General Disclaimer

One or more of the Following Statements may affect this Document

- This document has been reproduced from the best copy furnished by the organizational source. It is being released in the interest of making available as much information as possible.

- This document may contain data, which exceeds the sheet parameters. It was furnished in this condition by the organizational source and is the best copy available.

- This document may contain tone-on-tone or color graphs, charts and/or pictures, which have been reproduced in black and white.

- This document is paginated as submitted by the original source.

- Portions of this document are not fully legible due to the historical nature of some of the material. However, it is the best reproduction available from the original submission.

HOLLOW FIBER MEMBRANE SYSTEMS

FOR ADVANCED LIFE SUPPORT SYSTEMS

FINAL REPORT

BY

GEORGE J. ROEBELEN, JR.
AND
MICHAEL J. LYSAGHT

PREPARED UNDER CONTRACT NO. NAS 9-14682

BY

HAMILTON STANDARD
DIVISION OF UNITED TECHNOLOGIES CORPORATION
WINDSOR LOCKS, CONNECTICUT 06096

FOR

NATIONAL AERONAUTICS AND SPACE ADMINISTRATION
LYNDON B. JOHNSON SPACE CENTER
HOUSTON, TEXAS 77085

OCTOBER, 1976

HOLLOW FIBER MEMBRANE SYSTEMS

FOR ADVANCED LIFE SUPPORT SYSTEMS

FINAL REPORT

BY

GEORGE J. ROEBELEN, JR.
AND
MICHAEL J. LYSAGHT

PREPARED UNDER CONTRACT NO. NAS 9-14682

BY

HAMILTON STANDARD
DIVISION OF UNITED TECHNOLOGIES CORPORATION
WINDSOR LOCKS, CONNECTICUT 06096

FOR

NATIONAL AERONAUTICS AND SPACE ADMINISTRATION
LYNDON B. JOHNSON SPACE CENTER
HOUSTON, TEXAS 77085

OCTOBER, 1976

ABSTRACT

HOLLOW FIBER MEMBRANE SYSTEMS FOR ADVANCED LIFE SUPPORT SYSTEMS

By

George J. Roebelen, Jr.
and
Michael J. Lysaght

Contract No. NAS 9-14682

This report describes an investigation of the practicability of utilizing hollow fiber membranes in vehicular and portable life support system applications.

A preliminary screening of potential advanced life support applications resulted in the selection of five applications for feasibility study and testing.

As a result of the feasibility study and testing, three applications, heat rejection, deaeration, and bacteria filtration, were chosen for breadboard development testing; breadboard hardware has been manufactured and tested, and the physical properties of the hollow fiber membrane assemblies have been characterized.

FOREWORD

This report has been prepared by Hamilton Standard, Division of United Technologies Corporation for the National Aeronautics and Space Administration, Lyndon B. Johnson Space Center in accordance with the requirements of Contract NAS 9-14682, Hollow Fiber Membrane Systems for Advanced Life Support Systems. Complimenting Hamilton Standard in this program was Amicon Corporation, Lexington, Massachusetts, a researcher, developer, and producer of numerous hollow fiber membrane systems for commercial and biomedical applications.

Appreciation is expressed to the NASA Technical Monitor, Mr. P. B. McLaughlan, for his guidance and advice.

Hamilton Standard personnel responsible for the conduct of this program were Mr. Fred H. Goodwin, Program Manager, and Mr. George J. Roebelen, Jr., Project Engineering Manager. Mr. Michael J. Lysaght, Assistant Director of Research, was responsible for the effort at Amicon Corporation.

Appreciation is expressed to Mr. John S. Lovell, Chief, Advanced Engineering, Mr. Earl K. Moore, Technical Specialist, Mr. Edward H. Tepper, Senior Analytical Engineer, Mr. Ralph J. Petillo, Senior Test Engineer, and Dr. John R. Aylward, Research Scientist, all of Hamilton Standard, Dr. George Christopher of the United Technologies Research Center, and Mr. Frank Muolo, Lead Technician of Amicon Corporation, whose efforts made the successful completion of this program possible.

TABLE OF CONTENTS

TABLE OF CONTENTS
(Continued)

LIST OF FIGURES

LIST OF FIGURES
(Continued)

LIST OF FIGURES
(Continued)

LIST OF TABLES

INTRODUCTION

Hollow fiber membrane systems show promise in replacing existing components in life support systems because of their potential for reducing system weight, volume, cost, and complexity.

Conventional flat membrane systems have not been used in life support systems primarily due to the large volume and heavy membrane supporting structure required. Membranes in the form of small hollow tubes do not require any supporting structure, can withstand high pressure differentials without collapse or rupture, and consume considerably less volume than conventional flat membrane systems. Membrane tubes can be formed into bundles and, with suitable selection of membrane materials and matrices, will perform life support systems separative functions with high efficiencies and within small volumes.

This report describes the effort funded by NASA/JSC under Contract NAS 9-14682 during which a hollow fiber membrane applications and materials characterization study was performed, five promising applications were feasibility tested, and the three most promising applications, heat rejection, deaeration, and bacteria filtration, were breadboard level tested.

SUMMARY

The overall objective of the Hollow Fiber Membrane Systems for Advanced Life Support Systems program was to determine the practicability of utilizing hollow fiber membranes in vehicular and portable life support system applications.

An Applications Study and Materials Testing task was performed to define potential applications for hollow fiber membranes, to evaluate theoretically and experimentally a variety of materials for the most practicable applications, and to develop parametric information as a basis for the subsequent Breadboard phase. Of the five applications selected for study, carbon dioxide removal from a breathing gas stream, water vapor removal from a breathing gas stream, deaeration of water circuits, heat rejection using water as an expendable, and bacteria removal from PLSS water fill and drain circuits, three were demonstrated to have suitable performance characteristics to justify Breadboard studies: water deaeration, heat rejection, and bacteria filtration.

Breadboard units representing full size Shuttle PLSS assemblies for the bacteria filtration and water deaeration application and a half size Shuttle PLSS assembly for the heat rejection application were designed, manufactured, and tested.

Analytical evaluation of the data obtained from testing the breadboard units demonstrates the following:

- The bacteria filtration unit utilizing Romicon GM-80 acrylate fibers is completely retentive to bacteria and virus on a single shot basis.

- The deaeration unit utilizing Amicon SM-96 polysulfone fibers finds excellent application as a dissolved gas deaerator.

- The heat rejection unit utilizing Amicon SM-I polysulfone fibers has been demonstrated to possess excellent capability for heat rejection by water evaporation.

- Sizing criteria were established for the three applications.

- The heat rejection unit utilizing Amicon SM-I polysulfone fibers has been demonstrated to be capable of withstanding qualification level vibration testing equal to that imposed on Shuttle ECS hardware without sustaining damage.

3/4

CONCLUSIONS

The practicality of utilizing hollow fiber membrane devices for single shot bacteria/virus filtration, dissolved oxygen deaeration from a water stream, and heat rejection utilizing transport water has been demonstrated.

The feasibility of utilizing hollow fiber membrane devices for long term bacteria/virus filtration, dissolved hydrogen removal from a water stream, and carbon dioxide removal from a gas stream with an intermediate liquid sorbent loop has been indicated.

Removal of carbon dioxide and water vapor directly from a gas stream utilizing hollow fiber membrane devices has been demonstrated to be impractical due to the prohibitively large membrane area required to obtain suitable removal rates.

RECOMMENDATIONS

The studies and test results of this program have indicated that
hollow fiber membrane application effort should be expended in
the follow areas:

- Heat rejection using large diameter internally vented hollow
  fiber membranes.

- Membrane development aimed at producing a highly hydrophobic
  membrane for use in a liquid CO_2 sorbent system.

- Long term bacteria/virus filtration testing.

- Dissolved hydrogen removal from a water stream.

NOMENCLATURE

abs	absolute
acfm	actual cubic feet per minute
A	area
$\overset{\bullet}{A}$	angstrom
Btu	British thermal unit
cm	centimeter
c_p	heat capacity
C	molar concentration
CH_4	methane
CO	carbon monoxide
CO_2	carbon dioxide
°C	degree Celsius
d	diameter
D_{AB}	diffusivity of "A" in "B"
D_K	Knudson diffusivity
E	effectiveness
ECS	environmental control system
EMU	extravehicular mobility unit
f	Fanning friction factor
ft	feet
°F	degree Fahrenheit
g	gram
G	mass flux
h	liquid film thermal coefficient
hA	film conductance
hr	hour
HFM	hollow fiber membrane
H_2O	water
in	inch
I.D.	inside diameter
J	joule
k	thermal conductivity
kg	kilogram
kPa	kilopascal
$KHCO_3$	potassium bicarbonate
K_2CO_3	potassium carbonate

NOMENCLATURE
(Continued)

l	liter
lb	pound
L,l	length
LCG	liquid cooling garment
m	meter
max	maximum
mg	milligram
min	minute
ml	milliliter
mmHg	millimeters of mercury
M	molecular weight
NH_3	ammonia
N_A	molar flux
N_2	nitrogen
N_{GZ}	Graetz number
O.D.	outside diameter
O_2	oxygen
psi	pounds per square inch
psia	pounds per square inch absolute
psid	pounds per square inch differential
psig	pounds per square inch gauge
P	pressure
Pa	pascal (newton per square meter)
PP,P	partial pressure
PLSS	portable life support system
POS	portable oxygen system
P/N	part number
ΔP	pressure differential
Q	heat rejection rate
$\bar{r}$	mean pore radius
r	radius
R	universal gas constant
RO	reverse osmosis
s	second
S/N	serial number
t, T	temperature

NOMENCLATURE
(Continued)

UA	thermal conductance
V_A	molar volume
W	watt
$\dot{W}$	mass flow rate
X_A	mole fraction of specie A
Λ	difference, differential
μ	micron, viscosity
ρ	density
σ	surface tension

SEPARATIVE MEMBRANE TECHNOLOGY

Membranes, simply defined, are thin, separative barriers between two phases. They are generally constructed from naturally-occurring or synthetic plastic materials, although membranes for gas separation have been constructed from palladium, a metal, and boron silicate, a glass. Membranes may also be made in a variety of shapes, including tubes, flat sheets, or hollow fibers. The performance characteristics of a membrane are not defined simply by the choice of the material and its shape. Rather, transport depends upon several microscopic properties, such as the number of pores per unit area and the size of these pores, the percent of solvent (typically H_2O) imbibed by the membrane, the thickness of consolidated surface regions ("skins"), and the like. In short, the transport characteristics of a membrane result from an interplay of geometric and material considerations.

The mechanism of transport through a membrane is characterized as either "bulk-flow" or "diffusive." In the case of bulk-flow transport, the permeate species flows through discreet pores, linking one side of the membrane with the other. Separation here is accomplished by physical sieving, i.e., some of the pentrating species are small enough to go through the pores and others are not. Bulk-flow membrane separation is analogous to macroscopic filtration, as with a screen, grids, or the like, and is thus easy to conceptualize. Diffusive membranes, on the other hand, have no simple analogy in common experience. They contain no pores, and permeated species actually dissolve in the membrane material, then diffuse across the membrane and desorb at the downstream side. Rate of transport is dependent upon solubility of the permeate in the membrane material and upon the rate of its diffusivity; hence, two molecules which are exactly the same in size and shape could be effectively separated because they displayed different solubilities in the membrane material. Diffusive membranes have much lower throughput rates than bulk flow membranes but, as a general rule, can be utilized for more challenging separations (example, salt from water).

Regardless of whether transport is "bulk-flow" or "diffusive," certain fundamental principles will be followed:

- The relative rate of transport of two or more permeates (selectivity) is independent of membrane thickness. The absolute rate of transfer of each permeate decreases with increasing membrane thickness. Accordingly, from the viewpoint of separation efficiency alone, the thinnest possible membrane is always optimum. Mechanical considerations intervene, in practice, and set the minimum allowable thickness.

13

- The flow per unit area of any permeating species through a membrane is generally considered to be a product of a characteristic permeability and a driving force. In the final analysis, the driving force is thermodynamic activity or chemical potential; practically this is usually manifest as either pressure or concentration, or both. When the transport conditions are well defined, the performance of the membrane can be described simply in terms of the permeation coefficient which will be flux per unit area per unit time per unit of driving force.

- The resistance of the membrane to transport is only part of the overall system resistance. Additional hindrances to transport will be encountered in the boundary layers on both sides of the membrane and result from localized depletion of the permeates species and/or buildup of the rejected or non-transported solutes. Typically, the system resistances are two to three times that of the membrane resistance alone and, in many practical situations, the system resistance completely dominates the transport. It should be clear that in those cases no improvement could be realized by developing and utilizing a superior membrane.

Table I lists the different types of classes of currently significant membranes and gives the principal uses for each type. There are several ways of categorizing membranes. One is transport mechanism, i.e., the membrane is either diffusive or it is bulk-flow. Another is shape, i.e., the membrane may be in the form of flat sheet, tube, or a hollow fiber. Still a third is degree of water sorption; membranes are generally employed in water, and those which absorb it to a significant extent behave differently as a class from those which do not. Finally, microstructure is important. Some membranes are relatively homogeneous throughout; others, particularly the "anisotropic," have a very thin, consolidated region on one surface which rests atop an integral, expanded, sponge-like substrate. The anisotropic structure is essentially a compromise between the advantages of a thin barrier layer, as discussed earlier, and the requirement for mechanical strength and handleability.

Considerable investigative emphasis is currently being given to "composite" membranes, which attempt to crossover the traditional functional lines to achieve properties not available in existing categories. Typically, a composite membrane will be prepared from a bulk flow, ultrafiltrative matrix in whose pores has subsequently been immobilized a special diffusive barrier (for example, a liquid with high differential solubility to two gases). The resultant composite would be used as a diffusive barrier, even though its basic structure is for bulk flow.

TABLE I

TYPES AND USES OF PERMEABLE MEMBRANES

TYPE	GRADE	DEGREE OF WATER SORPTION BY MATRIX	COMPOSITION AND SHAPE	TYPICAL APPLICATIONS
DIFFUSIVE	→"REVERSE OSMOSIS"	Moderate	Anisotropic – flat sheet or Homogeneous – hollow fiber	Desalination of sea water or brackish water
	→"DIALYSIS"	High	Homogeneous – flat sheet or hollow fiber	Artificial kidneys; certain recharg-able batteries
	→"PERM SELECTIVE"	Low	Homogeneous – flat sheet	Research only
BULK FLOW	→ULTRAFILTRATIVE	Optional	Anisotropic – flat sheet and hollow fiber	Life science research in-vitro diagnostics *** Industrial Water purification
	→MICROPOROUS	Usually low	Homogeneous – flat sheet and hollow fiber	Bacterial or viral filtration; blood oxygenation
COMPOSITES	→"RO OR PS"	Mixed	Mixed – flat sheet	Research on all of the above

It is interesting to note that the membrane business is currently between $75 and $150 million worldwide on an annual basis, especially since the annual dollar volume of this business in 1961 was less than $1 million. The major current area, representing an estimated 70% of the total business, is biomedical. Membranes are the enabling components of artificial kidneys, which are the life-sustaining devices employed by upwards of 40,000 people worldwide. They are also used in artificial lungs or oxygenators during cardiac surgery, as well as in a variety of diagnostic and investigative purposes. Industrial ultrafiltration is the second largest category with "turn-key" membrane plants selling at anywhere from $50,000 to $2 million installed. Typical applications include: prepurification or "final filtration" of process water for polymerizations, microelectronics, or applications where extreme high quality water is required; purification of effluent streams before discharge as, for example, oil water streams or automotive paint tank overflow streams; and by-product recovery as in the citrus and dairy food industries. Still another major segment of the membrane business is the supply of devices for separation and concentration of biological and laboratory fluids. Finally, membrane desalination is still being studied as a method to provide potable water from brackish or sea water. This process is not yet economical in the United States, but in 1975 worldwide construction of membrane desalination plants was in the $10 to $20 million rate. Since the principal advantage of membrane desalination is its low fuel requirements, its attractiveness is expected to increase in the coming years.

Appendix A discusses the technology of membrane separations in considerably more detail.

PROGRAM PLAN

An Applications Study and Materials Testing task was performed to define potential applications for hollow fiber membranes, to evaluate theoretically and experimentally a variety of materials for the most practicable applications, and to develop parametric information as a basis for the subsequent Breadboard phase.

Breadboard units representing Shuttle PLSS assemblies for bacteria filtration, dissolved gas removal, and heat rejection applications were designed, manufactured, tested, and evaluated.

APPLICATIONS STUDY AND MATERIALS TESTING

The objectives of this phase were to define potential applications for using hollow fiber membranes in advanced portable and vehicle life support systems and to evaluate a variety of materials for each most practicable application to develop parametric information as a basis for the subsequent design phase.

APPLICATIONS DEFINITION

Potential applications for hollow fiber membranes (HFM) have been identified by reviewing representative schematics for Portable Life Support System, Portable Oxygen System, Shuttle Environmental Control System, and Space Station Environmental Control System. The results of this review are summarized in Table II where an "X" represents identification of a potential application, and an " ⊗ " represents those applications considered most practicable.

The most practicable applications selected for further study are:

    I.   Carbon dioxide removal from breathing gas stream.
   II.   Water vapor removal from breathing gas stream.
  III.   Deaeration of water circuits.
   IV.   Heat rejection using water as an expendable.
    V.   Bacteria filtration for PLSS water fill and drain circuits.

MATERIALS DEFINITION

Potential hollow fiber membrane materials have been identified by reviewing hollow fiber membranes currently available from HFM manufacturers, and a literature survey has been conducted to identify potential areas where membrane impregnants or post treatments would improve performance. Table III summarizes the results of this effort. An " ⊗ " represents identification of a potential material and, where applicable, a potential membrane impregnant or post treatment. The materials and impregnants or post treatments selected as most suitable for further study for each application follow.

CARBON DIOXIDE REMOVAL

    1.   XM-S Acrylic Material
          Anisotropic Structure
          0.051 cm (20 mil) I.D.

TABLE II

APPLICATIONS DEFINITION SUMMARY

X Represents Potential Application
(X) Represents Most Practicable Application

HOLLOW FIBER MEMBRANE FUNCTIONS	APPLICABLE SYSTEMS			
	PLSS	POS	SHUTTLE	SPACE STATION
A. Removal of CO_2 from the gaseous environment				
1. Can provide for CO_2 partial pressure control	(X)	(X)	(X)	(X)
2. Can be basis for a CO_2 partial pressure sensor using a HFM and a standard pressure transducer	(X)	(X)	(X)	(X)
B. Removal of N_2 from the gaseous environment				
1. O_2 enrichment from air to permit the denitrogenation of the astronaut	X	X	X	X
2. Purge suit of N_2 prior to or during an EVA	X	X	X	X
3. Can be basis for a N_2 partial pressure sensor using a HFM and a standard pressure transducer	X	X	X	X
C. Removal of O_2 from the gaseous environment				
1. Would be an alternate means of denitrogenization	X	X	X	X
2. Can be basis for an O_2 partial pressure sensor using a HFM and a standard pressure transducer			X	X
3. Can be basis of a direct O_2 partial pressure control regulator			X	X

TABLE II

APPLICATIONS DEFINITION SUMMARY (Continued)

HOLLOW FIBER MEMBRANE FUNCTIONS	APPLICABLE SYSTEMS			
	PLSS	PCS	SHUTTLE	SPACE STATION
D. Removal of Contaminants				
1. Can control contaminants in the environment and various fluid loops				
a. Removal of trace gaseous contaminants (H_2, CO, NH_3, benzene, etc.)	X	X	X	X
b. Filter out bacteria	Ⓧ		Ⓧ	Ⓧ
c. Filter out particulate contaminants from gases and liquids	X	X	X	X
d. Remove freon 21 from water			X	X
e. Reclaim wash and flush water				Ⓧ
E. Removal of H_2O from H_2, CH_4, O_2 and cabin air				
1. Removal of water vapor from the gaseous environment for relative humidity control	Ⓧ	Ⓧ	Ⓧ	Ⓧ
2. Removal of H_2O from electrolysis and CO_2 reduction subsystem gases			Ⓧ	Ⓧ

TABLE II

APPLICATIONS DEFINITION SUMMARY (Continued)

HOLLOW FIBER MEMBRANE FUNCTIONS	APPLICABLE SYSTEMS			
	PLSS	POS	SHUTTLE	SPACE STATION
F. Removal of gases from H_2O				
1. H_2O produced by fuel cells is saturated with H_2 which can come out of solution and cause blockage in suit or other water coolant transport circuits			Ⓧ	
2. Maintenance operations on coolant loops can inject gases which may cause pump activation or loop blockage and degraded performance or increased corrosion	Ⓧ		Ⓧ	Ⓧ
G. Remove H_2O from feces			X	X
H. Fluid Concentration Control				
1. Membranes can control the mixture concentration of various fluids				
a. Biocide concentration			Ⓧ	Ⓧ
b. Urine pretreat concentration control			Ⓧ	Ⓧ
2. Temperature sensitive membranes can control fluid temperatures (replacing electromechanical valves)			X	X

TABLE II

APPLICATIONS DEFINITION SUMMARY (Continued)

HOLLOW FIBER MEMBRANE FUNCTIONS	APPLICABLE SYSTEMS			
	PLSS	POS	SHUTTLE	SPACE STATION
I. Wick Transport Devices				
1. Replace sublimators	⊗		⊗	
2. Replace integral wick boilers	⊗		⊗	
3. Act as heat pipes	X		X	X
J. Hollow Fiber Applications (Nothing passes through the wall)				
1. Tube bundle heat exchangers	X	X	X	X
2. Flow restrictors with high dirt capacity and laminar pressure drop characteristics	X	X	X	X
3. Pressure damper to avoid stability problems	X	X		
4. Long cylindrical storage vessels with hemispherical ends. The fiber/cylindrical section can be bent into any shape to attain good volume utilization.	X	X	X	X

TABLE III

HOLLOW FIBER MEMBRANE MATERIALS SUMMARY

MATERIALS	HOLLOW FIBER TYPE	COMMENTS	HEAT REJECTION	DEAERATION	CO_2 REMOVAL	H_2O REMOVAL	BACTERIAL FILTRATION
1. Acrylics	Bulk Flow, ultrafiltrative	"XM"	PNS	PNS	PNS	PNS	⊗
2. Acrylics	Composite with glycerine	--	PNS	PNS	PNS	⊗	PNS
3. Acrylics	Composite with carbonate salts	--	PNS	PNS	⊗	PNS	PNS
4. Acrylics	Composites with polyvinyl alcohol	--	PNS	PNS	PNS	⊗	PNS
5. Acrylic	Composite with enzymes	--	PNS	PNS	⊗	PNS	PNS
6. Silicone polycarbonate	Diffusive	No longer available	NA	NA	NA	NA	NA
7. Silicone rubber	Diffusive	Only available as flat sheet	NA	NA	NA	NA	NA
8. Teflon	Bulk Flow, microporous	"Goretex"	⊗	⊗	PNS	⊗	PNS
9. Teflon	Bulk Flow, composites	Didn't hold impregnants	NA	NA	NA	NA	NA
10. Kypar	Bulk Flow, microporous or	Not commercially available and	ETM	ETM	PNS	ETM	PNS
11. Other fluorocarbons	ultrafiltrative	equivalent to off-the-shelf materials	ETM	ETM	PNS	ETM	PNS
12. Polypropylene	Bulk Flow, microporous	Only available as flat sheet	NA	NA	NA	NA	NA
13. Other polyolefins	Bulk Flow, microporous	Only available as flat sheet	NA	NA	NA	NA	NA
14. Cellophane	Diffusive	"Biofiber"; "Cuprophan"	⊗	PNS	PNS	⊗	PNS
15. Cellophane	Composite with enzymes	--	PNS	PNS	⊗	PNS	PNS
16. Cellophane	Composite with carbonate salts	--	PNS	PNS	⊗	PNS	PNS
17. Cellulose acetate	Diffusive, RO	"Loeb" type membrane	ETM	PNS	PNS	ETM	PNS
18. Ethyl cellulose	Bulk Flow, microporous	Only available as flat sheet	NA	NA	NA	NA	NA
19. Other cellulosic esters	Bulk Flow, microporous	Only available as flat sheet	NA	NA	NA	NA	NA
20. Other cellulosic esters	Diffusive	Variants on "Loeb" membranes	ETM	PNS	PNS	ETM	PNS
21. Other cellulosic esters	Bulk Flow, ultrafiltrative	--	ETM	PNS	PNS	ETM	PNS
22. Polysulfone	Bulk Flow, ultrafiltrative	"SH"	⊗	⊗	PNS	PNS	PNS
23. Polymethyl pentene	Bulk Flow, ultrafiltrative	--	ETM	ETM	PNS	PNS	PNS
24. Other hydrophobic thermoplastics	Bulk Flow, ultrafiltrative	--	ETM	ETM	PNS	PNS	PNS

CODE: ⊗ = Material tested; ETM = Material essentially equivalent to membranes which were tested; NA = Material not available as hollow fibers; PNS = The properties of this fiber (from literature or theoretical consideration) rendered it unsuitable for the application.

Impregnants:

a. Water with 0.25% surfactant (DSS)
b. Carbonic anhydrase with phosphate buffer
c. 30% solution of tetraethyl ammonium carbonate

2. Bio-Fiber 50 Cellulosic Material
Homogeneous Structure
0.020 cm (8 mil) I.D.

Impregnants:

a. Water
b. Carbonic anhydrase with phosphate buffer
c. 30% solution of tetraethyl ammonium carbonate

WATER VAPOR REMOVAL

1. XM Acrylic Material
Anisotropic Structure
0.051 cm (20 mil) I.D.

Post Treatments:

a. Polyvinyl alcohol
b. Glycerinization

2. Type A Gore-Tex Teflon Material
Microporous Structure
0.08 cm (1/32 inch) I.D.

3. Bio-Fiber 50 Cellulosic Material
Homogeneous Structure
0.02 cm (8 mil) I.D.

DEAERATION

1. SM-96 Polysulfone Material
Anisotropic Structure
0.02 cm (8 mil) I.D.

2. SM-I Polysulfone Material
Anisotropic Structure
0.051 cm (20 mil) I.D.

3. Type A Gore-Tex Teflon Material
Microporous Structure
0.08 cm (1/32 inch) I.D.

HEAT REJECTION

1. SM-96 Polysulfone Material
    Anisotropic Structure
    0.02 cm (8 mil) I.D.

2. SM-I Polysulfone Material
    Anisotropic Structure
    0.051 cm (20 mil) I.D.

3. Type A Gore-Tex Teflon Material
    Microporous Structure
    0.08 cm (1/32 inch) I.D.

4. Bio-Fiber 50 Cellulosic Material
    Homogeneous Structure
    0.02 cm (8 mil) I.D.

BACTERIA FILTRATION

GM-80 Acrylate Material
Anisotropic Structure
0.051 cm (20 mil) I.D.

LABORATORY PARAMETRIC TESTING

Scale model testing has been performed on each of the hollow
fiber membranes, and impregnants or post treatments where ap-
plicable, selected in the previous sections. The purpose of this
task is to generate parametric data to allow selection of the
most promising materials for each application and, ultimately,
selection of the three most promising applications to be pursued
further in the subsequent breadboard development efforts.

It became apparent during the materials definition task that the
most meaningful data would be obtained by constructing scale
model modules for each of the hollow fiber membranes materials.
As a result, twelve different scale model modules were con-
structed, some in duplicate for different applications, to cover
each combination of hollow fiber membrane material and, where
applicable, each impregnant or post treatment. This effort is
considerably larger than the five scale model modules anticipated
at the inception of the program.

An evaluation of the benefits to be gained from high speed photo-
graphy of the heat rejection vaporization process indicated that
the vapor would be totally invisible, and that any liquid/vapor

action in the individual pore region would be several orders of magnitude smaller than could be observed with conventional high speed photography. It was decided to delete the high speed photography and divert the effort into the expanded scale model module manufacturing and testing effort.

Vibration testing, originally targeted for this portion of the program, was postponed to the breadboard development test portion of the program to allow testing of a module more representative of flight configuration.

In addition to testing the bacteria filtration unit as a bacteria filter, it was decided to explore the capabilities of the unit as a virus filter.

CARBON DIOXIDE REMOVAL

Scale model modules were prepared containing the selected materials, XM-S acrylic and Bio-Fiber 50 cellulosic, each impregnanted with water, buffered carbonic anhydrase, and 35% solution of tetraethyl ammonium carbonate. Figures 1 and 2 describe the membrane devices and show photomicrographs of the sectioned non-impregnated hollow fiber membrane. Testing was performed using the setup shown in Figure 3 where N_2 or CO_2 is introduced into the inside of the dead ended hollow fiber membranes, and the gas flow through the membrane walls is measured. The intent of this testing is to generate data describing the N_2 and CO_2 flux through the membrane and thereby produce a value of membrane selectivity for CO_2 to N_2.

Table IV and V summarize the flux values and membrane selectivities (CO_2/N_2) for each of material and impregnant combinations under consideration.

WATER VAPOR REMOVAL

Scale model modules were prepared containing the selected materials, XM acrylic post treated with polyvinyl alcohol and with glycerine, untreated Type A Gore-Tex telfon, and untreated Bio-Fiber 50 cellulosic. Figures 4, 5, and 6 describe the membrane devices and show photomicrographs of the sectioned untreated hollow fiber membrane. Testing was performed using the setup shown in Figure 7 where nitrogen gas partially saturated with water vapor was passed through the inside of the hollow fiber membranes, and dry sweep gas was passed across the outside of the hollow fiber membranes. The water vapor removal rate is calculated by measuring the throughput flow rate and the inlet and outlet dew point. The results are summarized in Table VI. Water vapor removal with immeasurable gas loss was obtained with each of the XM acrylic modules. The Bio-Fiber 50 cellulosic fibers dried out and ruptured before data could be obtained. No water vapor removal was detected with the Type A Gore-Tex teflon module.

500μ

50X

50μ
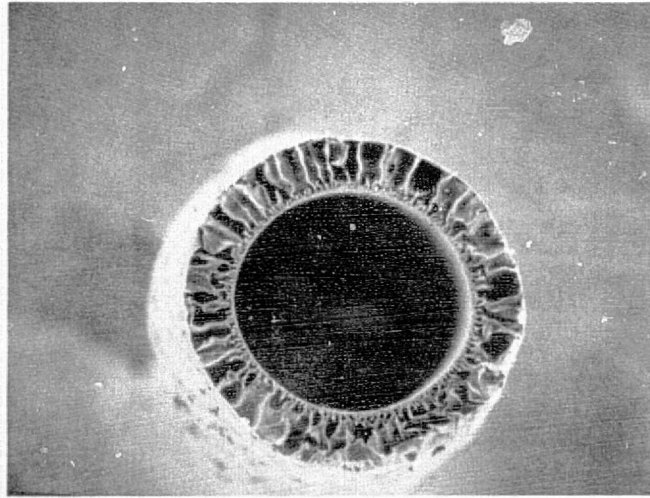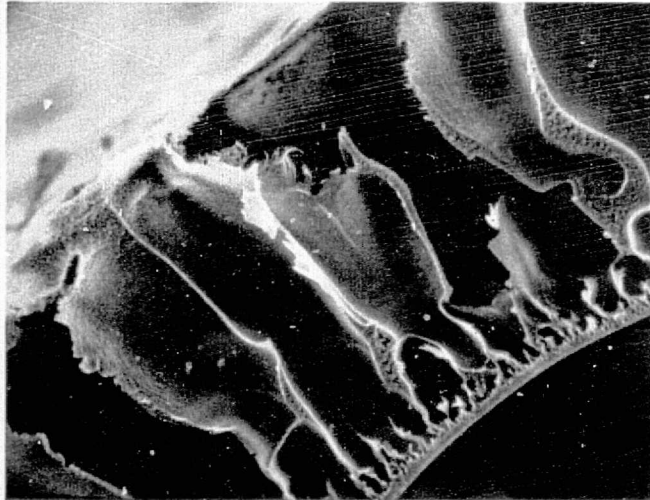
400X

MEMBRANE CHARACTERISTICS

- XM-S from Amicon
- Anisotropic Structure
- Acrylic Material
- 20-mil ID

DEVICE CHARACTERISTICS

- 400 Fibers
- 3.5 Inches Active Length
- 5.0 Inches Total Length
- 575 cm^2 Area for Transport

IMPREGNANTS

Water with 0.25% surfactant (DSS)
Phosphate buffer with carbonic anhydrase
35% solution of tetraethyl ammonium carbonate

SS 12989-8

FIGURE 1 XM-S MEMBRANE FOR CO_2 REMOVAL
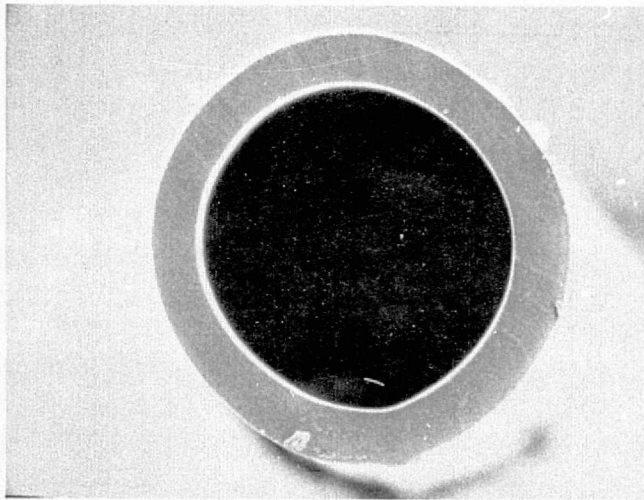
200X

2000X

MEMBRANE CHARACTERISTICS

- ' Bio-Fiber 50 from Bio-Rad
- ' Homogeneous Structure
- ' Cellulosic Material
- ' 8-mil ID

DEVICE CHARACTERISTICS

- ' 400 Fibers
- ' 6-Inches Active Length
- ' 8 Inches Total Length
- ' 400 cm^2 Area for Transport

IMPREGNANTS

Water
35% Tetraethyl ammonium carbonate
Carbonic anhydrase in phosphate buffer

SS 12982-8

FIGURE 2 BIO FIBER 50 MEMBRANE FOR CO_2 REMOVAL

HAMILTON STANDARD Division of UNITED TECHNOLOGIES™

Low Flow Bubble Meter

High Flow Bubble Meter

Hygrometer

Inlet Pressure Gauge

Valve

Hollow Fiber Module

RH Probe

N₂ or CO₂

Humidity Bubbler
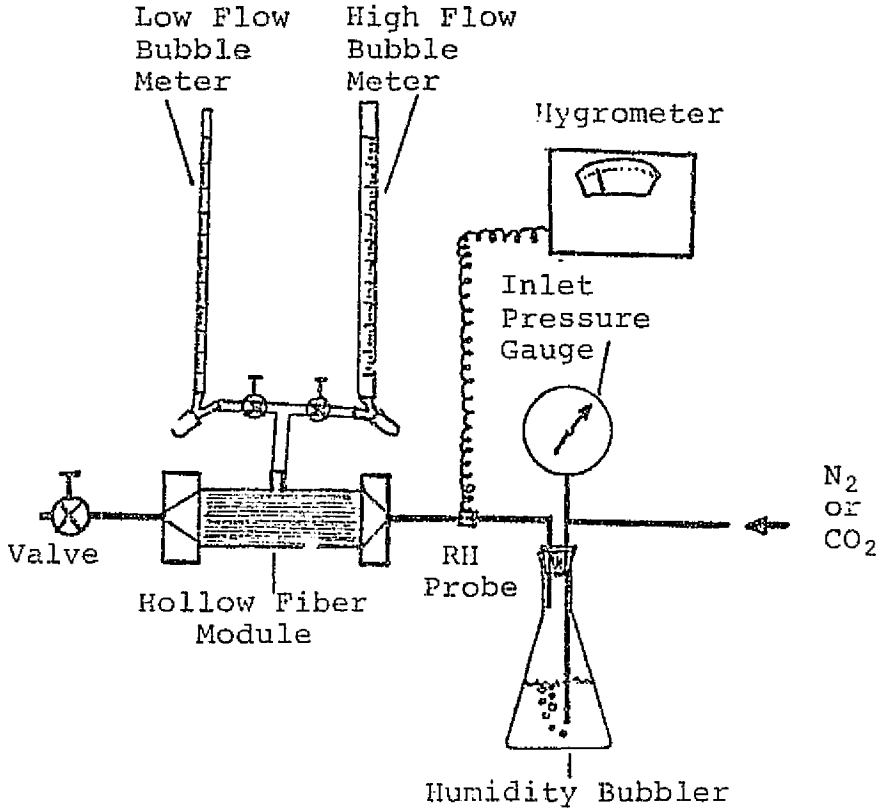
GAS PERMEATION TEST CONFIGURATION

FIGURE 3

TABLE IV
APPLICATION: CO_2 REMOVAL

CANDIDATE: XM FROM AMICON
AREA: 575 cm^2

Impregnant		Flux - cm^3/min at 26.6 kPa (200 mmHg) Total Membrane Pressure	Normalized Flux cm^3/hr-kPa-m^2	Membrane Selectivity
None	CO_2	8,800	16.5 x 10^6	0.68
	N_2	13,000	24.1 x 10^6	
Water with 0.25% Surfactant	CO_2	3.18	5,925	6.4
	N_2	0.50	930	
Carbonic Anhydrase Buffered	CO_2	2.8	5,216	4.7
	N_2	0.6	1,116	
Tetraethyl Ammonium Carbonate 35%	CO_2	1.3	2,425	26
	N_2	0.05	89.6	

TABLE V
APPLICATION: CO_2 REMOVAL

CANDIDATE: BIO-FIBER 50 FROM BIO-RAD
AREA: 400 cm^2

Impregnant		Flux - cm^3/min at 26.6 kPa (200 mmHg) Total Membrane Pressure	Normalized Flux cm^3/hr-kPa-m^2		Membrane Selectivity
Water	CO_2	0.373	CO_2	992	18
	N_2	0.018	N_2	55	
Carbonic Anhydrase Buffered	CO_2	0.706	CO_2	1,895	39
	N_2	0.018	N_2	55	
Tetraethyl Ammonium Carbonate (35% Aqueous)	CO_2	0.122*	CO_2	---	
	N_2	0.0**	N_2	---	

*Declined with time.
**None detected after two hours.

29

50X
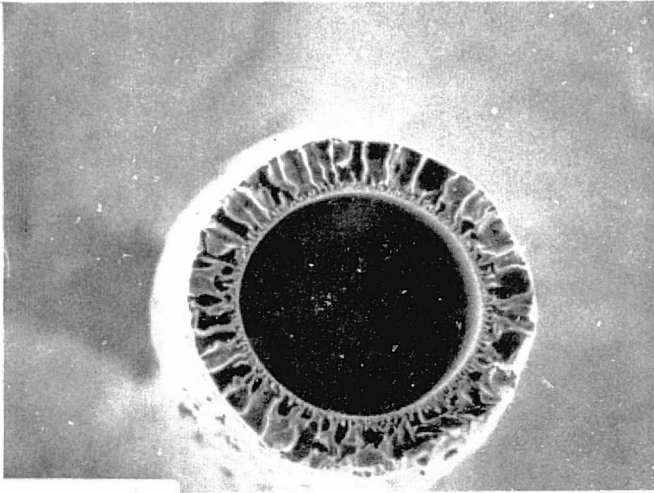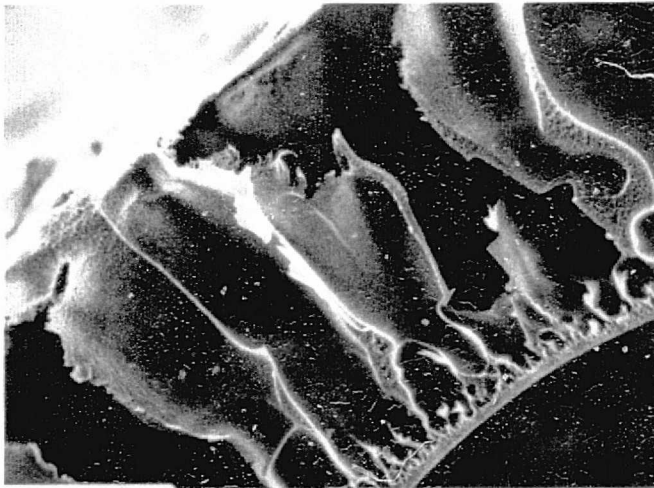
400X

MEMBRANE CHARACTERISTICS

* XM FROM AMICON
* ACRYLIC MATERIAL
* ANISOTROPIC STRUCTURE
* 20-MIL ID

DEVICE CHARACTERISTICS

* 400 FIBERS
* 3.5 INCHES ACTIVE LENGTH
* 5.0 INCHES TOTAL LENGTH
* 575 CM^2 AREA FOR TRANSPORT
* PERFORATED CASING

POST TREATMENTS

POLYVINYL ALCOHOL
GLYCERINIZATION

SS 12988-8

FIGURE 4 XM MEMBRANE FOR H_2O REMOVAL

30X

50X

MEMBRANE CHARACTERISTICS

· TYPE A GORE-TEX FROM GORE

· MICROPOROUS

· TEFLON MATERIAL

· 1/32" ID

DEVICE CHARACTERISTICS

· 100 FIBERS

· 3.5 INCHES ACTIVE LENGTH

· 5.0 INCHES TOTAL LENGTH

· 250 CM^2 AREA FOR TRANSPORT

· PERFORATED CASING

SS 12984-8   FIGURE 5 GORE—TEX MEMBRANE FOR H$_2$0 REMOVAL

31
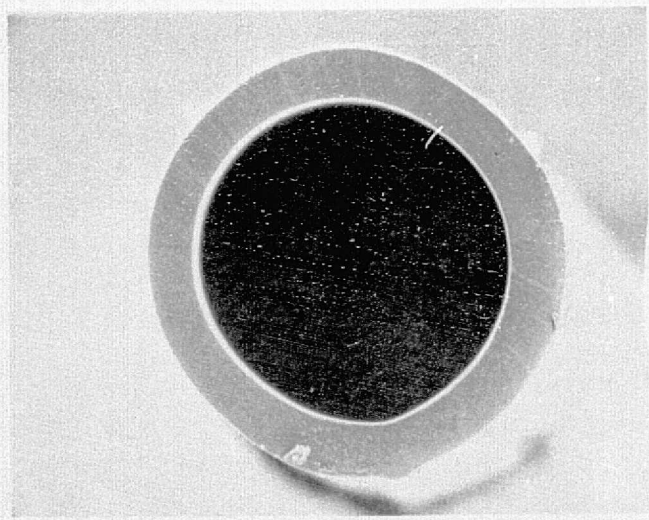
200X
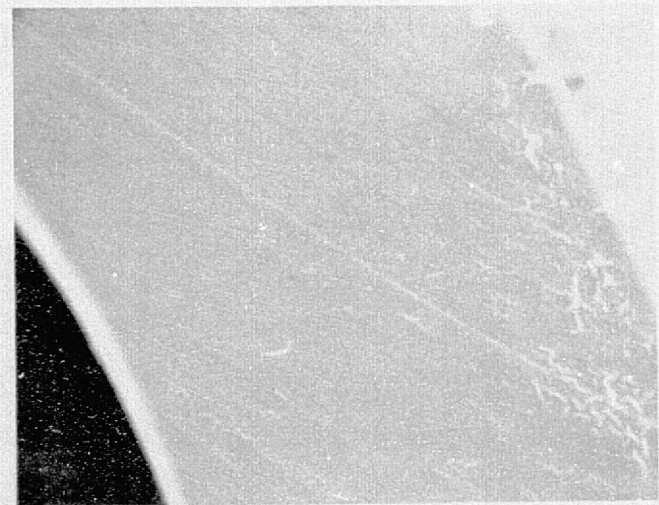
2000X

MEMBRANE CHARACTERISTICS

    Bio Fiber 50 from Bio-Rad

    Homogeneous Structure

    Cellulosic Material

    8-mil ID

DEVICE CHARACTERISTICS

    400 Fibers

    6-Inches Active Length

    8 Inches Total Length

    400 cm^2 Area for Transport

FIGURE 6 BIO FIBER 50 MEMBRANE FOR H_2O REMOVAL

SS 12982-8

22

HAMILTON STANDARD Division of UNITED TECHNOLOGIES
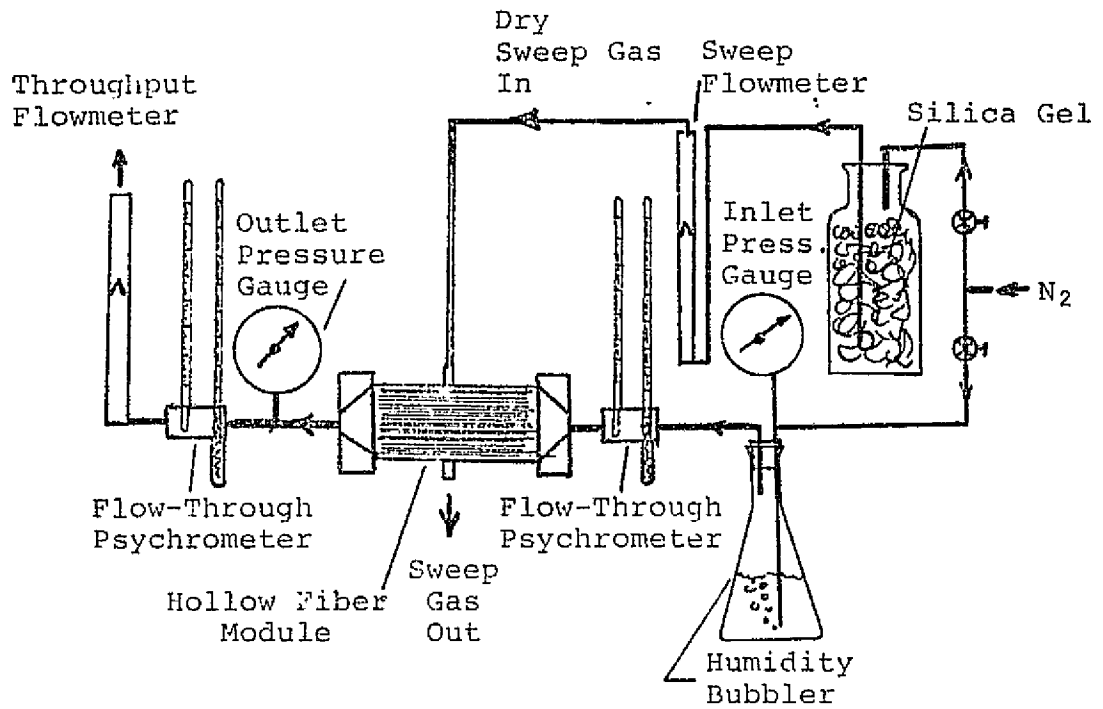
MOISTURE PERMEATION TEST CONFIGURATION

FIGURE 7

TABLE VI
APPLICATION: WATER VAPOR REMOVAL

TEST: DEHUMIDIFICATION OF AIR STREAM

RESULTS

Candidate	Water Vapor Removal mg/min at H2O Partial Pressure	Normalized Water Vapor Removal g/hr-kPa-m^2
XM Fiber Post Treated With Glycerine	6.7 @ 2.19 kPa (16.5 mmHg)	128
XM Fiber Post Treated With Polyvinyl Alcohol	4.8 @ 2.13 kPa (16.0 mmHg)	103
Bio-Fiber	Dried and Broke	--
Gore-Tex	None Detected	0

TABLE VII
APPLICATION: HEAT REJECTION AND DEAERATION

TEST: PERMEABILITY TO LIQUID WATER @ 68.9 kPa (10 psi)

RESULTS

Candidate	Measured Permeation cm^3/min	Normalized Permeation g/min-kPa-m^2
Polysulfone 0.02 cm (8 mil) I.D.	0.10 @ 850 cm^2	1.72
Polysulfone 0.051 cm (20 mil) I.D.	2.2 @ 300 cm^2	67.5
Gore-Tex	0 @ 225 cm^2*	0
Bio-Fiber	0.33 @ 400 cm^2	5.58

*None detected after three hours.

DEAERATION

Scale model modules were prepared containing the selected materials, SM-96 polysulfone, SM-I polysulfone, and Type A Gore-Tex teflon. Figures 8, 9, and 10 describe the membrane devices and show photomicrographs of the sectioned hollow fiber membranes. Liquid hydraulic permeation testing was performed on each module using the setup shown in Figure 11 where liquid water at 68.9 kPa gauge (10 psig) was flowed through the inside of the hollow fiber membranes, and the liquid permeate was collected and measured. Table VII summarizes the liquid permeation values for each of the materials under consideration.

Each of the membrane modules was tested for undissolved nitrogen removal and for dissolved oxygen removal from a liquid water stream flowing through the inside of the hollow fiber membranes. The outside of the membrane was subjected to varying levels of vacuum. Figures 12 and 13 show the test setup for undissolved nitrogen and dissolved oxygen, respectively. Tables VIII and IX summarize the test results.

HEAT REJECTION

A scale model module was prepared containing Bio-Fiber 50 cellulosic material and is described in Figure 14. This module and the SM-96 polysulfone, SM-I polysulfone, and Type A Gore-Tex teflon modules constructed for deaeration testing were considered in the heat rejection testing. Liquid hydraulic leakage was measured for the Bio-Fiber 50 module using the test setup of Figure 11, the results of which are included in Table VII.

Vacuum chamber testing per the test setup shown in Figure 15 to measure heat rejection rates was performed with membrane water inlet temperatures ranging from 18.3°C (65°F) to 41.7°C (107°F), water flow rate ranging from 11.34 to 113.4 kg/hr (25 to 250 lbs/hr), and chamber pressure ranging from 0.73 to 1.20 kPa (5.5 to 9 mmHg). The Gore-Tex membrane proved to be nonporous to water vapor and failed to reject heat under any of the test conditions. A graph of heat rejection versus log mean Δ P (difference between mean saturation pressure in the water flowing through the membranes and the chamber pressure) is shown in Figure 16. A theoretical maximum performance line that represents 100% effectivity is included on the curve for reference. Each of the polysulfone units were run at a chamber pressure of 0.27 kPa (2.0 mmHg) (below the triplepoint pressure). The 0.02 cm (8 mil) unit performed satisfactorily, but the 0.051 cm (20 mil) unit ruptured two membranes. The configuration of each of the membrane cartridges was such that the membranes were in relatively close contact with each other, creating a back pressure effect from the water vapor.
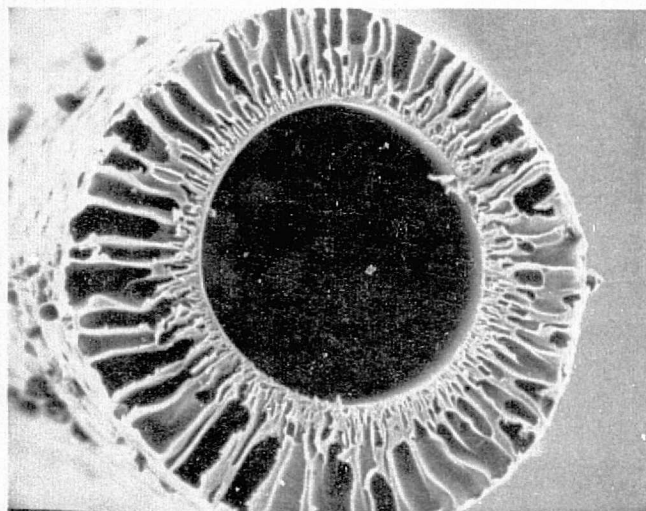
200X
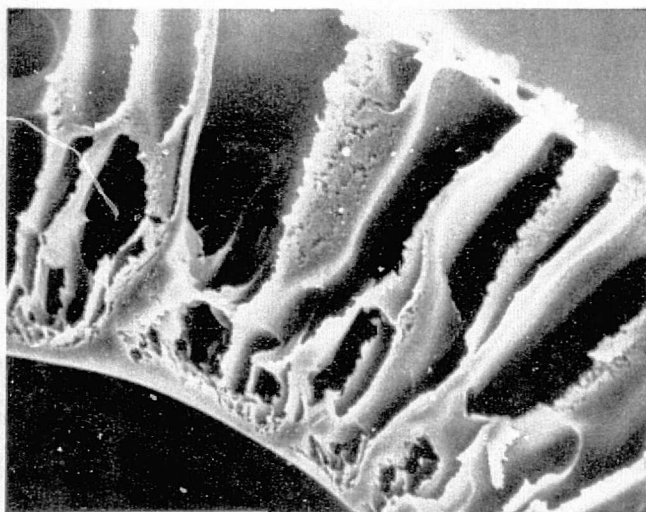
1000X

MEMBRANE CHARACTERISTICS
- SM-96 FROM AMICON
- ANISOTROPIC STRUCTURE
- POLYSULFONE MATERIAL
- 8-MIL ID

DEVICE CHARACTERISTICS
- 1500 FIBERS
- 3.5 INCHES ACTIVE LENGTH
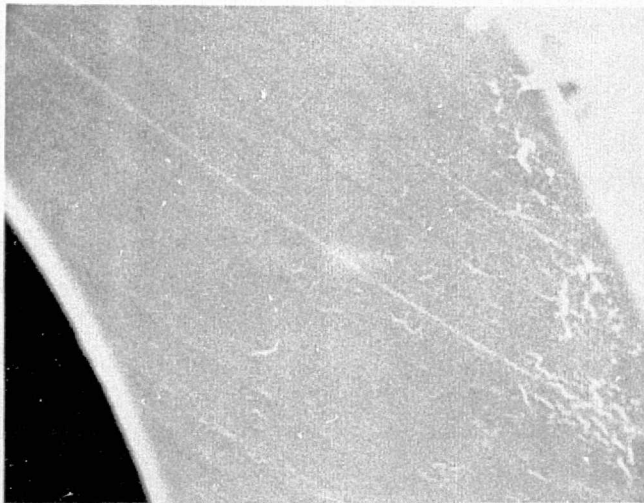- 5 INCHES TOTAL LENGTH
- 850 CM^2 AREA FOR TRANSPORT
- "OPEN" CASING

SS 12985-8   FIGURE 8 SM—96 MEMBRANE FOR HEAT REJECTION AND DEAERATION

50X
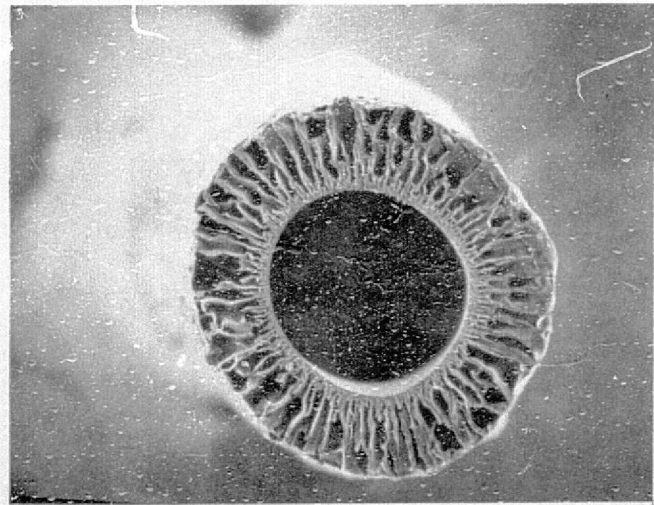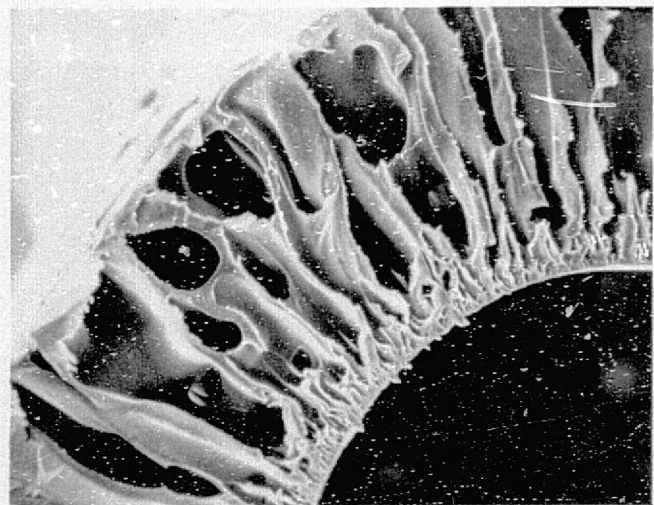
200X

MEMBRANE CHARACTERISTICS

- "SM-I" FROM AMICON
- ANISOTROPIC STRUCTURE
- POLYSULFONE MATERIAL
- 20-MIL ID

DEVICE CHARACTERISTICS

- 200 FIBERS
- 3.8 INCHES ACTIVE LENGTH
- 5.0 INCHES TOTAL LENGTH
- 300 CM^2 AREA FOR TRANSPORT
- "OPEN" CASING

SS 12986-8   FIGURE 9 SM-I MEMBRANE FOR HEAT REJECTION AND DEAERATION

30X

50X
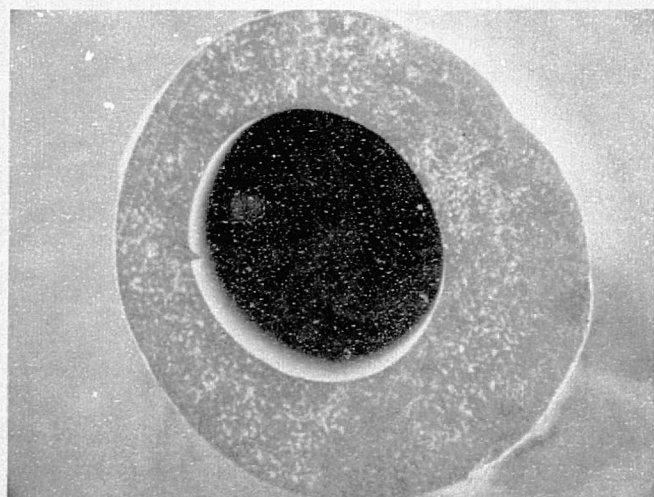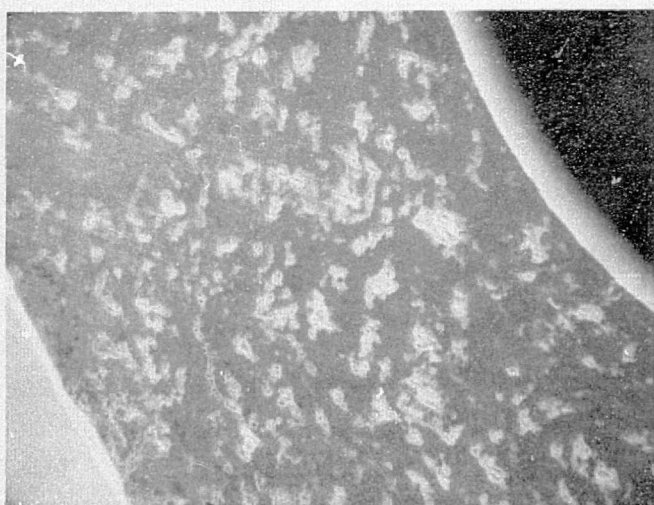
MEMBRANE CHARACTERISTICS

- Type A Gore-Tex from "Gore"
- Microporous Structure
- Teflon Material
- 1/32" ID

DEVICE CHARACTERISTICS

- 100 Fibers
- 3.5 Inches Active Length
- 5.0 Inches Total Length
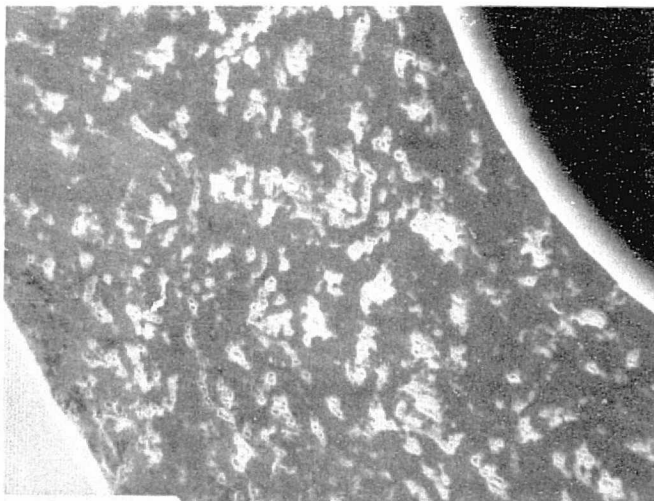- 225 cm^2 Area for Transport
- "Open" Casing

SS 12987-8   FIGURE 10 GORE—TEX MEMBRANE FOR HEAT REJECTION AND DEAERATION

Outlet
Gauge

Inlet
Gauge

Valve

Hollow
Fiber
Module

UF

Pump

Stopwatch

Graduated
Cylinder
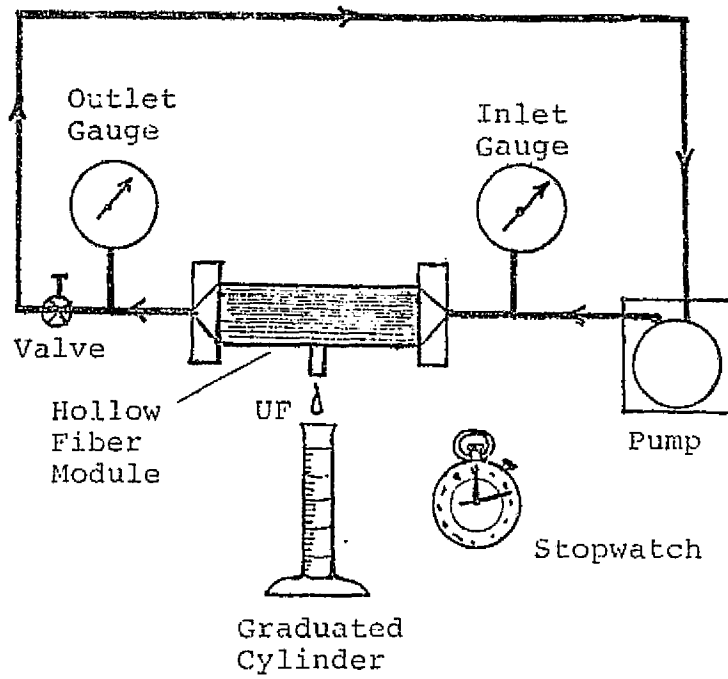
LIQUID HYDRAULIC PERMEABILITY TEST CONFIGURATION

FIGURE 11

FIGURE 12
UNDISSOLVED NITROGEN TEST
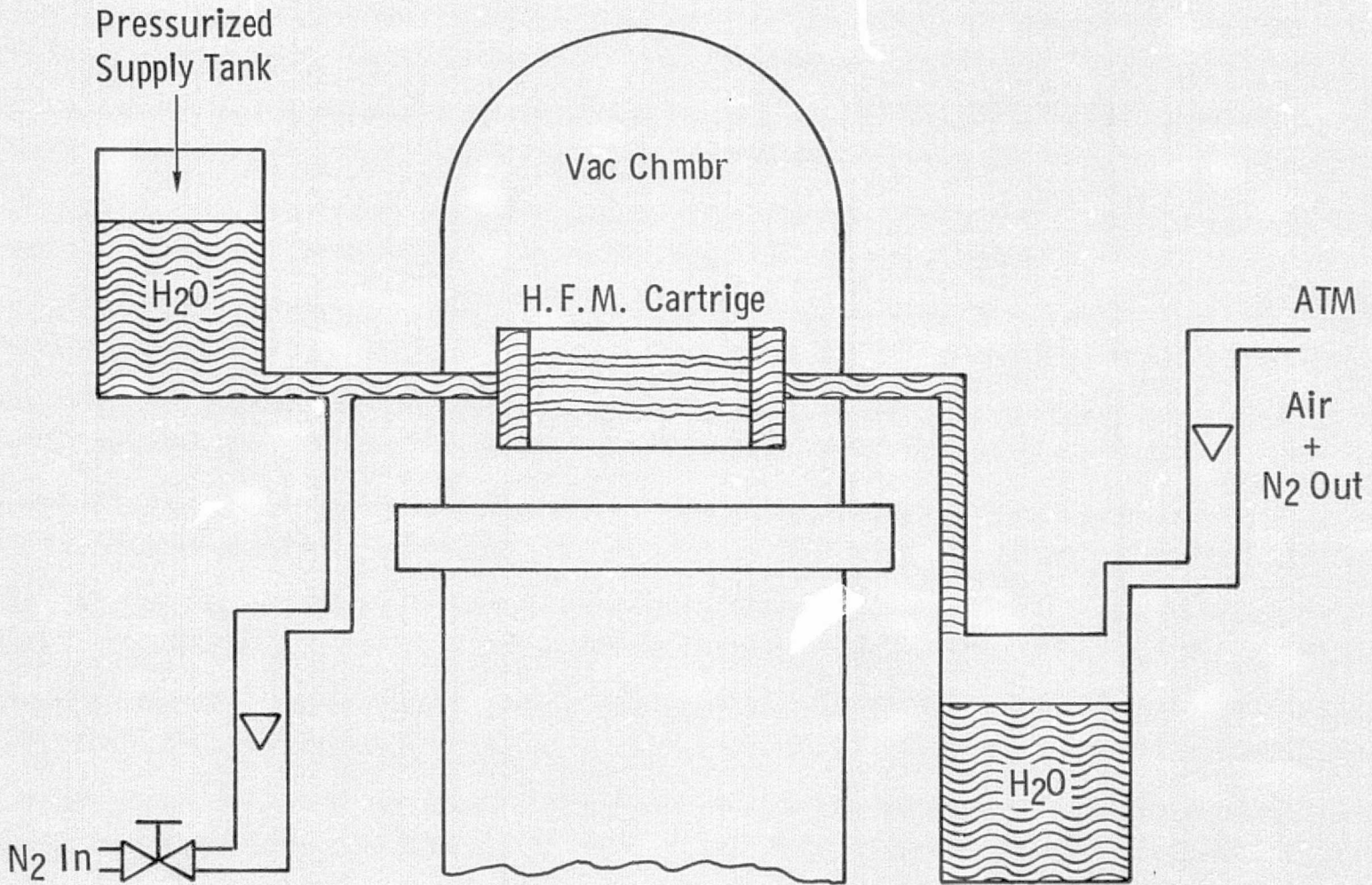
FIGURE 13
DISSOLVED OXYGEN TEST

Pressurized
Supply Tank

H2O

Vac. Chmbr

H.F.M. Cartrige

Inlet
Sample

Outlet
Sample

H2O
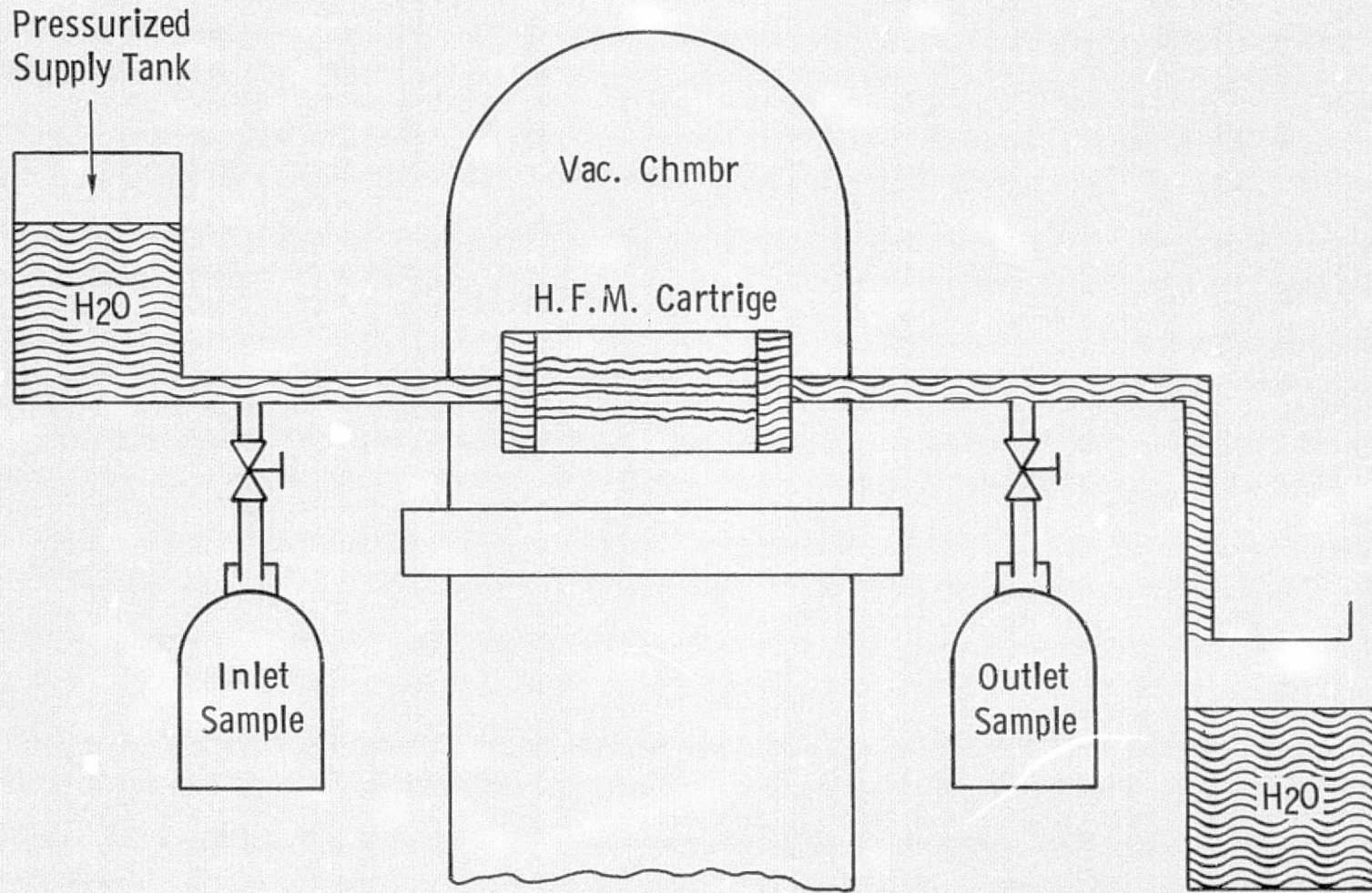
TABLE VIII
UNDISSOLVED NITROGEN TEST

Chamber Pressure	6.38 kPa abs (48 mmHg abs)	
Water Inlet Temperature	27.2°C (81°F)	
Water Flow	20.4 kg/hr (44.9 lb/hr)	

Test Sample	Introduced cm³/min	Permeated cm³/min	Percent
Polysulfone 850 cm² area 0.02 cm (8 mil) I.D.	21.2 42.8	1.2 15.8	5.7 36.9
Gore-Tex 225 cm² area 0.08 cm (1/32 inch) I.D.	21.2 42.8	4.2 12.8	19.8 29.9
Polysulfone 300 cm² area 0.051 cm (20 mil) I.D.	21.2 42.8	1.5 20.1	7.1 46.9

TABLE IX
DISSOLVED OXYGEN TEST

Chamber Pressure	6.88 kPa abs (51.7 mmHg abs)	
Water Inlet Temperature	27.2°C (81°F)	
Water Flow	20.4 kg/hr (44.9 lb/hr)	

Test Sample	Oxygen In	Oxygen Permeated
Polysulfone 850 cm² area 0.02 cm (8 mil) I.D.	10.0 g/m³	6.0 g/m³
Polysulfone 300 cm² area 0.051 cm (20 mil) I.D.	10.0 g/m³	3.0 g/m³
Gore-Tex 225 cm² area 0.08 cm (1/32 inch) I.D.	7.0 g/m³	None
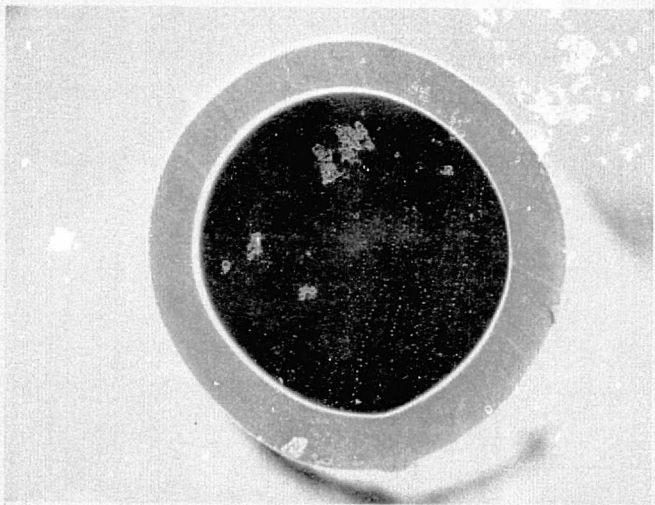
200X
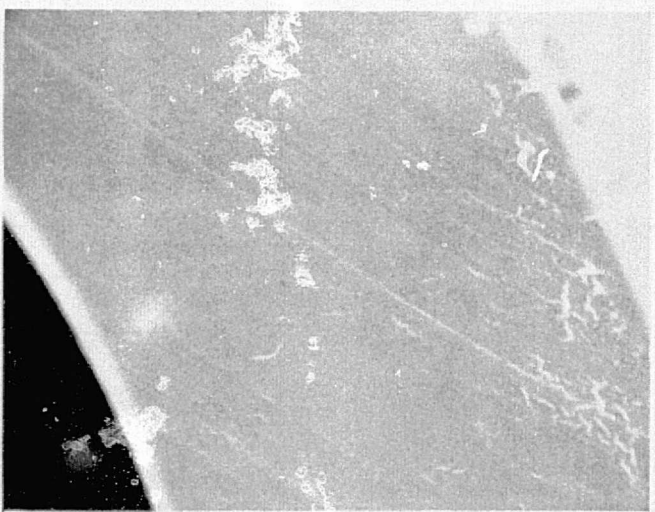
2000X

MEMBRANE CHARACTERISTICS

BIO FIBER 50 FROM BIO-RAD

HOMOGENEOUS STRUCTURE

CELLULOSIC MATERIAL

8-MIL ID

DEVICE CHARACTERISTICS

800 FIBERS

3.5 INCHES ACTIVE LENGTH

5.0 INCHES TOTAL LENGTH

400 CM^2 AREA FOR TRANSPORT

"OPEN" CASING

SS 12982-8

FIGURE 14 BIO FIBER 50 MEMBRANE FOR HEAT REJECTION

HEAT REJECTION TEST

N₂ supply

N₂ regul.

Water supply tank

HTR

SW.

T/C

P_IN

Flow rator

Vac Gage

ΔP

Vacuum chamber

Test sample

P_OUT

T/C

ATM. vent

To Vac

Water receiver tank
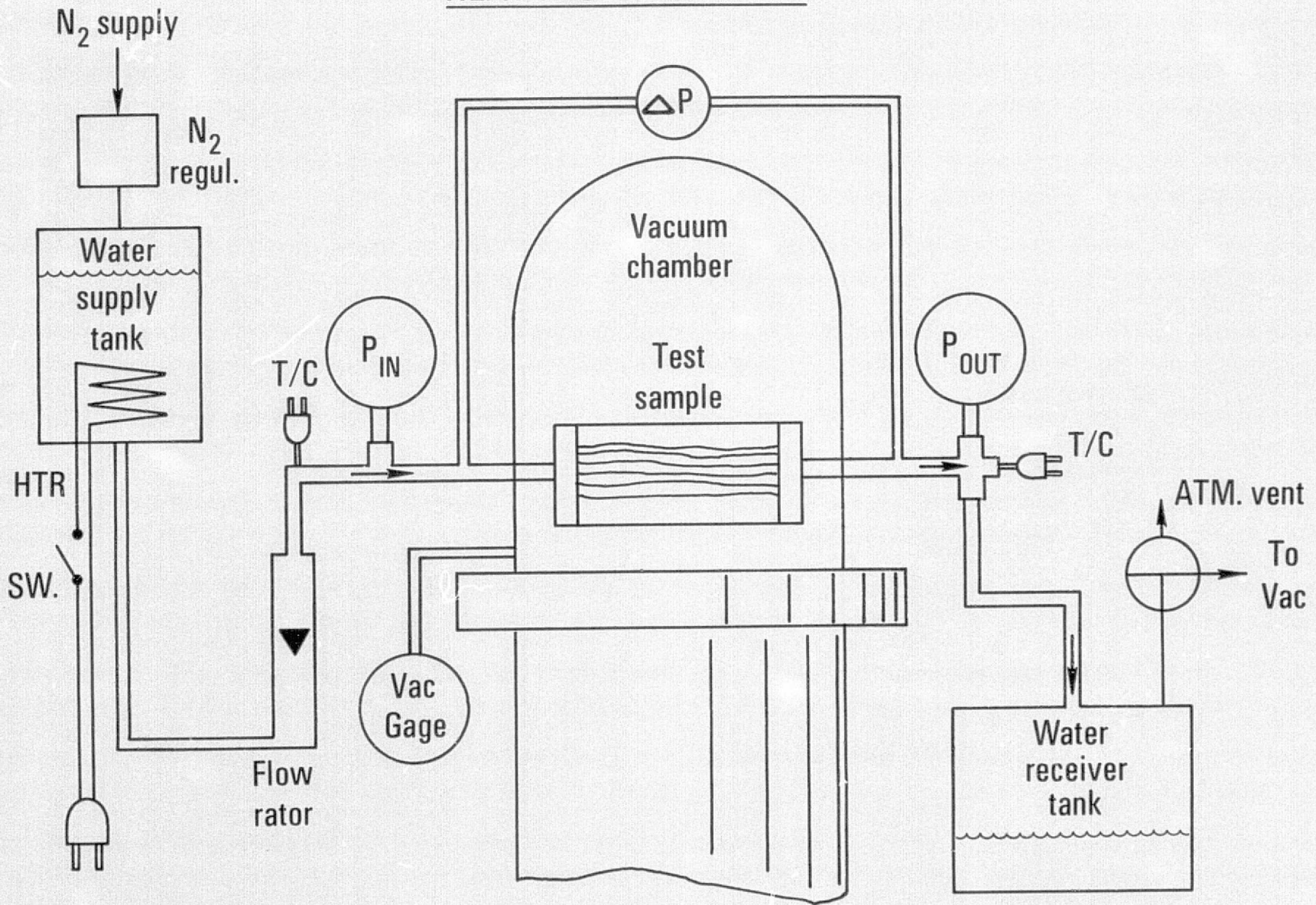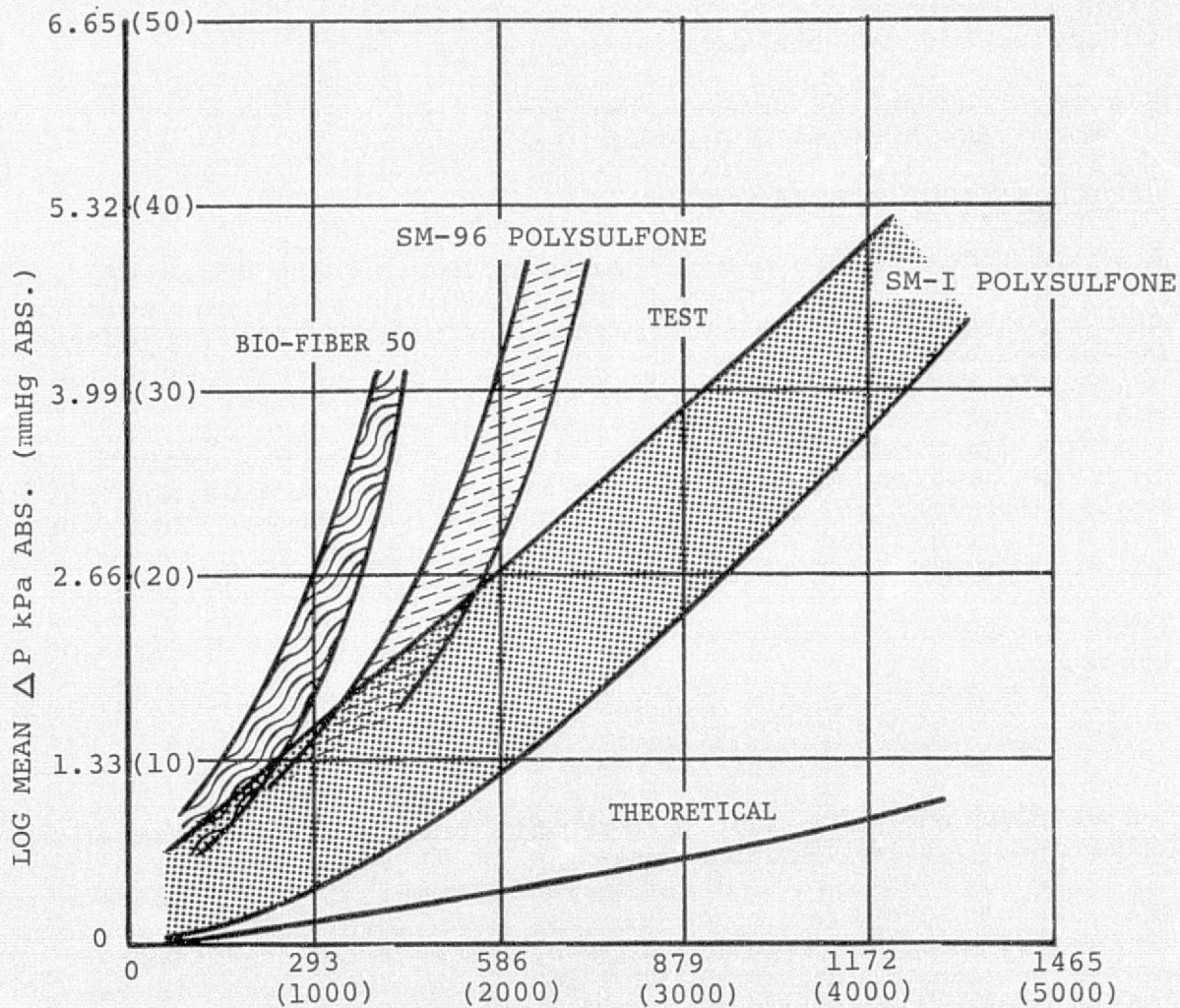
FIGURE 15

HEAT REJECTION Q~W (BTU/HR)

H.F.M. HEAT REJECTION PERFORMANCE

FIGURE 16

Two additional SM-I polysulfone modules were manufactured with the membranes "fluffed" to improve membrane separation and reduce back pressure. One of the modules was looser than the other and was designated L unit; the tighter one was designated T unit. Figure 17 presents this data which falls at the higher heat rejection side of the data of Figure 16.

Figure 18 shows the actual heat rejection test setups in Rig #8 of the Space Systems Department Laboratory.

BACTERIA/VIRUS FILTRATION

A scale model module was prepared containing the selected GM-80 acrylate material. Figure 19 describes the membrane device and shows photomicrographs of the sectioned hollow fiber membrane. Bacterial and viral retention testing was performed on the module using the test setup shown in Figure 20. Distilled water flux was measured using the test setup shown in Figure 11. Two retention tests were run. First, a bacteria mix was introduced into the dead ended inside diameter of the membranes and the permeate collected and cultured for bacteria content. Then the unit was sterilized, and a virus mix was introduced in the same manner and the permeate collected and cultured.

Table X summarizes the results of the Bacteria/Virus Filtration testing.

APPLICATIONS EVALUATION

For each of the five most practicable hollow fiber membrane applications, carbon dioxide removal, water vapor removal, deaeration, heat rejection, and bacteria filtration, a set of requirements and a subsystem schematic has been generated for a potential PLSS application. The test data obtained from the previous section has been evaluated, the most favorable membrane materials for each application have been discussed, and a suitability summary prepared.

CARBON DIOXIDE REMOVAL

The following requirements have been established for a PLSS CO_2 removal subsystem:

CO_2 Removal Rate	0.18 kg/hr (0.4 lb/hr)
Ventilation Loop CO_2 Partial Pressure	1.0 kPa (7.6 mmHg) max
Ventilation Flow	0.168 m^3/min (6.0 acfm)
Pressure Drop	0.25 kPa (1.0 in H_2O)

SM-I POLYSULFONE

AREA: 300 cm^2

X - L UNIT

O - T UNIT

TEST DATE: 4-30-76

FIGURE 17: LN $\triangle$ PH$_2$O VS. HEAT REJECTION

BELL JAR AND SCREEN

HOLLOW FIBER MEMBRANE
TEST MODULE
(INSIDE BELL JAR)

RIG #8 VACUUM CHAMBER

WATER SUPPLY TANK

SS 12285-4
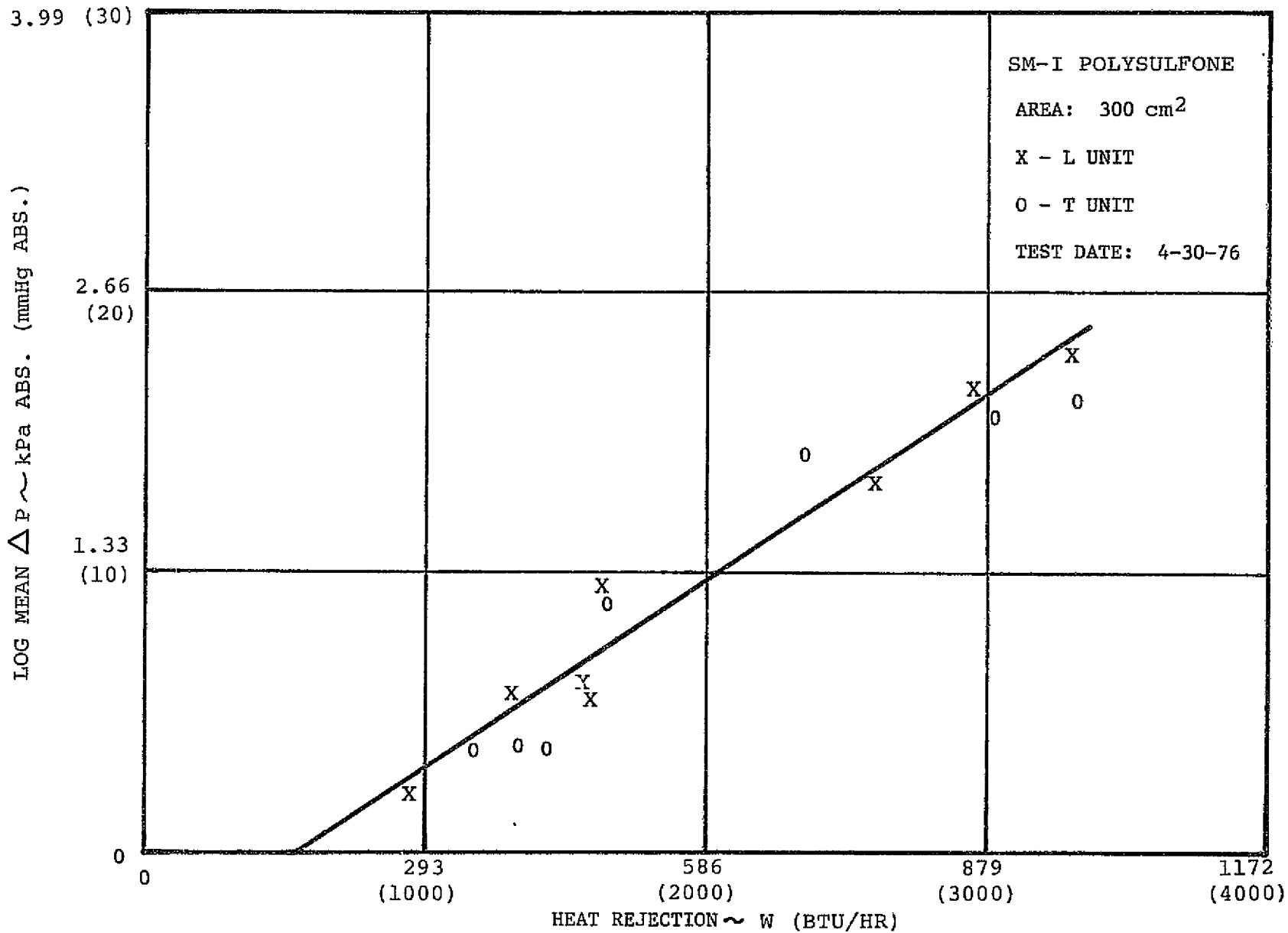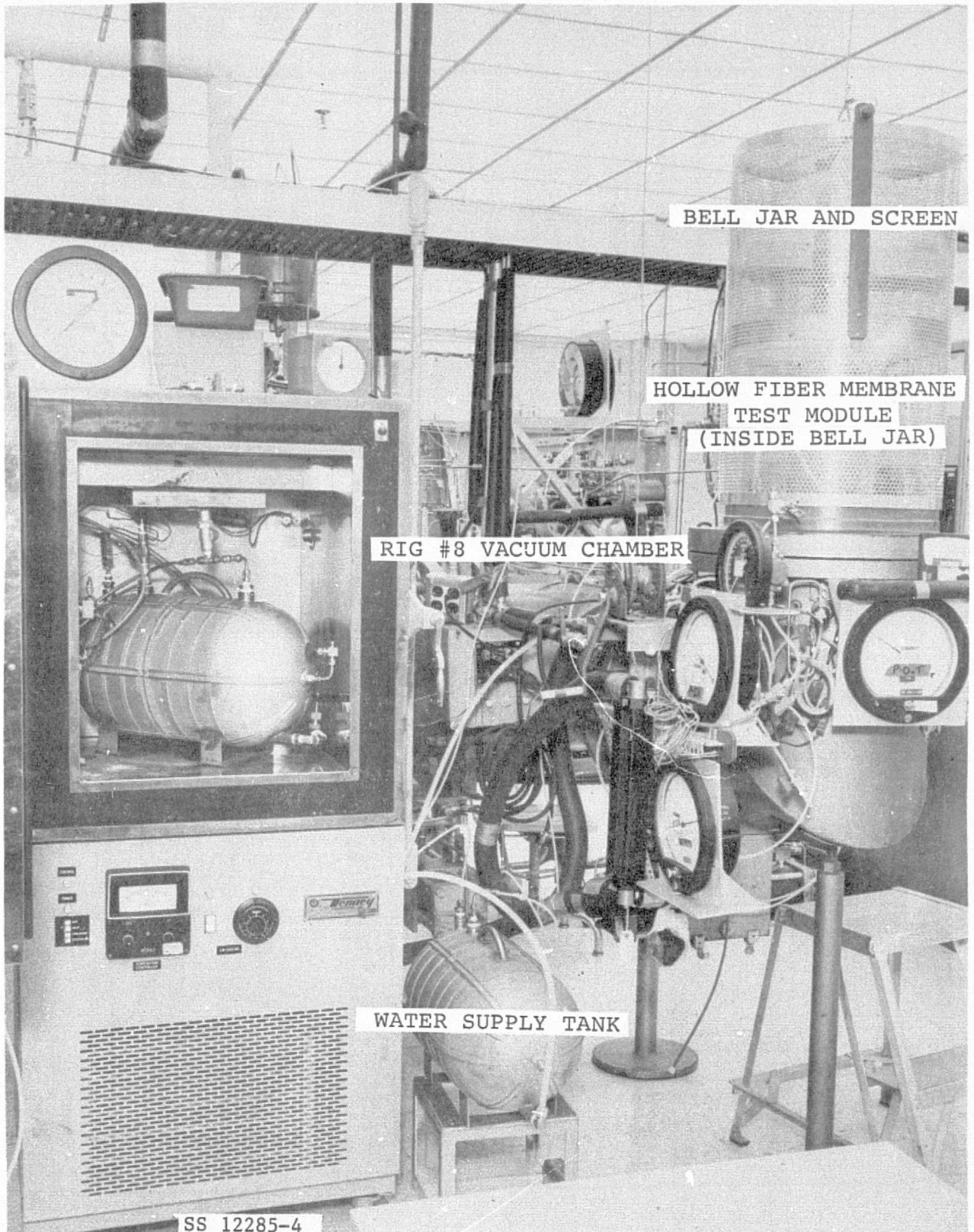
FIGURE 18   HEAT REJECTION TEST SETUP - RIG #8

50X
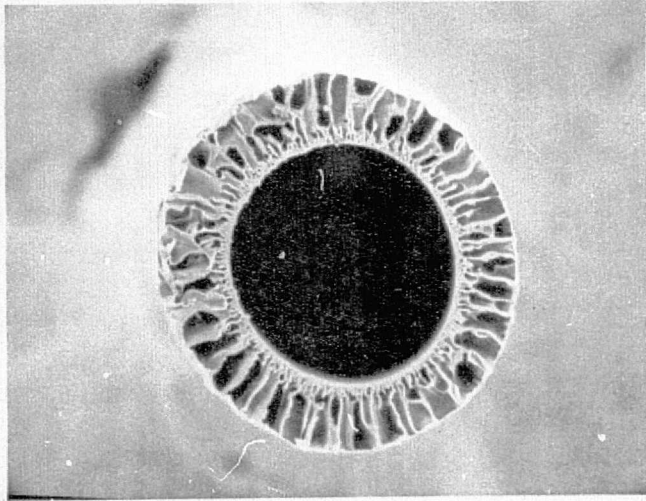
400X

MEMBRANE CHARACTERISTICS

- "GM-80" FROM ROMICON
- ANISOTROPIC STRUCTURE
- ACRYLATE MATERIAL
- 20-MIL ID

DEVICE CHARACTERISTICS

- 175 FIBERS
- 3.5 INCHES ACTIVE LENGTH
- 5 INCHES TOTAL LENGTH
- 250 CM^2 AREA FOR TRANSPORT
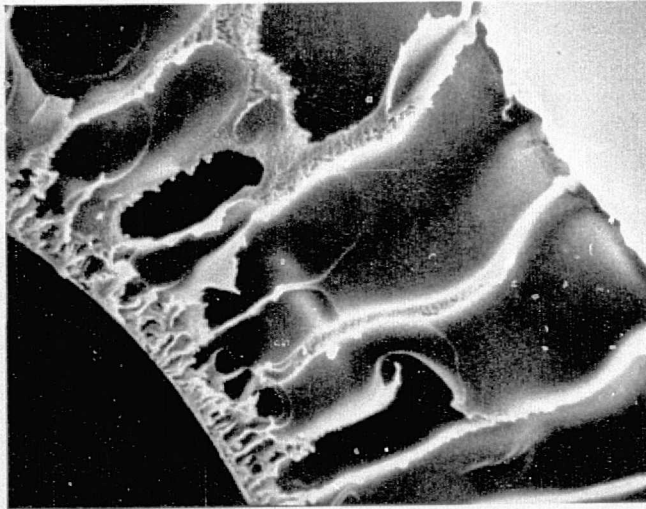
FIGURE 19 GN—80 MEMBRANE FOR BACTERIA REJECTION

SS 12983-8

Reservoir

Injection
Port

Hollow Fiber
Module

Dead Ended

Valve

Sample
Collection
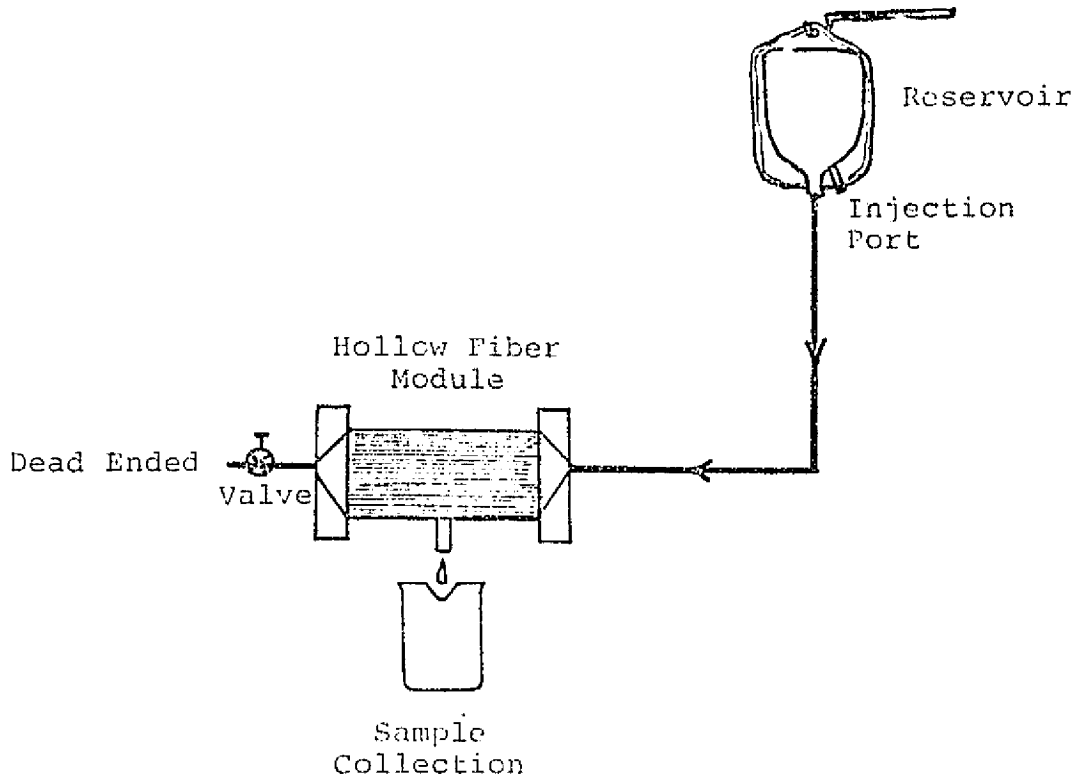
BACTERIAL AND VIRAL RETENTION TEST CONFIGURATION

FIGURE 20

TEST: Distilled Water Flux @ 20.7 kPa (3 psi)

   Results: Permeation of 140 cm^3/min @ area of 250 cm^2 or
   27 g/min-kPa-m^2 (23 lb/hr-ft^2-psi)

TEST: Bacterial Retention

Agent	ATCC No.	Colony Counts per cm^3 in Duplicate Culture	
		Challenge Fluid (upstream)	Ultrafiltrate (downstream)
Pseudomonas aeruginosa	9721	10^6	0
Escherichia coli	25922	10^6	0
Staphylococcus aureus	12600	10^6	0
Streptococcus pyrogens	10389	10^6	0
Klebsiella	23357	10^6	0
Proteus vulgaris	6380	10^6	0
Salmonella typhosa	13311	10^6	0

TEST: Viral Retention

Agent*	VR No.	Plaque Counts per cm^3 in Duplicate Culture	
		Challenge Fluid (upstream)	Ultrafiltrate (downstream)
Coxsackie virus A4	27	10^4	0
Echo Virus #2	32	10^4	0
Adenovirus-human type	1	10^4	0
Herpes Simplex	539	10^4	0
Vacinnia	118	10^4	0

*All viruses passed by 0.2µ "absolute" microporous filters. Viruses
were cultured in tissue cells. Retention @ 10,000 organisms/cm^3.

Figure 21 shows a schematic for a PLSS CO_2 removal subsystem when CO_2 is removed by subjecting the membrane outside diameters to a gas stream with low CO_2 partial pressure which in the PLSS case is vacuum. Suitable membrane selectivities of 25 or greater (CO_2 flux divided by N_2 flux) were obtained, but the projected CO_2 flux (removal rate) at 1.0 kPa (7.6 mmHg) was so low for the best membranes that a prohibitively large membrane area of 2,402 square meters or 60,000 units of the size tested, would be required to obtain the PLSS CO_2 removal rate of 0.18 kg/hr (0.4 lb/hr). Following is a summary of CO_2 partial pressure capabilities:

> CO_2 removal with competitive O_2 loss.
> Satisfactory CO_2 partial pressure capability.
> No back pressure regulator required.
> Prohibitively large membrane area, 2,402 m^2 (60,000 units
>   of the size tested) required to obtain PLSS CO_2 removal
>   of 0.18 kg/hr (0.4 lb/hr).

This concept has not been recommended for further evaluation.

WATER VAPOR REMOVAL

The following requirements have been established for a PLSS water vapor removal subsystem:

Water Vapor Removal Rate	0.204 kg/hr (0.45 lb/hr)
Outlet Dew Point	15.6°C max (60°F max)
Ventilation Flow	0.168 m^3/min (6.0 acfm)
Pressure Drop	0.075 kPa (0.3 in H2O)

Figure 22 shows a schematic for a PLSS water vapor removal subsystem where water vapor is removed by subjecting the membrane outside diameter to a gas stream with low water vapor partial pressure which in the PLSS case is vacuum. Water vapor removal with immeasurable gas loss was obtained with each of the acrylic XM cartridges, but the water vapor flux (removal rate) was extremely low. In order to obtain a typical PLSS removal rate of 0.204 kg/hr (0.45 lb/hr), a membrane area of 28 square meters, equivalent to 487 cartridges of the size testing, will be required. This size is prohibitive. Following is a summary of water vapor removal capabilities:

> Water vapor removal with negligible O_2 loss.
> Satisfactory outlet dew point capability.
> No back pressure regulator required.
> Prohibitively large membrane area, 28 m^2 (487 units of
>   the size tested) required to obtain PLSS removal rate
>   of 0.204 kg/hr (0.45 lb/hr).

This concept has not been recommended for further consideration.

PLSS H.F.M. CO_2 REJECTION SUBSYSTEM

VACUUM

$CO_2 + O_2 + H_2O$

$O_2 + CO_2 + H_2O$ → MEMBRANE SEPARATOR → $O_2 + H_2O$
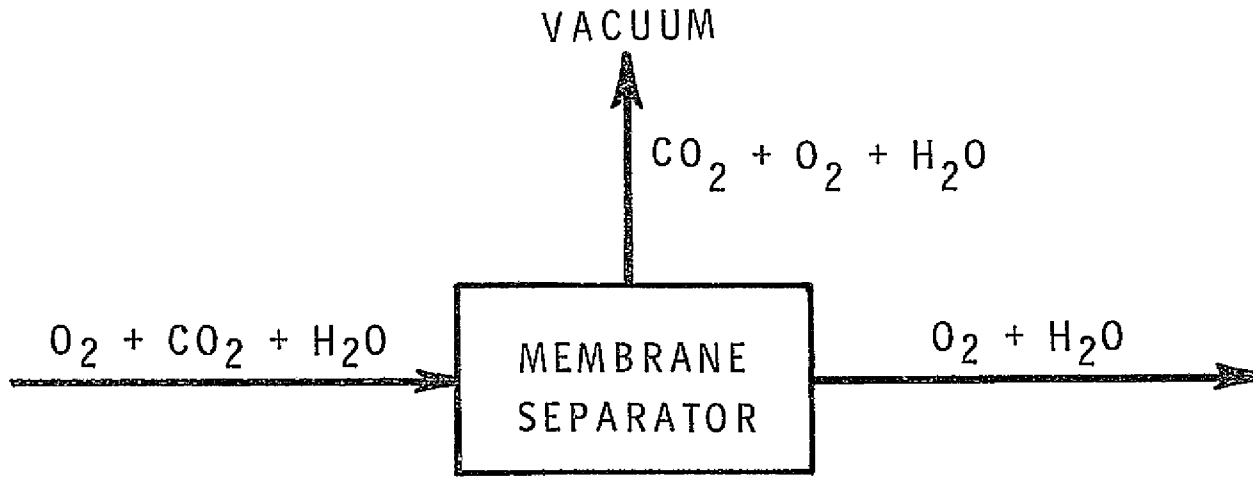
FIGURE 21

PLSS H.F.M. WATER VAPOR REMOVAL SUBSYSTEM

Vacuum

H_2O

D.P. = 18.3 - 32.2^{0}C

Vent Loop

Membrane
Subsystem

D.P. = 15.6^{0}C (60^{0}F)
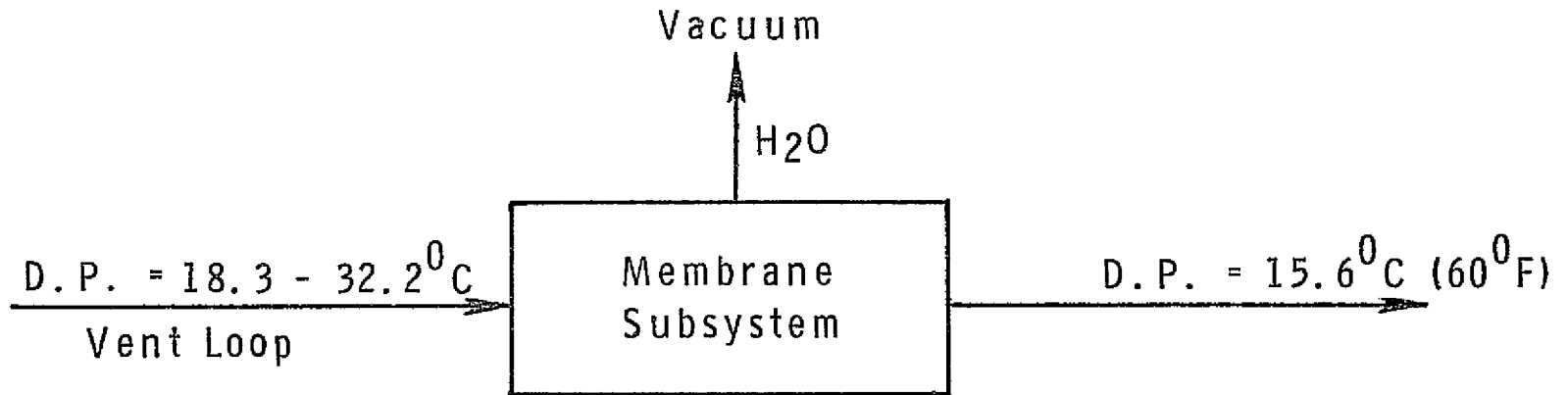
FIGURE 22

DEAERATION

The following requirements have been established for a PLSS
deaeration subsystem:

<table>
<tr><td>Undissolved Gas Removal</td><td>Complete Removal</td></tr>
<tr><td>Dissolved Gas Removal</td><td>23.1 kPa (3.35 psi)
Partial Pressure at 4.4°C (40°F)</td></tr>
<tr><td>Water Flow</td><td>18.1 kg/hr (40 lb/hr)</td></tr>
<tr><td>Water Pressure</td><td>68.9 kPa (10 psi) nominal</td></tr>
<tr><td>Water Temperature</td><td>4.4°C – 37.8°C (40°F – 100°F)</td></tr>
<tr><td>Pressure Drop</td><td>3.44 kPa (5 psi) maximum</td></tr>
</table>

Figure 23 shows a schematic for a PLSS deaeration subsystem
where dissolved and undissolved gas is removed by subjecting the
membrane outside diameters to a controlled low pressure.

Liquid water fluxes (permeation) of all the membranes are satis-
factorily low to obtain deaeration with insignificant cooling
(heat rejection). Testing to measure undissolved nitrogen re-
moval and dissolved oxygen removal was performed at a water inlet
temperature of 27.2°C (81°F) and a chamber pressure of approxi-
mately 6.65 kPa (50 mmHg) to minimize interactions from heat
rejection effects that would result at lower chamber pressures.
Good gas removal was achieved in both cases with both polysulfone
units. A potential PLSS application for water tank fill water
deaeration could be satisfied with one membrane cartridge of the
size tested.

Following is a summary of deaeration capabilities:

> Satisfactory removal of undissolved N_2.
> Superior removal of dissolved O_2.
> Satisfactory O_2 saturation pressure level capability.
> Competitive membrane area, 0.085 m^2 (one unit of the size
>   tested) required to obtain PLSS water tank fill water
>   saturation pressure of 23.1 kPa abs. (3.35 psia).

The size of a hollow fiber membrane unit for undissolved gas
removal is significantly larger than conventional screen-type
separators. Therefore, undissolved gas removal by hollow fiber
membranes is not competitive and has not been recommended for
further evaluation.

Dissolved gas removal by hollow fiber membranes appears to be
superior to existing methods and has been recommended for further
evaluation.

FIGURE 23. PLSS HFM DEAERATION SUBSYSTEM

Low press. O$_2$

Back press cont'l → VAC

Shuttle water tank

De-aerator

Water S.O.

Disconnect

Water tank

Water to LCG & heat sink

Shuttle
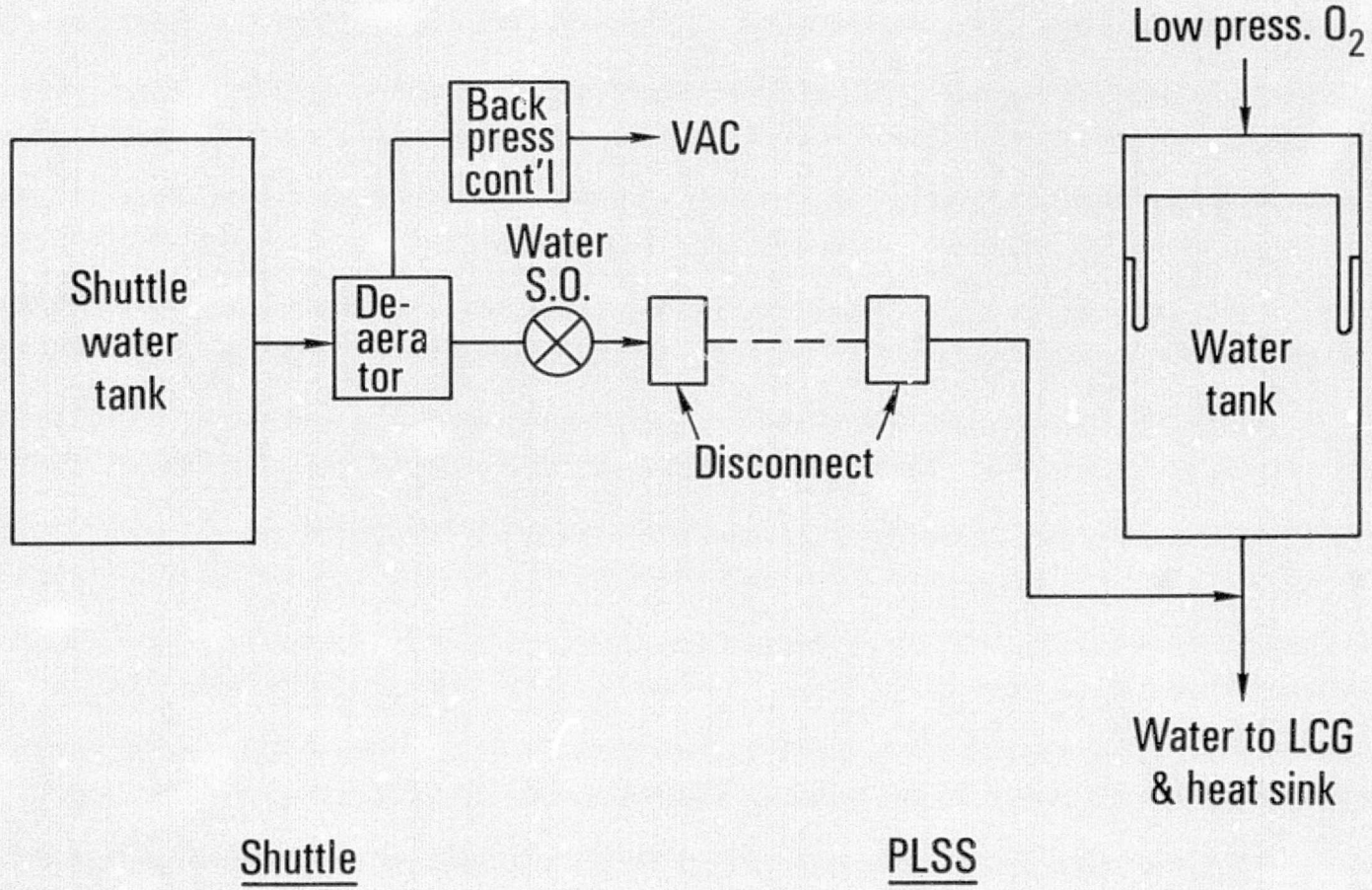
PLSS

HEAT REJECTION

The following requirements have been established for a PLSS heat rejection subsystem:

Coolant Flow	108.9 kg/hr (240 lb/hr)
Evaporant Flow	1.36 kg/hr (3 lb/hr) max
Unit Pressure Drop	4.8 kPa (0.7 psi) max
Coolant Outlet Temperature	11.4°C (52.5°F) max
Coolant Pressure	25.1-62.4 kPa (3.65-9.05 psi)
Heat Rejection	879 W (3,000 Btu/hr) max

Figure 24 shows a schematic for a PLSS heat rejection subsystem where heat is removed by subjecting the membrane outside diameters to a controlled low pressure and allowing water from the membrane inside diameter to permeate through the membrane wall and vaporize. Liquid permeation rates are satisfactorily low. Vacuum chamber testing to measure heat rejection rates was performed with membrane water inlet temperatures ranging from 18.3°C to 41.7°C (65°F to 107°F), water flow rate ranging from 11.3 to 113 kg/hr (25 to 250 lbs/hr), and chamber pressure ranging from 0.73 to 1.20 kPa (5.5 to 9 mmHg). The Gore-Tex membrane proved to be nonporous to water vapor and failed to reject heat under any of the test conditions. The Bio-Fiber 50 and each of the polysulfone membranes exhibited good heat rejection capabilities for all test conditions, with the SM-I polysulfone "fluffed" units being superior. A graph of heat rejection versus log mean ΔP (difference between mean saturation presssure in the water flowing through the membranes and the chamber pressure) is shown in Figure 16. A theoretical maximum performance line that represents 100% effectivity is included on the curve for reference.

One SM-96 polysulfone and one SM-I polysulfone unit was run at a chamber pressure of 0.27 kPa (2.0 mmHg) (below the triplepoint pressure). The SM-96 unit performed satisfactorily, but the SM-I unit ruptured two membranes. It is important to realize that a back pressure regulator will be required for the units as they now exist.

Following is a summary of heat rejection capabilities:

Superior heat rejection capability.
Competitive membrane area, 0.082 m^2 (2.7 units of the size tested) required to obtain PLSS heat rejection rate of 879 W (3,000 Btu/hr).
Back pressure regulator required.

Heat rejection by hollow fiber membranes appears to be competitive with existing methods and has been recommended for further evaluation.

FIGURE 24. PLSS H.F.M. HEAT REJECTION SUBSYSTEM

Vacuum

Back press.
regulator

From LCG

Membrane
evaporator

3000 Btu/Hr

Humidity
control HX
600 Btu/Hr

To LCG

Water press.
control

Vent
loop

H_2O
make-up
tank
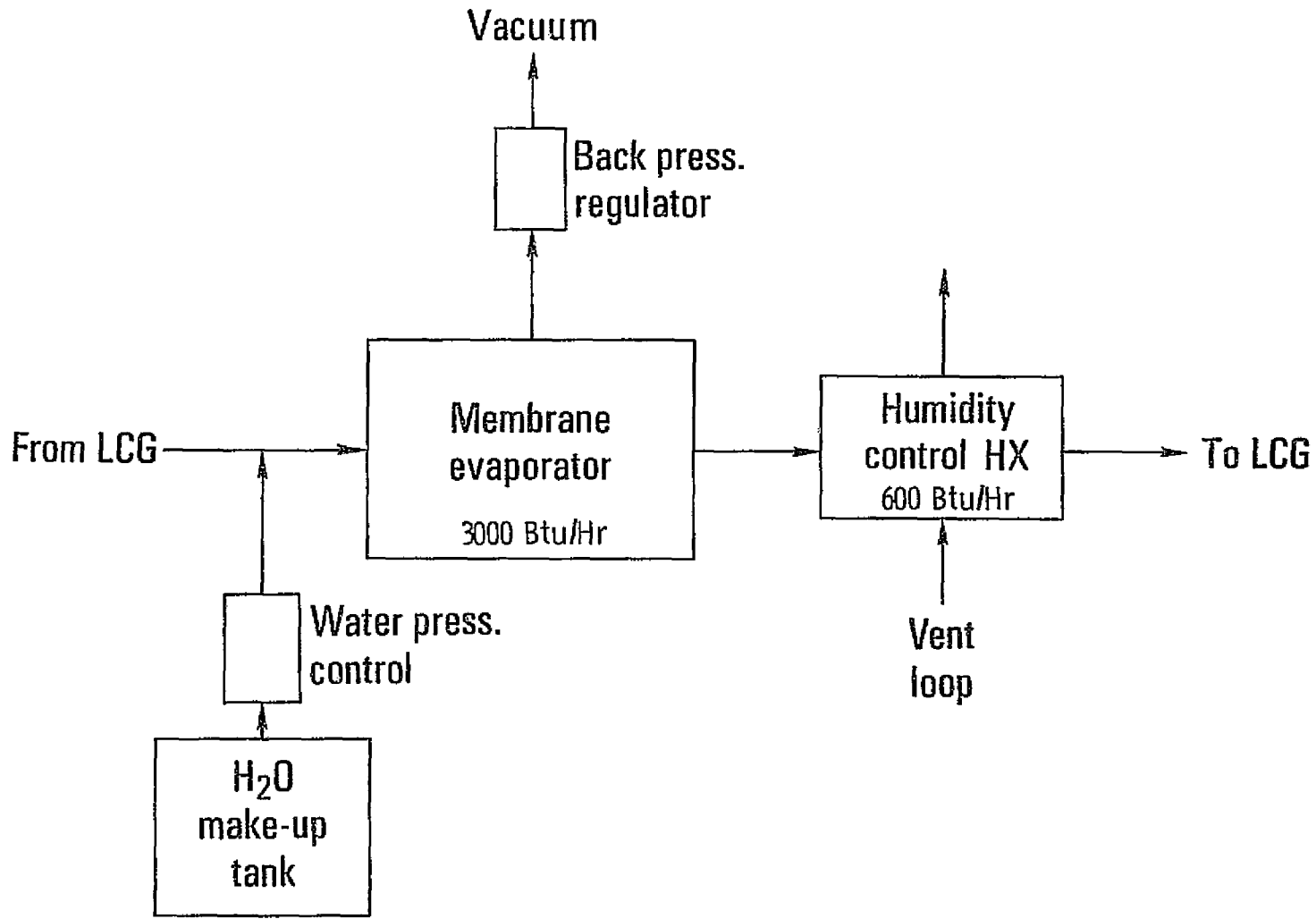
BACTERIA/VIRUS FILTRATION

The following requirements have been established for a PLSS
bacteria filter:

Filtration	100% Bacterial Retention
Fluid Flow	18.1 kg/hr (40 lb/hr)
Unit Pressure Drop	34.4 kPa (5 psi) max
Fluid Temperature	4.4°C-37.8°C (40°F-100°F)

Figure 25 shows a schematic for a PLSS bacteria filtration sub-
system where bacteria is retained within the hollow fiber mem-
branes when the potentially contaminated water stream is passed
through the membrane walls. Absolute bacteria filtration and
absolute virus filtration was obtained for a short term exposure.
Long term bacteria and virus exposure was not studied as it was
beyond the scope of this program. Following is a summary of
bacteria/virus filtration capabilities:

> Absolute bacteria filtration utilizing 10^6 colony counts
> per cubic centimeter.
> Absolute viral filtration utilizing 10^4 plaque counts per
> cubic centimeter.
> Competitive membrane area, 0.036 m^2 (1.5 units of the size
> tested) required to obtain PLSS water tank fill water
> protection.

Bacteria/virus filtration by hollow fiber membranes appears to be
superior to existing methods and has been recommended for further
evaluation.

APPLICATIONS SELECTION

Based on the results of the applications study and materials
testing described in the previous paragraphs of this section, the
following hollow fiber membrane applications have been selected
for further evaluation:

> I.   Water Deaeration
> II. Heat Rejection
> III. Bacteria Filtration

FIGURE 25. PLSS BACTERIA FILTER SUBSYSTEM

High press O$_2$

Press regul

Shuttle water tank

H.F.M. cartridge

Disconnect

Water S.O.

Water tank

H$_2$O press regulator

Shuttle

PLSS

Water to LCG. & heat sink
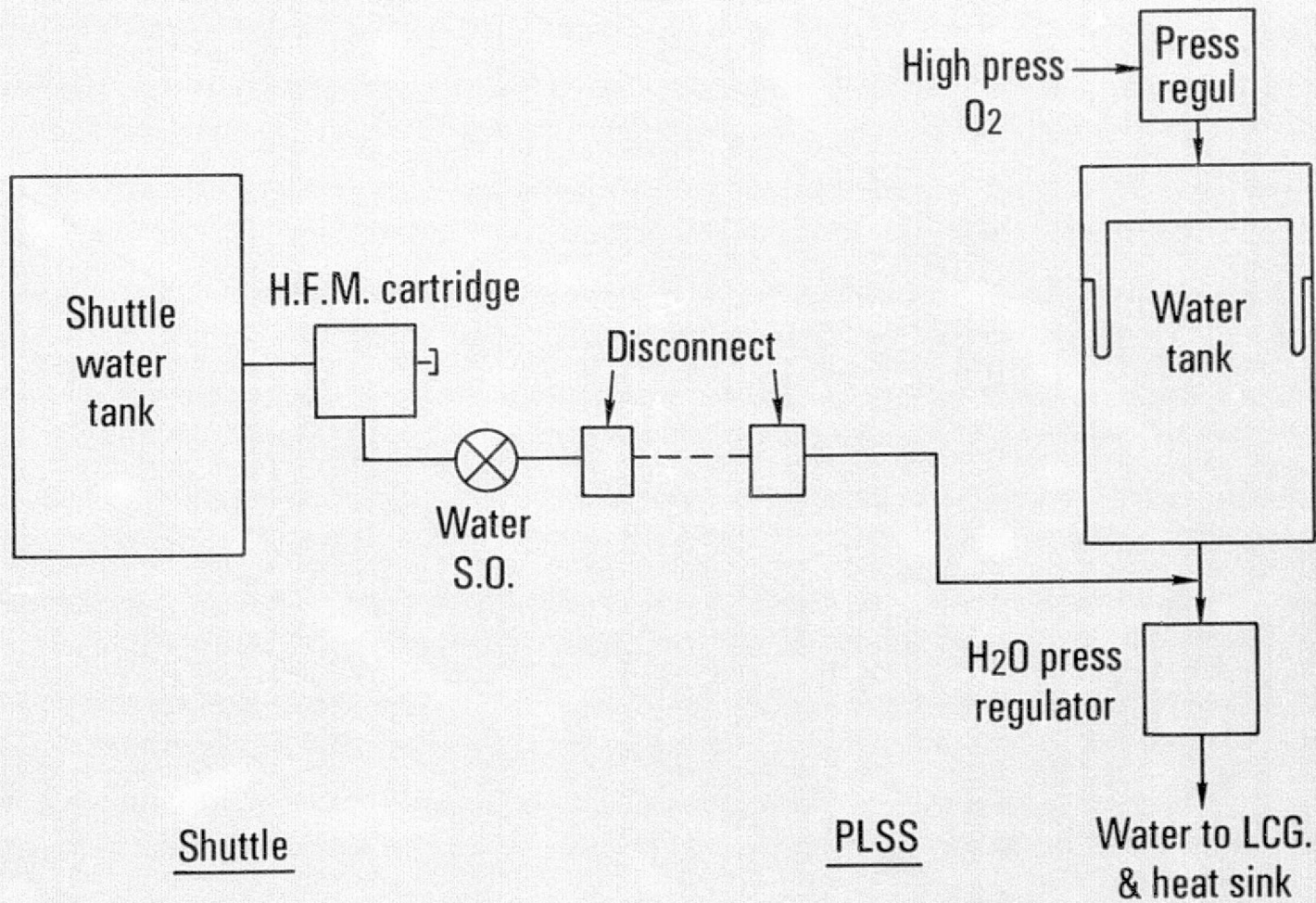
BREADBOARD DESIGN AND FABRICATION

PERFORMANCE ANALYSIS AND TRADE-OFF STUDIES

Application feasibility testing showed potential application in the areas of Bacteria Filtration, Heat Rejection, and Water Deaeration. Material development will be required before CO_2 removal can be considered.

Analysis effort has been accomplished to correlate the test data, size assemblies for Shuttle PLSS application, and perform a trade-off study against existing concepts. Areas for development where potential performance improvement can reasonably be anticipated are defined.

MEMBRANE CONFIGURATION

The predominant effort to correlate performance to membrane configuration has been centered around the Amicon SM-I and SM-96 anisotropic structure polysulfone fibers. These assemblies are characterized as follows:

	SM-I	SM-96
Fiber I.D., cm (in)	0.051 (0.020)	0.02 (0.008)
Number of Fibers	200	1500
Total Fiber Length, cm (in)	12.7 (5)	12.7 (5)
Active Fiber Length, cm (in)	8.9 (3.5)	8.9 (3.5)
Transport Area (I.D.), cm^2	300	850
Total Wall Thickness cm (mils)	0.009-0.013 (3.6-5.0)	0.004-0.005 (1.6-2.0)
Inner Wall:		
Thickness, micron	0.1-0.5	0.1-0.5
Fraction Open Area	0.005-0.05	0.005-0.05
Pore Size, Å	10-30	10-30
Outer Wall:		
Fraction Open Area	.45-.65	.45-.65
Pore Size, micron	1.0-3.0	1.0-3.0

All evaluation of membrane processes reported herein are based on average dimensional values where ranges have been provided by the manufacturer.

THEORETICAL RELATIONSHIPS

Liquid Transport

Laminar Flow – For a steady flow of Newtonian fluid in a tube of uniform diameter, the laminar pressure loss is described by the Hagen-Poiseuille relationship:

$$\Delta P = 3.4 \times 10^{-5} \quad \frac{\mu \ L \dot{W}}{d^4 \rho} \quad *$$

Turbulent Flow – In smooth pipe of constant diameter and of Reynolds numbers above 1,000 to 3,000, a transition to turbulent flow occurs and may be characterized by the Fanning equation:

$$\Delta P = 3.36 \times 10^{-6} \quad \frac{f \ L \dot{W}^2}{d^5 \rho}$$

Capillary Pressure Rise (Wicking) – The capillary pressure rise of water through hydrophilic materials may be estimated as follows assuming a zero contact angle:

$$\Delta P = (1.4 \times 10^{-5}) \quad \frac{2 \sigma}{r}$$

Liquid flow through the membrane system may be evaluated against these three relationships to determine the nature of the dominant process and thus permit extrapolation of the acquired data. Of primary interest are the following factors:

- Hydrostatic pressure loss for laminar flow is a linear function of flow rate.

- Hydrostatic pressure loss for turbulent flow varies with the square of flow rate.

- Capillary forces can dominate the available hydrostatic head and be the principal factor enhancing fluid flow through a porous structure. This flow will be independent of hydrostatic head.

Gas Transport

Knudson Diffusion – When the mean free path (the average distance a molecule travels before it collides with another molecule) is large compared to the pore diameter, collisions between the molecule and the wall affect the mass transport, and the phenomenum is termed Knudson diffusion. The following equations describe this process:

$$N_A = \frac{D_k}{RT \ell} \quad (P_1 - P_2)$$

$$D_k = 9,700 \quad \bar{r} \left(\frac{T}{M}\right)^{1/2}$$

$$G = 0.077 \quad \frac{\bar{r}}{R} \left(\frac{M}{T}\right)^{1/2} \quad (P_1 - P_2)$$

*Refer to Definition of Units at the end of this section.

Molecular Diffusion - When the pore diameter is very large compared to the mean free path, the steady state diffusion of one gas through a stationary layer of a second, non-diffusing gas is described by:

$$N_A = \frac{D_{AB}P}{RT\ell} \ln \left(\frac{1-X_{A2}}{1-X_{A1}} \right)$$

$$G = 7.94 \frac{D_{AB}PM}{RT\ell} \ln \left(\frac{1-X_{A2}}{1-X_{A1}} \right)$$

Typical diffusivities D_{AB} are shown in Table XI.

Laminar and Turbulent Flow - These processes are described by the relationships previously presented for liquid transport.

Diffusion through a Liquid - For dilute solutions the diffusion of specie A through stagnant B is described by:

$$N_A = \frac{D_{AB} \, C_{avg}}{\ell} \ln \left(\frac{1-X_{A2}}{1-X_{A1}} \right)$$

$$D_{AB} = \frac{14.0 \times 10^{-5}}{\mu_B^{1.1} \, V_A^{0.6}}$$

$$G = \frac{8.82 \times 10^{-3} \, c_{avg}}{\ell \, \mu_B^{1.1} \, V_A^{0.6}} \ln \left(\frac{1-X_{A2}}{1-X_{A1}} \right)$$

Absorption or Reaction Rate - In a process system involving chemical reaction and/or absorption (or desorption), the rate controlling step may not be diffusion but the actual rate of reaction or rate of absorption. These rates are not amenable to basic theoretical determination and must be derived from empirical results. Where information is available from the literature, it can be applied to the membrane separation processes to determine its potential as a rate controlling step.

Energy Transport

Heat Transfer Area - Although the nominal membrane transport area (i.e., 300 cm^2 for the Amicon SM-I) would normally be considered the heat transfer area, the system may be dominated by the distribution of pores in the inner wall. Total pore opening comprises only 1/2 to 5% of the total surface, and poor distribution would not distribute evaporant uniformly along the total tube surface, thus leaving only isolated points for heat transfer between the flowing fluid and the evaporant. Where energy transport is considered to be the limiting factor in a membrane process, the potential ineffective use of the available surface area must be noted.

TABLE XI

DIFFUSION COEFFICIENTS OF GASES
AND VAPORS IN AIR AT 25°C, 1 ATM

Substance	D, cm²/sec	$(\mu/\rho D)$
Ammonia	0.229	0.67
Carbon Dioxide	.104	.94
Hydrogen	.410	.22
Oxygen	.206	.75
Water	.256	.60
Carbon Disulfide	.107	1.45
Ethyl Ether	.093	1.66
Methanol	.159	0.97
Ethyl Alcohol	.119	1.30
Propyl Alcohol	.100	1.55
Butyl Alcohol	.090	1.72
Amyl Alcohol	.070	2.21
Hexyl Alcohol	.059	2.60
Formic Acid	.159	0.97
Acetic Acid	.133	1.16
Propionic Acid	.099	1.56
i-Butyric Acid	.081	1.91
Valeric Acid	.067	2.31
i-Caproic Acid	.060	2.58
Diethyl Amine	.105	1.47
Butyl Amine	.101	1.53
Aniline	.072	2.14
Chloro Benzene	.073	2.12
Chloro Toluene	.065	2.38
Propyl Bromide	.105	1.47
Propyl Iodide	.096	1.61
Benzene	.088	1.76
Toluene	.084	1.84
Xylene	.071	2.18
Ethyl Benzene	.077	2.01
Propyl Benzene	.059	2.62
Diphenyl	.068	2.28
n-Octane	.060	2.58
Mesitylene	.067	2.31

References: "International Critical Tables,"
vol. 5, 1928; Landolt-Bornstein, "Physikalische-
Chemische Tabellen," 1935.

Note: The group $(\mu/\rho D)$ in the above table is
evaluated for mixtures composed largely of air.

Wall Thermal Conductance - In the inner wall the available conductance is primarily through the membrane which comprises 95% or more of the structure. In the outer wall the membrane only occupies 35 to 55% of the volume, and conductance through the fluid in the remaining volume is added to the membrane conductance. Heat transport through the wall is governed by:

Inner Wall

$$Q = \left(\frac{kA}{\Delta L}\right)_{membrane} (t_h - t_c)$$

Outer Wall

$$Q = \left[\left(\frac{kA}{\Delta L}\right)_{membrane} + \left(\frac{kA}{\Delta L}\right)_{fluid} \right] (t_{hot} - t_{cold})$$

Liquid Film Thermal Conductance - In laminar flow inside a tube, assuming a parabolic velocity profile, the following equation describes the liquid film thermal conductance for values of the Graetz number above 10:

$$N_{GZ} = \frac{\dot{W}C_p}{kL}$$

$$h = 21 \frac{k}{d} (N_{GZ})^{1/3}$$

DATA CORRELATION

Tube Side Pressure Drop

Data for the Amicon SM-I and SM-96 are shown in Figures 26 and 27. The laminar model describes flow through the 0.02 cm (0.008 in) I.D. fibers over the full flow range tested. This model must be factored upwards (by approximately 1.5) to correlate the higher data. Exact causes for the difference between the data are not known but are probably due to fiber nonuniformity. The cross section is not necessarily circular and can be somewhat oval, reducing effective diameter. An error in assumed fiber diameter of only 10% could also account for the difference. Entrance and exit effects and the slight curvature of the tube along the axis are small effects (less than 5%) and should not be the cause of the noted variation.

For the 0.051 cm (0.020 in) fiber the flow regime is turbulent above a Reynold's number of 100 and correlates:

$$\Delta P = f(\dot{W})^{1.6}$$
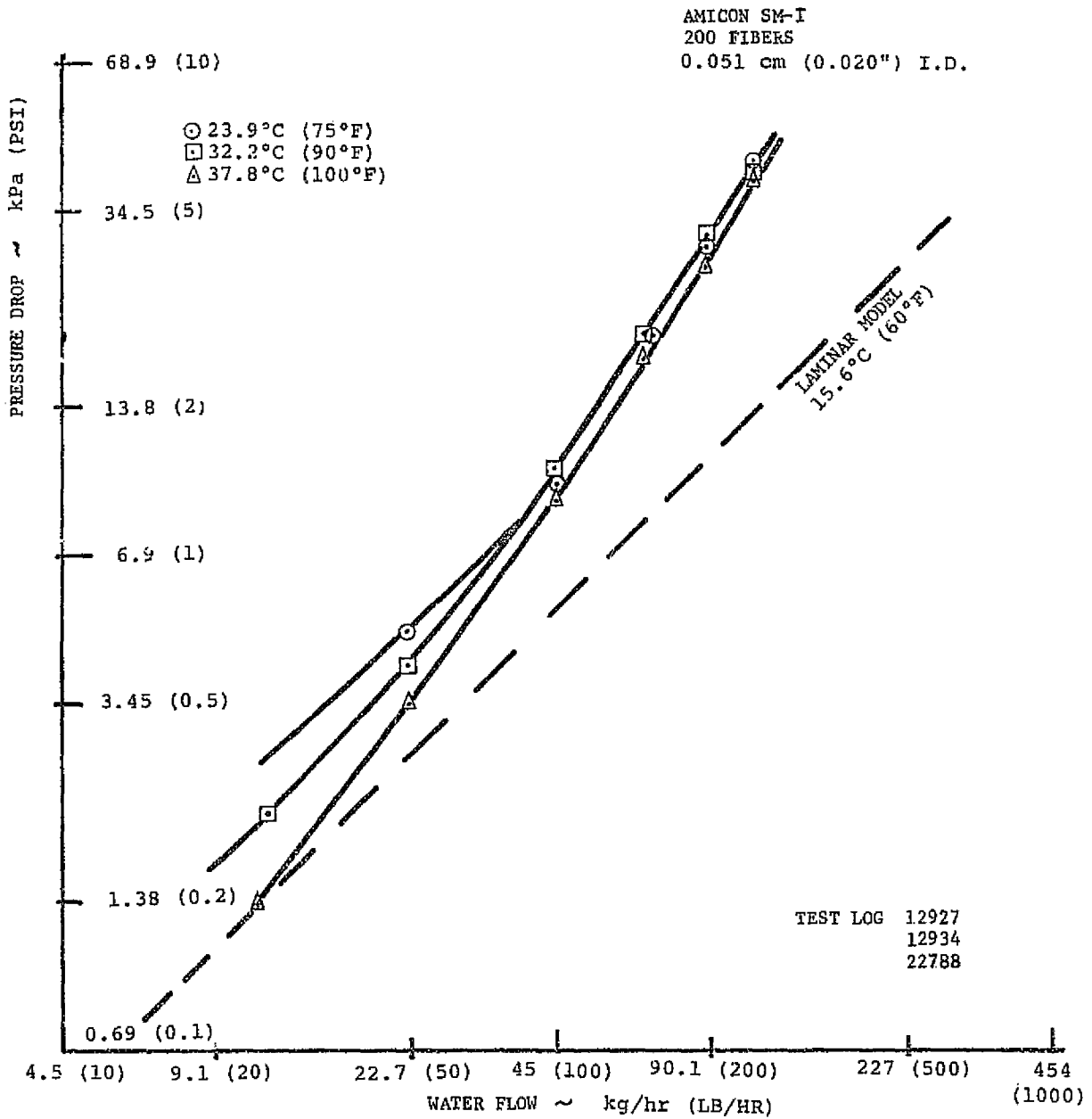
FIGURE 26 MEMBRANE TUBE SIDE PRESSURE DROP
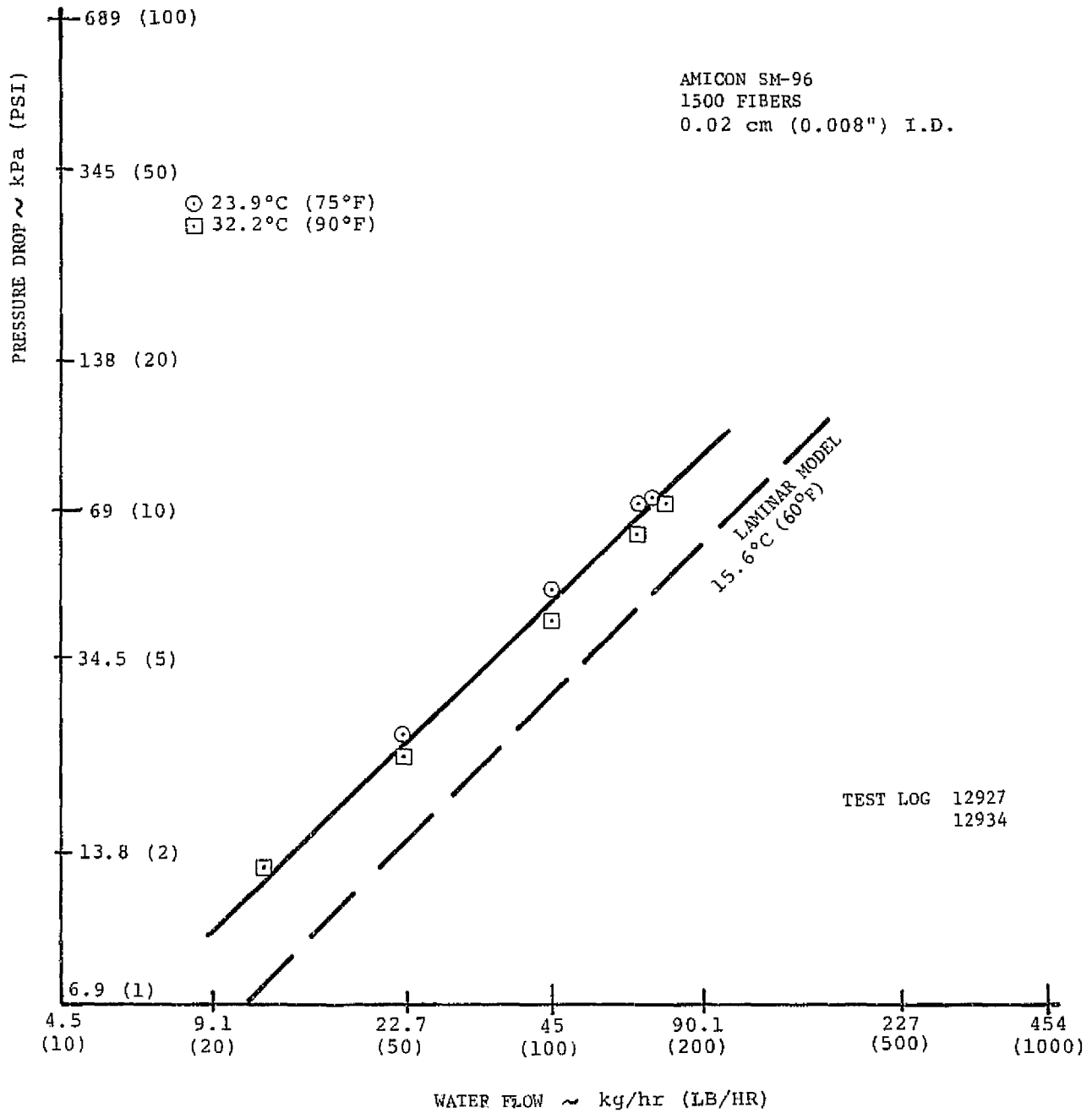
FIGURE 27 MEMBRANE TUBE SIDE PRESSURE DROP

rather than the 2.0 or 1.8 power expected. The flow below this range is transition and then laminar below a Reynold's number of 30. This early development of turbulent flow must be due to irregularities in the fiber I.D. disturbing the development of a laminar flow profile but not quite severe enough to produce fully turbulent flow. Some of this effect may also be present in the 0.02 cm (0.008") fiber but to a lesser extent.

The data and correlation are sufficient for sizing and extrapolation to meet development unit pressure drop requirements.

Transmembrane Flow

For those processes requiring transmembrane flow (bacteria retention, filtration), the flow versus hydrostatic pressure differential characteristic is of prime importance to unit sizing. Figure 28 presents data from typical Amicon SM-I and shows not only the linear flow versus ΔP relationship of laminar flow but also the variation due to the temperature effect on viscosity. Because of the complex and undefined nature of these flow passages, it is not recommended that forecast of performance be extrapolated from these data to new materials. A minimum of data should be sufficient, however, to extrapolate to a wide range of conditions. Also, because the device is an absolute surface filter, its pressure drop will vary with the volume of contaminant collected. The rate of pressure drop increase, which can be transposed into filter life, can only be predicted from knowledge of the contaminant level in the feed water. These values are yet to be defined for Shuttle systems.

Heat Rejection

Considerable effort was expended during the Applications phase to develop a correlation between the heat rejection test results and the assumed membrane transport processes. None really proved satisfactory. The primary basis for this investigation was the supposedly hydrophilic nature of the membrane material which leads to the assumption that the dominant process must be gas phase transfer. This process should correlate to gas ΔP; in this case the difference in water vapor pressure in the tube to chamber or tube O.D. pressure. In the outer shell, with a pressure difference of 2.7 kPa (200 mmHg), Knudson gaseous flow should be approximately 4.5 kg/hr (10 lb/hr), a value more than three times test results. In the inner shell mass flow for this same condition will not exceed 0.41 kg/hr (0.9 lb/hr) or a value one-third test results.
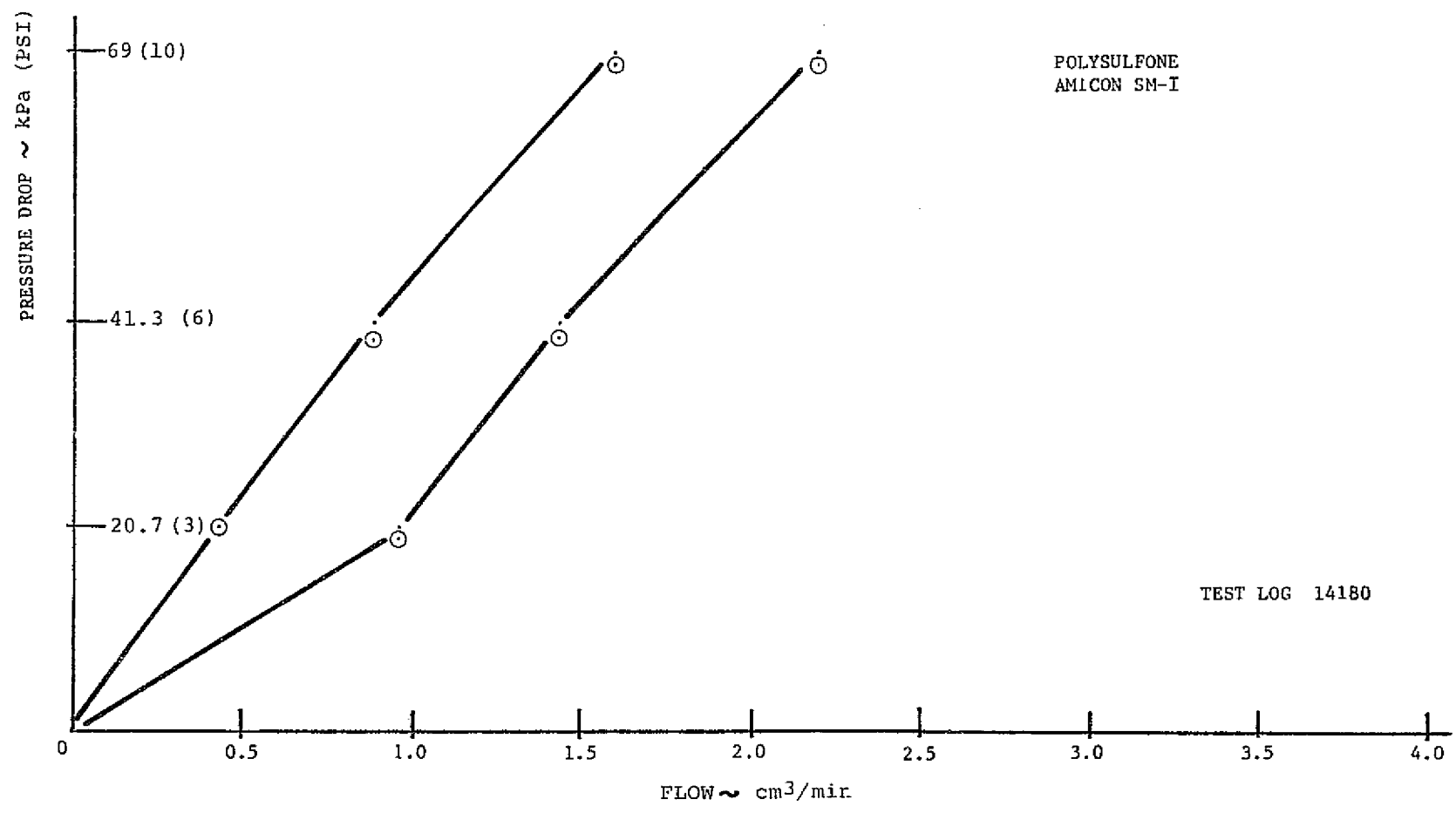
FIGURE 28 TRANS MEMBRANE HYDROSTATIC PRESSURE DROP

One other area was thought to be a controlling factor - shell side pressure drop. Two HFM 0.051 cm (20 mil) polysulfone, 300 cm², were tested in the heat rejection mode to determine the repeatability of these units' performance compared to performance acquired on the first unit. The newer assemblies were fabricated in an attempt to improve membrane to membrane separation. It was anticipated that this would result in a reduced shell side pressure loss and improved performance. Visual inspection of the two new assemblies indicated one had a fairly loose bundle appearance while the other was tight - similar to the first unit. The new units were designated 300-L (loose) and 300-T (tight). The results, shown in Figure 29, show no difference between the "loose" or "tight" bundle. These data generally confirm the previous results but at the higher limit (or slightly better) of the data spread giving indication that the "open bundle" has slightly improved performance.

In general, graphical analysis of data comparing performance, Q, to gas ΔP were inconclusive, and in some cases confusing, giving data trends opposite to that expected. Other means of correlation were sought. Hydrostatic liquid flow was considered but did not correlate. A heat rejection of 879 W (3,000 Btu/hr) in the Amicon SM-I unit was obtained in test, a transmembrane flow of 1.36 kg/hr (3 lb/hr) of water, with a hydrostatic pressure differential less than 138 kPa (20 psi). Extrapolating the data of Figure 28 would indicate that a ΔP of 960 kPa (140 psi) would be required for 1.36 kg/hr (3 lb/hr).

At this point, a change in direction in the data analysis was made. If the material were not hydrophobic but hydrophilic, capillary transport with evaporation at the fiber O.D. could account for the high rate of mass flow apparently independent of both hydrostatic pressure and vapor pressure differences. For this case the process limitation could correlate an energy transport limitation; i.e., the thermal conductance of the fiber wall and/or the liquid film on the fiber I.D. Assuming a polysulfone thermal conductivity of 0.255 W/°C-m (0.15 Btu/hr-°F-ft), a water thermal conductivity of 0.595 W/°C-m (0.35 Btu/hr-°F-ft), and a total heat transfer area of 300 cm², the thermal conductance through the fiber wall is 119 W/°C (226 Btu/hr-°F). Assuming laminar flow in the fiber, film thermal conductance ranges between 464 and 896 W/°C (800 and 1,700 Btu/hr-°F) at flows between 22.7 and 113 kg/hr (50 and 250 lb/hr). Turbulent flow correlation would predict higher values.

The major resistance is in the fiber wall (70% of the conductance is in the water contained in the pores), and the liquid film contribution was ignored in the remainder of the analysis.
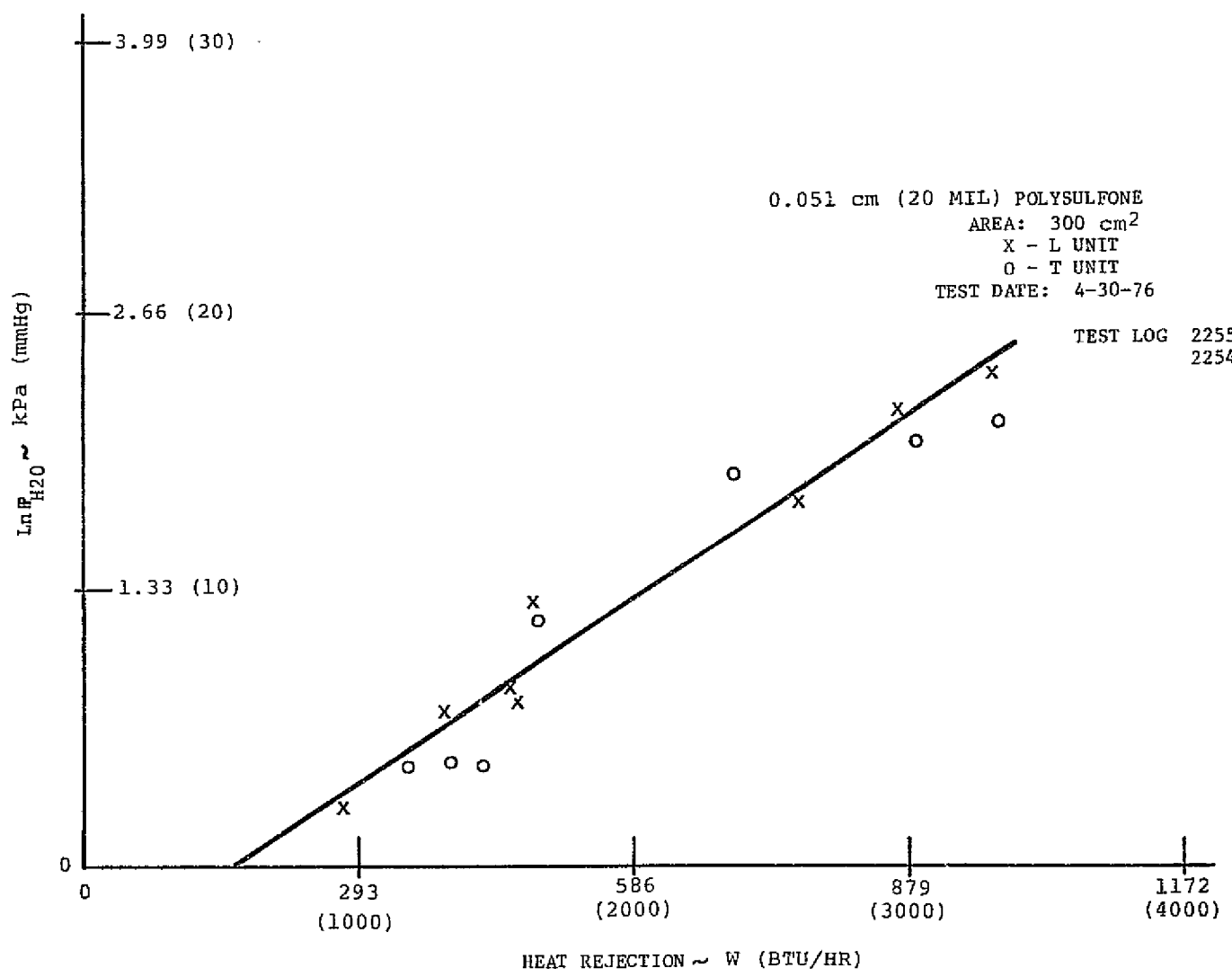
FIGURE 29: $Ln \Delta P_{H2O}$ VS HEAT REJECTION
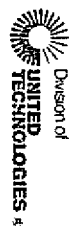
In an evaporative heat exchanger the flow stream capacity rate ratio:

$$\frac{(\dot{W} \ C_p)_{hot}}{(\dot{W} \ C_p)_{cold}}$$

can be considered zero, and the heat exchanger effectiveness is defined as:

$$E = \frac{(T_1 - T_2)_{hot}}{(T_1 - T_{sink})} = 1 - e^{-\frac{hA}{(\dot{W} \ C_p)_{hot}}}$$

$$T_{sink} = \frac{e^{\left(\frac{hA}{\dot{W} \ C_p}\right)} T_2 - T_1}{e^{\left(\frac{hA}{\dot{W} \ C_p}\right)} - 1}$$

Data from this test series (Amicon SM-I "L" and "T" units) was reduced and is shown in Figure 30 for assumed thermal conductances of 119, predicted, and 70.1 W/°C (226, predicted, and 113 Btu/hr-°F). Although the initial results indicate a rather strong dependence of sink temperature on total heat rejection – leading to the assumption that shell side pressure drop is affecting performance – it should be noted that lowering the thermal conductance by one-half produces a nearly constant sink temperature. No firm conclusions may be made from these data – the variables must be isolated such as by removing all shell side resistance to ensure a constant sink temperature.

A possible solution may lie in the Amicon SM-96 data acquired early in the program (12/11/75, 12/12/75). Although this assembly has almost three times the surface area of the SM-I, its performance was less than 70% of the SM-I. During the water seepage test (transmembrane flow) total flow through the SM-96 was only 2.6% of the SM-I performance leading to the conclusion that either it has significantly less open area, or the structure of the pores is much more restricting to flow. Extrapolating to the heat rejection mode it would follow that the heat rejection is dependent on evaporant flow area and, more importantly, on evaporant heat transfer area. Isolated flow points will only activate a small portion of the total available surface for heat transfer, and tested thermal conductance will be significantly less than predicted. Now, back to Figure 30, the reduction in UA from 119 to 70.1 W/°C (226 to 113 Btu/hr-°F) could be a logical move if, in fact, only one-half the apparent area is available for heat transfer.

FIGURE 30: SINK TEMPERATURE VS. HEAT REJECTION
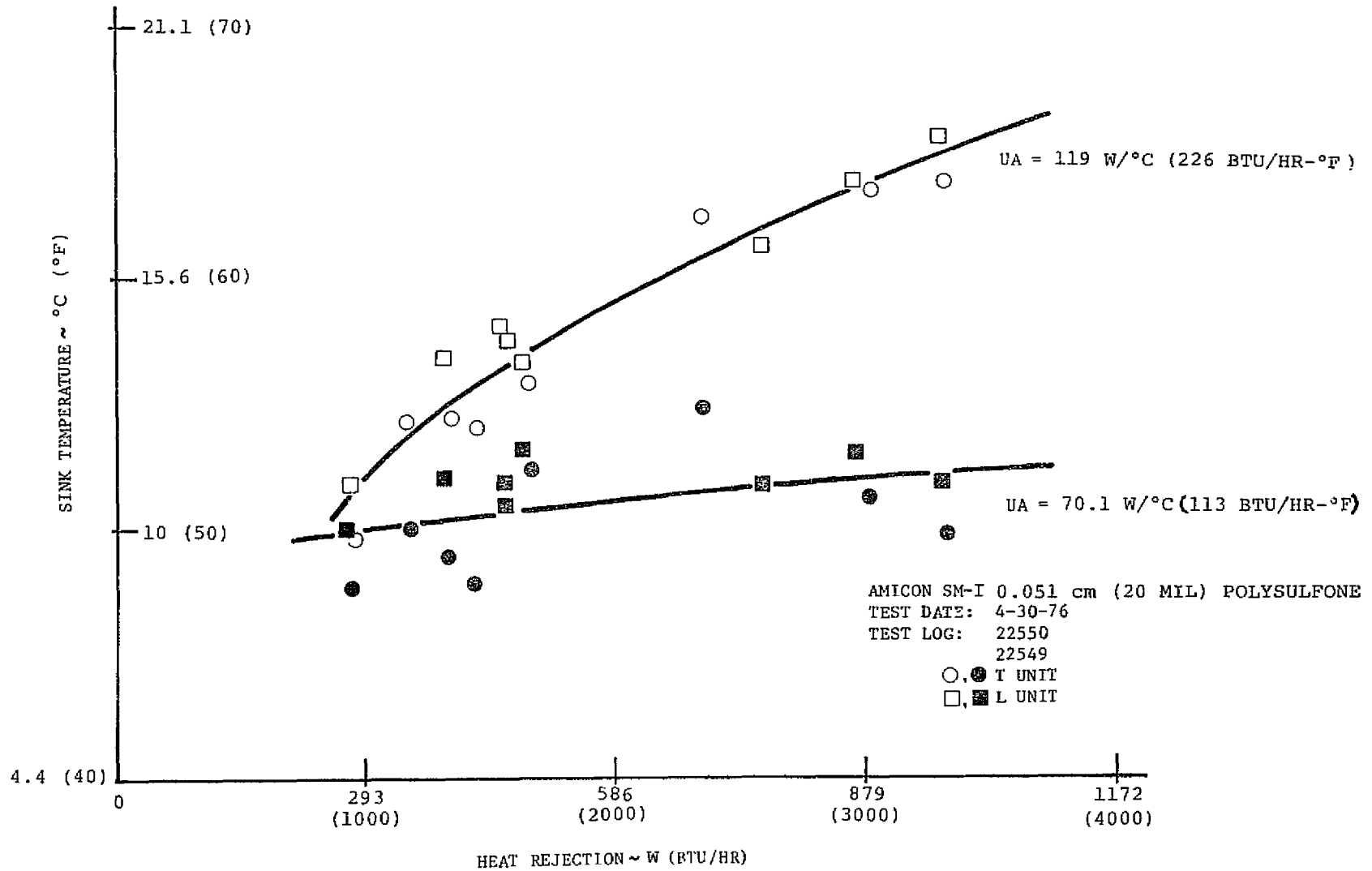
Deaeration

Test results obtained during the applications study were acquired for both the SM-I and SM-96 assemblies. Based on the prior analyses we would expect to be able to correlate the data to the diffusion of O_2 through water contained in both the inner and outer membrane wall. The results are summarized in the following table:

	Transmembrane O_2 Flow	
	SM-I	SM-96
Test Result, $\frac{\text{g-moles}}{\text{s}}$	5.1×10^{-7}	1.02×10^{-6}
Predicted, $\frac{\text{g-moles}}{\text{s}}$	0.84×10^{-7}	0.54×10^{-6}

Although the correlation would predict only 16-50% of the actual transport, the results are considered encouraging. The accuracy of data acquired during this test can be questioned due to the nature of the measurements and the test procedure. Deaeration remains a viable concept for Shuttle application.

CO$_2$ Absorption

At the Membrane Applications Study presentation in Houston on February 24, 1976, a system combining K_2CO_3 solution and membranes was included as shown in Figure 31. Two separate membrane assemblies are in this schematic. One interfaces the oxygen ventilation loop to provide CO_2 removal, dehumidification and gas cooling, while the other is exposed to space vacuum where the CO_2 is removed from the solution and dumped overboard, and water is evaporated to cool the solution. A back pressure valve is provided with this second membrane to maintain loop temperature control and prevent freezing. The solution passes through a heat exchanger to cool the LCG circuit and then back to the vent loop membrane assembly. A pump is provided for solution circulation plus a water makeup subsystem to replace the water lost in the evaporator and not added in the vent loop humidity control function.

System sizing for this concept is primarily driven by the LCG heat load which not only requires approximately 1.13 kg/hr (2.5 lb/hr) of evaporant but dictates solution flow rate be between 136 and 181 kg/hr (300 and 400 lb/hr) to keep the temperature rise across the heat exchanger below 5.5°C (10°F). Because of this high flow rate, solution strength need not be very high – the lower concentration will keep viscosity down, heat capacity up, and minimize pressure drop. The high flow rate is, however, a severe penalty on the system showing up mostly as pump power but also on membrane configuration to minimize pressure drop.

$$O_2 + CO_2 + H_2O$$

XM OR POLYSULFONE MEMBRANE SEPARATOR

K$_2$CO$_3$/KHCO$_3$ SOLUTION

$$O_2 + (H_2O)$$

PUMP

HX — LCG

H$_2$O

XM OR POLYSULFONE MEMBRANE SEPARATOR

$$CO_2 + H_2O$$

BACK PRESSURE VALVE

VACUUM
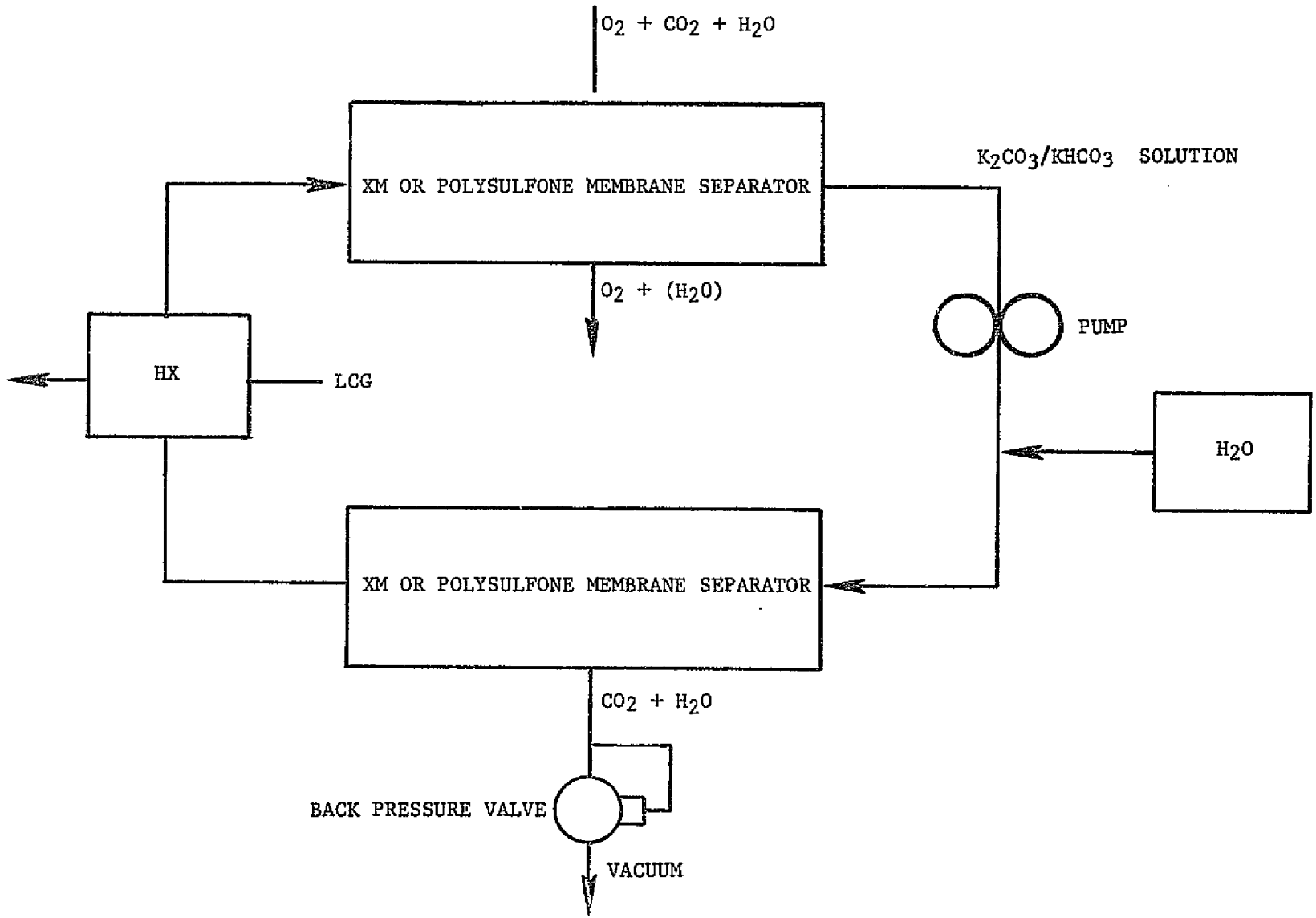
FIGURE 31: CO$_2$ + VENTILATION LOOP DEHUMIDIFICATION + LCG HEAT SINK

$$O_2 + CO_2 + H_2O$$

LCG

| | XM OR POLYSULFONE MEMBRANE SEPARATOR |

K2CO3 SOLUTION

OSMOTIC
MEMBRANE

H_2O

$O_2 + (H_2O)$

PUMP

POLYSULFONE

MEMBRANE

EVAPORATOR

XM OR POLYSULFONE MEMBRANE SEPARATOR

H_2O

$CO_2 + H_2O$

BACK PRESSURE VALVE

LCG

VACUUM
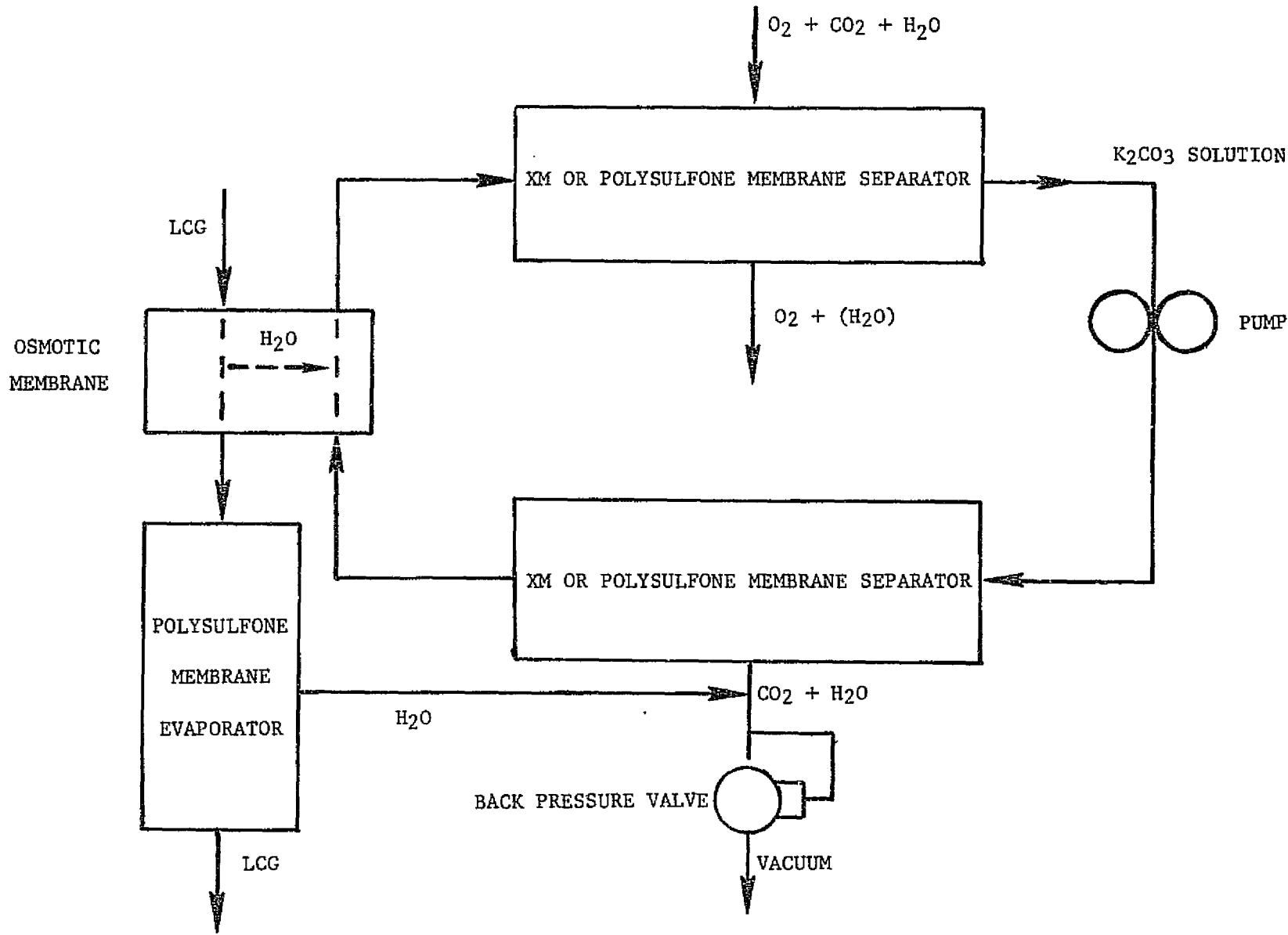
FIGURE 32:   VENTILATION LOOP REVITALIZATION

An improvement to this system is shown in Figure 32. Here, the LCG heat sink function is removed from the K_2CO_3 solution and replaced by a second membrane evaporator of the type we have shown feasible. Both membrane evaporator units discharge vapor to a common back pressure valve and may even be a single membrane assembly with dual headering (LCG plus K_2CO_3 solution). With this schematic the total heat load in the solution flow is limited to the ventilation loop revitalization which is composed of the following: Sensible – 29.3 W (100 Btu/hr); Latent – 140.6 W (480 Btu/hr); and Chemical (CO_2 absorption) – 35.1 W (120 Btu/hr). This total, 205.1 W (700 Btu/hr), is rejected to space in the evaporator where water is lost from the solution. Makeup water, 205.1-140.6 = 64.5 W (700-480 = 220 Btu/hr) required is received from the LCG transport circuit in the fourth membrane unit shown in this schematic. Water is transferred across this membrane by osmosis to automatically control solution concentration. Total solution flow for this system will be approximately 36.3 kg/hr (80 lbs/hr) and is dictated by temperature rise in the vent loop assembly.

Additional features worth noting in this schematic include:

Evaporator Assembly – With a common back pressure valve the solution will be cooled to a temperature slightly above the LCG due to water vapor pressure difference (Figure 34). This should not present any system problems. The CO_2 downstream pressure will be effectively near zero due to the washout effect of the water vapor (both from the solution and from the LCG coolant).

Water Makeup Assembly – This membrane will have to transfer water by osmotic pressure from the LCG to the solution. Transport of K_2CO_3 must be precluded. Solution concentration will automatically be controlled to a level determined by total solution hydrostatic pressure. This facet will dictate low solution K_2CO_3 concentration – on the order of 0.1 to 0.2 moles K_2CO_3 per liter.

This particular component is considered the highest risk of the membrane assemblies and was not considered for the initial test series. To minimize risk and ensure the acquisition of valid performance data, the system shown in Figure 33 was tested. Here water makeup is controlled by the pressure regulator to maintain a constant system K_2CO_3 concentration so long as no solute is lost.

Vent Loop Revitalization Assembly – Water is removed from the gas stream by direct vapor transfer through the membrane plus by condensation and then osmosis. The equilibrium water pressure of the solution is below that of water (Figure 34) and so can potentially reduce the vent loop dew point below the temperature of the solution.

$O_2 + CO_2 + H_2O$

XM OR POLYSULFONE MEMBRANE SEPARATOR

$O_2 + (H_2O)$

PUMP

PRESSURE CONTROL

LCG

$K_2 CO_3$ SOLUTION

XM OR POLYSULFONE MEMBRANE SEPARATOR

POLYSULFONE MEMBRANE EVAPORATOR

$CO_2 + H_2O$

H_2O

BACK PRESSURE VALVE

VACUUM
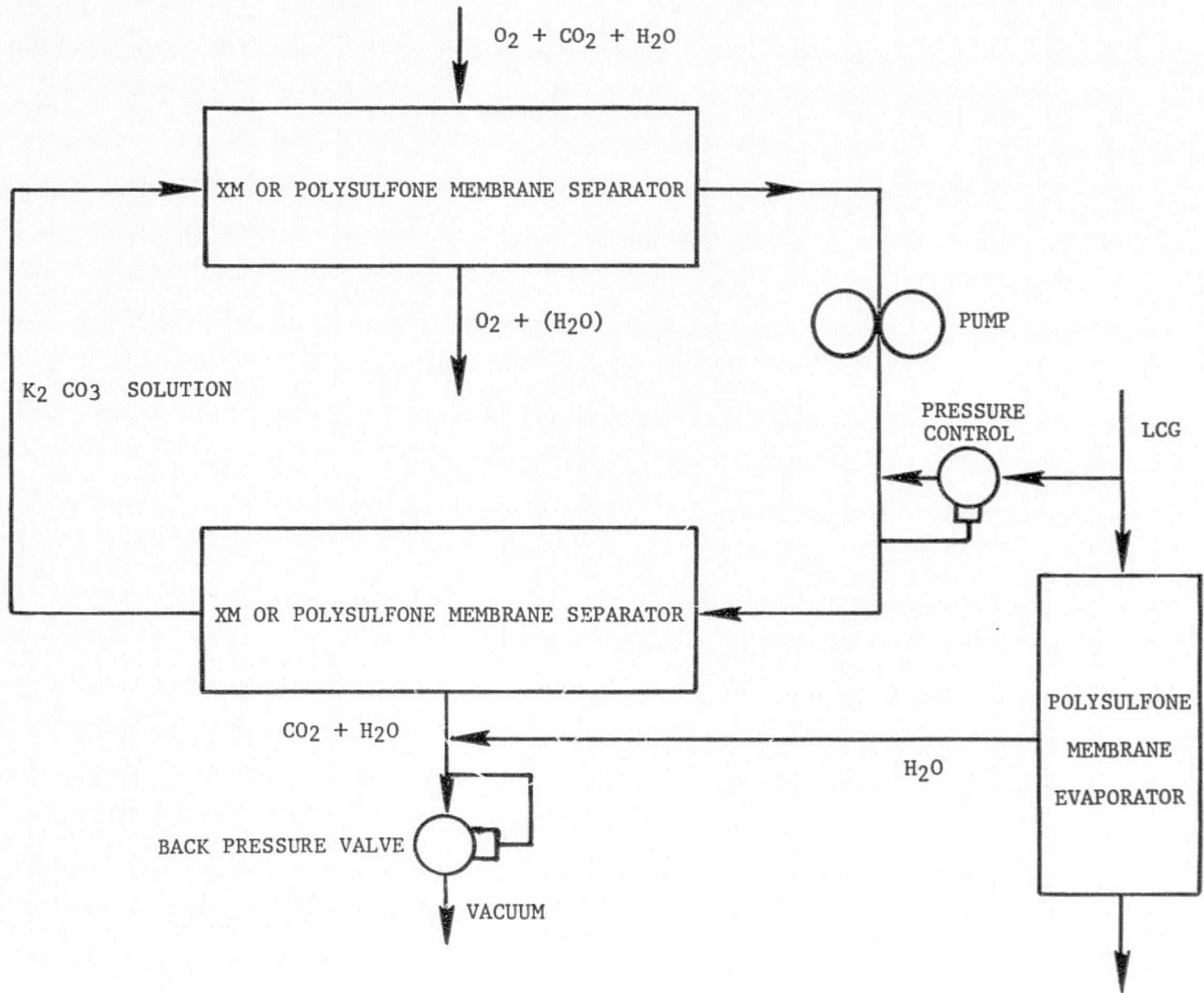
FIGURE 33: VENTILATION LOOP REVITALIZATION - RECOMMENDED TEST CONFIGURATION
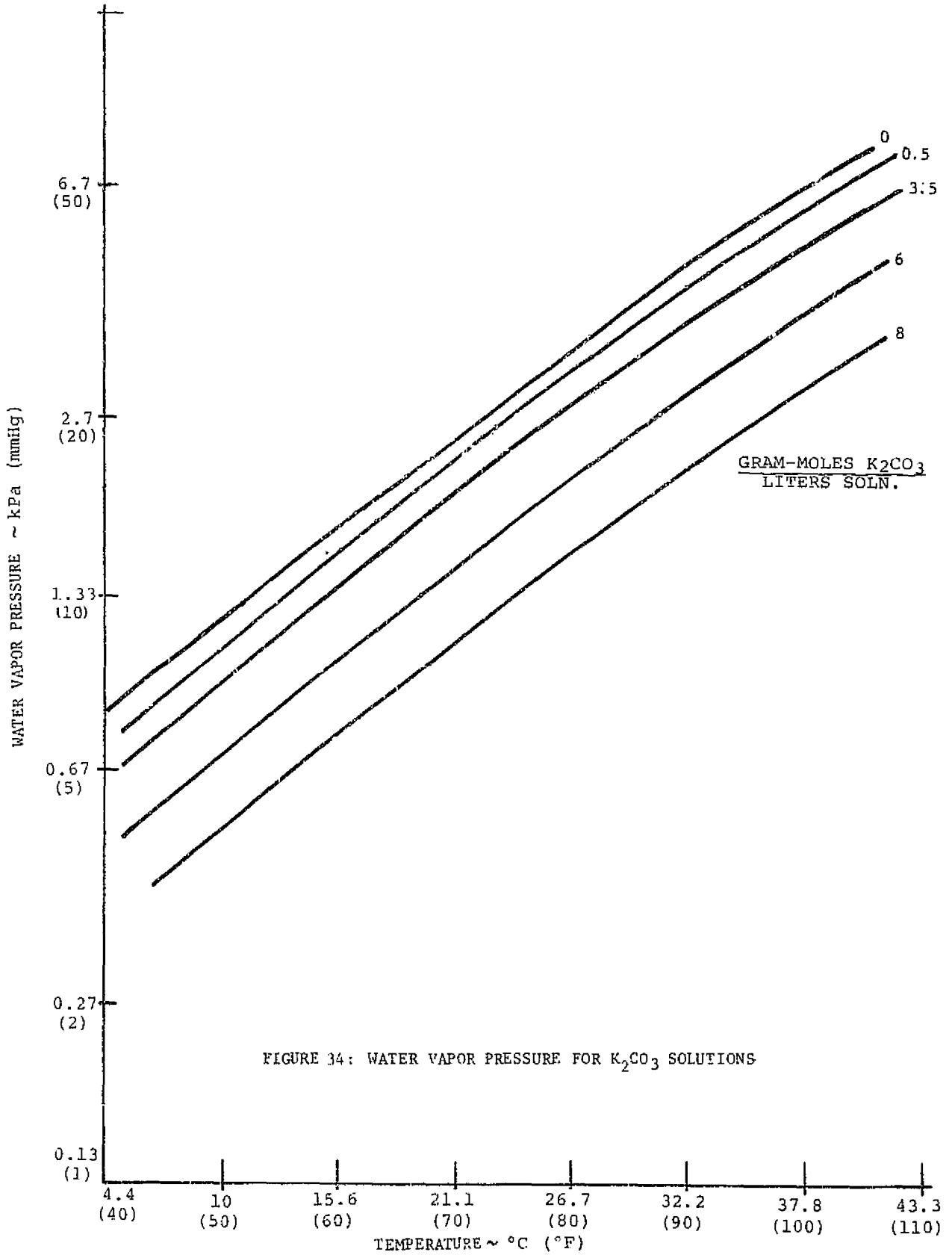
FIGURE 34: WATER VAPOR PRESSURE FOR K_2CO_3 SOLUTIONS

Figures 35 and 36 present CO_2 equilibrium pressure versus K_2CO_3 solution for 0°C (32°F) and 35°C (95°F) respectively. These curves were constructed from an empirical relationship in Perry's Chemical Engineering Handbook fifth edition and not from published data. Confirmation may be necessary at a later date.

The system of Figure 33 was tested with 1.0M and 2.5M K_2CO_2 and then with a 2.5M K_2CO_3 activated with 0.1M $NaAsO_2$ which has been shown to act as catalyst (two to three times greater reaction rate) for CO_2 absorption. All test results were essentially the same and are represented by Figure 37 which is catalyzed results. These absorption rates are extremely low and would essentially preclude further concept consideration. An analysis was conducted to determine the restricting membrane process and to determine if this restriction can be modified.

Liquid sorption rate can be ruled out based on the repetitive data for the three solutions tested. Diffusion in the flow stream appears to have some effect at the lower gas flows and partial pressures tested but not above 0.008 m^3/min (0.3 CFM) and 2.1 kPa (16 mmHg) (reference Figure 37).

The basic data point for correlation was 0.0012 kg/hr (0.0027 lb/hr) CO_2, 2.1 kPa (16 mmHg). Gas flow in the inner shell would be in the Knudson regime and for an average 0.025 open area fraction could transport 0.049 kg/hr (0.11 lb/hr) or 40 times the test result. If the inner pores were filled with liquid, diffusion of K_2CO_3 solution must be considered. CO_2 transport for this process would be 0.00145 kg/hr (0.0032 lb/hr) for an open area fraction of 0.025. This result is very close to test results and will be considered along with outer wall resistance.

If the outer wall (55% open) was also filled with liquid, an additional conductance of 0.36 x 10^{-4} kg/hr (0.8 x 10^{-4} lb/hr) must be considered. This result is too low. Gas diffusion in the outer wall is in the molecular regime at the ventilation loop pressures we are considering, 26.2 to 103 kPa abs. (3.8 to 15 psia). A diffusion rate of 0.16 kg/hr (0.36 lb/hr) can be expected for CO_2 through the non-flowing oxygen indicating that this area should not present any significant resistance to the adsorption process.

Based on these results it can be assumed that the solution wets the inner wall by capillary action but not the outer wall – unlike the heat rejection mode of operation. Apparently there is sufficient change in the surface tension from pure water to weak

HAMILTON STANDARD Division of UNITED TECHNOLOGIES
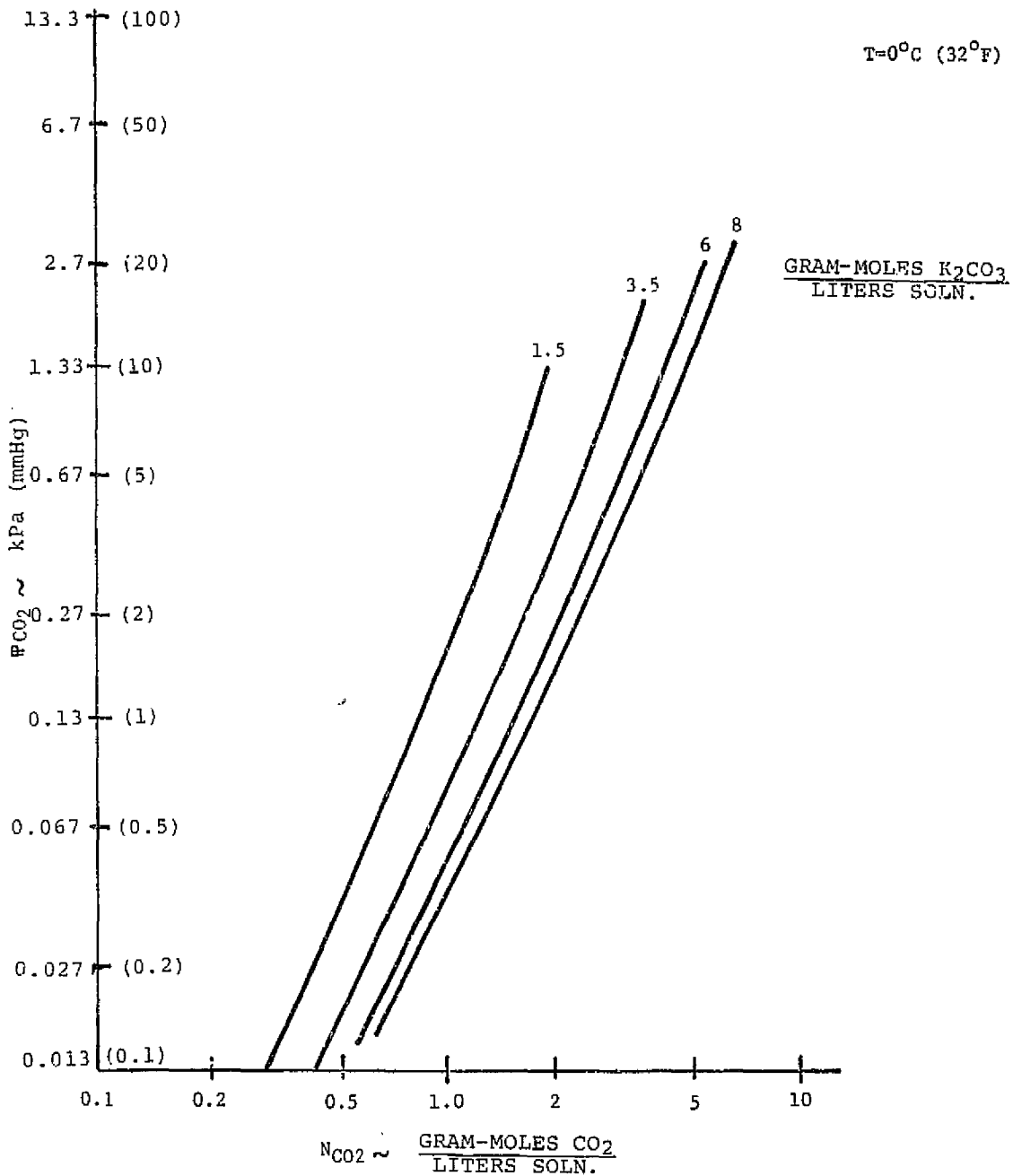
FIGURE 35: CO_2 VAPOR PRESSURE FOR K_2CO_3 SOLUTIONS, 0°C (32°F)-CALCULATED
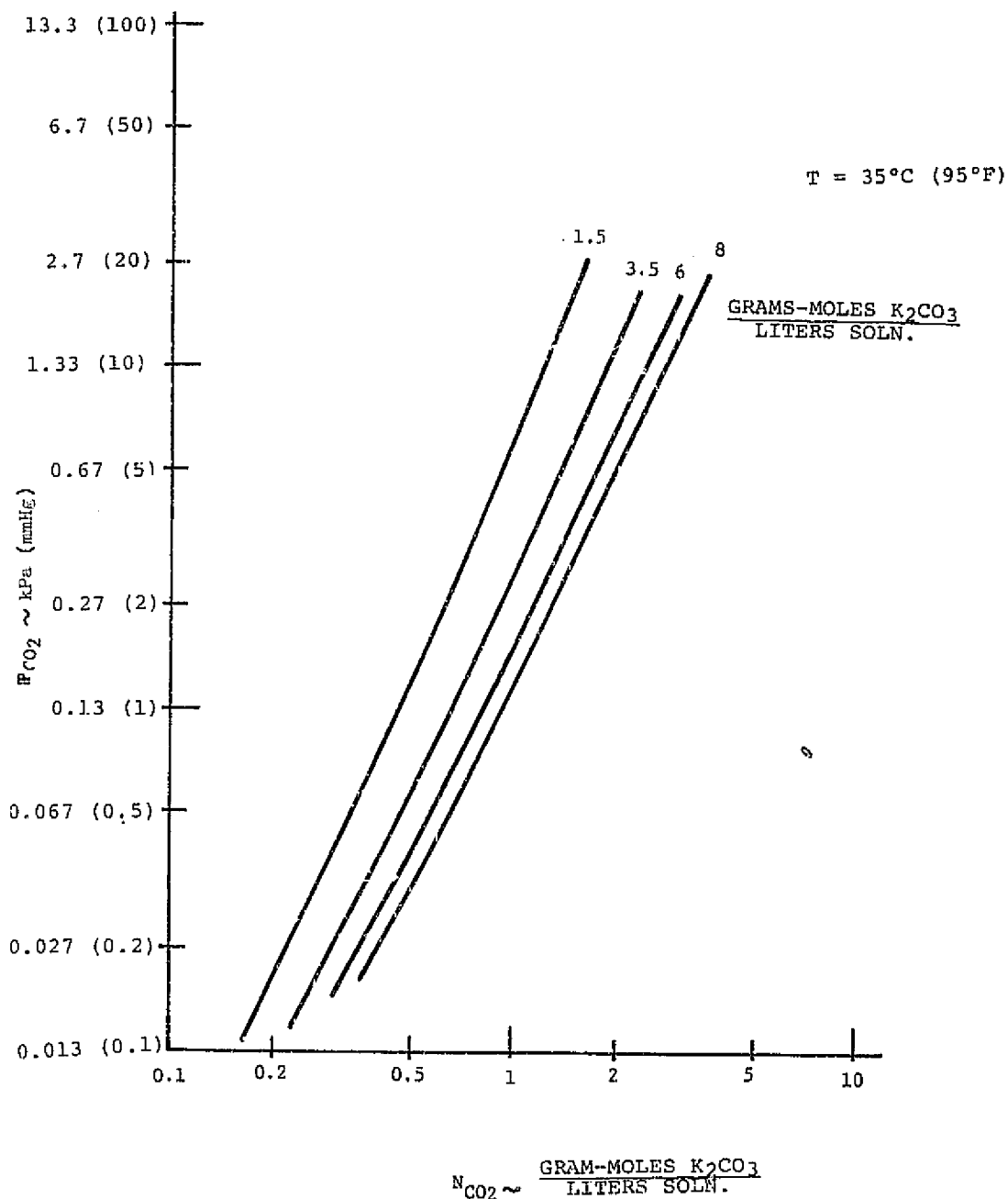
FIGURE 36: CO_2 VAPOR PRESSURE FOR K_2CO_3 SOLUTIONS, 35°C (95°F)-CALCULATED

● ,X = HIGH SOLUTION PRESSURE

○ = LOW SOLUTION PRESSURE

300 cm^2
K_2CO_2 + N_aASO_2
25M   0.1M

P_{CO_2} ≃ 2.13 kPa
(16 mmHg)

P_{CO_2} ≃ 0.93 kPa
(7 mmHg)

CO$_2$ TRANSFER RATE ∿ kg/hr x 10^3 (lbs/hr x 10^3)

GAS FLOW ∿ m^3/min (CFM)
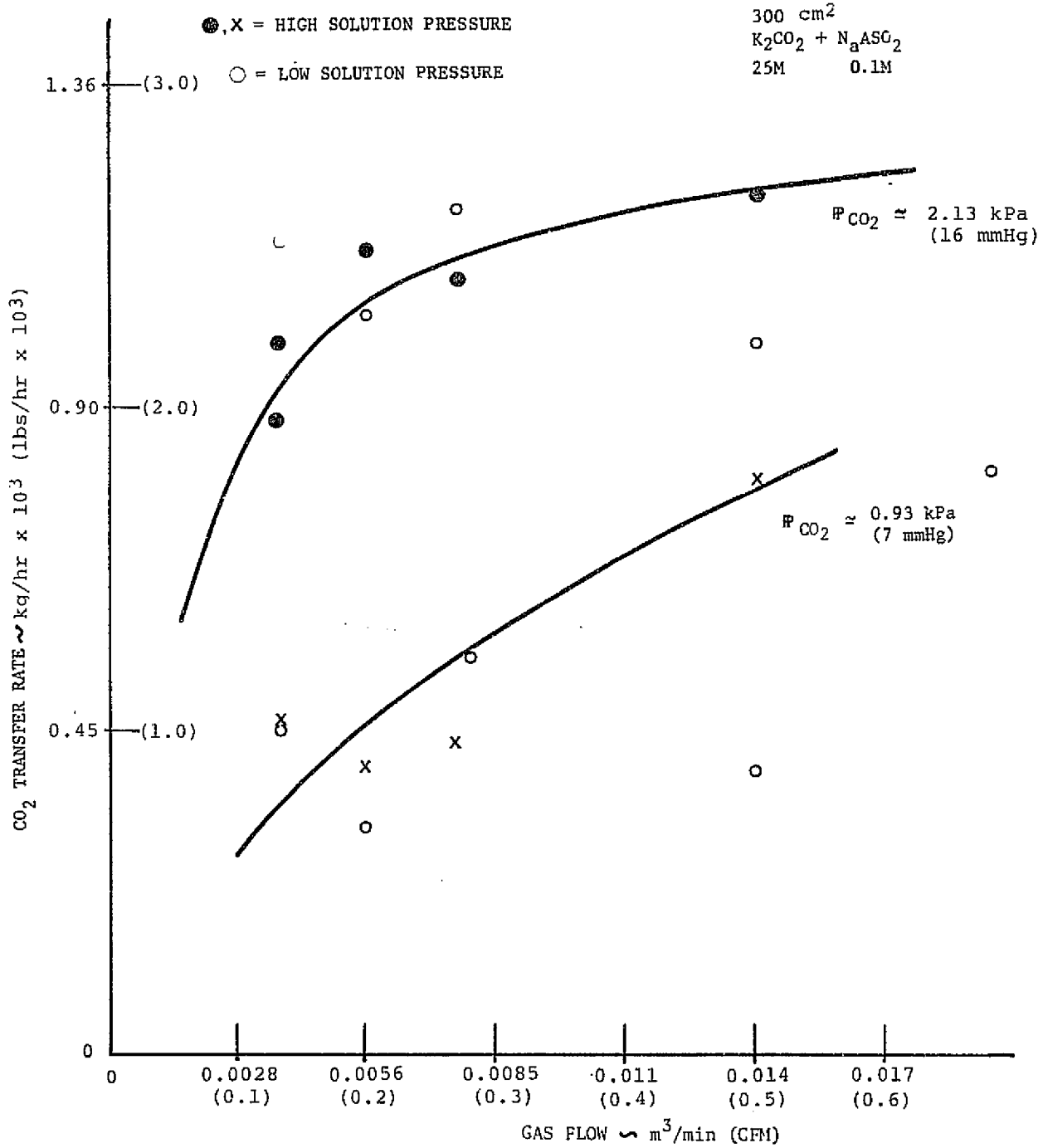
FIGURE 37: CO$_2$ TRANSFER RATE

solution to preclude capillarity of the larger pores in the outer structure. The overall transport process is assumed to be molecular diffusion of CO_2 through stagnant O_2 in the outer wall and the rate limiting step of $KHCO_3$ diffusion in a weak solution of K_2CO_3 in the inner wall.

Brief tests were conducted with the gas side (tube O.D.) pressure as much as 3.4 kPa (5 psid) above the solution in an attempt to force the liquid out of the pores. The result of no change in performance indicated that the capillary pressure rise was greater than 34.5 kPa (5 psi), and the reverse pressure had no effect.

DEFINITION OF UNITS

A	=	Area, ft^2
C	=	Molar Concentration, $g\text{-}mole/cm^3$
C_p	=	Heat Capacity, $Btu/lb\text{-}°F$
d	=	Diameter, in
D_{AB}	=	Diffusivity of "A" in "B", cm^2/s
D_K	=	Knudson Diffusivity, cm^2/s
E	=	Heat Exchanger Effectiveness, Dimensionless
f	=	Fanning Friction Factor, Dimensionless
G	=	Mass Flux, $lbm/hr\text{-}cm^2$
h	=	Liquid Film Thermal Coefficient, $Btu/hr\text{-}ft^2\text{-}°F$
k	=	Thermal Conductivity, $Btu/hr\text{-}ft\text{-}°F$
ℓ	=	Length, cm
L	=	Length, ft
M	=	Molecular Weight, $g/g\text{-}mole$
N_A	=	Molar Flux, $g\text{-}mole/s\text{-}cm^2$
N_{GZ}	=	Graetz Number, Dimensionless
ΔP	=	Pressure Difference, psid
P	=	Partial Pressure, atm
Q	=	Heat Transfer Rate, Btu/hr
$r, \bar{r}$	=	Radius, cm
R	=	Universal Gas Constant, $82.06\ cm^3\text{-}atm/g\text{-}mole\text{-}°K$
r	=	Mean Pore Radius, cm
t	=	Temperature, $°F$
T	=	Temperature, $°K$
V_A	=	Molar Volume of A at Normal Boiling Point, $cm^3/g\text{-}mole$
$\dot{W}$	=	Mass Flow Rate, lb/hr
X_A	=	Mole Fraction of Specie A
ρ	=	Density, lbm/ft^3
σ	=	Surface Tension, $dyne/cm$
μ	=	Viscosity, centipoise

SIZING FOR SHUTTLE PLSS APPLICATIONS

Membrane assemblies were sized for three Shuttle PLSS applications:

- Bacteria Filtration
- Water Deaeration
- Heat Rejection

Wherever possible, the sizing considered current manufacturing techniques and configuration to minimize development in this area.

BACTERIA FILTRATION

Requirements:

- Filtration: 100% bacterial retention
- Fluid Flow: 181 kg/hr (40 lb/hr)
- Unit Pressure Drop: 3.44 kPa (5 psi) max
- Fluid Temperature: 4.4°C-37.8°C (40°F-100°F)

The transmembrane flow/pressure drop was extrapolated using the laminar flow correlation to predict required surface area scaling from test data acquired during the applications study. The Romicon GM-80 assembly will be increased from 175 acrylate fibers to the required 250 fibers to provide a total flow area of 357 cm^2. Total fiber length 12.7 cm (5 in) and active length 8.9 cm (3.5 in) remains identical to the tested assembly.

The breadboard unit for this Shuttle PLSS application is full size.

WATER DEAERATION

Requirements:

- Feedwater Saturation: 37°C and 101 kPa abs. (98.6°F and 14.7 psia)
- Product Water Saturation: 4.4°C and 23.1 kPa abs. (40°F and 3.35 psia)
- Water Flow: 18.1 kg/hr (40 lb/hr)
- Unit Pressure Drop: 3.44 kPa (5 psi) max

Original size of the water deaerator was extrapolated through a transmembrane gas conductance empirically obtained from the applications study data using the dissolved gas log mean partial pressure across the membrane surface as the driving force for mass transfer:

$$\text{Gas Conductance} \quad = \quad \left[\frac{\text{Gas Transfer Rate}}{\cfrac{\mathbb{P}1 \; - \; \mathbb{P}2}{\text{Ln}\left(\cfrac{\mathbb{P}1 \; - \; \mathbb{P}\text{sink}}{\mathbb{P}2 \; - \; \mathbb{P}\text{sink}} \right)}} \right]$$

The Amicon SM-96 polysulfone membrane was selected for this application because of its low transmembrane liquid water transport and required a total active membrane surface area of 1,022 cm^2. Optimizing the assembly for minimum number of tubes and utilizing the allowable tube side pressure drop, the bundle would contain 1,860 fibers 0.02 cm (0.008 in) in diameter by 25.4 cm (10 in) overall length; active length is 21.6 cm (8.5 in). The same unit sized for the "standard" 12.7 cm (5 in) long fiber will contain 1,804 fibers.

Reevaluation of this sizing procedure (discussed under "correlation") has indicated that dissolved gas partial pressure may not be the process driving force but rather diffusion (mole fraction dominated) through the liquid contained in the fiber wall. Sizing a unit based on this hypothesis would predict a requirement of 1,480 cm^2 from "handbook" analysis and 784 cm^2 extrapolating from test data. Since there is insufficient data available to do more than predict the viability of the concept and the revised predictions bracket the earlier size, it would appear most feasible not to revise that size at this time.

The breadboard unit for this Shuttle PLSS application is full size.

HEAT REJECTION

Requirements:

- Coolant Flow: 108.9 kg/hr (240 lb/hr)
- Unit Pressure Drop: 4.8 kPa (0.7 psi)
- Heat Rejection: 879 W (3,000 Btu/hr) max
- Coolant Outlet Temperature: 11.4°C (52.5°F) max

Using the test results for the Amicon SM-I polysulfone as the basis for sizing an evaporator, active surface area of 818 cm^2 will be required to meet specification conditions. The assembly is very similar to those already constructed and tested being 12.7 cm (5 in) in overall length and 8.9 cm (3.5 in) active length but containing 545 fibers. With this size (based on wall thermal resistance), the sink temperature must be 8.9 to 10.6°C (48 to 51°F). This is equivalent to a shell side pressure of 1.13 to 1.28 kPa (8.5 to 9.6 mmHg) and will satisfy a UA variation between 162 and 325 W/°C (308 and 616 Btu/hr-°F).

The proposed breadboard unit for this application is half size and will contain 275 fibers of the same length as the full size unit. Two half size units in parallel would be equivalent to a full size unit.

Development potential of the HFM evaporator concept for this application is marginal because it is more costly than the sublimator. Both of the concepts require a heat exchanger of essentially equivalent cost. However, the HFM evaporator requires a temperature sensing back pressure valve with either a separate positive shutoff or manual override for intravehicular operation and storage. This valve requires significant development and is expensive. Schematics of the two systems are shown in Figure 38. Following is a weight, volume, and relative cost comparison between the sublimator and the HFM evaporator.

		Sublimator	HFM Evaporator
Weight	kg (lb)	4.8 (2.2)	4.4-4.8 (2.0-2.2)
Volume	cm^3 (in3)	1,180 (72)	819 (50)
Relative Cost		1.0	1.2

DESIGN CONCEPTING

The testing described in the Applications Study and Materials Selection Section was conducted using laboratory prototypes whose configuration was selected to facilitate measurement of the basic transport property in question. The breadboard design required a less procrustean approach. In the interest of simplicity, a single module design was employed for the three applications, bacteria filtration, deaeration, and heat rejection. The geometry of this module was selected to allow construction of full scale bacteria filtration and deaeration units, and half scale heat rejection units.

SUBLIMATOR
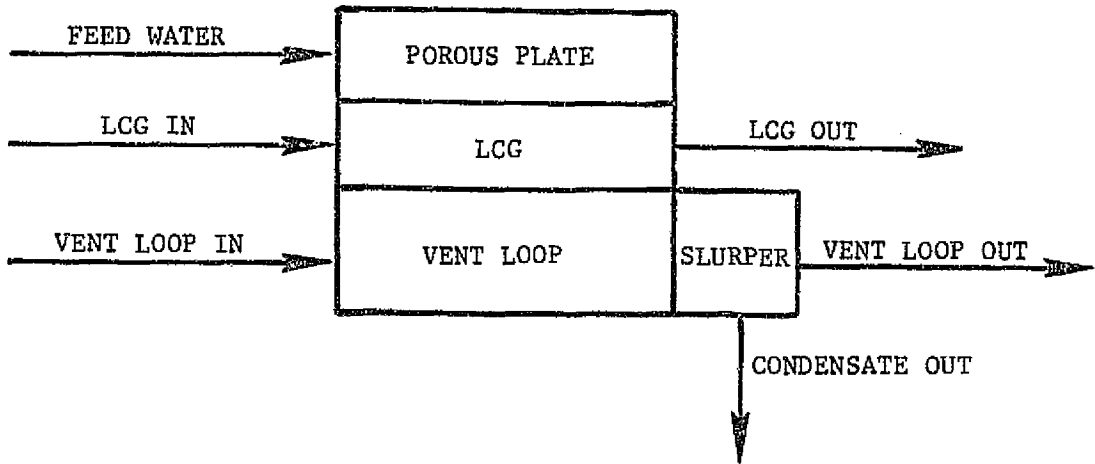
HFM EVAPORATOR
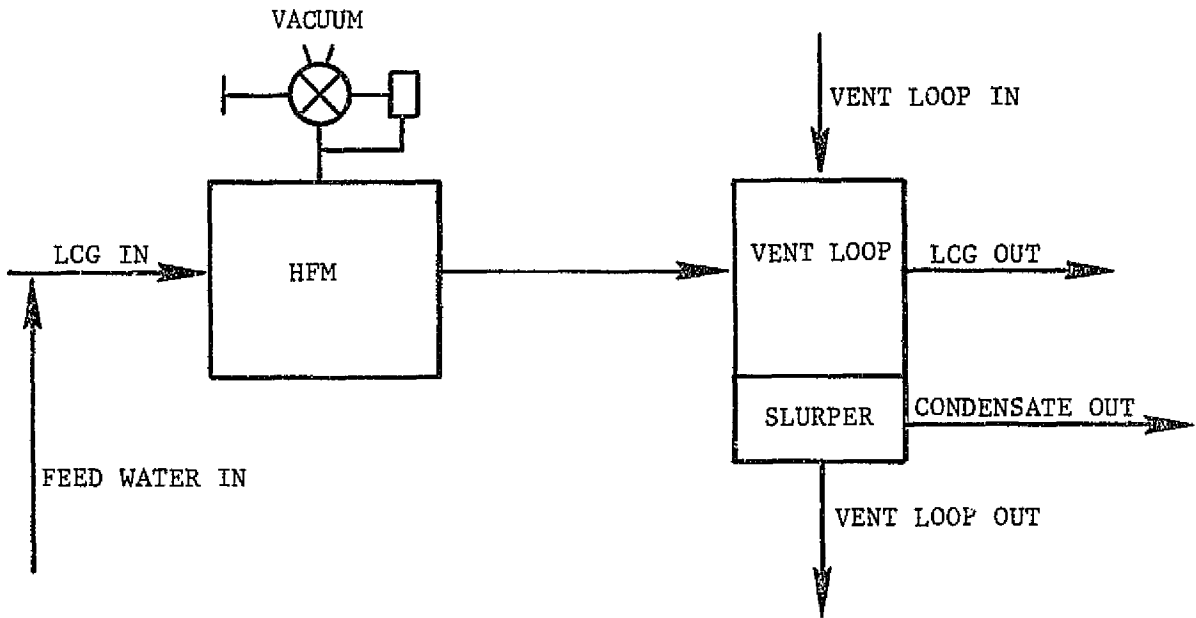
FIGURE 38: HEAT REJECTION SCHEMATICS

Design of the breadboard units involved two distinct tasks:

- Design of the module and housing.

- Determination of the spatial configuration of the fibers within the module.

MODULE AND HOUSING

The module was designed to provide free vapor access to and from the fibers, even at very low pressures, and to shield the hollow fibers from breakage or damage. The housing was designed to provide the required headering arrangements using a common hardware configuration. Figure 39 describes the construction of the three different hollow fiber membrane modules, and Figure 40 describes construction and makeup of the three different housing combinations.

Module

The module is configured as follows. An aluminum sleeve containing four oval windows is the outer container for the module. The hollow fiber membranes are contained within the sleeve and potted in epoxy at either end, such that access to the inside diameter of the membranes is achieved at either end of the sleeve, and access to the outside diameter of the membranes is achieved through the four oval windows.

A high-density polyethylene Vexar screen insert is placed just inside the tubing to protect the fibers from damage through the oval windows during handling. ("Vexar" is a DuPont trademark for a continuous, cylindrical screen whose two strands run at $\pm 45°$ to the axis line yielding diamond shaped openings.) The screen selected is rigid and has approximately 0.64 cm (0.25 in) by 0.64 cm (0.25 in) diamond openings. The Vexar adheres well to the epoxy. The epoxy potting compound is Amicon T-640, a two component epoxy resin material that has been used successfully during the parametric testing effort.

Housing

The housing contains aluminum end headers that fit over the end of the module to allow fluid connection of the membrane inside diameters to a common tube fitting. The headers are connected together by four aluminum rods (spacers) and a polycarbonate tube, trapped between the headers, provides a means for headering the outside diameters of the membranes for the bacteria filtration and the deaeration applications. The tube is omitted for the heat rejection application because it would inhibit the escape of water vapor.
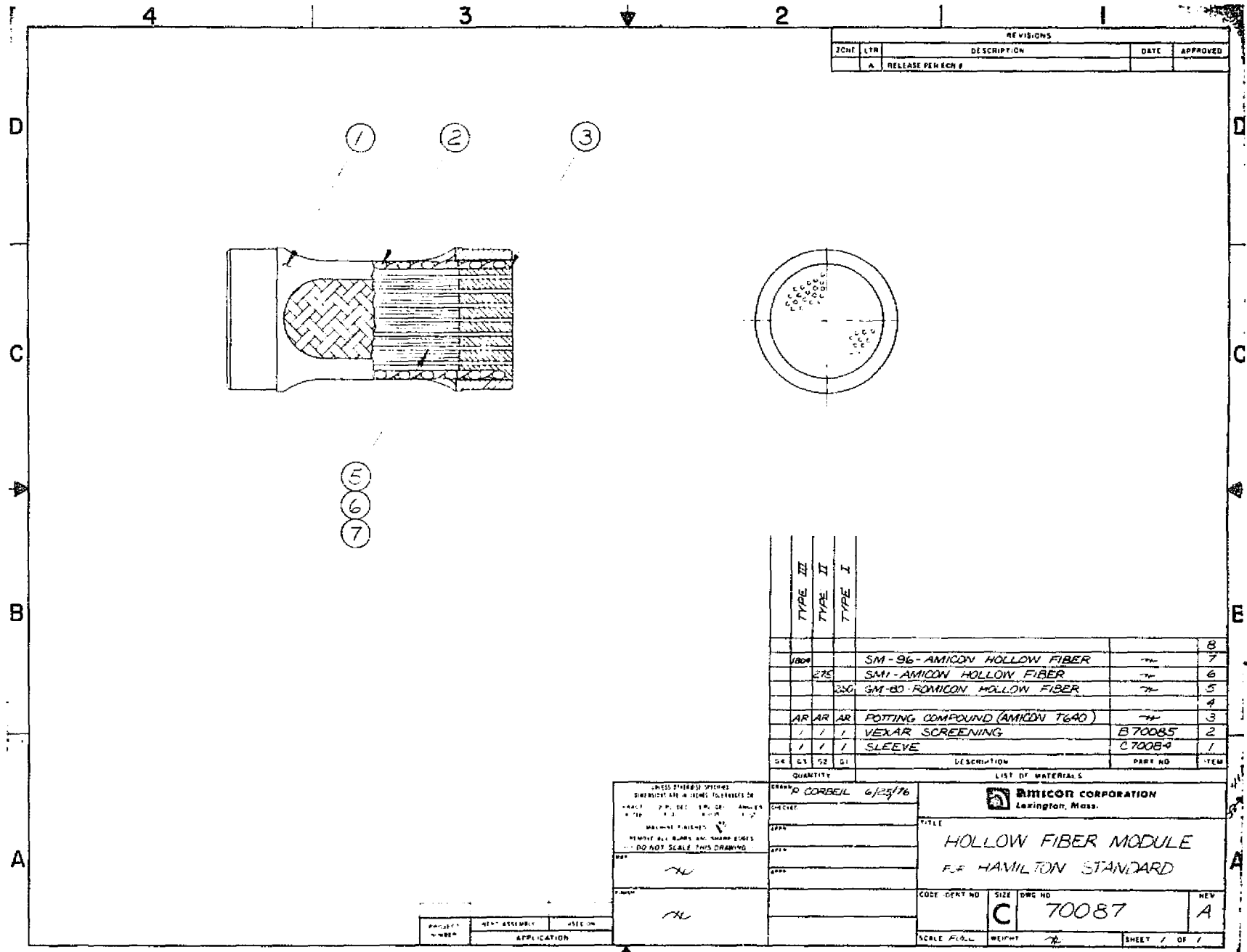
			REVISIONS		
ZONE	LTR	DESCRIPTION		DATE	APPROVED
	A	RELEASE PER ECN #			

	TYPE III	TYPE II	TYPE I	DESCRIPTION	PART NO	ITEM
						8
1804				SM-96-AMICON HOLLOW FIBER	—	7
	275			SM1-AMICON HOLLOW FIBER	—	6
		250		GM-80-ROMICON HOLLOW FIBER	—	5
						4
	AR	AR	AR	POTTING COMPOUND (AMICON T640)	—	3
	1	1	1	VEXAR SCREENING	B70085	2
	1	1	1	SLEEVE	C70084	1
Q4	Q3	Q2	Q1	DESCRIPTION	PART NO	ITEM
QUANTITY				LIST OF MATERIALS		

DRAWN R CORBEIL 6/25/76

amicon CORPORATION
Lexington, Mass.

TITLE

HOLLOW FIBER MODULE
FOR HAMILTON STANDARD

CODE IDENT NO	SIZE	DWG NO	REV
	C	70087	A

SCALE FULL   WEIGHT   SHEET 1 OF 1

FIGURE 39   HOLLOW FIBER MEMBRANE MODULE

FIGURE 40   HOLLOW FIBER MEMBRANE

11 FITTING   INSTALL W/ TEFLON PIPE TAPE
6 TUBE   -11 FITTING MUST NOT
7 BLOCK   EXTEND THROUGH -7 BLOCK.

-101 TUBE ASSY
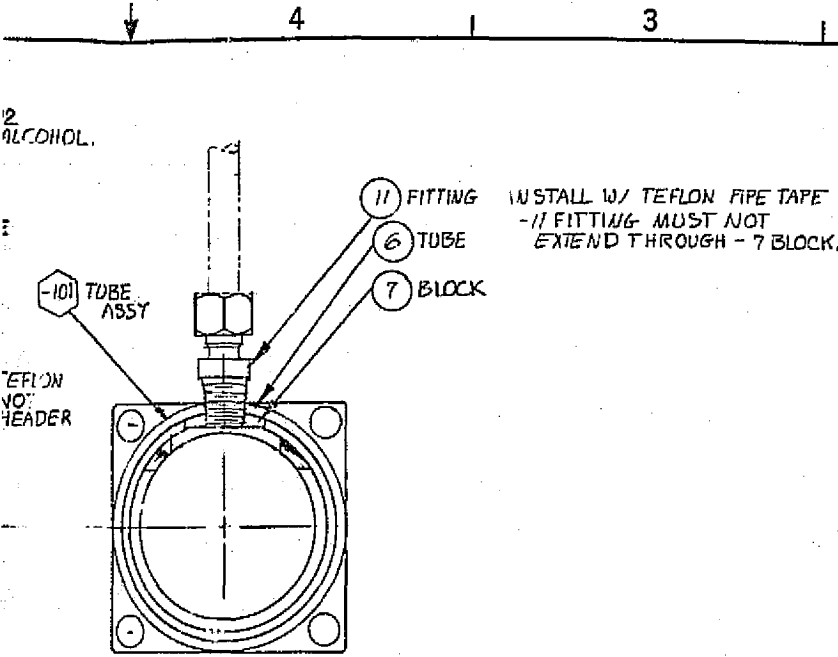
		REVISIONS			
AFFECTS PART-DIE	ZONE	LTR	DESCRIPTION	DATE	APPROVED
		A	REVISED TO REFLECT "AS BUILT" CONFIGURATION.	10-18-76	WCDun

D

C

SVSK92049

B

						FIND NO.	PART NO.		PART NAME	REMARKS
				1	16	AN913 D2		1/4 NPT PLUG	MATL ANODIZED ALUMINUM
	2		2	15	77-545-39		PACKING PREFORMED	VITON (PARKER COMPOUND)
	2	2	2	14	77-545-37		PACKING PREFORMED	VITON (PARKER COMPOUND)
	8	8	8	13	AN960-C8		WASHER (#8)	STAINLESS STEEL
	8	8	8	12	MS16995-27		SCREW (8-32 x .625)	STAINLESS STEEL
1	2	2	1	11	600-1-4-316		FITTING	SWAGELOCK P/N
2				10	MS 21208-C0815		HELICOIL	
	2	2	2	9	SVSK92049-106		HEADER	
1				8	SVSK92049-105		ROD	
	1			7	SVSK92049-104		BLOCK	
	1			6	SVSK92049-103		TUBE	
	4	4	4	5	SVSK92049-102		ROD ASSY	
		1	1	4	SVSK92049-101		TUBE ASSY	
	1			3	70087-G3		HFM MODULE	DEAERATION
		1		2	70087-G2		HFM MODULE	HEAT REJECTION
			1	1	70087-G1		HFM MODULE	BACTERIA FILTRATION

QTY PER ASSY — FIND NO. — PART NO. — REV LTR — PART NAME — REMARKS

ASSY NO: SVSK92049-102 | SVSK92049-101 | SVSK92049-3 | SVSK92049-2 | SVSK92049-1

INSPECT—TEST DESIGNATED AREA(S) PER
DES | SPECIFICATION(S)
A
B
C

ALL AREAS
ALL AREAS

MATERIAL
HARDNESS
HEAT TREAT SPEC
SURFACE COATING
MFG SPEC
MAKE FROM
PROD. CODE

UNLESS OTHERWISE SPECIFIED:
DIMENSIONS ± .010   ANGLES ± 2°
EXCEPT FOR DRILL END FORMS, FILLET RADII .005 TO .025, SURFACES HAVING A COMMON AXIS CONCENTRIC WITHIN .002 TIR.

MARK PART IDENTIFICATION: MIL-STD-130 PER HS393.
DRAWING INTERPRETATION PER HS1360. CLEANING, PRESERVATION AND HANDLING PER HS1550-C__P__

SEE DWG.

DRAWN W.C.Dean 6-18-76
CHECKED
DRAFTING
DESIGN W.U.Dean 6-21-76
MATERIALS
PROJECT E.Corbel 6-10-76
COST
FACTORY

NEXT ASSY | USED ON
APPLICATION

Hamilton Standard
WINDSOR LOCKS, CONNECTICUT · U.S.A.

HOLLOW FIBER MEMBRANE BREADBOARD UNIT

EXP MFG | PRELIM PROD. | F (DD.)

SIZE: D | CODE IDENT NO. 73030 | SVSK92049
SCALE: FULL | WEIGHT: | LB | SHEET

A

SPATIAL CONFIGURATION

During the application phase the fibers were packed somewhat tightly within the canister. Analyses suggested that loosely packaged, uniformly distributed fibers improved performance in applications based upon "liquid phase – vapor phase mass transport." Achievement of loosely-packed, uniformly distributed fibers were seen to require a major advance in fabrication technology. Accordingly, it was decided to fabricate all but one breadboard designated unit with loosely-packed, randomly-distributed fibers and to attempt to fabricate one unit with uniformly-spaced fibers. Uniform spacing was achieved by threading the fiber through two disc-shaped polypropylene mesh screens contained at either end of the shell.

HARDWARE FABRICATION

In all, eight modules were prepared for the program:

Bacteria Filtration:

    Two modules
    Romicon GM-80 membranes
    250 Fibers, active length 8.9 cm (3.5 in)
            total length 12.7 cm (5.0 in)

Water Deaeration:

    Two modules
    Amicon SM-96 membranes
    1,804 Fibers, active length 8.9 cm (3.5 in)
            total length 12.7 cm (5.0 in)

Heat Rejection:

    Three modules
    Amicon SM-I membranes
    275 Fibers, active length 8.9 cm (3.5 in)
            total length 12.7 cm (5.0 in)

    One module
    Amicon SM-I membranes with screen spacers
    275 Fibers, active length 8.9 cm (3.5 in)
            total length 12.7 cm (5.0 in)

Small prototype units were prepared for each incoming lot of fibers, and fiber properties were verified on these units (duly scaled) before committing to a full-sized unit. Experience has shown that lot-to-lot variation for the fibers can be high, but that good consistency is realized with a given lot. The GM-80 fibers for the bacterial retention unit and the SM-I fibers for the heat rejection unit were within specification on the first try. The first two lots of SM-96 fibers for the deaeration unit displayed too high a flux; the third passed.

After potting the fibers (by proprietary technique), the finished modules were permeation tested. As a double check, all units were also leak tested by Amicon's standard in-house procedure, i.e., permeability to two million molecular weight, color-tagged polysaccharide (blue dextran pharmacia). Membranes which passed water but sieved out the blue dextran were known to be integral and free of leaks. An extra deaeration unit had to be made because one of the first two failed its permeation test because of a leaky fiber.

The heat rejection module containing the screen spacers was constructed by threading the individual fibers through the screen spacers to form a spaced subassembly which was potted into the sleeve in the same manner as the other modules. The resulting matrix was very uniform, but many fibers were damaged in the threading process causing leaks. Attempts to seal off the damaged fibers were not successful so the unit could not be subjected to heat rejection testing.

Three individual housing assemblies were manufactured to provide a separate housing for each of the applications, thereby allowing the potential of completely independent testing. Figures 41, 42, and 43 are photographs of the bacteria filtration hardware, deaeration hardware, and heat rejection hardware, respectively.

OUTLET

INLET
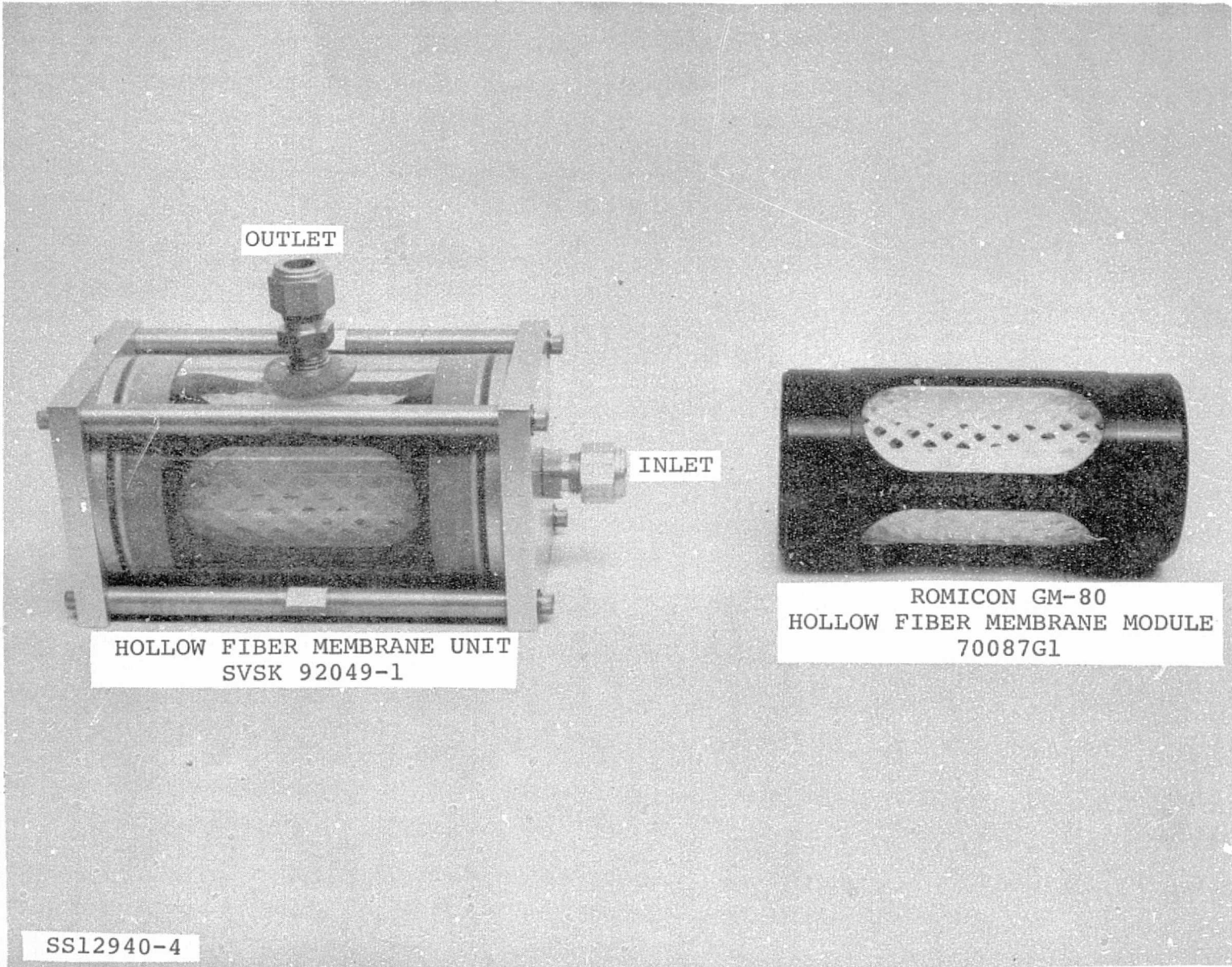
HOLLOW FIBER MEMBRANE UNIT
SVSK 92049-1

ROMICON GM-80
HOLLOW FIBER MEMBRANE MODULE
70087G1

SS12940-4

FIGURE 41   BACTERIA FILTRATION HARDWARE

VACUUM
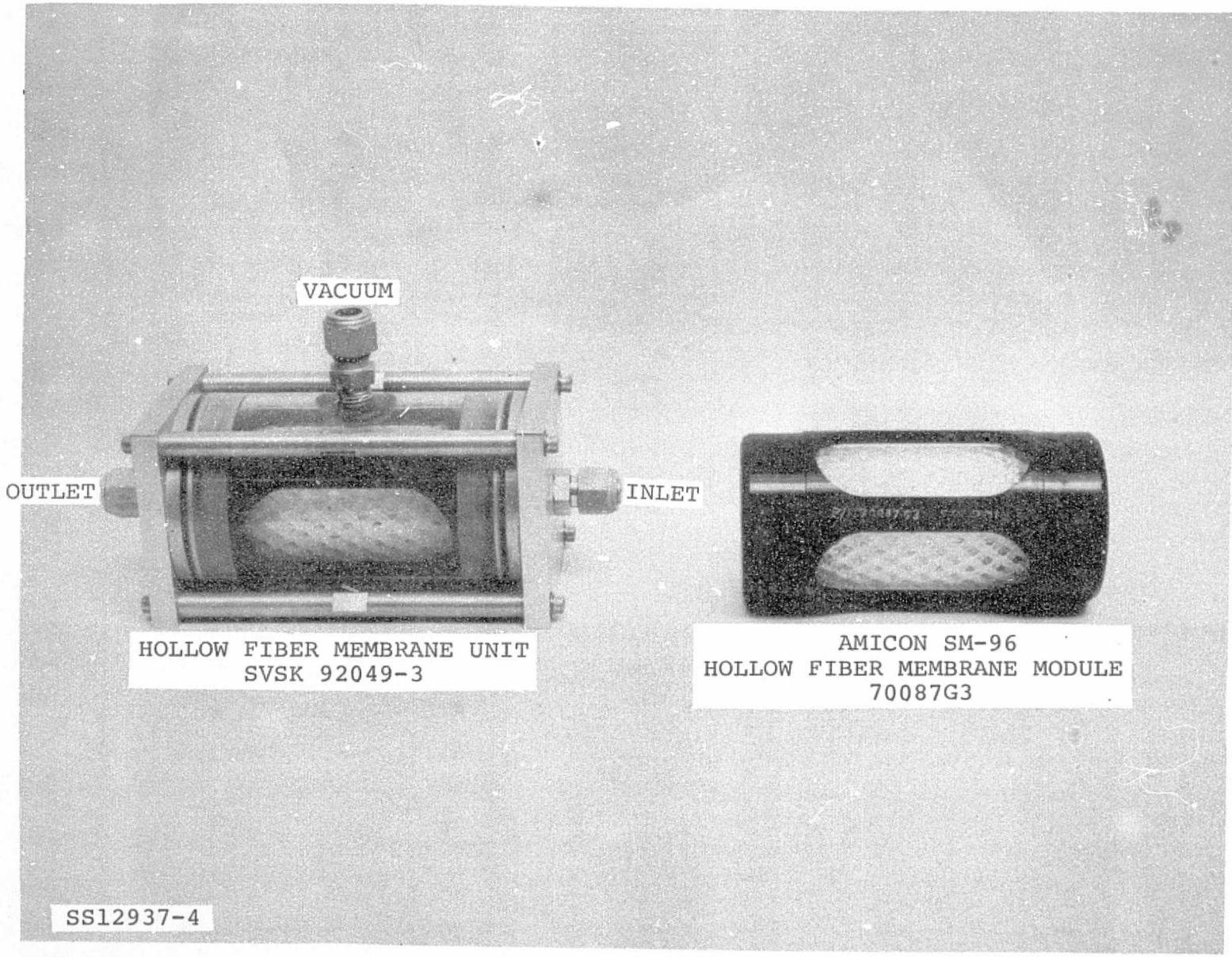
OUTLET

INLET

HOLLOW FIBER MEMBRANE UNIT
SVSK 92049-3

AMICON SM-96
HOLLOW FIBER MEMBRANE MODULE
70087G3

SS12937-4

FIGURE 42   DEAERATION HARDWARE

VACUUM AMBIENT

OUTLET

INLET

HOLLOW FIBER MEMBRANE UNIT
SVSK 92049-2

AMICON SM-I
HOLLOW FIBER MEMBRANE MODULES
70087G2

FIGURE 43   HEAT REJECTION HARDWARE

SS12939-4

BREADBOARD DEVELOPMENT TESTING

The objective of this task was to obtain data to allow verification of performance, evaluation of off-design conditions, verification of control modes, and the establishment of feasibility of the application. For each of the approved functional applications such as the bacteria filtration, dissolved gas deaeration, and heat rejection, a breadboard test was performed according to the Hollow Fiber Membrane Systems Test Plan included in Appendix B. In addition, a vibration test was conducted on a heat rejection HFM module to demonstrate that hollow fiber membranes are capable of withstanding exposure to vibration levels equivalent to the current Spacelab ECS qualification level.

Discussion of the Breadboard Development Testing task has been divided into three sections: Development Test Rationale, which presents the rationale for selecting the parameters to be tested; Development Testing, which presents the actual data obtained from the test program; and Test Evaluation, which evaluates the test results and generates parametric data for use in sizing hollow fiber membranes for subsequent application.

DEVELOPMENT TEST RATIONALE

BACTERIA FILTRATION

The purpose of the bacterial retention testing was to determine the capacity of the ultrafiltration canister to pass distilled water under a pressure gradient and, likewise, to retain bacterial and viral species.

Testing was to simulate an acute (or "single shot") situation with no attempt to determine filter life characteristics. If extended usage is anticipated, life testing will be required to see if flow will deteriorate due to pluggage or whether microorganisms which were originally retained by the membrane would eventually permeate.

Bacterial and viral agents were selected to be representative, not exhaustive. Since membranes reject on the basis of the size of the material to be rejected, it was believed that a representative distribution of bacterial sizes was most appropriate. For these tests all bacterial strains had traceable ATCC numbers, and all viral strains had traceable VR numbers. Pseudomonas aeruginosa was selected over pseudomonas diminui, even though the latter is smaller, because the former is more commonly encountered

and more often used as a reference molecule in the biological literature. In keeping with the representative nature of the study, retention of spore, fungi, and lichen were not quantitated, although it would appear that, so far as acute considerations are concerned, their retention could be inferred with reasonable certainty from the viral retention data.

DEAERATION

The purpose of the deaeration testing was to show the capability of the selected hollow fiber membrane unit to remove dissolved gas from a water stream. Dissolved oxygen was used in this test because of its adaptability to analysis.

Deaeration development tests were conducted with a representative hollow fiber membrane assembly containing 1,804 Amicon SM-96 fibers. Both proof pressure and leakage/permeation tests were run as quality control checks. Development performance data was obtained to determine the effects of water flow, chamber vacuum level, and dissolved oxygen concentration on deaeration performance. Originally, these data were intended to characterize solute diffusion through stagnant water contained in the membrane wall. Later, the data served to define characteristics which were apparently representative of solute diffusion through a flowing laminar stream inside a tube. Flow was varied between 6.3 and 28 g/hr-tube (0.014 and 0.061 lb/hr-tube) H_2O, while dissolved oxygen was varied between 7 and 32 g/m^3 (7 and 32 mg/l). Oxygen was utilized as the gaseous solute for all tests because of the relative ease and accuracy in determining its solution level with the available analysis equipment. Other gases would be expected to follow precisely the performance characteristics demonstrated in this test.

HEAT REJECTION

The heat rejection testing was performed to demonstrate that the selected hollow fiber membrane unit can provide a viable evaporative heat sink.

Membrane evaporator tests were defined to confirm conclusions reached during the Applications Study which predicted performance variation was a function of wall thermal conductance. In addition, the effects of module leakage/permeation level, which determines the unit's minimum heat rejection capacity on maximum thermal performance, was to be characterized. The units selected for test were 275 Amicon SM-I fiber assemblies specially selected by the manufacturer for low permeation.

Water flow was varied between 0.08 and 0.5 kg/hr-tube (0.18 and 1.1 lb/hr-tube), inlet water temperature between 13 and 32°C (55 and 90°F), and chamber vacuum between 1.2 and 1.3 kPa (8.6 and 9.8 mmHg). This is equivalent to an evaporant sink temperature between 8.9 and 10.9°C (48 and 51.7°F).

DEVELOPMENT TESTING

BACTERIA FILTRATION

Following fabrication of the test modules, a proof pressure test and a leakage/permeation test were conducted on each of the two units, P/N 70087G1, S/N 001 and S/N 002, to insure the integrity of the fibers and modules. Upon completion of the leakage/permeation test, the S/N 002 module was placed in a holder and subjected to a pressurized challenge solution in which bacteria agents had been injected. The ultrafiltrate which had passed through the membrane was collected and cultured to determine any presence of bacteria in the solution. The complete absence of bacteria in the ultrafiltrate would demonstrate successful performance of the unit. Upon completion of the bacteria challenge test, the S/N 002 module was sterilized and then subjected to a pressurized challenge solution in which viral agents had been injected. The ultrafiltrate which had passed through the membrane was collected and cultured to determine any presence of virus in the solution. The complete absence of virus in the ultrafiltrate would demonstrate successful performance of the unit.

Proof Pressure Test

Each of the test modules was placed in a holding fixture and plumbed according to Figure 44. With the module outlet closed, nitrogen pressure was slowly raised to an internal pressure of 124 kPa gauge (18 psig) and held for a minimum period of ten minutes. A visual observation showed that there was no rupture of the fibers or physical damage to either module.

Leakage/Permeation Test

With each module still plumbed in place per Figure 44, nitrogen pressure of 68.9 kPa gauge (10 psig) was slowly applied and held for 20 minutes. The leakage rate was measured by collecting the permeate in a gas collection bottle and found to be within the tolerance established in the test plan.

The modules were tested for pressure drop versus water flow characteristics using the setup of Figure 44. Water was flowed through the module at various driving pressures and the permeate flow rate recorded. Test results are shown in Table XII.

Leakage & Permeate
Collection

Pressure

Dead Ended — ⊗

Valve

Hollow Fiber
Module

N$_2$
or H$_2$O
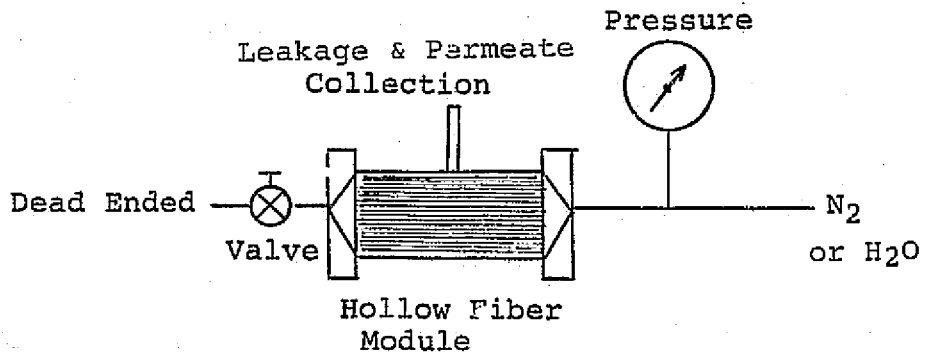
FIGURE 44 PROOF PRESSURE AND LEAKAGE/PERMEATION TEST SETUP

Subsequent to Bacteria/Virus testing and sterilization, the S/N 002 unit was retested for pressure drop versus permeate flow using the setup of Figure 44. These results are also shown in Table XII.

Table XII
Bacteria Filtration Leakage/Permeation Test

HFM Unit	Condition	Pressure	Fluid	Permeation Rate
70087G1 S/N 001	Pre-Bacteria	68.9 kPa gauge (10 psig)	N_2	0 cm^3/min
70087G1 S/N 002	Pre-Bacteria	68.9 kPa gauge (10 psig)	N_2	0 cm^3/min
70087G1 S/N 002	Pre-Bacteria	20.7 kPa gauge (3 psig)	H_2O	170 cm^3/min
70087G1 S/N 002	Post-Bacteria	34.5 kPa gauge (5 psig)	H_2O	126 cm^3/min
70087G1 S/N 002	Post-Bacteria	68.9 kPa gauge (10 psig)	H_2O	250 cm^3/min
70087G1 S/N 002	Post-Bacteria	103.4 kPa gauge (15 psig)	H_2O	376 cm^3/min
70087G1 S/N 001	Pre-Bacteria	6.9 kPa gauge (1 psig)	H_2O	105 cm^3/min
70087G1 S/N 001	Pre-Bacteria	13.8 kPa gauge (2 psig)	H_2O	208 cm^3/min
70087G1 S/N 001	Pre-Bacteria	20.7 kPa gauge (3 psig)	H_2O	307 cm^3/min

Bacteria/Virus Filtration

The hollow fiber membrane module, P/N 70087G1 S/N 002, was placed in the bacteria filtration fixture as illustrated in Figure 45. A challenge solution containing the bacterial agents and concentrations listed in Table XIII was formed by injecting suitable quantities of bacteria into the reservoir. The challenge solution was pressurized with nitrogen to 10 psig and allowed to pass through the membrane walls. The ultrafiltrate solution was cultured and analyzed for the presence of any of the bacteria agents.
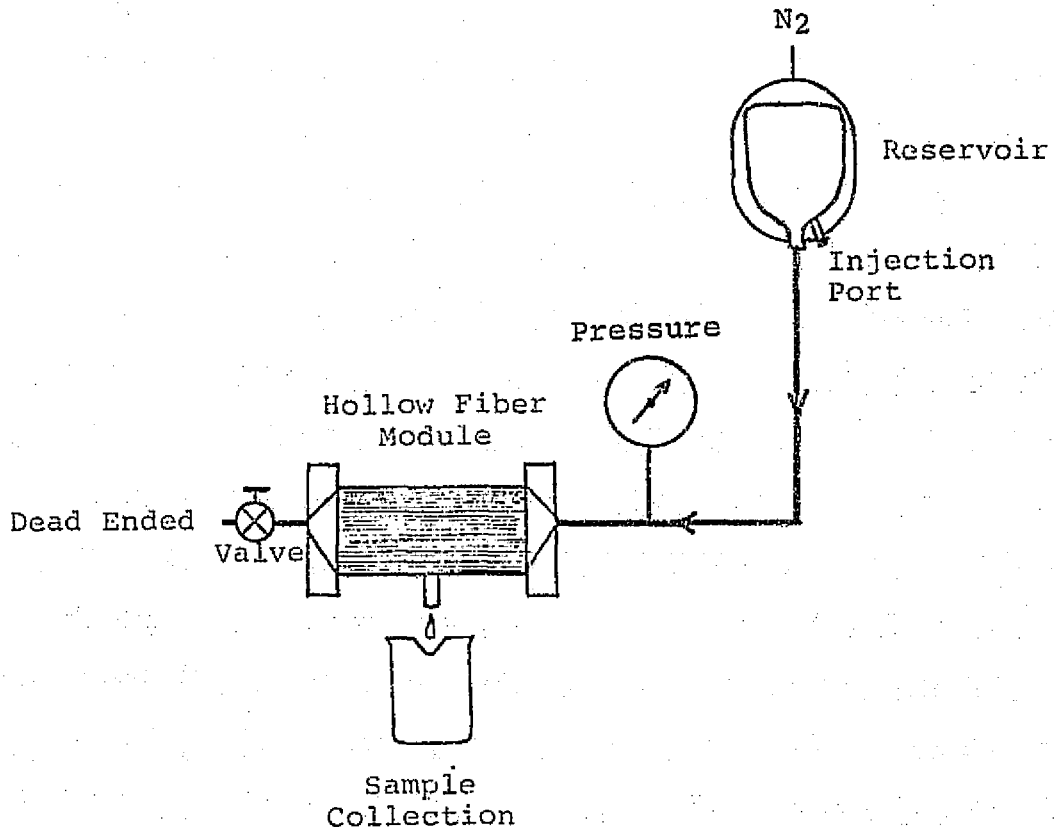
FIGURE 45 BACTERIAL FILTRATION SETUP

TABLE XIII
BACTERIA CHALLENGE SOLUTION AND ULTRAFILTRATE

	Colony Count per cm^3	
Agent	Challenge Fluid (Upstream)	Ultrafiltrate (Downstream)
Pseudomonas Aeruginosa	10^6	0
Escherichia Coli	10^6	0
Staphylococcus Aureus	10^6	0
Streptococcus Pyrogens	10^6	0
Klebsiella Species	10^6	0
Proteus Vulgaris	10^6	0
Salmonella Typhosa	10^6	0

TABLE XIV
VIRUS CHALLENGE SOLUTION AND ULTRAFILTRATE

	Plaque Count per cm^3	
Agent	Challenge Fluid (Upstream)	Ultrafiltrate (Downstream)
Coxsackie Virus A4	10^4	0
Echo Virus #2	10^4	0
Adenovirus-Human	10^4	0
Herpes Simplex	10^4	0
Vacinnia	10^4	0

The hollow fiber membrane module was sterilized, and the process was repeated for virus agents listed in Table XIV, followed by culturing and analysis of the ultrafiltrate solution. The results for the bacteria testing is listed in Table XIII, and the results for the virus testing is listed in Table XIV. Appendix C contains the Technical Report issued by the Microbiological Laboratory. Following the test, the module was sterilized and stored in an airtight container. The significance of the test results will be discussed in the following section.

DEAERATION

The candidate modules, P/N 70087G3, S/N 001 and S/N 002, were successfully proof pressure tested and leakage tested following manufacturing to insure the integrity of the fibers and modules.

The test module, S/N 002, was placed in the Rig #8 Vacuum Test Chamber in the Space Systems Department Space Laboratory. Oxygen enriched water was allowed to flow in various quantities through the membrane in the vacuum environment. Samples for analysis taken from the inlet and outlet of the test module provided evidence of the degree of deaeration.

Proof Pressure Test

Each test module was placed in a holding fixture and plumbed according to Figure 44. Figure 46 shows the actual test apparatus. Distilled water was allowed to flow through the membrane, and the outlet was closed. The water pressure was slowly raised to an internal pressure of 124 kPa gauge (18 psig) and held for a period of 10 minutes. A visual observation showed that there was no rupture in the fibers or physical damage to either of the modules.

Leakage/Permeation Test

With each module still plumbed in place per Figure 44, the water pressure was slowly increased to 68.9 kPa gauge (10 psig) and held for 20 minutes. Water leakage through the membrane was collected and measured during that time. Test results, shown in Table XV, indicate that the unit was within the tolerance set forth by the Test Plan and was suitable for deaeration testing. The above tests were performed following manufacture and also prior to the dissolved gas deaeration test.

VALVE

HOLLOW FIBER MEMBRANE MODULE

H2O SUPPLY TANK

N2 SUPPLY

PRESSURE GAUGE

TEST GAUGE

N2 PRESSURE REGULATOR

SAMPLE COLLECTION

SS12938-4
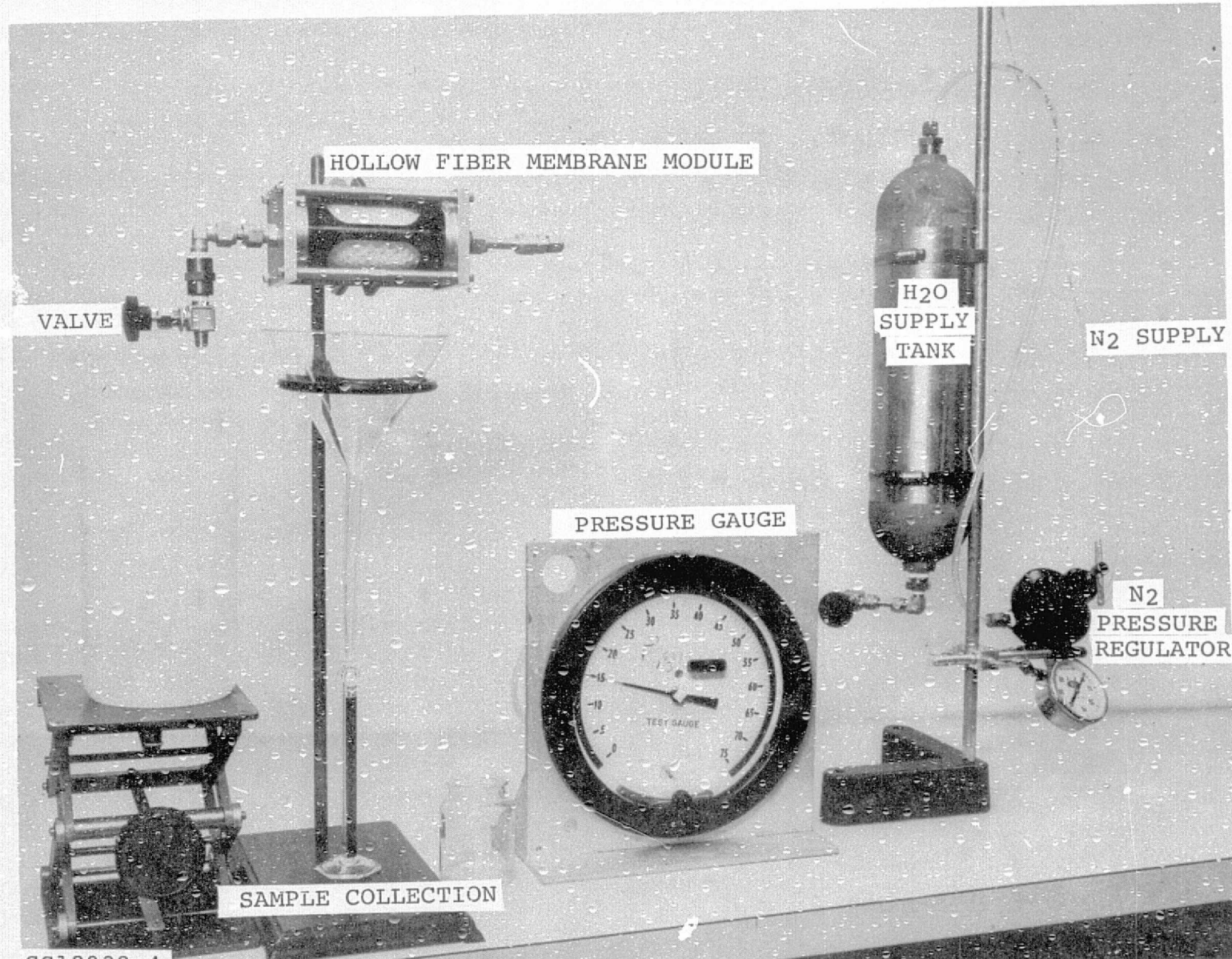
FIGURE 46   PROOF PRESSURE TEST AND LEAKAGE/PERMEATION TEST SETUP

TABLE XV
DEAERATION LEAKAGE/PERMEATION TEST

HFM Unit	Fluid	Pressure	Time	Permeation Rate
70087G3 S/N 001	H_2O	68.9 kPa gauge (10 psig)	20 min	1.45 cm^3/min
70087G3 S/N 002	H_2O	68.9 kPa gauge (10 psig)	20 min	1.00 cm^3/min

Deaeration of Dissolved Oxygen Test

The hollow fiber membrane module, P/N 70087G3 S/N 002, was placed in the holder located in the vacuum chamber of Rig #8 and plumbed as shown schematically in Figure 47. Figure 48 shows the actual Rig #8 test setup, and Figure 49 shows a close-up of the module in the vacuum chamber. The supply water, which was at room temperature, was highly saturated with oxygen by bubbling 42 cm^3/min through a sparger at 165 kPa abs (24 psia). This method provided a concentration up to 32 g/m^3 (32 mg/liter) of dissolved oxygen in the supply water. The chamber pressure was reduced to 3.5 kPa abs (0.5 psia), and the water allowed to flow through the membrane at the rate of 45.4 kg/lb (100 lb/hr). A sample of the outlet water was taken, and the remaining dissolved oxygen analyzed by the Azide Modification of the Winkler Method. The flow was reduced to 22.7 kg/hr (50 lb/hr) and 11.3 kg/hr (25 lb/hr) respectively with an outlet water sample taken at each condition for analysis. The chamber pressure was then reduced to 2.1 kPa abs (0.3 psia), and the flow restored to 45.4 kg/hr (100 lb/hr). A sample of exit water was taken and analyzed for remaining oxygen. The results of the analyses are recorded in Table XVI. The significance of the test results will be discussed in the following section.

HEAT REJECTION

The test modules, P/N 70087G2, S/N 001, S/N 002, and S/N 004, were submitted to proof pressure tests and leakage/permeation tests after manufacture to insure the integrity of the fibers and modules.

Heat rejection testing was performed by circulating water at various temperatures and flow levels inside the hollow fibers of the module which was placed in the Rig #8 vacuum chamber. The evaporation which took place through the membrane lowered the temperature of the exit water. Measurements were taken after each test condition had stabilized.

Proof Pressure Test

Each test module was placed in the pressure/leakage test fixture shown schematically in Figure 44 and the water lines plumbed accordingly. Figure 46 shows the actual test apparatus. The pressure in the water tank was slowly raised to 124 kPa gauge (18 psig) and held at that pressure for a minimum of 10 minutes. Visual observation showed that there was no rupture in the fibers or physical damage to the module.

Pressurized
Supply Tank

Vent

N_2

H_2O

Pressure

Vac. Chmbr

H.F.M. Cartrige

Receiver
Tank

Flowmeter

Inlet
Sample

Outlet
Sample

H_2O

O_2
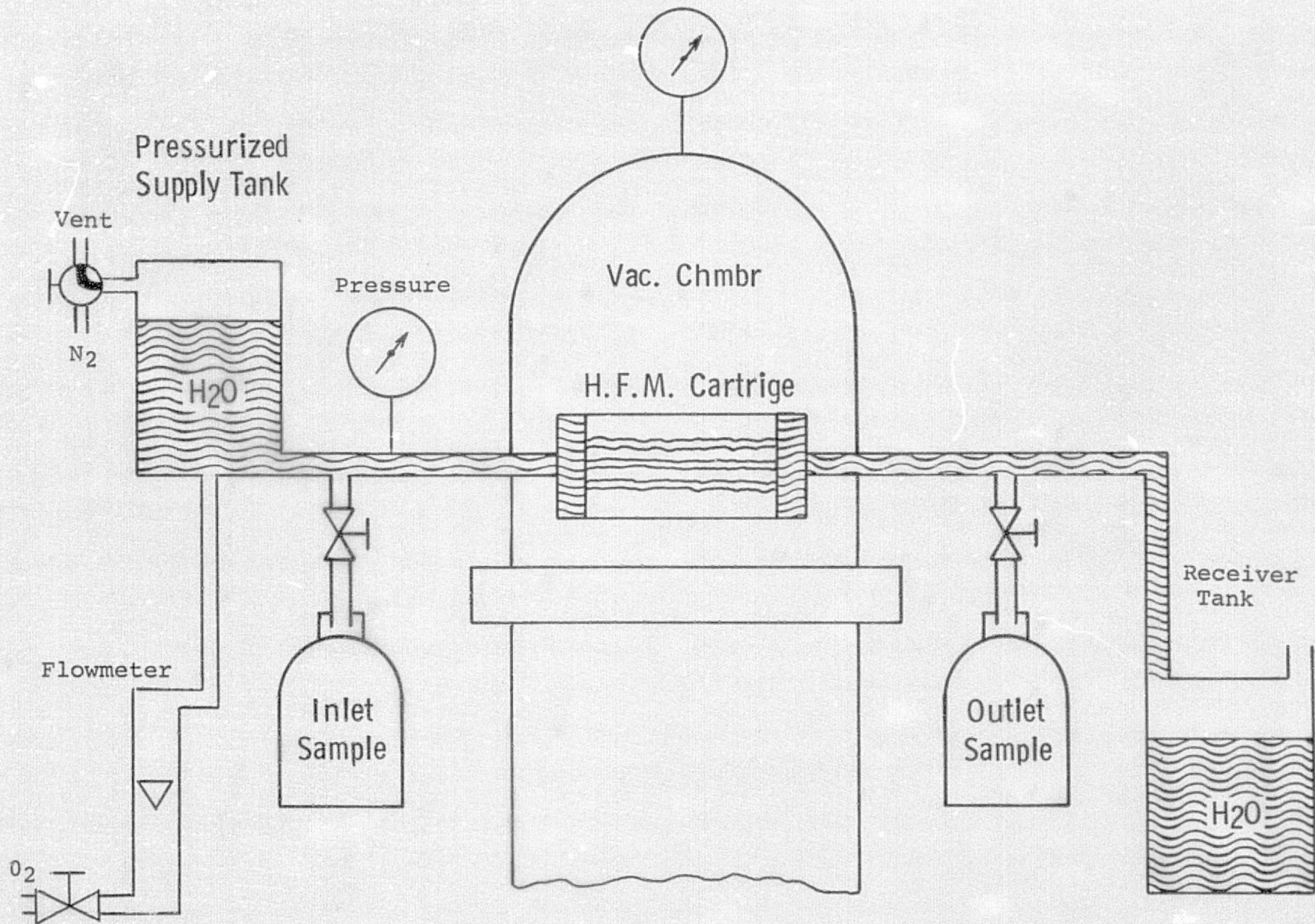
FIGURE 47 DISSOLVED OXYGEN TEST
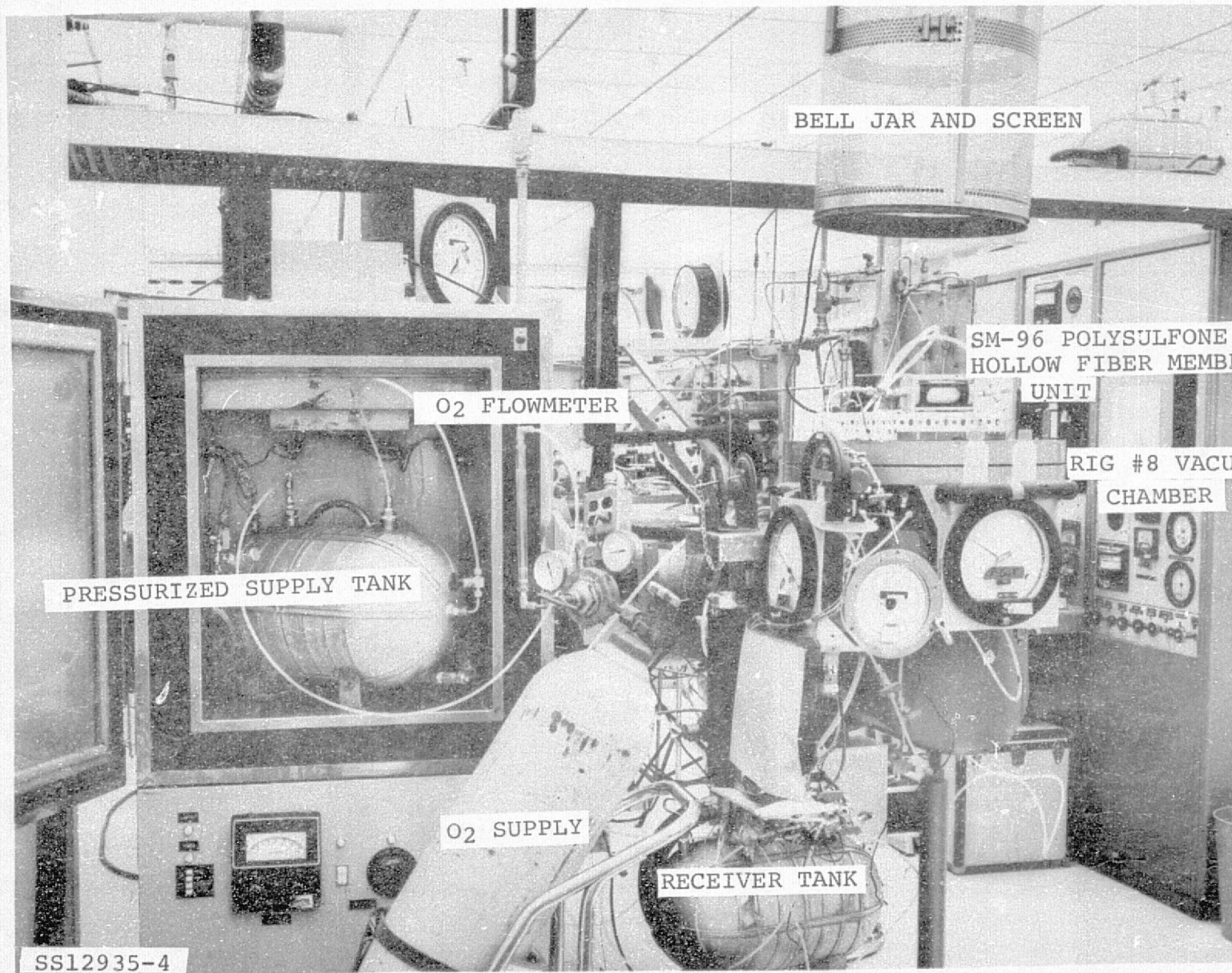
HAMILTON STANDARD
Division of
UNITED
TECHNOLOGIES™

SVHSER 7100

110

BELL JAR AND SCREEN

SM-96 POLYSULFONE
HOLLOW FIBER MEMBRANE
UNIT

O2 FLOWMETER

RIG #8 VACUUM
CHAMBER

PRESSURIZED SUPPLY TANK

O2 SUPPLY

RECEIVER TANK

SS12935-4

FIGURE 48   DEAERATION TEST SETUP

SM-96 POLYSULFONE HOLLOW FIBER MEMBRANE UNIT

THERMOCOUPLE

THERMOCOUPLE

RIG #8 VACUUM CHAMBER BASE

WATER SAMPLE BOTTLES

SS12936-4
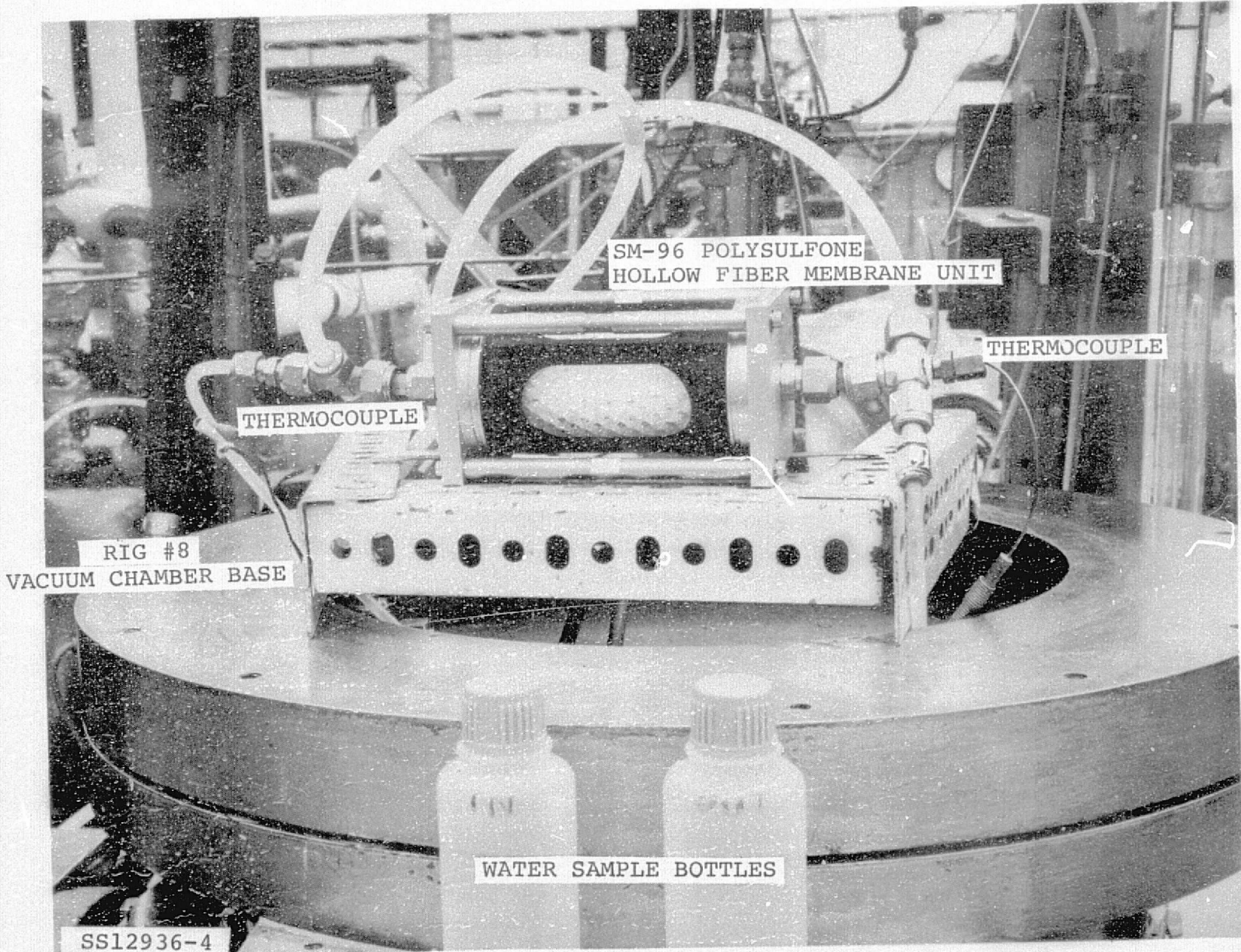
FIGURE 49   DEAERATION UNIT IN RIG #8 VACUUM CHAMBER

HAMILTON STANDARD Division of UNITED TECHNOLOGIES™

TABLE XVI
DEAERATION OF DISSOLVED OXYGEN TEST RESULTS

Module 70057G3 S/N 002

Chamber Press. kPa abs (psia)	Flow kg/hr (lb/hr)	Diss. O_2 g/m^3 (mg/l)	O_2 Removed g/m^3 (mg/l)
3.4 (0.5)	45.4 (100)	7 (7)	2 (2)
3.4 (0.5)	22.7 (50)	7 (7)	2 (2)
3.4 (0.5)	11.3 (25)	7 (7)	3 (3)
2.1 (0.3)	45.4 (100)	7 (7)	3 (3)
3.4 (0.5)	45.4 (100)	13 (13)	4 (4)
3.4 (0.5)	22.7 (50)	13 (13)	5 (5)
3.4 (0.5)	11.3 (25)	13 (13)	7 (7)
2.1 (0.3)	45.4 (100)	13 (13)	4 (4)
3.4 (0.5)	49.9 (110)	30 (30)	0 (0)
3.4 (0.5)	22.7 (50)	30 (30)	4 (4)
3.4 (0.5)	11.3 (25)	30 (30)	14 (14)
2.1 (0.3)	49.9 (110)	30 (30)	3 (3)
3.4 (0.5)	49.9 (110)	32 (32)	11 (11)
3.4 (0.5)	22.7 (50)	32 (32)	14 (14)
3.4 (0.5)	11.3 (25)	32 (32)	19 (19)
2.1 (0.3)	49.9 (110)	32 (32)	11 (11)
3.4 (0.5)	49.9 (110)	21 (21)	4 (4)
3.4 (0.5)	22.7 (50)	21 (21)	5 (5)
3.4 (0.5)	11.3 (25)	21 (21)	10 (10)
3.4 (0.5)	49.9 (110)	21 (21)	3 (3)

Leakage/Permeation Test

With each module still plumbed in place per Figure 44, the water pressure was slowly increased to 68.9 kPa gauge (10 psig) and held for 20 minutes. Water leakage was collected in a graduate and found to be within acceptable limits. Table XVII summarizes the leakage/permeation test results.

Heat Rejection Test

Each of the hollow fiber membrane modules, P/N 70087G2 S/N 001, S/N 002, and S/N 004, was placed, in turn, in the holder inside the vacuum chamber of Rig #8 and plumbed to the water lines as shown schematically in Figure 50. Figure 51 shows the actual test setup. The water tank was filled with distilled water at 18.3°C (65°F) and placed in the environmental chamber. The pump was started and water allowed to circulate at the rate of 136 kg/hr (300 lb/hr). The vacuum chamber pressure was reduced to 1.3 kPa abs (9.8 mmHg). When stability was attained, the inlet/outlet temperatures and pressures were recorded. The flow was then reduced in steps to 109 kg/hr (240 lb/hr), 81.6 kg/hr (180 lb/hr), 40.8 kg/hr (90 lb/hr), and 22.7 kg/hr (50 lb/hr) respectively. Temperature and pressure data were recorded when stability at each condition was attained.

The chamber pressure was further reduced to 1.14 kPa abs (8.6 mmHg), and the above flow levels were repeated with corresponding data on inlet/outlet temperatures and pressures recorded. With the chamber pressure remaining at 1.14 kPa abs. (8.6 mmHg), the water temperature was lowered to 12.8°C (55°F), and the flow conditions repeated. Data was recorded at temperature and pressure levels when stability was attained. Finally, the chamber pressure was increased to 1.3 kPa abs (9.8 mmHg), and the water temperature elevated to 32.2°C (90°F). Again, pressure and temperature were read following equilibrium at each flow condition. The data for the above tests is presented in Table XVIII. The significance of the test results will be discussed in the following section.

VIBRATION TESTING

The purpose of vibration testing of the hollow fiber membrane module was to determine the effect, if any, of subjecting the module to the Spacelab ECS qualification level vibration spectrum. Figure 52 shows the heat rejection module 70087G2 S/N 002 in place on the shaker head. Figure 53 shows the Spacelab ECS qualification level specification with tolerance band. The test duration time was ten minutes.

HAMILTON STANDARD Division of UNITED TECHNOLOGIES™

TABLE XVII
HEAT REJECTION LEAKAGE/PERMEATION TEST

HFM Unit	Fluid	Pressure	Time	Permeation Rate
70087G2 S/N 001	H_2O	68.9 kPa gauge (10 psig)	20 min	0.24 cm^3/min
70087G2 S/N 002	H_2O	68.9 kPa gauge (10 psig)	20 min	0.51 cm^3/min
70087G2 S/N 004	H_2O	68.9 kPa gauge (10 psig)	20 min	0.88 cm^3/min
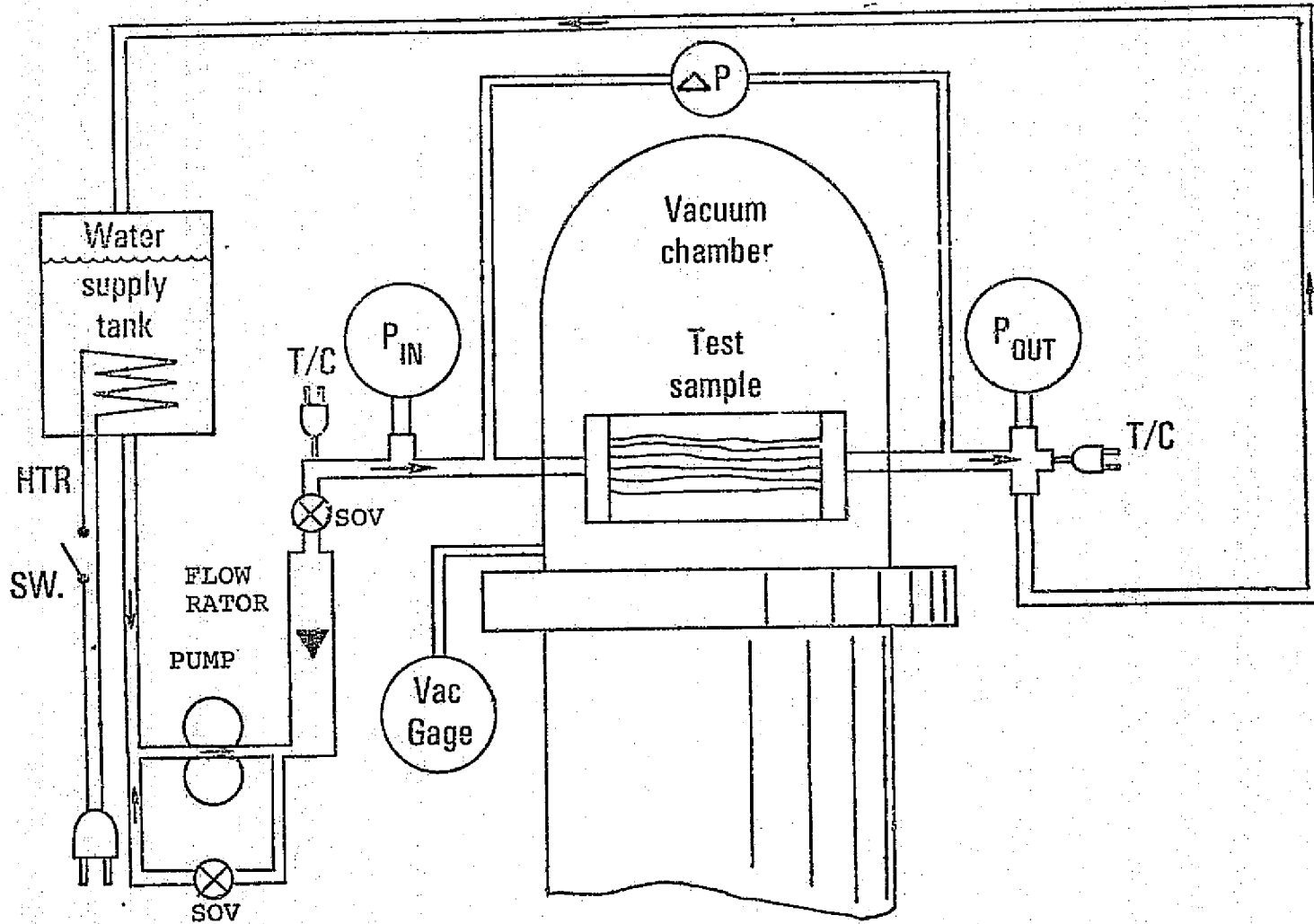
FIGURE 50   HEAT REJECTION TEST
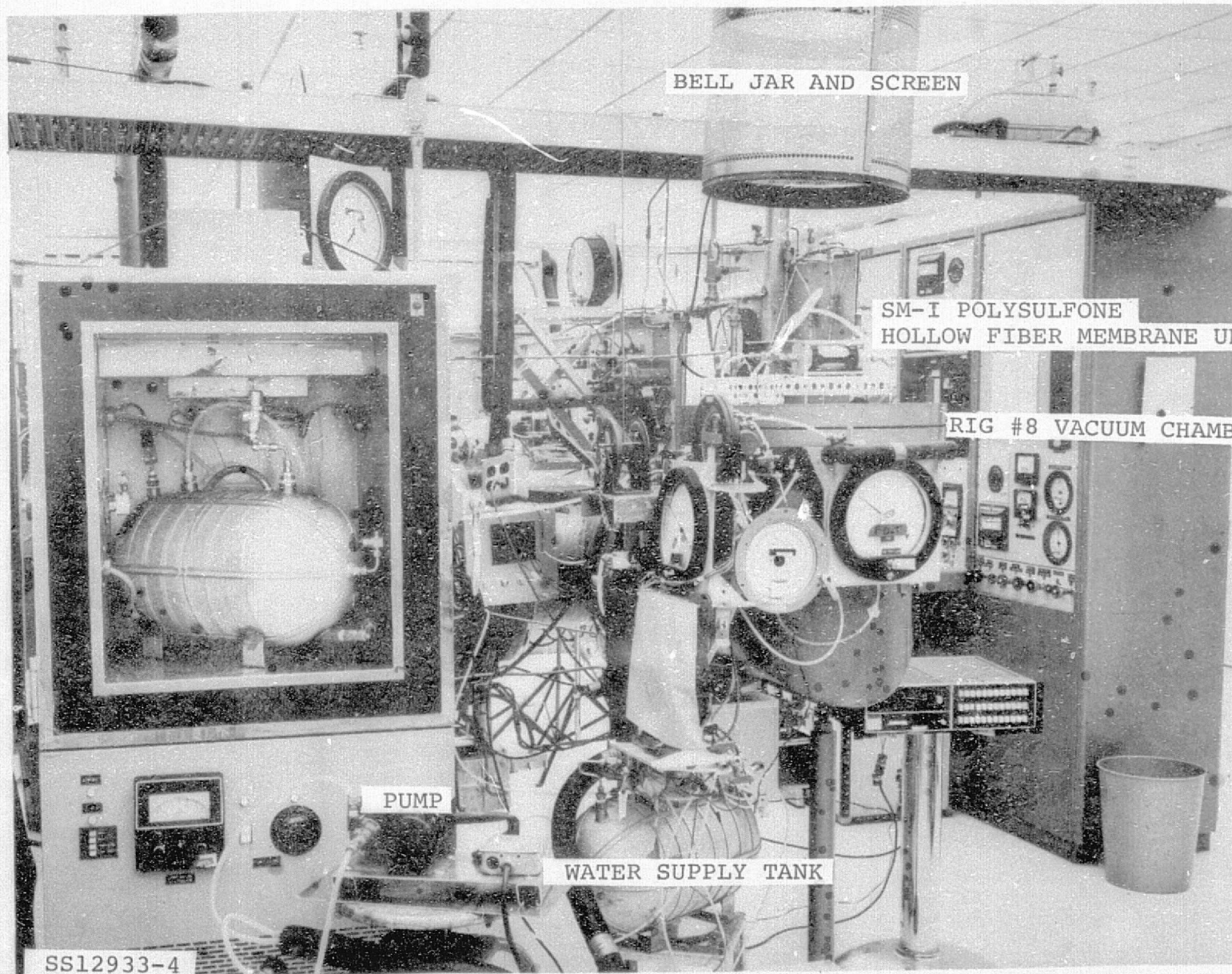
FIGURE 51   HEAT REJECTION TEST SETUP

BELL JAR AND SCREEN

SM-I POLYSULFONE
HOLLOW FIBER MEMBRANE UNIT

RIG #8 VACUUM CHAMBER

PUMP

WATER SUPPLY TANK

SS12933-4

HAMILTON STANDARD

Division of
UNITED
TECHNOLOGIES

SVHSER 7100

117

TABLE XVIII
Heat Rejection Test Results

Test Module: 70087G2-001

Test Log No.   13904

W		P		Pch		Ts		T_1		T_2		Q		UA	
kg/hr	(lb/hr)	kPa	(psi)	kPa	(mmHg)	°C	(°F)	°C	(°F)	°C	(°F)	W	(Btu/hr)	W/°C	(Btu/hr-°F)
118	(260)	22.7	(3.3)	1.31	(9.8)	10.9	(51.7)	31.5	(88.7)	25.6	(78.0)	815	(2782)	46.77	(88.74)
109	(240)	20.0	(2.9)	1.31	(9.8)	10.9	(51.7)	32.1	(89.8)	26.1	(78.9)	766	(2615)	42.63	(80.89)
81.6	(180)	13.8	(2.0)	1.31	(9.85)	11.1	(51.9)	32.2	(90.0)	24.5	(76.1)	733	(2502)	43.04	(81.68)
40.8	(90)	5.5	(0.8)	1.32	(9.9)	11.1	(52.0)	31.8	(89.3)	20.4	(68.8)	541	(1845)	37.83	(71.79)
22.7	(50)	4.1	(0.6)	1.31	(9.8)	10.9	(51.7)	31.6	(89.0)	17.0	(62.6)	387	(1320)	32.42	(61.51)
136	(300)	38.6	(5.6)	1.14	(8.6)	8.9	(48.0)	12	(54.7)	11.7	(53.0)	149	(510)	46.26	(87.78)
109	(240)	28.9	(4.2)	1.14	(8.6)	8.9	(48.0)	12	(54.4)	11.4	(52.5)	134	(456)	44.58	(84.60)
81.6	(180)	20.7	(3.0)	1.14	(8.6)	8.9	(48.0)	12.6	(54.6)	11.2	(52.2)	127	(432)	42.88	(81.36)
40.8	(90)	13.8	(2.0)	1.16	(8.7)	9.2	(48.6)	13.3	(55.9)	11.1	(51.9)	105	(360)	37.64	(71.43)
22.7	(50)	5.5	(0.8)	1.14	(8.6)	8.9	(48.0)	13.8	(56.9)	10.3	(50.5)	94	(320)	33.46	(63.49)
136	(300)	34.5	(5.0)	1.14	(8.6)	8.9	(48.0)	11.7	(53.1)	11.2	(52.2)	79	(270)	30.67	(58.19)
109	(240)	31.7	(4.6)	1.14	(8.6)	8.9	(48.0)	11.8	(53.3)	11.2	(52.2)	77	(264)	29.41	(55.81)
81.6	(180)	22.7	(3.3)	1.14	(8.6)	8.9	(48.0)	11.7	(53.0)	10.7	(51.2)	95	(324)	42.37	(80.39)
40.8	(90)	11.7	(1.7)	1.14	(8.6)	8.9	(48.0)	12.8	(55.0)	10.7	(51.2)	100	(342)	37.16	(70.52)
22.7	(50)	6.9	(1.0)	1.14	(8.6)	8.9	(48.0)	13.8	(56.9)	10.4	(50.7)	91	(310)	31.42	(59.62)

TABLE XVIII Continued

Test Module: 70087G2-002

W		P		Pch		Ts		T_1		T_2		Q		UA	
kg/hr	(lb/hr)	kPa	(psi)	kPa	(mmHg)	°C	(°F)	°C	(°F)	°C	(°F)	W	(Btu/hr)	W/°C	(Btu/hr-°F)
136	(300)	43.4	(6.3)	1.14	(8.6)	8.9	(48.0)	13.4	(56.2)	12.4	(54.4)	158	(540)	39.20	(74.38)
109	(240)	33.8	(4.9)	1.14	(8.6)	8.9	(48.0)	12.8	(55.1)	11.6	(52.9)	155	(528)	46.92	(89.03)
81.6	(180)	26.2	(3.8)	1.14	(8.6)	8.9	(48.0)	12.8	(55.1)	11.7	(53.1)	105	(360)	31.41	(59.60)
40.8	(90)	9.0	(1.3)	1.14	(8.6)	8.9	(48.0)	13.5	(56.3)	11.2	(52.2)	108	(369)	32.36	(61.40)
22.7	(50)	4.8	(0.7)	1.14	(8.6)	8.9	(48.0)	13.2	(55.9)	10.4	(50.7)	76	(260)	28.31	(53.72)
136	(300)	41.3	(6.0)	1.31	(9.8)	10.9	(51.7)	17.8	(64.1)	16.3	(61.4)	237	(810)	38.84	(73.70)
109	(240)	31.0	(4.5)	1.28	(9.65)	10.7	(51.3)	17.7	(64.0)	15.9	(60.7)	232	(792)	38.08	(72.26)
81.6	(180)	22.0	(3.2)	1.31	(9.8)	10.9	(51.7)	17.8	(64.1)	15.6	(60.0)	216	(738)	38.09	(72.28)
40.8	(90)	9.0	(1.3)	1.29	(9.7)	10.8	(51.5)	18.2	(64.7)	14.3	(57.8)	182	(621)	35.08	(66.56)
22.7	(50)	5.5	(0.8)	1.31	(9.8)	10.9	(51.7)	19.1	(66.3)	13.3	(55.9)	152	(520)	32.82	(62.28)
136	(300)	40.0	(5.8)	1.14	(8.6)	8.9	(48.0)	18.2	(64.7)	16.3	(61.3)	299	(1020)	35.98	(68.27)
109	(240)	29.6	(4.3)	1.14	(8.6)	8.9	(48.0)	18.2	(64.8)	16.0	(60.8)	281	(960)	34.39	(65.26)
81.6	(180)	22.0	(3.2)	1.14	(8.6)	8.9	(48.0)	18.2	(64.8)	15.4	(59.8)	264	(900)	33.52	(63.60)
40.8	(90)	10.3	(1.5)	1.14	(8.6)	8.9	(48.0)	18.8	(65.9)	14.1	(57.4)	224	(765)	30.54	(57.95)
22.7	(50)	5.5	(0.8)	1.14	(8.6)	8.9	(48.0)	18.8	(65.9)	12.5	(54.5)	167	(570)	26.70	(50.67)
136	(300)	34.5	(5.0)	1.31	(9.8)	10.9	(51.7)	31.2	(88.1)	26.3	(79.4)	765	(2610)	43.19	(81.95)
109	(240)	24.9	(3.6)	1.31	(9.8)	10.9	(51.7)	31.1	(88.0)	25.6	(78.0)	703	(2400)	40.76	(77.34)
81.6	(180)	17.2	(2.5)	1.31	(9.8)	10.9	(51.7)	31.2	(88.2)	24.4	(75.9)	649	(2214)	38.98	(73.97)
40.8	(90)	9.0	(1.3)	1.31	(9.8)	10.9	(51.7)	31.7	(89.0)	20.9	(69.7)	509	(1737)	34.56	(65.57)
22.7	(50)	4.1	(0.6)	1.31	(9.8)	10.9	(51.7)	31.9	(89.4)	17.6	(63.6)	378	(1290)	30.39	(57.67)

TABLE XVIII Continued

Test Module: 70087G2-004

W		P		Pch		Ts		T$_1$		T$_2$		Q		UA	
kg/hr	(lb/hr)	kPa	(psi)	kPa	(mmHg)	°C	(°F)	°C	(°F)	°C	(°F)	W	(Btu/hr)	W/°C	(Btu/hr-°F)
136	(300)	35.8	(5.2)	1.14	(8.6)	8.9	(48.0)	12.6	(54.6)	11.2	(52.1)	220	(750)	75.31	(142.9)
109	(240)	27.6	(4.0)	1.13	(8.5)	8.7	(47.6)	12.2	(54.0)	11.0	(51.8)	155	(528)	53.28	(101.1)
81.6	(180)	21.4	(3.1)	1.14	(8.6)	8.9	(48.0)	12.1	(53.8)	10.3	(50.6)	169	(570)	76.10	(144.4)
40.8	(90)	10.3	(1.5)	1.14	(8.6)	8.9	(48.0)	12.8	(55.1)	9.9	(49.9)	137	(468)	62.61	(118.8)
22.7	(50)	7.6	(1.1)	1.14	(8.6)	8.9	(48.0)	13.9	(57.0)	9.7	(49.5)	110	(375)	47.17	(89.5)
136	(300)	34.5	(5.0)	1.14	(8.6)	8.9	(48.0)	17.3	(63.1)	13.9	(57.0)	536	(1830)	81.84	(155.3)
109	(240)	25.5	(3.7)	1.15	(8.65)	9.1	(48.4)	17.6	(63.6)	13.6	(56.4)	506	(1728)	81.16	(154.0)
81.6	(180)	18.6	(2.7)	1.14	(8.6)	8.9	(48.0)	17.7	(63.9)	12.9	(55.3)	454	(1548)	73.83	(140.1)
40.8	(90)	9.0	(1.3)	1.14	(8.6)	8.9	(48.0)	18.0	(64.4)	11.1	(52.0)	327	(1116)	66.93	(127.0)
22.7	(50)	4.8	(0.7)	1.14	(8.6)	8.9	(48.0)	18.9	(66.0)	9.9	(49.9)	236	(805)	59.23	(112.4)
136	(300)	33.0	(4.8)	1.31	(9.8)	10.9	(51.7)	17.3	(63.1)	14.5	(58.1)	440	(1500)	91.28	(173.2)
109	(240)	24.1	(3.5)	1.30	(9.75)	10.8	(51.5)	17.7	(63.8)	14.3	(57.8)	422	(1440)	84.58	(160.5)
81.6	(180)	17.9	(2.6)	1.31	(9.8)	10.9	(51.7)	18.0	(64.4)	14.0	(57.2)	380	(1296)	79.42	(150.7)
40.8	(90)	9.0	(1.3)	1.31	(9.8)	10.9	(51.7)	18.6	(65.5)	12.5	(54.5)	290	(990)	75.62	(143.5)
22.7	(50)	4.8	(0.7)	1.31	(9.8)	10.9	(51.7)	19.4	(67.0)	11.7	(53.0)	205	(700)	64.93	(123.2)
136	(300)	26.9	(3.9)	1.14	(9.6)	10.7	(51.2)	32.8	(91.1)	23.4	(74.1)	1494	(5100)	87.80	(166.6)
109	(240)	20.7	(3.0)	1.32	(9.9)	11.2	(52.1)	32.1	(89.7)	22.0	(71.6)	1273	(4344)	83.06	(157.6)
81.6	(180)	15.2	(2.2)	1.31	(9.8)	10.9	(51.7)	31.8	(89.3)	20.3	(68.5)	1097	(3744)	76.42	(145.0)
40.8	(90)	7.6	(1.1)	1.31	(9.8)	10.9	(51.7)	32.0	(89.6)	15.9	(60.6)	765	(2610)	68.72	(130.4)
22.7	(50)	5.5	(0.8)	1.31	(9.8)	10.9	(51.7)	32.3	(90.1)	13.1	(55.5)	507	(1730)	60.92	(115.6)
136	(300)	27.6	(4.0)	1.31	(9.85)	11.1	(51.9)	30.7	(87.3)	22.4	(72.4)	1310	(4470)	86.38	(163.9)
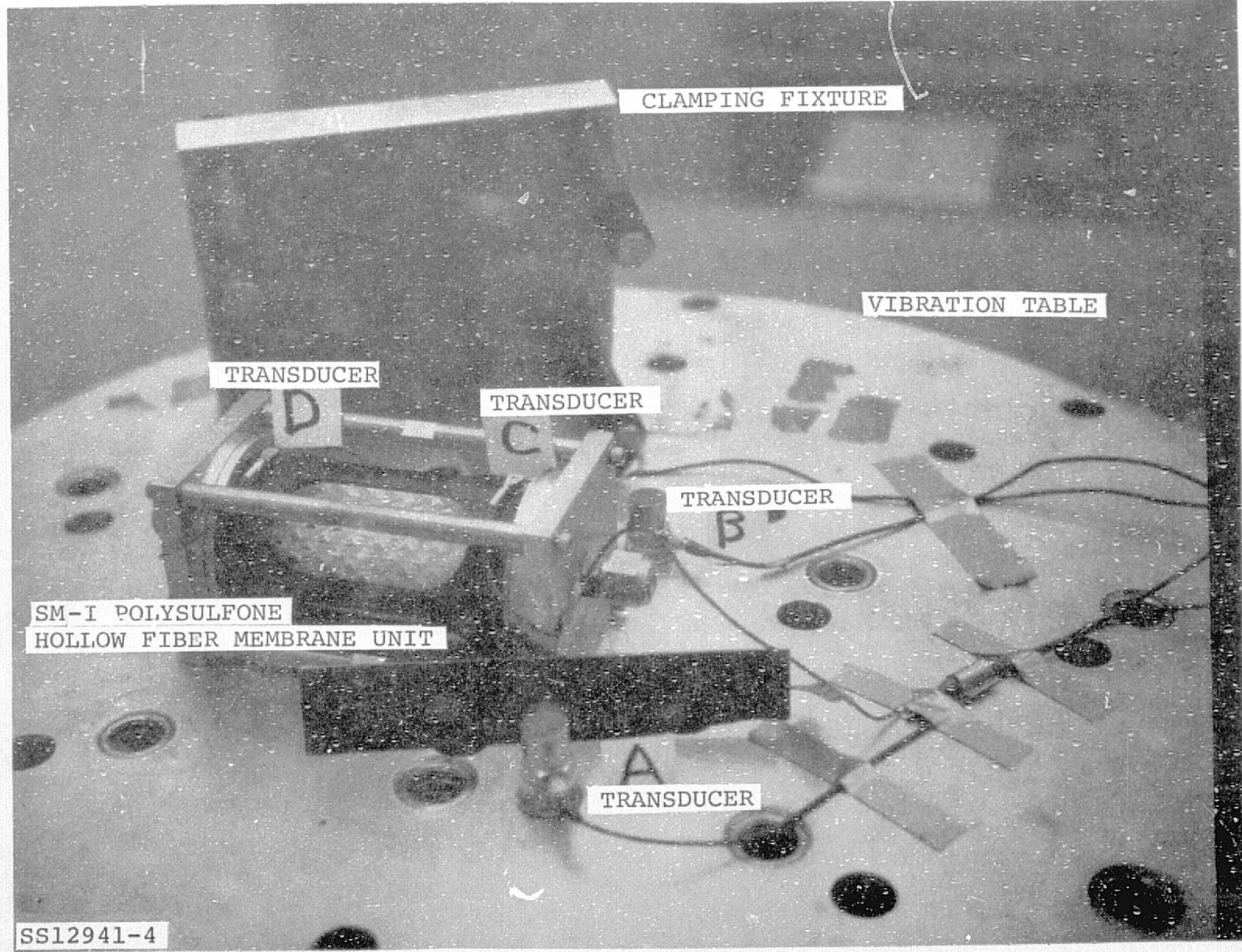
FIGURE 52   VIBRATION TEST SETUP

A leakage test was run on the module using the test setup of
Figure 44 before and after vibration testing to uncover any
structural change that occurred to either the fibers or the
module.

Figures 54 and 55 show the frequency response at point C and D
respectively, as defined by Figure 52. These figures show that
the vibration was introduced to the module with minimum amplifi-
cation or attenuation. Vibration was conducted in one axis only,
the axis perpendicular to the fiber orientation. The second axis
is identical to the first, i.e., perpendicular to the fiber
orientation, and the third axis, coincident with the fiber orien-
tation, was judged significantly less severe than the first two
axes.

Upon completion of vibration testing, the module was visually
examined, and no damage was noted.

Post vibration leakage was measured at 0.15 cm^3/min of H_2O at
68.9 kPa (10 psi) pressure differential, sufficiently close to
the previbration leakage of 0.14 cm^3/min of H_2O at 68.9 kPa
(10 psi) pressure differential to conclude that no internal
damage occurred. This leakage is transmembrane permeation; a
broken membrane would increase the leakage rate significantly.

TEST EVALUATION

The hollow fiber membrane hardware evaluated and tested during
the conduct of this program represents new components with viable
potential in many applications. An understanding of the heat
and/or mass transport phenomena which dominate a particular new
process is necessary to conceive new applications and to permit
accurate scaling of development data to a new situation. Tailor-
ing the material and structure configuration to a desired end
permits even more flexibility in design optimization for achiev-
ing characteristics compatible to a potential application.

Analytical models correlating acquired data to published rela-
tionships are a valuable aid in this development process. The
three applications selected for test are excellent examples of
the many and varied performance characteristics obtainable with
HFM technology. The results of this development testing has
shown that:

-   The Romicon GM-80 bacteria filter can be sized based on
    laminar transmembrane flow.
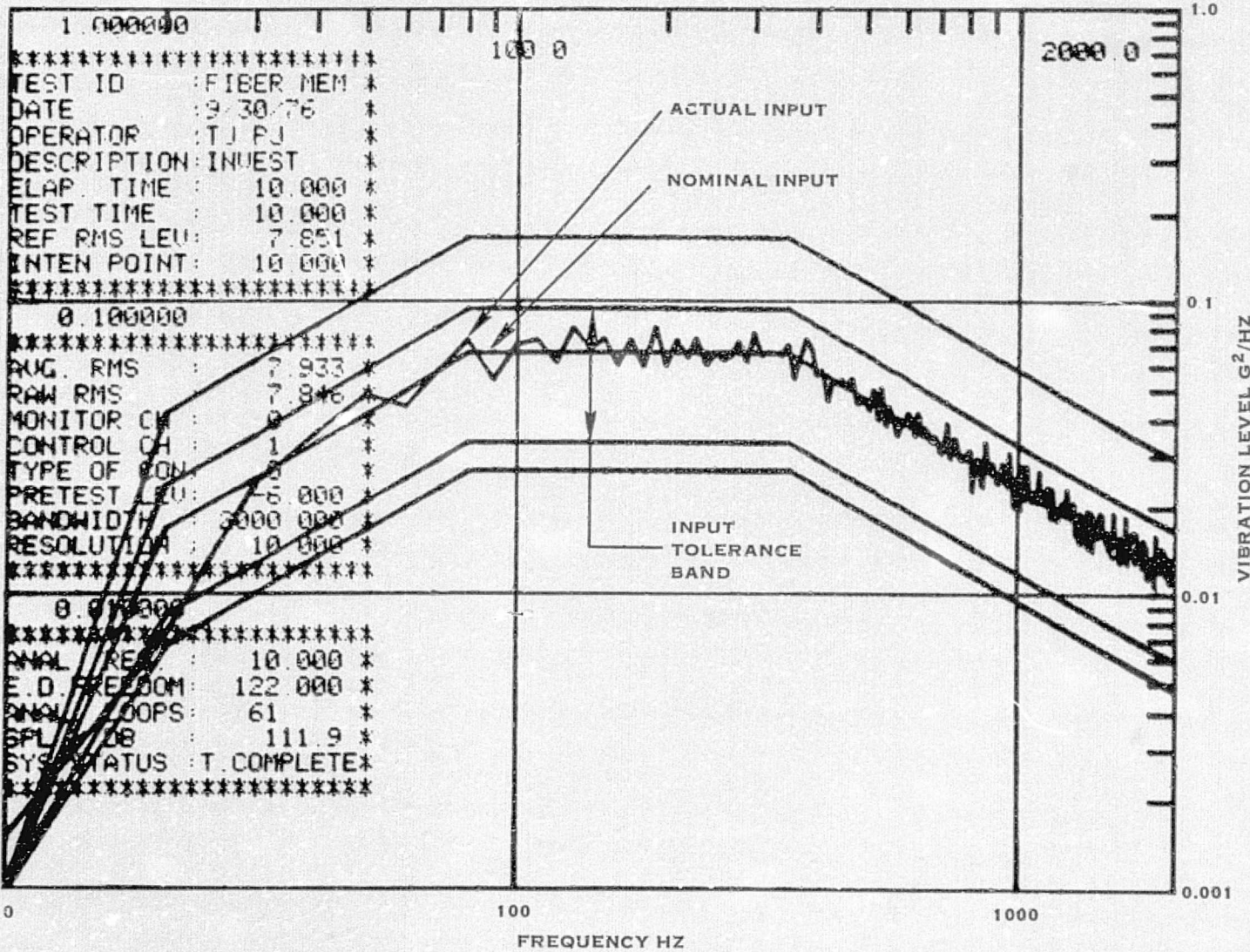
FIGURE 53. MODULE VIBRATION INPUT LEVEL
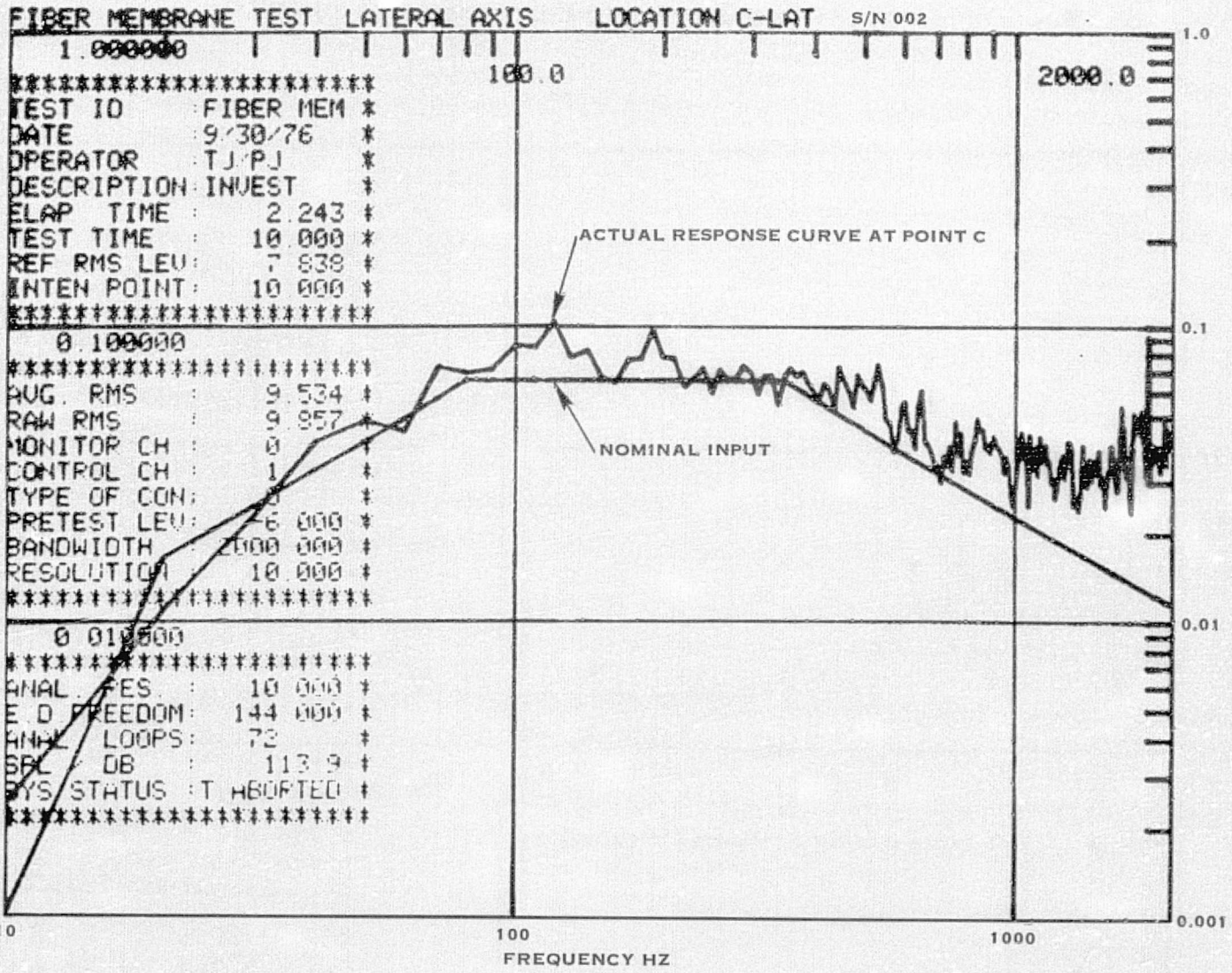
FIGURE 54. MODULE VIBRATION RESPONSE AT POINT C
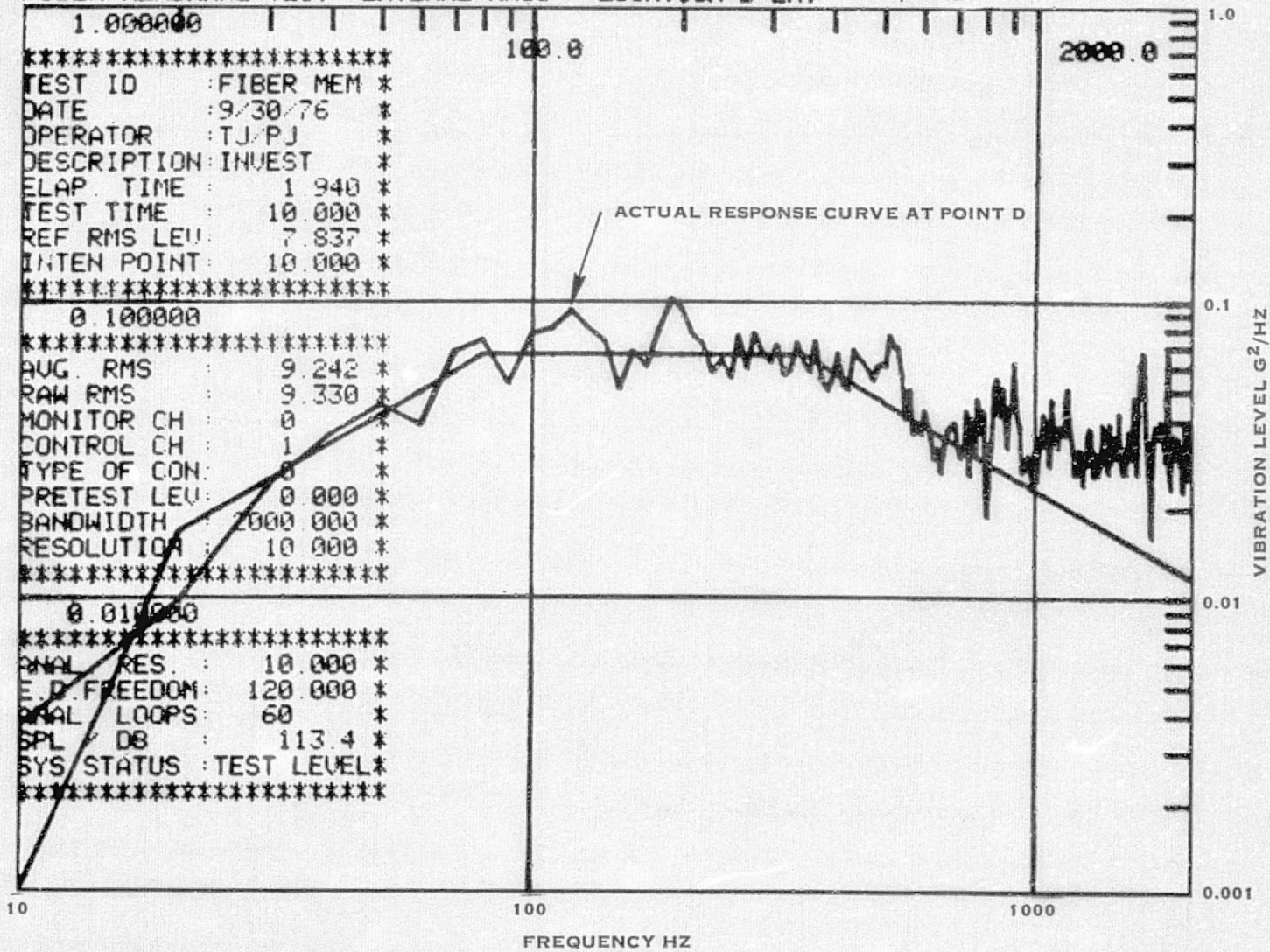
FIGURE 55. MODULE VIBRATION RESPONSE AT POINT D

- Amicon's SM-96 unit finds excellent application as a deaerator with sizing governed by dissolved gas diffusion from the fiber flow stream to the inner fiber (membrane) wall.

- Heat rejection by water evaporation from the Amicon SM-I unit is determined by heat transfer, at active sites in the fiber wall, through the wall thickness itself, and through the laminar film within the flow stream. Control of the number and distribution of active sites can be enhanced by post-manufacturing treatment.

- The heat rejection unit containing Amicon SM-I 0.051 cm (20 mil) polysulfone fibers can withstand current Spacelab ECS vibration qualification levels without sustaining structural damage to the fibers or the module.

BACTERIA FILTRATION

The GM-80 unit was completely retentive to bacteria and virus on a single shot or acute basis. Bacterial retention had been expected and predicted, and program work was confirmatory. However, viral retention by such a high flux membrane is a new discovery and represents one of the major contributions of this program to separative membrane technology.

Transmembrane pressure drop is shown in Figure 56. These data are correlated by laminar flow relationships. Initial difference in transmembrane flow between S/N 001 and S/N 002 is due to normal production variability and is anticipated for this product. The increased flow resistance of S/N 002 after test and sterilization was unexpected however. Pressure drop more than doubled; possibly due to the sterilization process or pluggage from the filter performance test (conducted prior to sterilization). Data relating pressure drop to performance life are required to separate these effects. In any event, the huge bacteria dosages utilized during testing are many orders of magnitude greater than those anticipated during actual mission usage where we are retaining random bacteria, and reusage after sterilization was not considered a requirement.

The pressure drop/flow performance for both units, as shown in Figure 56, meets the predicted value. Further testing would be required to evaluate sterilization cycles versus life effects if sterilization becomes a realistic requirement.
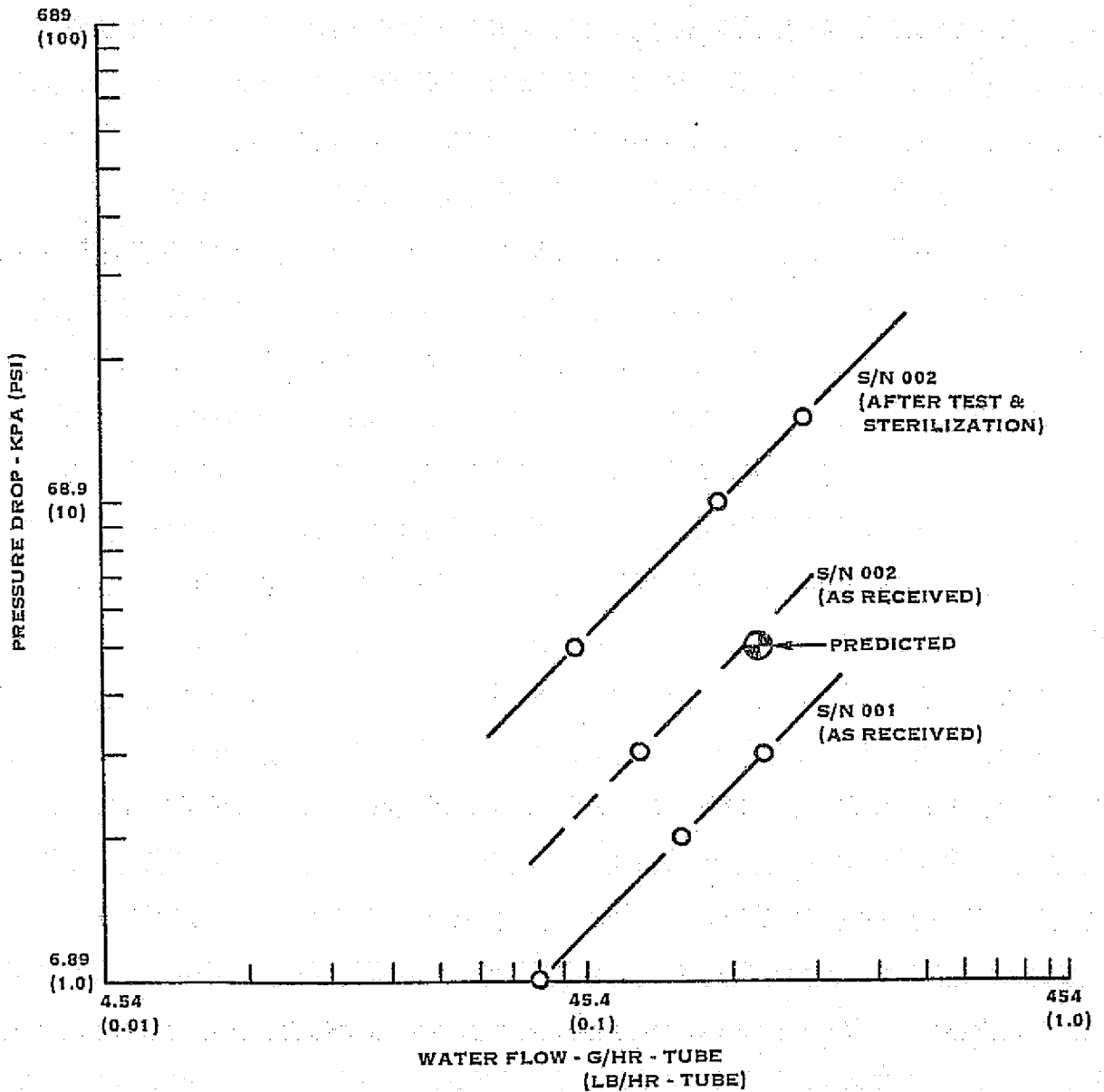
FIGURE 56. ROMICON GM-80 TRANS MEMBRANE FLOW VS. PRESSURE DROP

DEAERATION

Initial attempts to correlate the deaeration test results to relationships describing gas diffusion through stagnant liquid (as would be the case for liquid in the wall pores) were not encouraging. Data scatter is definitely a concern to this evaluation, but an overriding factor present throughout the analysis is an unpredicted variation in diffusivity with flow rate. As flow through the tubes increases, oxygen transport tends to increase. Figure 57 demonstrates this trend where oxygen throughput has been normalized by the average oxygen concentration in solution. Normalized flow was anticipated to be constant over the range of test flows.

These data have directed our thoughts to diffusion within the flow stream inside the tube with the strong potential that much, if not all, of the tube wall porosity is void of liquid. Since the dissolved gases represent very small concentrations in the liquid phase, diffusion within the laminar stream can be a controlling parameter. Therefore, added diffusional resistance through liquid in the tube wall would only retard performance, and an optimum design would utilize a hydrophobic membrane with no water in the wall porosity. Gas pressure drop through the pores is negligible due to the extremely low mass flow rate and can be considered negligible in the analysis. This conclusion was substantiated when variation in the downstream or chamber vacuum pressure level had no perceptable effect on performance.

Diffusion through a laminar flow will be described by

$$\text{Effectiveness, } E = \frac{C_1 - C_2}{C_1 - C_W} = f\left[\frac{\dot{W}}{L}\right]^x$$

where the molar concentration, C, is for dissolved oxygen at the inlet, outlet, and tube wall conditions. Since tube length, L, was constant for this test series, its effect on performance could not be confirmed. There is no reason to suspect, however, a condition not predictable from the above relationship. Figure 58 presents the data results in terms of component effectiveness versus mass flow rate. Data scatter remains distracting, but the effect of flow variation becomes more obvious. Extrapolation to new designs can be made using this figure as follows:

Requirements:

Water Flow: 18.1 kg/hr (40 lb/hr)

Unit Pressure Drop: 34 kPa (5 psi) maximum
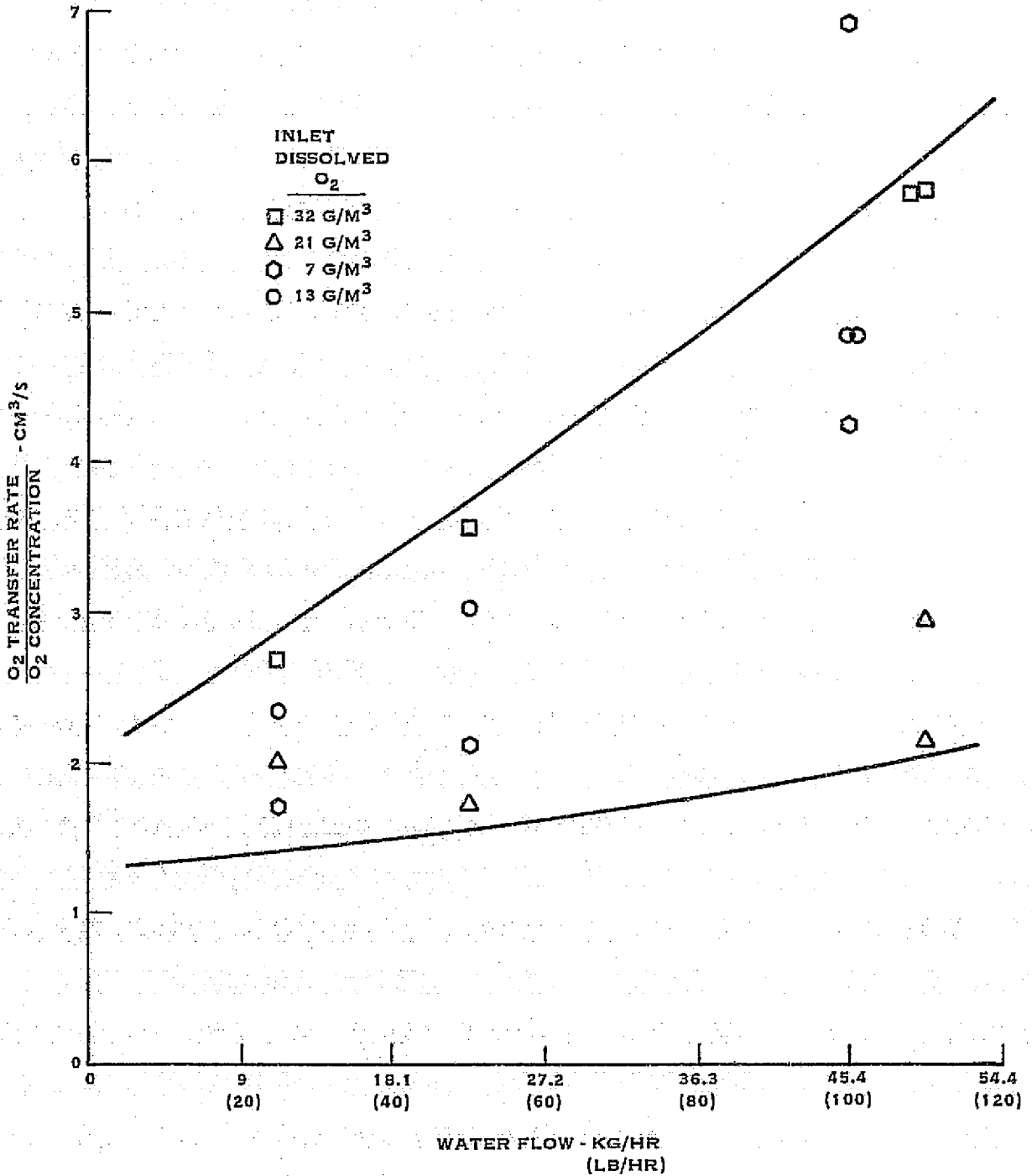
FIGURE 57. NORMALIZED OXYGEN THRUPUT VS. FLOW

$$E = \frac{c_{O_{2_1}} - c_{O_{2_2}}}{c_{O_{2_1}} - c_{O_{2_W}}}$$

REF: TEST LOG 13509, 13510 & 13716

DESIGN CURVE

EFFECTIVENESS

1.0

0.1

4.54
(0.01)

45.4
(0.1)

WATER FLOW - G/HR - TUBE
(LB/HR - TUBE)
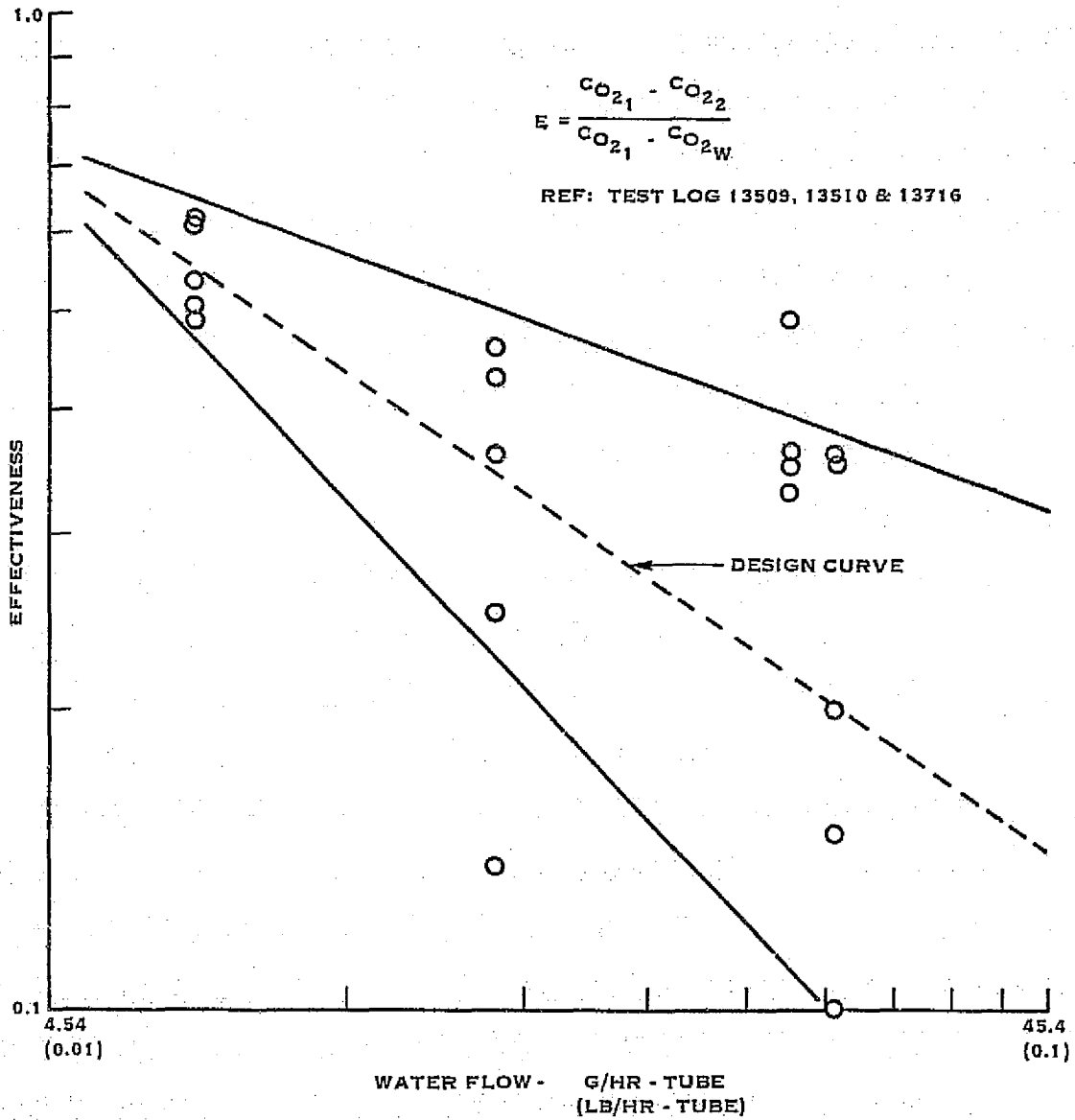
FIGURE 58. DEAERATOR EFFECTIVENESS VS. FLOW

129

Feedwater Saturation: 37°C and 101 kPa (98.6°F) and 14.7 psia) ($C_{O_{21}}$ = 9.92 x 10^{-7} g-moles/cm^3)

Product Water Saturation: 4.4°C and 23 kPa (40°F and 3.35 psia) ($C_{O_{22}}$ = 4.19 x 10^{-7} g-moles/cm^3

$$E = \frac{C_1 - C_2}{C_1 - C_W}$$

$$= \frac{(9.92 - 4.19)\ 10^{-7}}{(9.92 - 0)\ 10^{-7}} = 0.58$$

From Figure 58,

$$\dot{W} = 5.9 \text{ g/hr-tube } (0.013 \text{ lb/hr-tube})$$

$$\text{Number Tubes Required} = \frac{40}{0.013} = 3077 \text{ tubes}$$

From Figure 59,

Unit ΔP = 6.89 kPa (1.0 psi)

This particular design could benefit substantially from a longer tube. Doubling the active length, for example, cuts the tube requirement in half and only raises pressure drop to 15 kPa (2.2 psi).

HEAT REJECTION

In sizing a system to accomplish the maximum desired heat rejection rate, consideration must be directed also toward performance at minimum heat rejection rate. For the HFM, the minimum heat rejection rate should exceed the heat of vaporization available from the transmembrane leakage to preclude liquid buildup on the downstream side of the membrane. A minimum thermal load of 117 W (400 Btu/hr), equivalent to 170 cm^3/hr leakage, has been selected for design purposes.

To accomplish this relatively low leakage rate, units were especially selected during manufacture to be at the low end of the leakage spectrum. Units tested during the Applications Study phase had a leakage of 0.66 cm^3/hr-tube at 68.9 kPa (10 psi) ΔP, while the units tested during this Breadboard Development phase had leakages between 0.052 and 0.13 cm^3/hr-tube.
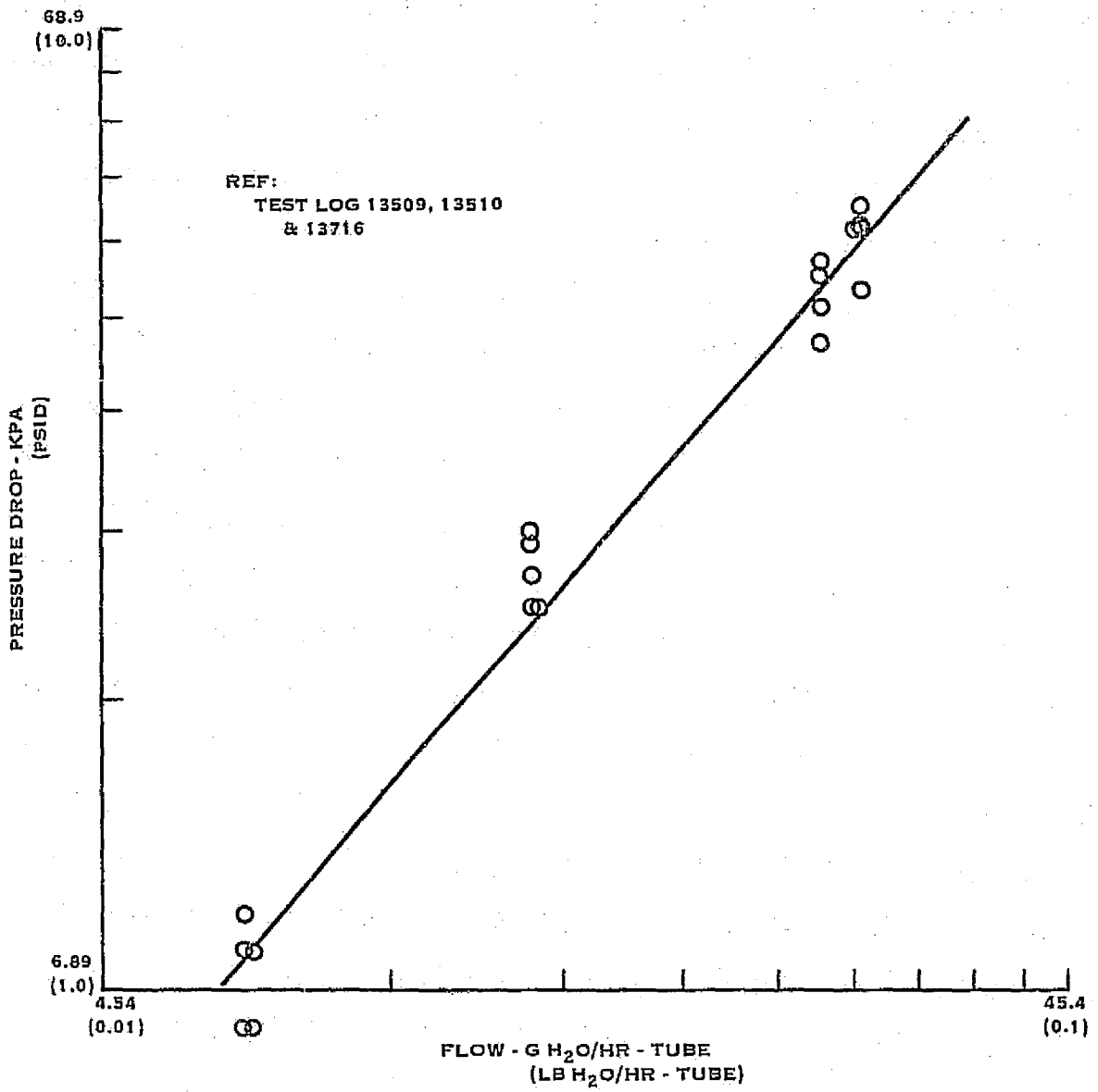
FIGURE 59. AMICON SM-96 PRESSURE DROP VS. FLOW

Heat rejection test results are shown in Figure 60. Since these were half size assemblies, the minimum anticipated result was a UA of 81.2 watts/°C (154 Btu/hr-°F) at 54.4 g/hr (120 lbs/hr), considerably above the 34.3-36.9 watts/°C (65-70 Btu/hr-°F) actually experienced with S/N's 001 and 002. At this point, it was recognized that the relationship between thermal conductance, UA, and leakage, postulated during Applications Study Analysis, was producing the reduced performance. S/N 004 was treated with a surfactant solution and performance increased (Figure 60) to a level above that acquired during the Applications phase, while S/N 004 leakage was increased from 0.13 cm^3/hr-tube to only 0.19 cm^3/hr-tube. We can now conclude that leakage is only a secondary factor in predetermining heat rejection - increased leakage tends to associate with increased heat transfer, but other stronger factors are dominating.

The polysulfone material apparently is slightly hydrophobic and will only pass water (transmembrane) through some large range of pore diameter at 68.9 kPa (10 psid). In the "as-received" condition, smaller pores remain void of liquid and contribute little to the heat transfer mode due to excessive steam flow restriction and back pressuring. Treatment with surfactant has permitted additional (and maybe all) of the pores to be filled with water. Although the pore contains water, surface tension at the discharge boundary or fiber O.D. apparently prevents hydrostatic leakage. Evaporation is not hindered, however, and makeup water will continue to flow into the wetted pore so that heat transfer performance is substantially improved. As long as the membrane assembly is not allowed to dry out (a condition requiring retreatment with surfactant), heat transfer performance will remain stable at the elevated performance. Treatment with surfactant has provided the means to minimize leakage and comply with minimum heat load requirements while maintaining sufficiently high performance potential to favorably trade off the system.

Prior analyses had concluded that the liquid film thermal resistance could be considered negligible in the system, especially at flows above 0.45 kg/hr-tube (1 lb/hr-tube). The data of Figure 61 indicate some contribution from film resistance - witness the increase in UA, or lowering the film thermal resistance, with increase in flow. Analysis of these data would produce liquid conductances, hA, approximately one-half predicted values. This would correlate the thesis that poor pore distribution would effectively reduce heat transfer area below the apparent value of the assembly. Extrapolation of test unit performance to other configurations or performance points must consider both wall thermal conductance, KA/ΔX, and film conductance, hA. Unit sizing should be based on the pressure drop of Figure 62 and the thermal performance of Figure 61.
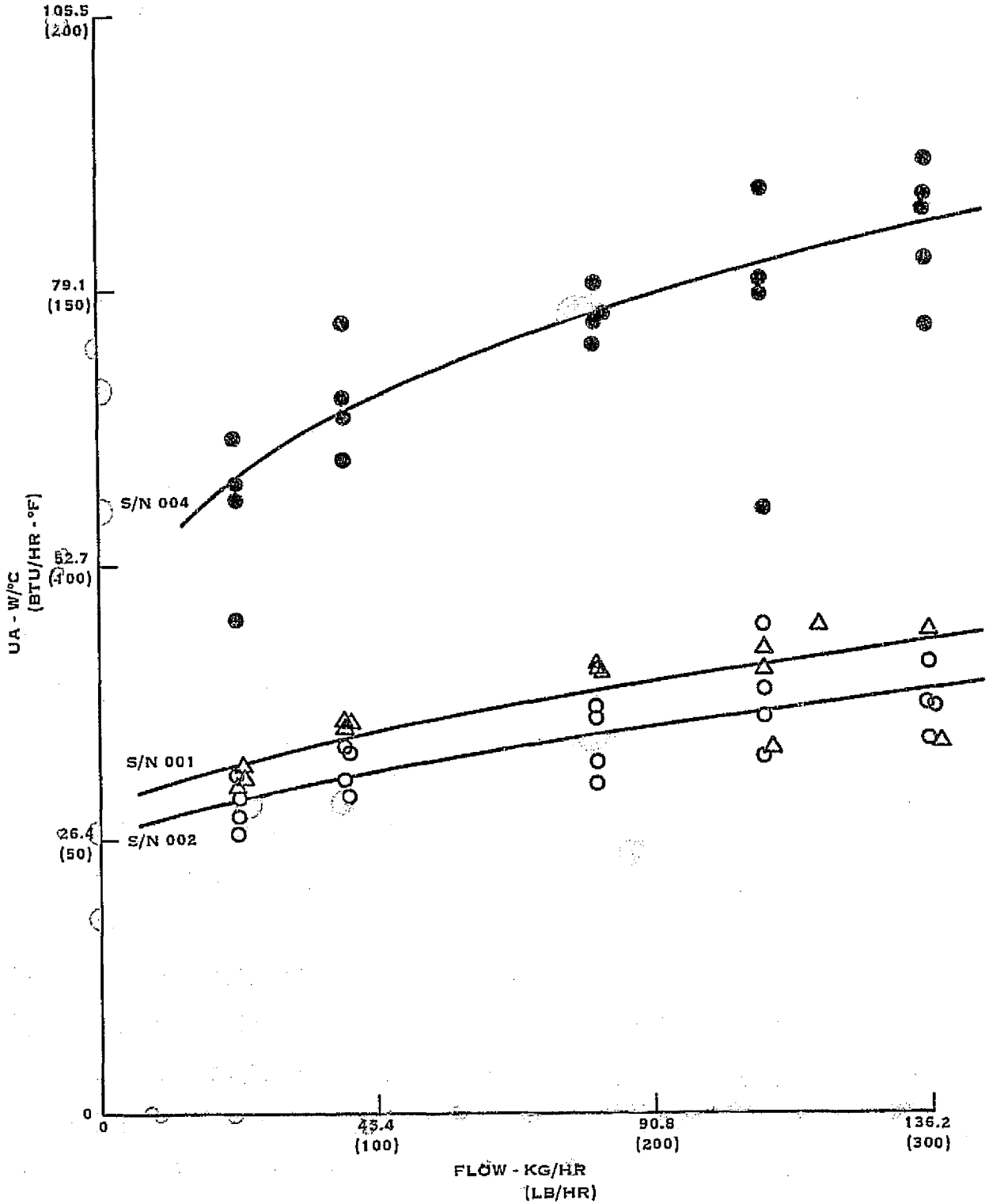
FIGURE 60. HEAT REJECTION TEST RESULTS
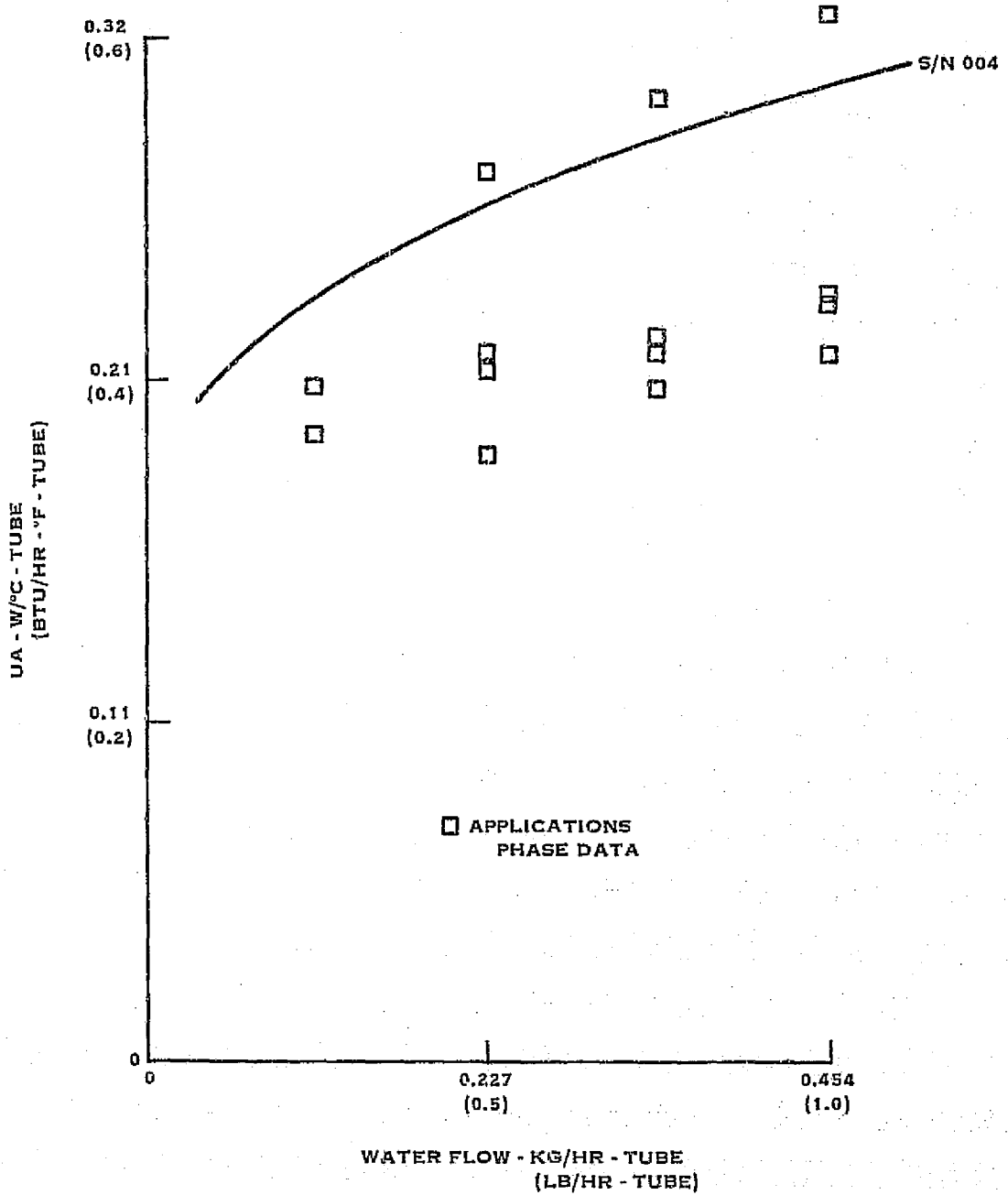
FIGURE 61. AMICON SM-I THERMAL PERFORMANCE

Division of
UNITED TECHNOLOGIES™
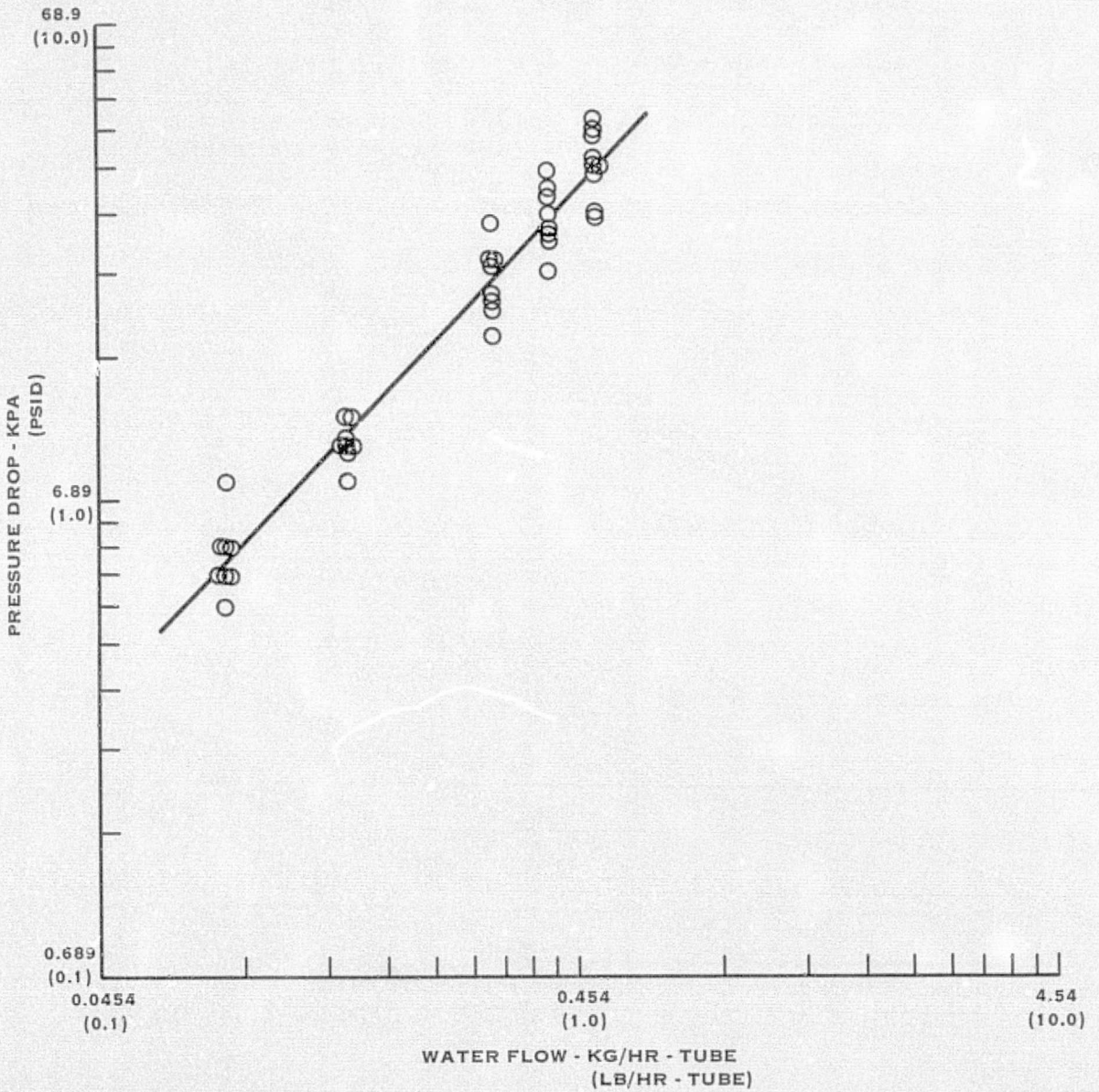
FIGURE 62. AMICON SM-1 PRESSURE DROP VS. FLOW

135

As an example, we will size a unit to meet the following Shuttle
EMU Evaporator requirements:

> Coolant Flow: 109 kg/hr (240 lb/hr)
>
> Unit Pressure Drop: 4.8 kPa (0.7 psi)
>
> Heat Rejection: 879 W (3000 Btu/hr) maximum
> 120 W (400 Btu/hr) maximum
>
> Coolant Outlet Temperature: 11.4°C (52.5°F) maximum

Select a sink temperature = 8.9°C at 1.13 kPa
(48°F at 8.5 mmHg)

$$\Delta T_{LCG} = \frac{Q}{W C_p}$$

$$= \frac{(3000)}{(240)(1.0)} = 6.9°C \ (12.5°F) \ \triangle$$

Coolant Inlet Temperature = $T_2 + \Delta T$

$$= (52.5) + (12.5)$$

$$T_1 = 18.3°C \ (65°F)$$

Membrane $\Delta T_{ln} = \dfrac{T_1 - T_2}{\ln \dfrac{T_1 - T_s}{T_2 - T_s}}$

$$= \frac{(65) - (52.5)}{\ln \dfrac{(65) - (48)}{(52.5) - (48)}} = 5.2°C \ (9.4°F)$$

$$UA_{required} = \frac{Q}{\Delta T_{ln}}$$

$$= \frac{(3000)}{(9.4)} = 168 \ W/°C \ (319 \ Btu/hr\text{-}°F)$$

From Figure 62:

Water Flow = 0.079 kg/hr-tube (0.175 lb/hr-tube)
at 4.8 kPa (0.7 psi)

Number of tubes required = $\dfrac{240}{0.175}$ = 1371 tubes

From Figure 61:

UA = 0.22 W/°C-tube (0.42 Btu/hr-°F-tube)
at 0.079 kg/hr-tube (0.175 lb/hr-tube)

Actual UA = (0.42)(1371) = 304 watts/°C (576 Btu/hr-°F)

Water pressure drop is controlling in this design, and a substantial margin of safety (81%) is provided in the thermal performance.

APPENDIX A

HOLLOW FIBER MEMBRANE TECHNOLOGY

CONTENTS

B-1 INTRODUCTION

It is the purpose of this section to review and summarize the many technologies involved in the production and use of hollow fiber membranes. This appendix includes polymer chemistry, film forming materials, fiber production (including hollow fibers), transport of liquids, vapors and gases through barriers which may be porous or non-porous solids, homogeneous gels or crystalline materials or combination of these in the form of anisotropic materials.

This information serves as a starting point for the conduct of this hollow fiber membrane program, and is drawn largely from data compiled by Hamilton Standard Division (and United Aircraft Corporation as a whole) over the past fifteen years during which research and development programs were carried out involving separations of liquids, gases and solids and for which membranes of various sorts were considered or used. Specifically, these UAC programs have involved the use of active or passive semi-permeable membranes for separation of gas mixtures such as CO_2, from O_2 and N_2, H_2 from CO and CO_2, O_2 from N_2, and H_2 from O_2; separation of gases from liquids; separation of liquids from soluble and insoluble solids (such as the purification of contaminated water by reverse osmosis (hyperfiltration).

The membrane materials examined during these studies included regenerated cellulose, cellulose acetate, polyacrylonitrile, polyvinychloride, and silicone rubber. In general, flat membranes were formed and used, but in a few cases hollow fiber membranes were obtained and tested. Ultra thin flat membranes were also produced and tested after transfer to a support material. In addition, membranes containing materials added to permit facilitated transport of hydrogen and oxygen gases were produced and tested.

During this period of time Dr. K. Kammermeyer, a recognized expert in the field of transport through membranes, serves as a consultant to Hamilton Standard, and Drs. H. Eyring, H. Mark, M. Szwarc, and I. Miller acted as consultants for United Aircraft Corporation.

B-2 GENERAL

The term "membrane" includes all configurations of materials which serve as an interface between two fluids and across which liquids or vapors and gases may be transported. A crucial condition is that this interface or membrane must be a partial barrier to transport between the two regions.

Included within the scope of the term, as used, are porous plates through which liquids or gases are transported by hydrodynamic flow, and films through which only diffusive transport can occur. Since it is unlikely that perfect examples of these two extremes actually exist, it may be expected that all "real" membranes will permit transport, to some degree, by both hydrodynamic flow and diffusive processes.

Usually the membrane is a thin film. Because both organic and inorganic polymeric materials can be shaped into a wide variety of forms with tailored macromolecular morphology, good physical properties, a wide range of chemical properties, and a fair degree of physical and chemical stability, they represent the principal supply of available membranes. Implicit in the concept of membranes is selectivity. Although the transport of a single material in a polymer is a valid subject of study, the search is for finer and sharper differences in transport.

Transport through membranes has been observed and studied for the past 140 or so years and the results of such studies has accounted for approximately 30,000 publications in areas covering membrane preparation, characterization, experimental phenomena, mathematical and thermodynamic analysis, biological studies, separation processes, and commercial equipment.

Types of Membranes

It is convenient to consider three types of membrane structures classified by the mode of transport through the membrane wall.

1. Microporous membranes have a structure that enables fluids to flow through them according to the normal equations of hydrodynamics. The effective pore size is at least several times the mean free path of the molecules in the fluids, namely from several microns down to about 100 A.

2. Molecular diffusion membranes lie at the other extreme and have a structure in which the transported molecules individually dissolve. Extruded plastic films, metal foils, films cast from "good" solvents, and glasses normally will yield membranes of this type. Strictly speaking, one should not speak of "pore size" for the structure of this class of membranes.

(Continued)

3.   Ultra filter membranes are an intermediately structured type in which transport is partially by a porous mechanism, but membrane-penetrant interactions are also important. To describe the transport hydrodynamically, the equations must be modified since the effective pore size is comparable with molecular size. If one starts from solubility considerations, one generally sees the influence of a tailored morphology. Regenerated cellulose, polyelectrolyte complexes and membranes made from leached defect structures fall in this intermediate class. The effective pore size of these membranes is usually from 7 to 50 A. Obviously the mode of transport through a given membrane depends on the size of the molecules being transported in relation to the microstructure of the membrane.

Hamilton **U**
Standard **A**®
DIVISION OF UNITED AIRCRAFT CORPORATION

B-3 HISTORICAL

The transfer of materials across cell walls was an early area for study by biologists of the 19th century. These same early investigators also experimented with every type of membrane available in studying the phenomena associated with colloids. For these studies of osmosis, natural membranes such as animal intestines and peritoneal membranes were extensively used. Later, artificial membranes were developed. Examples of these were the inorganic gel-like material deposited in a porous ceramic tube used in classical studies of osmosis by Pfeffer and the somewhat later membranes of parchment and of nitrocellulose used for studies in dialysis.

This latter material was devoloped during the early years of the present century and represents a start in the study of permeation and separation using synthetic membranes. Separations were primarily on the basis of molecular weight or particle size and the use of membranes of this kind provided a means for purification of crude invertase solutions in pioneer work in enzyme chemistry.

B-4 MEMBRANE REQUIREMENTS

The functional properties of membranes dominate their choice and use. Mechanical properties are also important. A number of membrane processes related to present interests are summarized in Table B-1. In each, the porosity of the membrane, or its morphology leading to effective porosity, is a crucial property. These processes include: gas separations, pervaporation, pressure permeation (reverse osmosis), dialysis and ultrafiltration. Not only must a morphology be achieved which permits making the appropriate separation, but the membrane must be reasonably stable to temperature changes, have acceptable chemical resistance, maintain its morphology during wet-dry cycling of permeants, and for some processes maintain its micro-structure under severe pressure changes. The membrane must be as thin as possible and, for applications associated with living organisms, should be non-toxic.

Some of the important physical properties to be considered, when designing membranes with long useful life, are tensile strength, tear strength, dimensional stability over a wide range of thermal and chemical conditions, abrasion resistance, flexibility, resistance to stress cracking under wet-dry cycling, regidity to withstand compaction in high pressure processes, toughness and morphological stability.

TABLE B-1
SUMMARY OF MEMBRANE PROCESSES

Process	Driving Force	Membrane	Primary Flux	Comment
filtration	pressure	microporous	solvent	particulate matter retaining by sieving
ultrafiltration	pressure	ultrafilter	solvent	colloids and large solutes retained
pressure permeation	pressure	solution-diffusion	selective transport of most mobile component	for gases and liquids; called "reverse osmosis" for solute removal; diffusion coefficients constant in membrane
pervaporation	vacuum	solution-diffusion	selective transport of most mobile component	diffusion coefficients have gradient in membrane; downstream side dry

B-5 SYNTHESIS OF ORGANIC POLYMERS

The organic polymers used in forming the synthetic organic membranes of interest in separation processes, are produced by the chemical reaction of specific reactive molecules. These molecules have the ability to form high molecular weight products by either an addition process or by a condensation process.

Addition polymers are produced from monomer molecules which contain one or more carbon-to-carbon double bonds. They may be produced using either a single kind of monomer molecule or a mixture of kinds of monomer. The polymerization may be pictured to occur as follows:

$$X \quad \begin{matrix} R & & R \\ C & = & C \\ R & & R \end{matrix} \longrightarrow \left(\begin{matrix} R & & R \\ -C & - & C- \\ R & & R \end{matrix} \right)_X$$
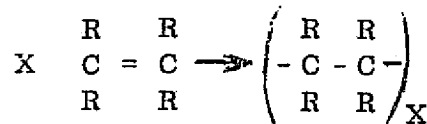
Typical products of this type of polymerization are:

> polyethylene
> poly (vinyl chloride)
> poly (vinyl acetate)
> poly acrylonitride
> poly (methacrylic esters)
> poly propylene

Condensation polymers are produced by reaction of two kinds of monomer compounds, each of which are bifunctional, and the reaction is accompanied by the splitting out of a by-product formed from part of each of the reacting molecules.

The polymerization can be pictured to occur as follows:

$$R'' \begin{matrix} C \overset{O}{\diagup} \!\!- OH \\ \diagdown C - OH \\ \underset{O}{\overset{||}{}} \end{matrix} \quad + \quad \begin{matrix} HN \overset{R}{} \\ \diagdown R' \\ H - N \diagdown R \end{matrix} \longrightarrow$$

$$\left(\begin{matrix} O & & O & R \\ \overset{||}{} & & \overset{||}{} & \overset{|}{} \\ --C - R'' - C - N - R' - N --- \end{matrix} \right)_X \quad + \quad H_2O$$
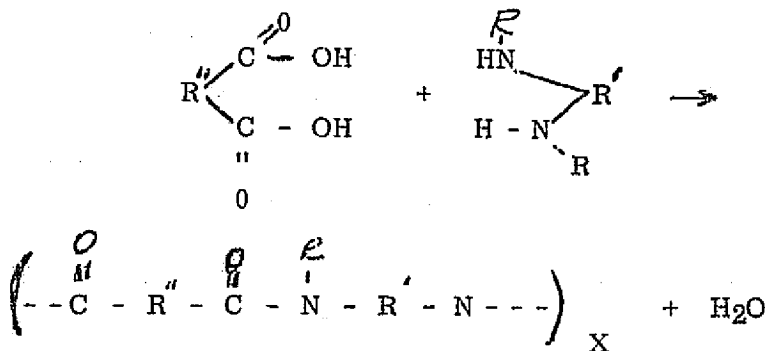
Typical products of this type of polymerization are:

(Continued)

Typical products of this type of polymerization are:

> polyesters
> polyamides
> urea-formaldehyde resins
> melamine-formaldehyde resins

Most of the examples cited in the product listings represent polymeric materials which are primarily linear polymers and could be formed into thin films (either flat membranes or hollow fibers).

The actual conditions under which the polymerizations are carried out, determine to a large degree the suitability of the products for membrane separation use.

The polymerizations can be carried out in bulk (the monomers in liquid form), in solution in a solvent, or in dispersion (finely dispersed in a non-solvent). The reactions may be initiated by heat or by addition of chemical additives. Each method has inherent advantages and disadvantages. Bulk polymerization results in minimum contamination of the product but the reactions may be strongly exothermic and the product has a broad molecular-weight distribution with possibilities of insoluble gel particles in the product.

Solution polymerization permits ready control of heat of polymerization but leads to difficulties in complete removal of solvent and initiators.

Suspension polymerization provides good temperature control but the finely-divided particles of product polymer may be contaminated with dispersing agent and with the initiators used for the reaction.

It can be expected that performance of membranes made with products from the several polymerization processes will be different even though the gross products are nominally the same. The molecular weight and molecular weight distribution of the polymers are important factors in membrane performance. These factors therefore must be considered in the development of a HFM for gas and liquid separations.

B-6 STRUCTURE OF FILM-FORMING POLYMERS

The ability of certain polymers to form fibers or films can be traced to several structural features at different levels of organization rather than to any one particular molecular property.

For a complete description of fiber/film structure, three levels of molecular organization must be considered, each relating to certain aspects of fiber behavior and properties. Of prime importance is the organochemical structure, which defines the structure of the repeating unit in the base polymer and the nature of the polymeric link. This level of molecular structure is directly related to chemical properties, moisture sorption, and swelling characteristics, and indirectly related to all physical properties. The next level of molecular organization is the macromolecular structure which describes the family of polymer molecules in terms of chain length, chain-length distribution, chain stiffness, molecular size, and molecular shape. Finally, the supermolecular organization provides a description of the arrangement of the polymer chains in three-dimensional space. This level of molecular organization is particularly important in the natural fibers which contain various aggregations of polymer chains that are intermediate between the polymer molecule and the fiber.

The natural and man-made fibers/films have certain regions in which the molecular chains are arranged in near perfect register, and where the laws of x-ray diffraction are obeyed. In other regions the molecular chains are not ordered and may be described as being in random-coil configuration. The two-phase crystalline-amorphorous structure of film-forming polymers was for a long time the working model used to interpret film properties. It was subsequently replaced by the fringed-micellar model, wherein the sharp boundary between a crystalline and an amorphous region disappeared in favor of a more gradual transitional region. This concept was eventually formulated in terms of a lateral-order distribution according to which structural regularity varies from the perfectly ordered or crystalline state to the completely disordered or amorphous state in a continuous manner.

Regardless of whether films and fibers are visualized as two-phase systems (crystalline and amorphous), as systems of continuously varying structural perfection (lateral-order distribution), or as single-phase crystalline systems with imperfections and defects, the same general picture emerges: a polymeric substance with a high degree of three-dimensional structural regularity. An important feature of this three-dimensional regularity is that the molecular chains, or aggregates of polymeric chains, are preferentially oriented with respect to the fiber axis. This orientation is induced in all man-made films and fibers by various drawing processes during manufacture.

(Continued)

In keeping with the structural definition of films and fibers as semicrystalline, irreversibly oriented polymers, three general requirements of molecular structure for film or fiber-forming polymers may be formulated. First, the polymer chains must be linear rather than three-dimensional and must have relatively high molecular weight. There is no single value of molecular weight that can be given as optimum since this depends to a large extent on other structural factors. However, in general, it appears that the chain length must be at least 1000 A, on the average, to be useful. In the lower ranges of molecular weight the dependence of fiber and film strength, for example, is quite pronounced; however, increasing the molecular weight above a certain level does not reflect itself in increased strength.

The second general requirement of polymer structure for useful film formation is the degree of linear symmetry. The presence of large, bulky side groups on the polymer backbone would hinder chain interactions by physically or sterically preventing the chains from assuming the stable close-neighbor positions that lead to crystallinity and orientation. It is possible to obtain useful materials from polymers where side groups are present by controlling steric regularity. Stereoregular polymers such as isotactic polypropylene, are excellent film-forming polymers since the methyl side groups are arranged in a dimensionally regular manner along the backbone chain and therefore do not interfere with chain packing.

The third general requirement is one which considers the interaction among polymer chains by control of molecular flexibility. In the absence of restraining forces, polymer chains would assume random-coil configurations and would not be capable of either crystallization or irreversible orientation. The restraining forces against random-coil formation may be the presence of specific intermolecular cohesive forces such as ionic bonds, dipolar interactions, dispersion forces, van der Waals forces, and hydrogen bonding.

B-7 MANUFACTURE OF FILMS AND FIBERS

The polymeric materials suitable for film or fiber use are usually thermoplastic
and with relatively little cross-linking in the molecular structure. For these reasons
the actual formation of films or fibers is normally carried out by extruding the
molten polymer through dies or by casting or spinning solutions of the polymers
in selected solvents or mixtures of solvents.

The production of hollow fibers represents a sophisticated modification of solid
fiber production technology and is discussed in detail in the next section.

The forming processes mentioned for fiber production are known as melt spinning,
wet spinning and dry spinning. Historically, the last two methods preceded the
melt spinning process because most of the natural polymers available were degraded
at temperatures below their melting points and processing was only possible from
solution. (The process referred to as "spinning" in the manufacture of fibers
actually refers to the formation of fibers by extrusion.) These processes were
initially developed for textile use.

In wet spinning, the solution of polymer is extruded through fine holes in a spin-
neret into a liquid coagulant which precipitates the polymer in a filamentary form.
In dry spinning, the solution is extruded into hot gas or vapor which rapidly evaporates
the solvent to leave filaments. In melt spinning, the molten polymer is extruded
into cool gas or vapor, and its rapid solidification produces filaments.

A useful fiber does not necessarily result from the primary formation process.
When the polymer molecules have undergone little or no orientation during extrusion,
the resulting fiber is weak. To introduce orientation, the filaments are stretched
or drawn immediately after extrusion or as a separate operation.

Although fiber strength is important, the process of molecule orientation may have
a detrimental effect on other properties. Permeability properties of fibers and
films are often decreased by excessive orientation.

Fiber Production

Spinnerets -- The main spinning processes have one important item in common,
the spinneret, which is a plate containing orifices through which the molten or
dissolved polymer is extruded under pressure. For melt or dry spinning it is
made of stainless steel or a nickel alloy, but for wet spinning, if the spin bath is
corrosive, a precious metal such as platinum alloy or tantalum is used instead.
Glass spinnerets have also been used in wet-spinning processes. For melt spinning,
the spinneret is a flat plate, flush with or recessed in its mounting whereas for
wet or dry spinning it is usually thimble shaped with the orifices in the end face
so that the spinneret projects a short distance into the liquid or gas. The

(Continued)

spinnerets for use with molten polymers are relatively thick, on the order of 1/4 – 1/8 inch, and individual holes are in the range of 0.007 – 0.030 inches in diameter, the wider end of the range being used for the more viscoelastic polymer melts. For use with solutions the metal spinnerets are thinner.

The number of holes in a spinneret may range from a very small number to many thousands depending on the limitations of the specific spinning process. The arrangement is important, particularly where heat transfer controls the solidification rate. Preferred patterns include rectilineal rows of holes, concentric annuli, and irregular arrangements, the particular pattern being chosen to give even cooling in all filaments or regular access of coagulant to the spinneret face.

For hollow fibers, introduction of inert gas at the center of an orifice is effective. Also effective is extrusion through an incomplete annulus since surface tension forces cause the molten polymer to complete the ring. Only if the extruded polymer is of high viscosity will the fiber retain the shape imposed in this way.

Spinneret hole size does not control fiber size. The size of a melt-spun or a solvent-free solution spun fiber is controlled by two factors, the throughput of polymer per hole (T, lb/hr) and draw-down speed (W, ft/min) according to the relation

$$\text{fiber size} \sim T/W$$

Fibers which are typically spun from a melt are given in Table B-2. Included are the melting points and the spinning temperatures.

Table B-2 Typical Melt-Spun Fibers

Structure	Melting point, °C	Spinning temp, °C
Polyamides		
poly(hexamethylene adipamide) (nylon-6,6)	264	280-290
poly(hexamethylene sebacamide) (nylon-6,10)	215	
poly(pentamethylene carbonamide) (nylon-6)	220	270-280
poly(decamethylene carbonamide) (nylon-11)	187	
poly(metaxylylene adipamide) (MXD,6)	243	280-290
Polyesters		
poly(ethylene terephthalate)	264	280-300
poly 1,4-bis(methylene)cyclohexane terephthalate (1:2 cis:trans)	290	310-320

(Continued)

Table B-2 (Continued)

Structure	Melting point, °C	Spinning temp, °C
Polyolefins		
polyethylene	115–125	250-300
polypropylene	167	250-300
poly(4-methylpentene)	250	280-320
Saran		
poly(vinylidene chloride) copolymers	120-140	175

Fibers which are typically produced by wet-spinning and the solvents and coagulents used are shown in Table B-3.

Table B-3 Typical Wet-Spinning Solvents and Coagulants

Fiber	Solvent	Coagulant
Viscose rayon	water (solution of sodium salt of xanthate ester of cellulose)	dilute H_2SO_4 + sodium sulfate + zinc sulfate
cuprammonium rayon	aqueous cuprammonium hydroxide	water
poly(vinyl alcohol)	water	aqueous sodium sulfate
polyacrylonitride	dimethylacetamide	aqueous dimethylacetamide
"	dimethylformamide	hot kerosene
"	"	aquerous dimethylformamide
"	ethylene carbonate-water (85:15)	aqueous ethylene carbonate
"	60% zinc chloride	40-50% zinc chloride
"	50% sodium thiocyanate	10% sodium thiocyanate
"	65-80% nitric acid	25-40% nitric acid
"	70-75% sulfuric acid	50-55% sulfuric acid
Modacrylic fiber	acetonitrile	aqueous acetonitrile
"	acetone	water
poly(vinylchloride)	cyclohexanone	water+isopropanol+cyclohexanone
poly(hexamethylene terephthalate)	conc. sulfuric acid	40-60% sulfuric acid

A-13

(Continued)

It is seen that generally the coagulant is simply a more dilute form of the solvent.

The equipment used in the wet-spinning process typically consists of a solution vessel, a pump delivering through a filter to a holding and deaeration tank, then metering gear pumps delivering through filters to spinnerets. The spinnerets are immersed in tanks containing the coagulant. The coagulated fibers pass over a guide to driven rolls.

With viscose, freshly made solutions must be "ripened" to the proper molecular weight and viscosity before spinning. With other fibers, provided the solutions are free of gel particles and of controlled viscosity, no delay is required.

Precipitation of the polymer in the coagulant involves mass transfer in two directions simultaneously, as solvent diffuses out of the extrudate into the bath and non-solvent or precipitant diffuses in the opposite direction. The fine structure of the fiber is determined during the coagulation process and is not materially altered during subsequent regeneration or drying of the gel structure. The rate of coagulation has a profound effect on fiber properties. The important variables affecting the fine structure are the concentration and temperature of the polymer solution, the composition, composition and temperature of the coagulant bath, and the stretch applied during spinning. The relative importance of these variables differs from fiber to fiber. The coagulant must have free access to all the extruded fibers without turbulence in order to minimize variation in structure from fiber to fiber or along a single fiber.

In dry spinning the processes involved are similar to those used in wet spinning up to the spinneret. The polymer solution passes through the spinneret holes into a cabinet into which hot solvent-poor gas or vapor is introduced at one end, and from which solvent-rich vapor emerges at the other end. The gas flow is commonly counter-current to the fiber. The gas temperature may range from 80 - 130 C for the lower boiling solvents, and from 200 -400 C for the relatively non-voltile solvents. The gas used is usually air or inert gas. Inert gases are needed when the fibers are oxidation sensitive.

Typical dry-spinning solvents are listed in Table B-4.

Fiber Drawing

Fiber manufacturing processes convert an isotropic polymer into a highly anisotropic form. This they accomplish by constraining the macromolecules to adopt conformations in which the main chain is roughly parallel to the fiber axis. The more nearly the chains lie parallel to the axis, the more highly oriented the fiber is said to be. Orientation is produced at the spinning stage by passing the molten

(Continued)

Table B-4 Typical Dry-Spinning Solvents

Fiber	Solvent
secondary cellulose acetate	acetone + 2-6% water
cellulose triacetate	methylene chloride + methanol
polyacrylonitrile	dimethylformamide; dimethyl acetamide
modacrylic fiber	acetone
poly(vinyl chloride)	carbon disulfide + acetone
chlorinated poly(vinyl chloride)	carbon disulfide + acetone
crys' lline poly(vinyl chloride)	ketone + aromatic hydrocarbon
vinyl chloride copolymers (vinyon)	acetone, methyl ethyl ketone
poly(vinyl alcohol)	water

or dissolved polymer through a narrow orifice, then drastically reducing its diameter by collecting it at a high linear speed and removing the solvent if present. In some cases, such as acetate, the orientation produced at this stage gives the fiber sufficient strength in an axial direction, but often a further stretching or drawing operation is required. Here two types of polymer may be distinguished. Some, such as viscose, will stretch if sufficiently plasticized, for example by residual solvent, but the stretching is not localized during the process. Others, including the crystallizable thermoplastic polymers, undergo a process known as "cold drawing", whereby the filament under tension extends irreversibly to several times its original length and does so at a localized draw point known as a "neck".

The cold drawing process is exothermic, and may be understood in terms of heat liberated by the work of stretching during conversion of the fiber into the more stable oriented form, reducing the viscous forces opposing extension at the neck. The glass-transition temperature (T_g) of the polymer is important here, since the resistance to extension in the glassy state is very high and makes it difficult to establish stable cold-drawing conditions. With a polymer whose T_g is well above room temperature, and indeed often in fibers whose T_g is below room temperature, it is useful to heat the fiber before drawing. Plasticizers, by lowering T_g can have the same effect. Stretching a fiber in the plastic state, as in drawing, is much more effective in orienting the structure than stretching in viscous liquid form, as largely occurs in the spinning process. Still further orientation may be induced by heating the drawn fiber under tension to a high temperature at which, if unconstrained, it would shrink; this process serves also to increase the crystallinity of the fiber, most dramatically when the fiber, due to having a high T_g,

(Continued)

has passed through the earlier stages without substantial crystallization.

As mentioned earlier, the orientation of the molecules in the fiber have an important effect on transport properties of the fiber. In general, increased orientation leads to lower permeabilities and greater specificities.

Quality Control

It is doubtful whether there is any industry more dependent on strict standards of quality control than the manufacture of polymeric hollow fibers. The strict control of polymer molecular weight is essential for control of the spinning or forming process. The presence of any particulates in the spinning dope can cause non-uniformities in wall thickness of hollow fibers and could lead to pin holes in the walls or blockage of the annulus of the hollow fiber.

As indicated earlier, all steps in the production process must be very tightly controlled in order to maintain reproducible membrane micro structures.

B-8 HOLLOW FIBER MEMBRANES

The development of thin organic polymeric membranes in hollow fiber form shows great promise of making membrane separation processes, demonstrated with flat membranes, commercially feasible on the basis of unit sizes and cost.

The principal advantages of hollow fibers over flat membranes are:

1. They are mechanically strong and require no additional support in separation devices;

2. They expose a large amount of active surface in relation to the volume of the containing vessel;

3. Their production by a continuous spinning process should result in more uniform membranes, and should offer a lower cost means of producing large areas of active membrane.

Although the potential of hollow-fiber membranes has not been as fully developed as that of flat membranes, there appears to be no reason why comparable properties cannot be achieved with hollow fibers. There also appears to be no reason why most of the polymers which have been formed into flat membranes could not be spun into the hollow fiber form.

Presently a number of polymeric materials are available in hollow fiber form for use as gas separators, reverse osmosis, ultrafilter and dialysis applications, and experimental oxygenators for blood.

The materials used include regenerated cellulose, cellulose esters, polyamides, polyesters, polysulfones, teflon and related fluorocarbons.

Spinning of Hollow Fibers

As indicated earlier, the technology developed for hollow textile fibers, particularly in the manufacture of spinnerets, has been very useful in the development of hollow-fiber membranes.

Hollow fibers for use as membranes have been made by three conventional synthetic-fiber spinning methods: (1) wet spinning (spinning from a polymer solution into a liquid coagulant); (2) dry spinning (spinning from a solution of a polymer in a volatile solvent into an evaporative column); and (3) melt spinning. In all cases the tubular cross section was formed by extruding the molten polymer or polymer solution through an annular die or spinneret. Spinneret design and precision of manufacture are critical features of successful hollow-fiber spinning.

(Continued)

1. One annular spinneret design has a solid pin supported in the center of a circular orifice. The polymer is extruded through the annulus. With this spinneret design, it is generally necessary to incorporate a gas-forming additive in the polymer melt. The gas fills the core of the fiber as it emerges from the annulus and prevents collapse until the fiber solidifies.

2. Another spinneret design has a hollow needle or tube supported in the center of the orifice. An inert gas or liquid is injected through the needle to maintain the tubular shape until the fiber solidifies or coagulates.

3. A third type of hollow-fiber spinneret has a C-shaped orifice. Generally the tips of the C overlap. The polymer solution or melt welds into a tube after extrusion through the C-shaped die. The gas required to keep the fiber hollow is drawn in through the gap in the extruded fiber upstream from the weld point.

A patent description of hollow-fiber spinning describes the use of a type 2 spinneret with a 44 mil OD x 36 mil ID annular orifice [a]. The spinneret was used to melt spin-hollow fibers of a modified nylon polymer with final dimensions of 2 mil OD x 1 mil ID. The size reduction was achieved by rapidly drawing the fiber away from the spinneret face. In this case the draw rate was 465 yd/min. In wet or dry solvent spinning, the draw rates are generally lower; however, some additional size reduction is obtained by the solvent loss. Size reduction can also be achieved by a postspinning drawing operation; however, the orientation that generally occurs on cold drawing can significantly reduce the permeability of hollow-fiber membranes.

Hollow-fiber membranes, like their flat-membrane counterparts, often require special handling techniques to maintain or achieve the optimum permeation properties. Procedures reported include (1) spinning of plasticized fibers, (2) processing the fibers in a wet swollen state, (3) replasticizing fibers after spinning, and (4) chemical modification of the fiber after spinning.

Applications

Reverse Osmosis - Among the applications for hollow-fiber membranes, the greatest attention has been given to their use in desalination of water by reverse osmosis. Saline water is placed in contact with a suitable membrane at a pressure exceeding the osmotic pressure of the solution. Fresh water, or water with a lower salt content, permeates the membrane and is collected for use. A concentrated brine is discharged from the high-pressure side of the membrane as a waste stream.

Reverse osmosis development has been directed primarily toward the production of fresh water from natural brackish waters; however, reverse osmosis units have also

(Continued)

been tested in a variety of other water-and waste-treatment applic tions, including recovery of water and concentration of wastes from sewage effluents (raw sewage, primary or secondary effluent), acid mine drainage, high-salinity irrigation drainage, and paper-mill effluent.

For a membrane with a given specific permeability, the fresh-water output or flux of a reverse osmosis device is directly proportional to membrane area and pressure driving force, and inversely proportional to membrane thickness. Membrane area can be maximized and thickness minimized in the hollow-fiber form. Fine hollow fibers provide a thin, self-supporting membrane with the very high surface-to-volume ratio desirable for reverse osmosis.

Reverse Osmosis Membrane Properties – The important properties for a membrane are flux, salt rejection, and durability.

Flux – The water permeation or flux rate of hollow fiber membranes can be expressed as gallons per day per square foot of membrane area (gfd) based on the outside diameter of the fiber. (Hollow-fiber reverse osmosis devices are generally operated with the pressurized saline water on the outside of the fibers and fresh-water permeation inward from the outside.) Flux rates of 0.05 – 4.0 gfd have been reported.

Salt Rejection – The selectivity of a reverse osmosis membrane is often expressed as the salt rejection, SR, which is defined by the equation

$$\% \, SR \; = \; \frac{C_f - C_p}{C_f} \; X \; 100$$

where C_f = salt concentration in feed water and C_p = salt concentration in permeate. The salt rejection required in reverse osmosis application depends upon the proposed water use. Generally, for the production of potable water, a permeate concentration of $<$ 500 ppm is desired. Thus, a salt rejection on the order of 85 – 95% is required for brackish-water desalination (1000 – 5000 ppm) and $>$ 98.5% for seawater desalination (35,000 ppm).

The rejection of a reverse osmosis membrane varies with the solute composition in the feed water. Multivalent ions are generally rejected better than monovalent ions. Rejection of dissolved materials other than salts is often of importance particularly in the treatment of waste water. Dissolved components that are soluble in the membrane are rejected poorly (i.e., ketones in cellulose acetate membranes). Another factor that influences salt rejection is the pH.

(Continued)

Membrane Life - The durability of a reverse osmosis membrane is influenced by both the membrane properties and the nature of the system in which it is operating. Failure can be caused by membrane compaction, fiber collapse, fouling (slimes or scale), chemical degradation, or biological degradation.

Hollow fiber membranes which have been used for the reverse osmosis process are principally cellulose acetate and nylon although phenolic resin fibers have been reported.

Cellulose Acetate

The first report of the use of hollow-fiber membranes for reverse osmosis appeared in 1963 [b]. Cellulose triacetate fibers were produced by a laboratory-scale wet-spinning process. The fibers produced ranged in size from 35 to 70 OD with 7 - 10 walls. Small laboratory test cells were prepared with these fibers. A 1% sodium chloride solution was passed through the fibers at 200 psi. (The direction of permeation in this case was outward from the inside.) The flux rates were very low (ca 0.001 gfd), reflecting the fact that the fibers had been oven dried prior to testing. Characteristically, cellulose acetate or triacetate membranes prepared initially in a water-swollen state undergo an irreversible dehydration and shrinkage upon drying, with a corresponding decrease in water flux. The initial salt rejection in these early tests was greater than 99%. The rejection decreased with time, due possibly to a slow hydrolysis of the acetate groups. Membrane hydrolysis rates have been found to be lower in solutions containing multivalent ions. The control of pH can also be used to retard hydrolysis.

Another report of hollow cellulose acetate fibers produced by a wet-spinning process describes similar results with wet and dried fibers [c]. The water-swollen fibers gave good salt rejection and high water flux (0.7 gfd at 200 psi); however, the fibers collapsed under prolonged application of pressure. When the same fibers were air-dried prior to pressure testing, they were stable up to 1000 psi; however, the water flux was reduced to 0.05 gfd at 500 psi.

Hollow cellulose acetate and triacetate fibers have also been produced by a modified melt-spinning process [d]. An extractable plasticizer is blended with the polymer prior to spinning. The plasticizer lowers the spinning temperature, which reduces thermal degradation of the polymer. In one example, a cellulose triacetate blend containing 43% Sulfolane plasticizer is spun at 235°C, whereas the melting point of unplasticized triacetate is approximately 300°C.

The use of a water-extractable plasticizer has the added advantage of increasing the water permeability of the hollow-fiber membrane. When the plasticized fibers are leached in water, the water uptake of the fiber increases with increasing plasticizer

(Continued)

content. There is a corresponding increase in water flux with increasing membrane water content. The relationship of flux to plasticizer (Sulfolane) content is shown in Table B-5. Water-extractable plasticizers that have been used in spinning hollow fibers of cellulose acetate and cellulose triacetate include dimenthyl sulfoxide, 2-pyrrolidone, γ-butyrolactone, triacetin, Sulfolane, and caprolactam.

Table B-5   Effect of Plasticizer Content on Water Flux
(Hollow Fibers with 10μWalls; Pressure, 200 psi; Feed, Distilled Water)

Sulfolane content, wt %	Flux, gfd
28.6	0.07
31.0	0.10
33.3	0.13
35.3	0.15
37.3	0.16

Another modified melt-spinning process was reported for the production of hollow cellulose acetate or triacetate fibers having improved water permeability [e]. In this process, the additives blended with the cellulose acetate or cellulose triacetate polymers consist of a compatible plasticizer such as Sulfolane and a polyol. In one example a blend containing 66.7 wt % cellulose acetate (40% acetyl), 20% Sulfolane, and 13% tetraethylene glycol is spun into hollow fibers. The fibers are leached in water at 60°C and have a salt rejection greater than 90% and a water flux six times as great as a control containing no glycol.

A method for altering the selectivity and permeability of cellulose ester membranes has been reported which involves post-treating the fibers in a swelling solution [f]. The solution contains a plasticizer for the cellulose ester and a secondary additive which is a non-solvent for the membrane. As an example, a cellulose triacetate membrane is treated for 10 minutes at 25°C in a 50% solution of Sulfolane in water and then washed in water at 60°C. The water permeability of the membrane increases five to sevenfold with no decrease in salt rejection.

Asymmetric hollow fibers with a rejecting thin skin and a highly permeable substructure have been prepared by coating a regenerated-cellulose hollow fiber with a thin outer layer of cellulose acetate or solution spinning a dilute cellulose acetate system in which the skin is obtained by evaporation of a volatile diluent [g]. In the former process, the cellulose acetate is mixed prior to spinning with materials that are non-solvents at room temperature, but upon heating form a homogeneous melt which can be subsequently

(Continued)

extruded and cooled to form a gel. The spinning dopes generally contain 10 -40%
cellulose acetate in triethylene glycol and diethylene glycol monomethyl ester. The
dope forms a homogeneous melt at 100 - 150°C and gels at 90°C. The melt can be
extruded through an annular spinneret and cooled in a gelation bath. Phase separation
occurs during gelation. The water content of the gel fibers after extraction of the
plasticizers is 65 - 70%, indicating a highly porous structure. The water-swollen
hollow fibers are regenerated in 0.2 N sodium hydroxide and coated with a thin cellulose
acetate layer from a chloroform solution. Reverse osmosis test data were not re-
ported.

The Monsanto Research Corporation has accomp'shed the development of a solution-
spinning technique for the production of asymmetric hollow fibers. These fibers are
prepared by spinning a 25 wt % cellulose acetate dope containing acetone and formamide
in a 60:40 weight ratio. Fibers are spun from the dope with a dry jet-wet spinning
system having the spinneret position above a coagulation bath. This air gap permits
evaporation of the volatile component in the spinning dope, which is an essential re-
quirement for preparing asymmetric hollow fibers. Generally, high salt rejection is
achieved by post-treating the coagulated fiber in water at 70 - 80°C for 5 minutes.

A small laboratory-scale device for reverse osmosis is shown in Figure B-1. A small
loop of fiber is sealed in epoxy resin near the open end. These fiber loops are then
assembled into high-pressure tubing and saline water is pumped through the tubing
over the outside surface of the fibers at a pressure exceeding the osmotic pressure
of the solution. Desalted water that permeates the fiber walls is discharged from the
open end of the loops. Zones of reduced flow outside the fibers can result in re-
duced water productivity and rejection. Consequently, a very high flow rate is main-
tained through the pressure casing to ensure that the results from these loop cells
reflect the hollow-fiber characteristics and not the design characteristics of the device.
In sealing up from laboratory test units to full-scale hollow-fiber cartridges, the dis-
tribution of brine over the outside of the fibers is an important design consideration.

Nylon

Hollow fibers of modified nylon have been used in commercial-scale desalination
units sold by DuPont. These modified nylon fibers are claimed to have greater
biological and mechanical stability than cellulose acetate fibers and a wider operable
pH range. The chemical nature of the nylon hollow fibers used in early B-5 permeators
from DuPont has not been disclosed. However, there is evidence that formic acid-
treated nylon fibers were used in this device. This unit clearly demonstrated the
ability of the nylon membrane to desalt brackish sulfate waters, although rejection
of chloride ions was poor.

Hamilton Standard _____ U A®
DIVISION OF UNITED AIRCRAFT CORPORATION
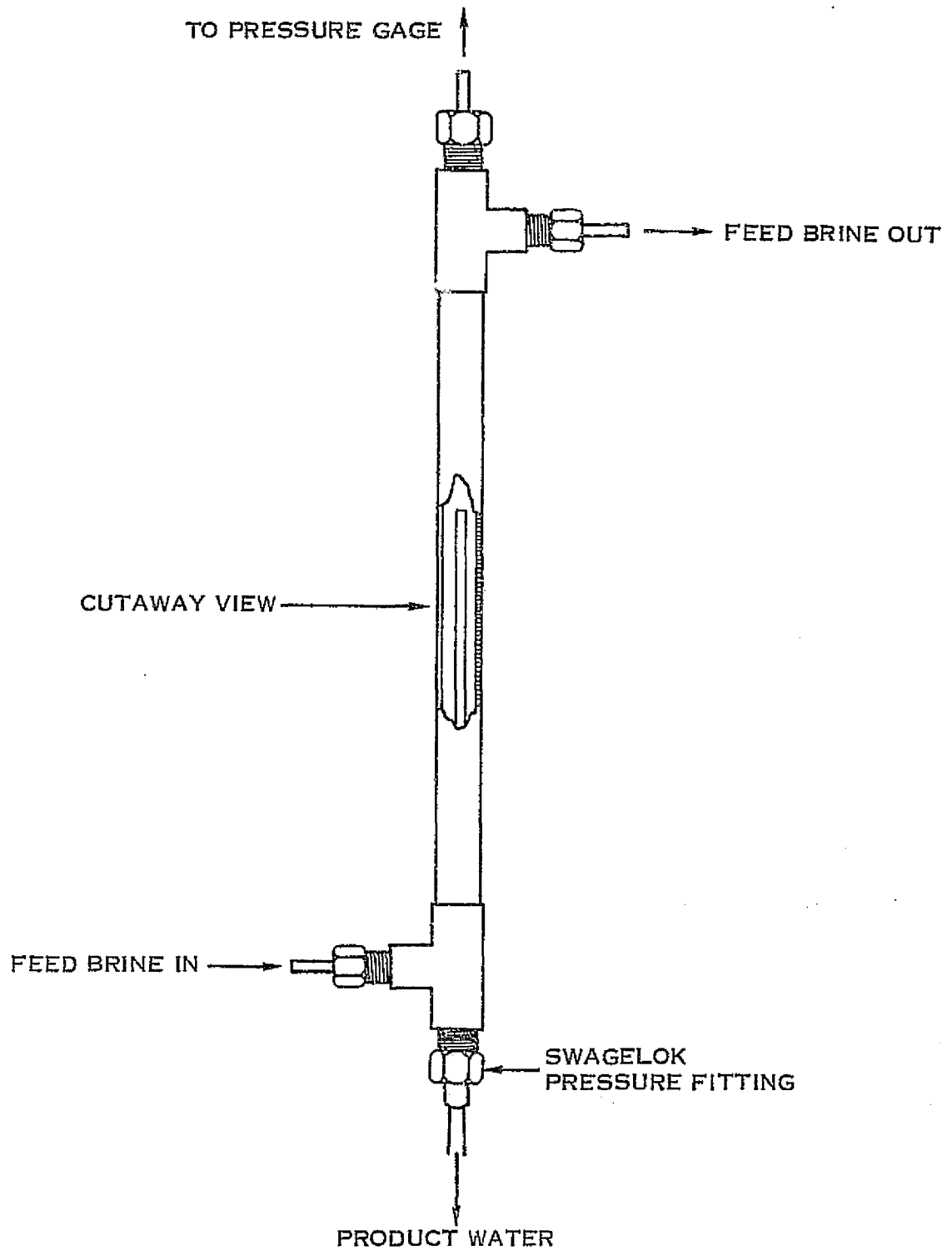
FIGURE B-1. HOLLOW-FIBER TEST CELL FOR
LABORATORY EVALUATION

(Continued)

Nylon-6 or nylon-6, 6 hollow fibers can be swollen in solutions containing either certain protonic acids, lyotropic salts, or Lewis acids to increase their water permeability. The treatment results in a weight loss for the hollow fibers ranging from 1 to 70% depending upon the duration and severity of the treatment. The increase in water permeability obtained by this treatment is believed to result from the formation of microvoids by dissolution of the less-ordered portions of the polymer and increased crystallinity of the more-ordered portions. In one example, hollow nylon-6,6 fibers (53 μ OD by 27 μ ID) were treated in an aqueous solution containing 65% formic acid at 25°C for 4 hours. The treated bundle was washed in water and not allowed to dry during cell assembly. In a reverse-osmosis test run at 550 psi with a feed solution containing 1500 ppm dissolved mixed sulfate salts, the water flux was 0.09 gfd and the salt rejection 95.6%.

Nylon hollow fibers of varying permeability and selectivity have been prepared and tested. With the original permeator there were difficulties with wet oxygenation of the nylon membrane fibers and pressure-drop instability within the device.

Improvements were achieved by development asymmetric hollow fibers made of an aromatic polyamide. The permeator has a shell-and-tube configuration similar to a single-end heat exchanger. The looped fibers are potted at one end in an epoxy resin. Saline water under pressure enters the shell side through a distributor-tube located in the center of the fiber mat. The brine flows radially from the distributor tube through the fiber mat, collects at the flow screen, and flows the length of the shell to a concentrate or brine exit port near the same end as the feed port. The desalted water, which permeates the fiber walls inward from the outside, is discharged from the open end of the fibers on the low-pressure side of the tube sheet. Typical characteristics for the permeator are as follows: fiber OD 84 fiber ID 42 operating pressure (external to fibers) 400 psi, operating pH range 5-9, product water capacity 2000 gallon per day, sodium chloride passage less than 10%, permeating area 1500 ft^2, and chlorine tolerance 0.05 ppm on a continuous basis.

Dialysis

Dialysis is a way of separating relatively small molecules from large ones. The success of dialysis depends on whether conditions can be found in which there is an adequate difference in the rates of diffusion of solutes through the membrane. The rate of diffusion of a simple solute through a membrane depends on the solute concentration, the membrane permeability. Commercial applications of dialysis were frequently related to recovery and purification of process streams.

(Continued)

In 1960, dialysis began to be used in the medical field as a substitute for the human kidney. The blood of these patients is purified by dialysis with cellulose membranes against an isotonic saline solution.

The early commercial dialyzers and artificial kidneys were bulky and inefficient.

The development of small semipermeable hollow fibers or capillaries provided the basis for the design of smaller and more efficient commercial dialyzers. With this membrane geometry, enormous support-free membrane area can be generated economically and assembled into dialyzers that possess a minimum holdup volume. The rigidity of the small, thick-walled, semipermeable cylinders provides a well-defined fluid flow path with a resultant minimum in liquid-side transfer resistance. The first hollow-fiber dialyzer to be introduced commercially was the hollow-fiber artificial kidney. This hollow-fiber hemodialyzer contains 11,000 hollow fibers of cellulose of approximately 200 μ ID giving a total surface area of 10 ft^2. The cellulose hollow fibers are produced by hydrolyzing or deacetylating cellulose acetate fibers which are similar to those already discussed in connection with reverse osmosis. With wall thicknesses of only 20-25 μ these fibers allow the efficient passage of solute having a molecular weight of up to 2000-4000. The blood to be cleansed is passed through the inside of the hollow fibers while the isotonic saline solution is distributed over the outside of the fibers. Metabolic wastes, such as urea, uric acid, and creatinine, rapidly diffuse from the blood through the membrane and into isotonic saline solution.

With this device, highly efficient transfer of these solutes has been achieved. Hemodialysis therapy lasting more than two years has demonstrated the expected advantanges of this membrane configuration.

Industrial devices ranging in size from 1 to 150 ft^2 of transfer area are under development. One and 20 ft^2 sizes have been released commercially. These two devices provide for rapid and simple laboratory dialysis separation.

Two cellulosic membranes are available in each size. The transport properties of these membranes and devices can be found in Table B-6. In addition to providing efficient dialytic conditions, the hollow fiber concept can be readily utilized to remove water or concentrate solutions by applying a transmembrane pressure across the hollow fibers. The removal of water by this method is known as ultrafiltration in contradistinction to reverse osmosis, since the dialysis fibers are readily permeable to low-molecular-weight solutes and no significant osmotic back pressure is generated across these fibers during the water removal. Consequently, the advent of semipermeable dialytic hollow fibers provides the unique opportunity to combine dialysis with ultrafiltration. This unit operation is particularly suited to the purification and concentration of high-molecular-weight biological species or polymers.

TABLE B-6

TRANSPORT CHARACTERISTICS OF HOLLOW-FIBER BEAKER UNITS

Unit	Molecular-Weight Cut-Off	Water Flux At Standard Operating Conditions	Sodium Chloride Transfer
dialyzer	5,000-10,000	$1 \text{ cm}^3/\text{min}/\text{ft}^2$	99.9% removal from 100 ml in 40-60 min
ultrafilter	30,000-40,000	$10 \text{ cm}^3/\text{min}/\text{ft}^2$	99.9% removal from 100 ml in 40-60 min

Ultrafiltration

Low-molecular-weight solutes can be separated from liquids containing polymeric or other high-molecular-weight materials without phase change by employing membrane ultrafiltration. As in reverse osmosis the driving force is hydraulic pressure and the solution components are separated on the basis of molecular size and shape. Membrane ultrafiltration operates at less than 100 psi because the membranes generally reject solutes greater than 500 in molecular weight, which provide only minor osmotic contributions. Flat-membrane ultrafiltration has generated considerable interest in several industrial areas, most notably, in the food and pharmaceutical industries. With ultrafiltration membranes the solvent flux through the membrane increases rapidly as the molecular-weight cut-off increases. Consequently, ultra-filtration membranes show a flux an order of magnitude higher, even at lower operation pressures, than that of reverse-osmosis membranes. However, to achieve the full potential of the ultrafiltration membranes, concentration polarization at the membrane surface must be controlled. This is generally accomplished by designing equipment that will maximize the transport of rejected solutes away from the membrane. Typically, back diffusion is augmented by operating at high fluid shear rates at the membrane surface, which necessitates either increasing the flow velocity or decreasing the channel height. Hollow fibers, with their well-controlled and minimal channel height, offer an attractive possibility of an ultrafiltration membrane configuration.

Two examples of hollow-fiber ultrafiltration devices have been described to date. These are the ultrafiltration artificial kidney under development by Amicon in collaboration with the University of Pennsylvania[h] and laboratory ultrafiltration devices offered commercially by The Dow Chemical Company. The former is a 4 ft^2 shell-and-tube ultrafiltration device which has been used experimentally to remove toxins from uremic dogs by ultrafiltration of their blood and reconstitution with makeup saline solution. The Dow devices have surface areas of 1 and 15 ft^2 with a comparable solute flux and can be used for laboratory separations of solutes greater than 70,000 in molecular weight.

Gas Permeation

The Permasep gas-permeation device introduced by Du Pont is primarily intended for two applications[I, J]: (1) to upgrade carbon monoxide synthesis gas by removing as much as 95% of the hydrogen, which can then be recycled to other processes, and (2) the recovery of high-purity hydrogen from hydrogen synthesis gas and from crude

(Continued)

refinery high-pressure hydrodesulfurizer gases. With these latter two gases the methane is concentrated and can be recycled for other uses. The commercially available Permasep devices are fabricated with hollow Dacron polyester fibers of 36μ OD and 18μ ID. The permeator shells are 12 in. in internal diameter and just under 18 ft. long, each containing more then 32 million hollow fibers.

Another gas-permeation device is the "artificial lung" which substitutes for normal respiratory function during open heart surgery. No hollow-fiber artificial lungs are commercially available at this time; however, at least three have been reported to be under development (K, L, M). The artificial lung must be able to oxygenate up to 5 liters/min venous blood to at least 95% saturation, which generally requires an uptake of 300 ml/min of oxygen. Concomitantly, the artificial lung must be able to remove an equal quantity of carbon dioxide. The most widely used artificial lungs oxygenate and strip carbon dioxide by contacting blood with oxygen gas. Although this blood-gas interaction is known to denature plasma protein, in most cases the body is able to compensate for this denaturation if the by-pass duration is less than 2-4 hr. Significant decrease in protein denaturation has been observed if a membrane is placed between the blood and gas phases. Consequently, the membrane oxygenator appears to be the artificial lung of choice. However, commercially available membrane oxygenators suffer from insufficient oxygenation capacity and are expensive devices that are difficult to rebuild prior to each clinical operation. Therefore, a compact and efficient artificial lung fabricated of semipermeable hollow fibers should be ideal for this application.

Future Trends

Currently, there is evidence to suggest that hollow fiber membrane devices will play a major role in blood oxygenation, artificial-kidney therapy, ultrafiltration, industrial dialysis, and reverse osmosis and life support system applications. In the medical area, hollow-fiber-membrane devices will be particularly important because of their high surface area to priming volume ratio and high transport efficiency resulting from well-defined blood channels, as well as their ease of operation and potential disposability.

Hollow fibers are also well suited to ultrafiltration because the thin channels in combination with high wa... ar, facilitate back diffusion of the higher-molecular-weight species that are rejected at the membrane surface.

(Continued)

Hollow fibers are an attractive membrane configuration for industrial dialysis.
Widespread use of dialysis as a unit operation is now greatly impeded by the high
initial capital cost, even though the operating cost can be quite low. Hollow-fiber
dialysis equipment can be fabricated at a significantly lower cost than devices with
flat membranes. Many of these advantages accrue to reverse-osmosis devices as
well. A recent study indicates that the cost for desalinating brackish water is com-
parable between hollow-fiber units and the two best flat-membrane configurations,
even though the hollow fibers have a flux rate of only one tenth that of the flat membranes.
Since it is unlikely that the flat membranes will be able to retain this flux advantage
over hollow fibers, it seems reasonable to assume that hollow fibers will also play
an important role in reverse osmosis.

Most important of all, the subject of membrane transport by primary chemical bond
formation rather than longer range secondary forces will be developed. This will
result in the preparation of synthetic membranes with a thermodynamic driving force
generated at or in the membrane itself rather than applied from an external source of
energy. Another benefit from membranes employing direct chemical bonding for
transport will be total separations rather than partial ones. These advances should
bring the goal of perfectly separating semipermeable interfaces in sight.

B-9 Polymers for Microporous Membranes

Thin films of cellulose, cellulose esters, polypropylene, nylon, poly (vinyl chloride),
polycarbonate and epoxy resins have sound application as microporous membranes.
This type of membrane is produced with pore size from 100 $\overset{o}{A}$ to 10μ, and can be
made by leaching out incorporated salts, soaps, water-soluble polymers such as
poly (ethylene oxide), or starch. Matrixes such as the cellulose esters can be cast
from precisely formulated mixed solvents with controlled evaporation procedures
to yield a predetermined pore size with a uniformity of ± 5%.

Cellulose triacetate has been used because of its stability to various humidity con-
ditions and because of its high tensile strength. Membranes made from this material
may be autoclaved (heated at pressure) without significant change in pore size.

Regenerated cellulose is a choice material when resistance to organic solvents is
required.

Where resistance to strongly acid or alkaline media is required, membranes of poly
(vinyl chloride), poly (vinylidene fluoride), poly porpylene or polyethylene are
satisfactory.

(Continued)

Among the inorganic polymers, leached borosilicate glass, unfired, produces a microporous membrane with pores controllable from 40 to 200A°.

General examples of the production of microporous membranes by addition of additives are:

1.   Cellulose acetate cast from a "good" solvent such as acetone containing additives such as organic phosphates, amides, organic acids, sulfoxides is a good ultrafilter. If the additive is omitted and only a good solvent is used, a dense membrane of very low aqueous permeability results.

2.   Cellulose nitrate with additives in the casting solution yields membranes with controlled porosity. The pore size may be varied from 20 A° to 2μ.

3.   Gelatinous ultrafiltration membranes can be made from crosslinked poly (ethylene oxide), crosslinked poly vinylpyrolidone, or crosslinked poly (vinyl alcohol)

B-9.1 Convective Transport Through Hydrophilic Porous Membranes

In microporous membranes whose surfaces are wetted by a contacting liquid, it is considered that capillary forces cause the membrane pores to be filled with the liquid and that vaporization of the liquid occurs at the liquid-gas interface. In such a case any solutes present in the liquid may also be carried into the pores and tend to increase the solute concentration within the liquid in the membrane. An increase in concentration of solute decreases the activity of the liquid and therefore reduces the partial pressure of the vapor in contact with the liquid.

The equilibrium level of solute in the membrane will be determined by the balance between liquid loss for vaporization and solute back diffusion from the pores to the bulk liquid. Pore size, pore volume and thickness of the membrane determines the resistance to flow within the membrane.

Gases in contact with such a wetted membrane may permeate the membrane by diffusion through the liquid in the membrane. The thickness of the liquid is equivalent to that of the membrane.

B-9.2 Convective Transport Through Hydrophobic Porous Membranes

In microporous membranes whose surfaces are not wetted by a contacting liquid or its vapor, vapor permeation proceeds by a different mechanism. If the interfacial tension and pore size of the membrane are such that penetration of liquid into the pores does not occur, the interface between a gas phase and the vapor of the liquid will be on the liquid side of the membrane. Vapor permeation then follows the mechanism associated with Knudsen effusion and the membrane barrier resistance will be low relative to other transport modes.

(Continued)

Since the liquid does not penetrate into the pores, solutes in the liquid will also be excluded. There can be a concentration polarization at the membrane surface due to vaporization of liquid but this can be taken care of hydrodynamically.

Also, since the membrane acts as a porous divider permeable only to gases, the transport of gases are governed by the Knudsen coefficients and the net partial pressures of the gases on each side of the membrane.

B-9.3 Polymers for Separation by Diffusive Transport

When membranes of the solution-diffusion type are made from polymers with limited ability to swell in the medium being transported, there can be significant differences in the diffusion coefficients of even closely related small molecules. This difference coupled with differences in solubilities of the small molecules in the polymer matrix leads to separation of mixtures by differential transport of components. The limited swelling of the membrane may be due to low solubility of the diffusants in the membrane; to a high degree of crosslinking in the membrane polymer; or may be because one face of the membrane is dry (as in pervaporation).

Much work has been carried out in developing this type of membrane for separations of salts from water by reverse-osmosis. The most used membrane for desalination by diffusive pressure-driven transport is cellulose acetate having a degree of acetylation of 2.4. An asymmetric membrane developed by Loeb, Sourirajan and others [o] has made this method of desalination a practical process.

It consists of a thin (about 0.3μ) layer of dense cellulose acetate supported by an integral, spongy, microporous layer about $50-100\mu$ thick of the same material. The thin, dense layer differentiates between the transport of water and many salts with high efficiency and with good flux owing to the thinness of the diffusion layer.

Since most pressure permeation is carried out at 600-1500 psi, some compaction of the membrane, with a dimination of flux, is observed and is a major problem.

Many polymers have been evaluated for the treatment of aqueous solutions. In addition to cellulose acetate, the mixed acetate propionate, acetate butyrate esters, and their combinations have been of interest. Among those having significant desalination properties [p] and which therefore may be presumed to have interesting separating properties for other water-soluble solutes, are polyacrylonitrile, poly (vinylene carbonate), nylon-6,6, nylon-6,10, poly(isobutyl vinyl ether), polytetrahydrofuran, poly(ethyl acrylate), poly (hydroxyethyl methacrylate), and a copolymer of ethylene dimethacrylate and hydroxyethyl methacrylate. If the polymer to be evaluated is not directly suitable for membrane formation, it can be formed into a graft copolymer with cellulose. In this form triallyl phosphate and methyl vinyl ketone have been used. A polymer alloy of ethylcellulose and poly(acrylic acid) also had good desalinating properties.

(Continued)

Separation of organic mixtures by pressure-driven solution-diffusion membranes has been carried out primarily by pervaporation. In pervaporation a mixture of liquids, often heated, on the upstream side of a membrane is driven through the film by a vacuum applied to the downstream side, which is consequently dry. The gradient of diffusion coefficients within the membrane, often varying by several orders of magnitude owning to a gradient of morphology from the wet to the dry side, leads to sharper semipermeability but lower flux rates than pressure permeation. Most of the data in the sparse, published literature deal with mixtures of simple organic solvents such as: xylene-heptane, hexane-acetone, carbon tetrachloride-chloroform, methanol-ethylene glycol, benzene-cyclohexane, etc. For organic systems as well as aqueous ones cellulosic compounds are the basis for many semi-permeable membranes. Regenerated cellulose itself, ethylcellulose, cellulose acetate, and acetate butyrate have been used. Typical crosslinking agents for these film-forming polymers are formaldehyde, butyraldehyde, and toluene diisocyanate. Other membrane materials used for organic permeants are polyethylene, polypropylene, poly(vinyl chloride), saran, poly (tetrafluoroethylene), rubber hydrochloride, nylon-6,6, poly(ethylene terephthalate), and poly(vinyl alcohol).

B-9.4 Membranes for Separating Gases

Generally the diffusion of gases through polymeric membrane approaches the model of noninteracting molecular permeants whose transport is controlled by size and solubility. For example, helium from natural gas and other sources can be purified by the use of high-purity silica glass membranes, since this smallest of gas molecules (2 A^0) can pass through via defects in the glass structure. Although permeation rates are increased by heating the glass membrane, the selectivity is diminished by increased lattice vibrations and expansion. Organic membranes for helium and hydrogen purification are designed with the opposite principle in view: namely, rejection of the methane and other larger molecules. This is done by using the less crystalline fluorocarbon films such as perfluorinated ethylene-propylene copolymer and a copolymer of tetrafluoroethylene and a perfluorinated dioxolane. The latter membrane has high separation factors for helium (up to 700) and hydrogen (up to 150) from methane and shows some separation of oxygen from air (separation factor of about 3.5).

Another organic polymeric membrane being studies today for gas separation is silicone rubber. This material has the highest gas permeability of polymeric films.

It has received much attention as an artificial gill, since it passes carbon dioxide faster than oxygen; yet when used under water it is plasticized by water on the outside, making it asymmetric and thereby favoring the influx of oxygen. These two phenomena act in concert to make it possible to support life for small animals under water. A table of gas permeabilities is shown for representative polymers in Table B-7. This table gives an indication of the degree of separation which can be achieved by the solution-diffusion mechanism.

TABLE B-7
GAS PERMEABILITY CONSTANTS OF SOME POLYMERS AT 25°C

Polymer	Gas Permeability Constant [a] to				
	Hydrogen	Helium	Nitrogen	Oxygen	Carbon Dioxide
natural rubber	500	308	84	230	1,330
polybutadiene	420		64.5	191	1,380
polychloroprene	136	45	11.8	40	250
poly(vinyl chloride)	36		0.4	1.2	10.2
poly(vinylidene chloride)	0.76	3.7	0.01	0.05	0.29
polyethylene (0.932 g/ml)	86	74	11.7	55	265
ethylcellulose	82	260	84	265	430
fiorinated ethylene-propylene copolymer	110	400	21.5	59	17
poly(ethylene terephthalate)	6	11	0.05	0.3	1
silicone rubber		2,530	2,000	6,000	28,000
chlorosulfonated polyethylene	142	95	11.6	28	208
cellulose acetate butyrate	210	140	16	60	310
polyamide	10		0.2	0.38	1.6

[a] In cc (STP)- mm/cm^2 - sec - cm Hg x 10^{10}

B-10   TRANSPORT PROPERTIES OF MEMBRANES

Permeability

Permeability is the measure of ease with which an intact material can be penetrated by a given gas or liquid. Although the general term "permeability" may apply to any form or shape of a material, the property is most important and most conveniently studied in the passage of matter through a thin film or membrane. Membranes are generally described as permeable, semipermeable (permeable to some substances but not to others), or permselective (permeable to different extents to different molecular species under equal driving force). A given membrane, however, may be described by any of these terms depending upon the nature of the penetrant or penetrants being considered (eg, cellulose is permeable to water, permselective to water-glucose solutions, and semipermeable to water-protein solutions).

Membranes may be homogeneous or heterogeneous. A homogeneous membrane is defined as one which has uniform properties across all its dimensions. Only a few membrane materials would fit this definition. Most films have either some anisotropy due to molecular orientation during the manufacturing process or fillers, additives, voids, or reinforcing materials which would cause them to be classified as heterogeneous. Another important class of heterogeneous membranes is comprised of laminates, such as coated cellophane. Many polymers contain crystalline and amorphous regions, and must be classified as heterogeneous.

The terms permeability and permeability coefficient are defined in various ways by different authors.

Permeability Coefficient

The permeability coefficient of a material to a gas or vapor can be defined as the cubic centimeters of vapor at STP permeating through a material of unit area (cm^2) and unit thickness (cm) under a partial pressure difference of one centimeter Hg per unit time (sec), regardless of the mechanism involved. These units will be used wherever possible, ie, (ml at STP) (cm)/(cm^2) (sec) (cm Hg).

Since permeability coefficients in these units have values for most polymers in the range of 10^{-7} to 10^{-12} many larger number units have been used in practical application studies. The most common of these is in units of (g)(mil)/(m^2)(24hr)(atm). The various units may readily be converted from one to another. In the case of permeability to liquids or vapors, the vapor pressure at ambient temperature is necessary to convert the values to the proper units mentioned above.

Since permeability coefficients are often highly temperature dependent, values should be quoted at a given temperature. In the case of organic vapors, and often with water vapor, the permeability coefficients are dependent on the vapor pressures themselves, and it is necessary to specify the exact conditions of measurements.

(Continued)

In general, the permeability coefficient P at a given temperature may be (a) almost constant for all vapors and independent of pressure (capillary flow or pinhole), (b) a constant for a particular vapor and independent of pressure (the ideal activated diffusion process), and (c) a coefficient which varies with vapor pressure (nonideal activated diffusion process).

Principal Models of Permeation (Q, R)

The term permeability does not imply anything about mechanism, and several permeation mechanisms may be operating concurrently during the measurement of flux of penetrant. Permeation of relatively small molecules through a membrane may occur by at least three processes: (a) flow through pores or pinholes in the membrane, (b) diffusive flux of molecules dissolved in the membrane, and (c) con concurrent operation of the above mechanisms.

Flow Through Pores

In a nonhomogeneous membrane, permeation of small molecules may occur through preexisting pores or capillaries, and in this case the size of the permeant relative to pore and the viscosity of the permeant are the controlling factors governing permeability. The simplest type of flow mechanism is viscous flow, in which the volume of penetrant q passing through a capillary of radius r and length Δx in unit time is given by Poiseuille's equation (eq. 1) where n is the viscosity of the

$$q = \pi r^4 \Delta p / 8 \eta \Delta x \tag{1}$$

permeant and Δp is the pressure drop across the capillary. The permeant flow per unit area of capillary and per unit time is therefore given by equation 2 where β is

$$q / \pi r^2 = \beta r^2 \Delta p / 8 \eta \Delta x \tag{2}$$

a tortuosity factor which increases the effective length from Δx to $\Delta x / \beta$. Hence the membrane flux can be given as equation 3, where ϕ is the volume fraction of capillary in the membrane.

$$q = \frac{\phi \beta r^2}{8 \eta} \frac{\Delta p}{\Delta x} \tag{3}$$

Accordingly, the permeability coefficient P defined previously corresponds to equation 4. For all penetrants that do not interact with the membrane, ie, for which

$$P = \phi \beta r^2 / 8 \eta \tag{4}$$

ϕ and r are independent of the penetrant, the permeability coefficients are inversely proportional to the viscosities of the penetrant.

The viscosity of gases is directly proportional to temperature and, accordingly, permeability of gases through porous media shows a small but negative temperature dependence.

(Continued)

For liquid permeants, viscosity is generally inversely proportional to temperature, and the temperature dependence is positive. In liquid permeation the pore radius is often calculated by assuming that the flux goes only through the capillaries and the volume fraction of fluid in the entire membrane is the volume fraction of capillaries. The equivalent pore radius so obtained may serve as a parameter for characterizing membrane permeability. However it should be borne in mind that such numbers arise from a hypothetical model of membrane behavior and may not correspond to physical reality.

When permeation occurs by a flow mechanism the pressure drop across the membrane is the driving force regardless of the phase of the penetrant, ie, whether it is a gas or liquid. It should be emphasized that simple viscous flow as described above is only one of a number of modes of flow through pores. As the size of the pore approaches the mean free path of a gas, for example, Knudsen flow and other mechanisms become operative.

Activated Diffusion

In a membrane which has no pores or voids permeation of small molecules occurs by an activated diffusion process. In this process the penetrant dissolves and equilibrates in the membrane surface, and then diffuses in the direction of lower chemical potential. At the second boundary equilibrium with the fluid is again established. If the boundary conditions on both sides of the membrane are maintained constant, a steady-state flux of the components will be established which can be described at every point within the membrane by Fick's first law of diffusion (eq. 5) where Q_i is the mass flux (g/cm^2-sec), D_i is the local diffusivity (cm^2/sec),

$$Q_i = - D_i \frac{dc_i}{dx} \qquad (5)$$

c_i the local concentration of component i (g/cm^3), and x the distance through the membrane measured perpendicular to the surface . When more convenient the mass units can also be expressed as volume units, eg, cm^3 at standard temperature and pressure.

If the rate of arrival and removal of the permeant at both membrane-fluid boundaries is large compared with its rate of penetration, as is commonly the case with gases, then the fluid-phase composition remains constant up to the membrane surface.

(Continued)

In gas permeation partial pressure, p_i, of a component i outside the membrane is usually measured. This pressure, p_i, is directly proportional to activity and it is related to the membrane concentration of penetrant at the surface by Henry's

$$C_i = S_i p_i \qquad (6)$$

law (eq. 6) where S_i is the Henry's law constant of component i (or its solubility coefficient) in the membrane material. Equation 5 may then be rewritten as equation 7.

$$Q_i = -D_i S_i \frac{dp}{dx} \qquad (7)$$

The terms $D_i S_i$ may be combined into a permeability coefficient P_i, giving equation 8.

$$Q_i \, dx = -P_i dp_i \qquad (8)$$

It is possible for both the diffusion coefficient and the solubility to vary with the composition of the penetrant-membrane mixture. However, for the simple case of permanent gases which do not interact strongly with the membrane, P is a constant and equation 8 may be written in its integrated for (eq. 9).

$$P_i = \frac{Q_i x}{\Delta p_i} \qquad (9)$$

Measurement of Permeability

The measurement of permeability is carried out by two basic methods, (a) transmission methods and (b) sorption-desorption methods. In the transmission method two sections of a chamber are separated by the membrane to be tested and a concentration gradient of the penetrant is applied across the membrane. This can be accomplished with or without a total pressure difference between the sides. The rate of transmission can then be determined by a number of techniques. In sorption-desorption methods samples are rapidly brought into a liquid or vapor of known activity, and from the rate of sorption and desorption and the equilibrium sorption value the diffusion coefficient and the solubility coefficient can be calculated. The permeability coefficient may then be estimated from these two values.

Permeabilities measured by those two basic principles agree only when the sorption and the diffusion of penetrant in the polymer membrane are ideal. Because of the generally accepted concept of "permeability" and also the phenomenological aspect of the permeation process, it is usually better to measure the permeability by the transmission methods.

Transmission Methods

The amount of penetrant passing through the membrane in unit time can be measured

(Continued)

by a variety of methods such as refractive index or interferometry, thermal conductivity, chemical analysis or colorimetry, gravimetric techniques, mass spectroscopy, gas chromatography, and pressure-volume-temperature measurements of gases. Virtually any kind of method which can quantitatively determine the amount of penetrant can be utilized for permeability measurement.

The most accurate method of measuring permeability constants by the transmission method is the measurement of steady state permeation rates. However, permeation of many penetrants through the majority of polymer membrances occurs as an activated diffusion process; in that case, the increase of the measured parameter is not a simple linear function of time and is accompanies by a characteristic time lag. The time lag is related to the diffusion constant of the penetrant in the polymer, and is a characteristic parameter which depends only on the nature of polymer and the thickness of the membrane and does not depend on the method of measurement. Therefore, regardless of the sensitivity, the accuracy, and the time required for a particular measurement, one must make sure that the permeation reaches the steady state. For many polymers in readily available thicknesses and for many gases and vapors, the time lag often exceeds a few hours.

Factors Influencing Permeability

Temperature

The dependence of both D and S on temperature generally follows a relationship of the type given by equations 10 and 11 where Hs is the apparent heat of solution and E_D

$$S = S_0 \exp(-Hs/RT) \tag{10}$$

$$D = D_0 \exp(-E_D/RT) \tag{11}$$

the activation energy for the diffusion process, and the subscript zero refers to a standard state. Consequently, the permeability coefficient, P, follows a similar relationship (eq. 12).

$$P = P_0 \exp(-E_p/RT) \tag{12}$$

In equation 12

$$E_p = H_S + E_D \tag{13}$$

The sorption of a gas or vapor in a polymer may be divided into two processes, condensation of the vapor followed by mixing. Thus, H_S can be expressed as the sum of the heat of condensation and the heat of mixing (eq. 14).

(Continued)

$$H_S = H_{cond} + H_{mix} \tag{14}$$

For permanent gases, such as hydrogen, helium, oxygen, or nitrogen, H_{cond} is negligible and H_S is determined largely by H_{mix}. For permanent gases, therefore, the heat of solution is small and positive and S increases slightly with increasing temperature. For condensable vapors, such as sulfur dioxide, ammonia or water, H_S is negative owing to the large heat of condensation, and S decreases with increasing temperature.

The activation energy E_D is always a positive quantity. Therefore, the overall permeation energy E_p is positive for permanent gases. With a condensable vapor such as water in polystyrene, however, the heat of condensation is of opposite sign and nearly equals the diffusion energy. The net result is a permeability nearly independent of temperature.

Membrane Thickness

From equation 8 it can be seen that the permeability coefficient should be independent of thickness. In practice, however, it becomes very difficult to avoid pinholes in very thin membranes. When preparing a film from a melt or from solution the outside surfaces are cooled much more rapidly than the interior. This may produce a "skin effect" which becomes much more important in very fine films. Generally, the permeability coefficient of films thicker than 0.001 inch tends to become independent of thickness. In the Loeb type(s) membrane used in reverse osmosis, however, a thin skin controls the permeability and the apparent permeability coefficient increases with increasing membrane thickness.

Density of Polymer

In general, the density of a polymer, as related to the free volume content, is a good measure of the pre-existing hole volume or "looseness" of the polymer structure. The lower density polymers are therefore generally more permeable.

Molecular Weight

The molecular weight of a polymer has been found to have little effect upon the rates of diffusion and permeation except in the very low range of molecular weights not normally encountered in coherent films.

Chemical Structure

Chemical modification of a polymer, including copolymerization and substitution reactions, can have a pronounced effect on P, D, and S. In general, if the cohesive-

(Continued)

energy density of the polymer increases as a result of modification, it will decrease
the value of the diffusion coefficient. However, the effect of change in the cohesive
energy on the solubility coefficient depends entirely on the cohesive energy of the
penetrant vapor. Since the solubility would be expected to increase as the cohesive-
energy densities of the vapor and the polymer become more nearly equal, the increase
in the cohesive energy of the polymer can be in either direction; ie, if it approaches
the value of the vapor the solubility will be increased; however, if it departs from the
value of the vapor, the increase in cohesive energy of the polymer eventually de-
creases the solubility of the vapor. Accordingly, the overall permeability will depend
on the magnitude of changes in both D and S. These relationships may be illustrated
by the example of esterification of cellulose.

Upon esterification of cellulose the cohesive energy decreases, since highly polar
hydroxyl groups are replaced by ester groups. This causes the increase of the diffusi-
bility of any penetrant in the polymer, but the effect of the esterification on the solu-
bility of penetrant depends on the nature of the penetrant. For example, the solubili-
ties of the permanent gases which have very small cohesive energies will be increased
by the decrease in the cohesive energy of the polymer due to the esterification. How-
ever, their magnitude is relatively unimportant, since the difference between the co-
hesive energies of the gases and that of the polymer are overwhelmingly large and
consequently the contribution of the solubility to the overall permeability is relatively
small. Therefore, the permeability of the permanent gases increases as a result of
the esterification. On the other hand, in the case of water vapor the change in the
solubility is in the opposite direction. Since water has a cohesive energy that is de-
cidedly higher than that of most polymers, the decrease in the cohesive energy of the
polymer increase the difference in cohesive energy between the polymer and the
penetrant, leading to the lowering of the solubility. Furthermore, the solubility plays
a predominant role in the overall permeability of water vapor, and the magnitude of
the change in solubility is more than enough to compensate for the increase in the
diffusibility. Accordingly, the water-vapor permeability decreases on the esterifica-
tion of cellulose despite the increase in the diffusibility of the penetrant in the polymer.

Crystallinity

The crystallites can be considered impermeable; consequently, the higher the degree
of crystallinity the lower the permeability to gases and vapors.

Orientation

The permeability in an amorphous polymer below or not too far above its glass-transi-
tion temperature is somewhat dependent on the degree of molecular orientation of the
polymer, and is normally reduced, as compared to higher temperatures, although
small strains sometimes increase the permeability of certain polymers.

(Continued)

The orientation of elastomers well above their glass-transition temperature has relatively less effect on the overall transport property.

Crosslinking

Crosslinking will decrease the permeability mainly due to the decrease in the diffusion coefficient. The effect of crosslinking is more pronounced for large-molecular-size vapors.

Plasticizers

The addition of a plasticizer to a polymer usually, but not always, increases the rates of vapor diffusion and permeation.

Glass Transition

Polymers may undergo transitions from the glassy state to a rubbery or leatherlike condition over the temperature range in which their permeability is of interest. In generaly, above the glass-transition temperature, T_g, heats of solution are larger (less negative) and activation energies are larger (more positive) than below the transmission. An Arrhenius temperature dependency exists on both sides of T_g but different values of the constants may have to be used (T, U). For small penetrants the glass-transition may not have an effect. If the penetrant is highly sorbed by the polymer it may also plasticize the polymer and lower the glass-transition temperature.

Condensable Vapors and Polymer Swelling

The extent to which a homogeneous polymer will absorb a vapor or liquid depends on the closeness of their chemical constitution. When the penetrant has similar polarity or, more precisely, as the cohesive-energy density of the penetrant and polymer approach the same value, more penetrant dissolves in the polymer and the polymer becomes swollen. Under these circumstances both the solubility coefficient, S, and the diffusion coefficient, D, from equation 7 are likely to be concentration dependent and so consequently is the permeability coefficient, P. An integrated permeability coefficient, $\bar{P}$, is often used as a convenient method of describing permeation between two vapor pressures (eq. 15). Film thickness is also concentration dependent, but the usual practice is to

$$\bar{P} = \frac{Q_x}{p_2 - p_1} \tag{15}$$

use the unswollen film thickness and incorporate all corrections into the integrated permeability coefficient.

(Continued)

For strongly swelling penetrants it is also obvious that in steady state permeation a nonlinear concentration profile must exist. Most of the resistance to transport is also localized on the outflow side. The situation is analogous to permeation of composite membranes.

In a strongly swollen membrane, relaxation of stresses produced during membrane manufacture may take place. When this happens the permeability at all degrees of swelling will be changed. For characterization of intrinsic polymer properties a membrane should be conditioned by exposure to liquid or high vapor concentration. For control of manufactured materials it may be more desirable to consider only the conditions under which the membrane will be used.

Liquid and Vapor

Permeability of a polymer membrane to saturated vapor and to liquid should be the same in principle. In practice it is difficult to measure permeability of saturated vapor and an extrapolation technique is often used. Swelling often increases very rapidly near saturation and the extrapolations may not be valid. Contact with a liquid may also induce morphological changes.

Permeability Ratios and Mixed Vapors

For noncondensable gases, Stannett and Szuarc (V) predicted that the permeability ratio of a pair of gases should be relatively constant over a series of polymers. Table B-8 confirms this as it shows that the ratio of permeabilities of carbon dioxide to nitrogen varies by a factor of only two, while the permeabilities varied by 5000. Data of Stern show that the ratio of permeabilities of methane and nitrogen vary by a factor of about fifteen in a series of membranes in which the permeabilities varied by more than 2×10^6. Helium-nitrogen and helium-methane permeability ratios in the same series of polymer membranes varied by factors of 2.5×10^2 and 6.5×10^2, respectively. It is probable that the permeation mechanism for helium is different from that of the other gases.

Permeability Constants of Polymeric Materials

The permeability of many of the common polymers to oxygen, carbon dioxide, and water vapor at 30°C is given in Table B-9.

The overall activation energies are included in Table B-9 wherever reliable values are known. These may be used to calculate the permeabilities at other temperatures using the relationship shown in equation (a) where P_1 and P_2 are the permeability constants

TABLE B-8. PERMEABILITY TO CARBON DIOXIDE AND NITROGEN AT 30°C

FILM	$P_{CO_2}{}^a \times 10^{11}$	$P_{N_2}{}^a \times 10^{11}$	RATIO
saran	0.29	0.0094	30.9
polyester[b]	1.53	0.05	30.6
nylon	1.6	0.10	16.0
rubber hydrochloride,[c] unplasticized	1.7	0.08	21.2
poly(butadiene-co-acrylonitrile)[d]	746	2.35	31.7
butyl rubber	518	3.12	17.4
methyl rubber	75	4.8	15.7
poly(ester-amide-diisocyanate)[e]	186	4.9	37.9
poly(butadiene-co-acrylonitrile)[f]	186	6.04	30.9
rubber hydrochloride,[g] plasticized	182	6.2	29.4
poly(butadiene-co-acrylonitrile)[h]	309	10.2	29.1
neoprene	250	11.8	21.1
polyethylene	352	19	18.5
butadiene-styrene elastomer	1210	63.5	19.6
polybutadiene	1380	64.5	21.4
natural rubber	1310	80.8	16.3

[a] cm^3 (STP) - cm/cm^2-sec-cm Hg.

[b] Mylar, DuPont

[c] Pliofilm N, Goodyear Tire & Rubber Co.

[d] Hycar OR 15, B. F. Goodrich; 61% butadiene; 39% acrylonitrile.

[e] Vulcaprene.

[f] Hycar OR 25; B. F. Goodrich; 68% butadiene; 32% acrylonitrile.

[g] Pliofilm P4, Goodyear Tire & Rubber Co.

[h] Perbunan, Farbenfabriken Bayer A. G.; 80% butadiene, acrylonitrile 20%

TABLE B-9. PERMEABILITY OF POLYMERS TO OXYGEN, CARBON DIOXIDE, AND WATER VAPOR AT 30°C AND ITS TEMPERATURE DEPENDENCE[a]

POLYMER	OXYGEN		CARBON DIOXIDE		WATER VAPOR	
	$P \times 10^{10}$	E_p	$P \times 10^{10}$	E_p	$P \times 10^{10}$	E_p
butyl rubber	1.3	10.7	5.2	9.9	120	
cellophane[b]	0.002		-0.006		d	
cellulose acetate	0.8	5.0	2.4	4.3	6,800	0
ethylcellulose	26.5	4.2	41.0	1.3	12,300	0.4
natural rubber	23	7.5	131	6.1	2,600	
nitrile rubber	1.0	12.0	7.5	10.5		
nylon – 6, 6[b]	0.04	10.4	0.16	9.7	70	
polycarbonate	1.5	4.6	8.5	3.8	1,400	
polyethylene						
low density	5.9	9.9	28.0	8.2	100	8.0
high density	1.1	8.8	4.3	7.4	15	7.5
poly(ethylene terephthalate)	0.04	6.4	0.15	6.2	175	0.7
polypropylene	2.3	11.4	9.2	9.1	68	10.1
polytrifluorochloroethylene	0.02	10.9	0.05	11.1	0.2	
poly(vinyl acetate)	0.5	13.4[c]	4.6		10,000	
poly(vinyl alcohol)[b]	0.003		0.01		d	
poly(vinyl chloride)			1.0	12.2	170	
poly(vinylidene chloride)	0.005	15.9	0.03	12.3	1.0	17.5
rubber hydrochloride	0.02	12.8	0.17	8.6	10	6.8

Units: P -- (ml at STP) (cm)/ (cm^2) (sec) (cm Hg); E_p = kcal/mole. The vapor permeabilities vary with type and condition of the polymer. The values given are as far as possible for the unmodified materials. See equation (a) for permeability at other temperatures.

[b] Dependent on relative humidity; values given are for dry films.

[c] Above 25°C only.

[d] Very high and humidity dependent.

TABLE B-10.   EFFECT OF RELATIVE HUMIDITY ON GAS
PERMEABILITY AT 21°C

Material	Oxygen		Carbon Dioxide	
	0% rh	75% rh	0% rh	75% rh
plain cellophane, unmodified	0.033	1.2	0.13	2.3
coated cellophane	0.05	1.0	0.16	6.4
rubber hydrochloride	2.8	2.8	17.5	17.6
glassine	23.0	11.0		
nylon – 6 – 6	0.020	0.033	0.12	0.24

[a] Units: (ml at STP) (cm) / (cm^2) (sec) (cm Hg) $X 10^{10}$, thickness
not specified.

(Continued)

$$\log P_2 \; = \; \log P_1 \; + \; \frac{1000 \, E_p}{4.6} \left(\frac{1}{T_1} - \frac{1}{T_2} \right) \tag{16}$$

at temperatures T_1 and T_2, respectively, and E_p is the activation energy in kcal/ mole. For a few of the polymers, the permeabilities depend on the relative humidity and these are marked accordingly.

As was mentioned earlier, the permeation of organic vapors through polymer films is much more complicated due to the pressure-dependent solubility and the concentration-dependent diffusion coefficient. Although extensive studies have been made on the permeability, solubility and diffusivity of various organic vapors in polyethylene, relatively little data are available for other polymers. Since the solvent action of organic vapors varies from polymer to polymer, the permeability cannot be compared in a similar fashion as is possible for permanent gases and water vapors.

In general, the gases permeate in approximately the same ratio through all polymers. The effectiveness of a barrier against a particular gas can be gaged, therefore, from its permeability constants for other gases. Water vapor and organic vapors, however, permeate in a much more specific fashion and the permeability constant is largely governed by the solubility factor. It is much more difficult, therefore, to estimate the permeability of a polymer toward water or organic vapors without actual measurement.

As the solvent power and concentration of sorbed copenetrant increase, the effect on vapor diffusion and permeation becomes more apparent. The presence of water vapor was found to have an accelerating effect on the concurrent sorption and diffusion of organic vapors in polymers such as poly(vinyl acetate) and cellulose acetate which sorb a significant amount of water vapor (W). Similarly, the increased water sorption of polymers with increasing relative humidity also leads in some cases to increasing gas transmission rates. Some practical results illustrating this are shown in Table B-10. It is interesting to note that the permeability of glassine actually decreases a little at high humidity. This is because of closing of the pores as the glassine swells with increasing humidity.

A similar case of a swelling penetrant increasing the gas transmission rate of a second gas was noted by Stannett and Szuarc (X). In this case it was observed that oxygen, in the presence of large amounts of carbon dioxide, permeated polyethylene at rates three times as fast as in the pure state.

(Continued)

It is clear that changes in both solubility and diffusivity will affect overall permeability behavior. Both the nature of the penetrant and that of polymer will affect both of the above properties.

Nature of the Penetrant

The solubility of the penetrant will be greatly affected by its polarity, or its cohesive-energy density, and the similarity of these quantities with that of the polymer. It is clear, for example, that a hydrocarbon such as n-hexane should have higher solubility in polyethylene than, for example, methyl bromide, and this is indeed the case. It should be borne in mind that cohesive-energy densities are often similar for materials of quite different structure.

The diffusivity of a penetrant is mainly dependent on its size and shape and numerous attempts have been made to put this relationship on a more quantitative basis. The data for the simple gases shows a scattered relationship between the energy of activation for diffusion and the first and second power of the molecular diameter. In the case of organic molecules the shape factor becomes high important.

Nature of the Polymer

Besides the effects of similar cohesive energy densities on the solubility of a penetrant in a polymer, the nature of the polymer structure, ie, its morphology, can also be important. In the case of semi-crystalline polymers, solubility occurs only in the non-crystalline regions, and the solubility is roughly proportional to the amorphous content. With highly drawn polymers other factors are involved, and the order of solubility of a series of solvents can sometimes be changed in that the size and shape of the penetrant may be come the governing factor. Cross-linking, in general, tends to reduce solubility with the more highly swelling penetrants but otherwise has little effect except at very high degrees of cross-linking.

The diffusivity of a penetrant in a polymer can best be interpreted in terms of the Eyring picture of viscosity or diffusion. The polymer can be visualized as a tangled mass of polymer chains with the "holes" between them. At normal temperatures there is considerable segmental mobility and the holes are continually forming and disappearing as a result of thermal motion. Diffusion of a penetrant takes place by a succession of "jumps" from hole to hole under the influence of the gradient of concentration or, better, the chemical potential. The energy of activation for diffusion can then be related to the cohesive energy of the polymer, ie, the energy associated with hole formation. The pre-exponential factor of the diffusion constant, on the other hand, can be associated to some extent with the number of holes or looseness of the polymer structure, ie, the free volume.

(Continued)

The effect of crystallinity on the diffusivity is quite complex. In general, the crystal-line regions interrupt the flow lines and lead to increased tortuosity of the diffusion path. In addition, the crystallites act as cross-links restraining the mobility of the chains. These two effects have been studied by Michaels and co-workers (Y), the former effect is by far the most important. The dependence of the diffusion constant on the amorphous content is complex. For some polymers such as poly(ethylene terephthalate), it is first-power dependence, whereas for certain grades of poly-ethylene it is almost second power. This, coupled with the linear dependence of the solubility on the amorphous content, leads to an overall dependence of the permeabi-lity constant on the second to third power of the amorphous content.

Cross-linking has an effect on the diffusivity. For example, in the case of poly-ethylene one cross-link per about thirty monomer units leads to a reduction of the diffusion constant by one-half (Z).

It is difficult in comparing the relative permeabilities of a series of polymers to clarify the role of the various factors which contribute to the observed differences. However, a consideration of the variables discussed briefly above does help in pre-dicting the permeation properties of a polymer with fair accuracy.

Preliminary Materials List

Gas and vapor permeabilities through synthetic membranes, for CO_2, O_2, N_2 and water vapor have been compiled from available literature. The polymeric materials for which data is available probably represent all of the types which would be con-sidered for application of present interest.

In most cases the permeation data was obtained with flat films of the polymeric materials. Since the permeability depends on the chemical state of the polymeric material and not on the geometric configuration, it is assumed that the data cited below is directly applicable to hollow fiber membranes of the same materials. It must be remembered that such factors as polymer crystallinity, presence of plas-ticizers, and polymer molecular weight all affect the permeation of gases and vapors. These factors are usually not measured and therefore wide and unexplained variations are frequently found for the permeation of a given gas through different preparations of supposedly identical polymeric films.

The data report was generally obtained with single gases and not with mixtures of gases or vapors. Since the presence of a specific gas in a mixture can have a pro-nounced effect on the permeation of other gases in the mixture, the ratios of per-meabilities which can be derived from the data tabulated in Table B-11 must be used with caution.

TABLE B-11. MATERIALS PROPERTIES

| | $P \times 10^{10}$ Units cc (STP) cm/cm^2-sec-cm Hz | | | |
POLYOLEFINS	CO_2	O_2	N_2	H_2O
Polyethylene				
low density	26.5	5.5	1.17	–
	28.	5.9	2.0	210
	16.	3.0	1.1	100
medium density	15.	3.2	1.9	–
high density	3.5	1.1	.25	–
	4.3	1.1	.33	12-15
unspecified	12-19	2.8-3.5	.8-1.2	
Polypropylene extruded biaxially oriented	9.2	2.3	.44	70
	1.8	.6	.09	–
	4.8	1.4	.29	–
uncoated	3.2	1.0	.12	–
coated	.003-.03	.001	.002-.01	–
Polycis-isoprene	23.5	5.7	–	–
Poly 4-methyl pentene-1	9.4	3.6	–	–
Ethylene-propylene copolymer	16.	4.4	–	–
Ethylene-octene-1 copolymer	1.9	.6	–	–
Polyisobutylene	1.1	.4	–	–
POLYAMIDES				
Nylon 6	.06	.015	.005	–
Nylon 6-6	.12-.24	.02-.03	–	70
	.16	.04	–	–
	.06	.03	.002	–
Nylon 11	.9	.2	.02	
Nylon 12	.9-2.0	.31-.56	.08-.11	–
Nylon	.16	.038	.01-.02	70-1700
CELLULOSICS				
Cellophane (regenerated cellulose)	v. low	.002	–	–
	.0024-.036	.0012-.03	.003-.01	v. high
	.13 @ 02 RH	.03 @ 02 RH	–	–
	2.3 @ 75% RH	1.2 @ 75% RH	–	–
Cellulose acetate	5.1-6.0	.8	–	–
Cellulose triacetate	2.4	.8	–	6800
	2.4-18	.4-.78	.16-.5	1500-10,600
	5.3	.9	.18	–
Cellulose acetate butyrate	36.	5.7	1.5	–
	31.	6.0	1.6	–
Ethyl cellulose	30.	12.	3.6	–
	133.	23.	8.4	3000
	41.	26.5	8.4	12,300

TABLE B-11. MATERIALS PROPERTIES (CONTINUED)

	$P \times 10^{10}$ Units cc (STP) cm/cm^2-sec-cm Hz			
FLUOROPLASTICS	**CO$_2$**	**O$_2$**	**N$_2$**	**H$_2$O**
Polyvinyl fluoride (Tedlar)	.09	.02	.004	330
	.07	.02	.004	-
Polytetrafluoroethylene (Teflon)	-	-	-	36
Polytrifluorochlorocopolymer (KdF)	.048-1.25	.025-54	.009-.013	.3-36.0
	.02	.05	-	.2
FEP fluoroplastic	1.7	5.9	2.15	50.
Poly (vinylene fluoride-hexa fluoro propylene) Viton A	7.8	1.5	.44	52.
Fluorinated ethylene propylene copolymer	10	4.5	2.0	-
Poly (vinyl acetate)	4.6	.5	-	10,000
ACRYLONITRILE COPOLYMERS				
Vinyl nitrile rubber	1.45	.3	.03	-
Acrylonitride-butdiene-styrene	1.0-1.2	.3-.4	.03-.06	-
Poly (styrene-acrylonitrile)	1.08	.34	.046	900
Poly (butadiene-acrylonitrile)	7.5-64	.96-8.2	.24-2.5	1,000
Nitrile rubber	7.5	1.0	-	-
OTHER				
Rubber Hydrochloride (Pliofilm)	1.7-80.	.23-13.5	-	-
	.17	.02	-	19
	1.8- 6.0	.18-1.8	.03-.05	-
	.17-1.8	.025-.54	.008-.62	25-1900
Butyl rubber	17.5	2.8	-	-
	5.2	1.3	.32	40-200
Polyurethane elastomer	2.7-10	.45-1.9	.25-.7	350-12,500
	14-40	1.5-4.8	.49	350-12,500
Polybutadiene	138	19.1	6.45	4,900
Polystyrene	.54	2.1	-	-
Butadiene styrene copolymer (Buna S)	124	17.2	6.35	2,400
Polysulfone	5.7	1.4	.24	high
Polyvinyl alcohol	.01	.003	-	2,900-14,000
	1.2 (50%RH)	.7 (50% RH)	-	-
Polyimide	.27	.15	.03	-

TABLE B-11.   MATERIALS PROPERTIES (CONTINUED)

	$P \times 10^{10}$ Units cc (STP) cm/cm^2-sec-cm Hz			
	CO$_2$	O$_2$	N$_2$	H$_2$O
Polyester (terephthalate)	.15	.04	--	175
	.10	.03	.005	
	.09	.002-.036	--	130-230
	.10-.15	.036-.048	.004-.006	--
Polycarbonate	8.5	2.0	.3	700
	8.5	1.5	--	1,400
	6.6	1.8	.3	--
Ethylene-vinyl acetate copolymer	36	2.1	2.1	--
Polyvinylchloride	1.0	--	--	170
	1.0-3.7	.12-.6	.04-.17	260-630
	.48-4.8	.12-1.2	.02-.18	--
nonplasticized	.1-.3	.02-.15	--	--
plasticized	.6-18	.15-12	--	--
Vinylidene chloride-vinylchloride copolymer	.03-.3	.005-.04		
Silastic	25.3	6.4	--	--
Silicone rubber	600-3000	100-600	--	--
	2,800	600	200	--
Neoprene (polychloroprene)	25.0	4.0	1.18	1,800
Vinylidene chloride (Saran)	.03	.005	.001	1.4-100
	.03	.005	--	1.0
Natural Rubber	133	23	8.4	3,000
	131	23	--	2,600
Epoxy (Epon-1001)	.086-1.4	.05-1.6	--	--
Polyformaldehyde (Delrin)	.19	.038	.02	500-1000
Chloro sulfonated polyethylene	20.8	2.8	1.16	1,200
Polybutadiene	138	19.1	6.45	4,900
	79	14	--	--

FACILITATED TRANSPORT MEMBRANE
FOR CO$_2$

	$P \times 10^{10}$			Separation Factor
Membrane	CO$_2$	O$_2$	N$_2$	CO$_2$/O$_2$
Porous Cellulose Acetate impregnated with aqueous solution of cesium bicarbonate and sodium arsenite	21.4	.0052	--	4,100
Copolymer of polyethylenimine, polyvinylbutyral and Epon 834	3.44	.113	.0746	30.4

C. 3

B-11 FACILITATED TRANSPORT OF CO_2

The facilitated transport process by which the permeation of CO_2 across a membrane is chemically augmented has been described by Ward and Robb[aa] and the process has been subjected to analysis by Ward.[bb]

In its simplest form a facilitated transport system consists of a gas A and nonvolatile species B and AB in a liquid film. The gas A can react reversibly with B. If the equilibrium constant, K, for the reaction $A + B \overset{K}{\rightleftharpoons} AB$ is favorable, when a concentration difference in A is maintained across the film there is established a concentration difference in AB which is in the same direction as that in A. A concentration difference in B is also established which is opposite in sense to that in A.

Because of these concentration differences there is a net transport of both A and AB in the same direction across the liquid film and a net transport of B equal and opposite to that of AB.

Since the total flux of A containing species across the film is equal to the flux of A plus the flux of AB at any point in the film, the flux of A is facilitated or augmented as the result of the nonvolatile species AB and B.

In the CO_2 study the nonvolatile species B, in the liquid film was the bicarbonate ion, HCO_3^-.

With this system using gas mixture of 5% CO_2-95% O_2 at atmospheric pressure in one side supported liquid film containing $CsHCO_3$, and a total pressure of 2.5 to 4 cm Hg. on the low pressure side a separation factor for CO_2/O_2 permeation of 1500 was obtained. When the rate of the reaction of CO_2 with H_2O to form HCO_3^- was accelerated by means of a catalyst, the separation factor was increased to 4100.

A version of the facilitated transport of CO_2 was studies by Miller[cc]. In this case a weakly basic polyneric membrane was used. Again an improvement in the CO_2/O_2 separation factor was observed but a much smaller magnitude than that found with the bicarbonate system.

These results suggest that mobile or fixed carriers may be incorporated into polymeric membrane separator units by which the transport of one gas of a mixture may be augmented and permit single pass separation of even trace amounts of impurity gases in a gas stream.

Trace Gas Removal

The rates of generation and the allowable levels of a number of trace contaminants are presented in Table (B-12). Carbon monoxide, ammonia and hydrogen sulfide are gases which might be removed by a modified hollow fiber process.

B-11.1 CO Removal

The low levels of carbon monoxide which enter a circulating gas stream have been historically removed on an oxidation catalyst. Reliance on separation by selective permeation through polymeric membranes appears to be unattractive because of the low levels of carbon monoxide.

A concept involving the incorporation of a finely divided oxidation catalyst on the impure gas side surface of hollow fiber membranes appears to have merit. It is proposed that the catalyst be incorporated into membranes which permit facilitated transport of CO_2. Impure gas containing both CO and CO_2 first contacts the oxidation catalyst which connects the CO to CO_2, the CO_2 produced and that present in the incoming gas would then be removed in the CO_2 selective membrane.

The feasibility of depositing catalyst on the surfaces (inside) of hollow fibers has been demonstrated in fuel cell applications.

Low temperature catalysts for CO oxidation are also available.

A potential problem relates to the active life of catalysts operating at ambient temperatures in gas which may contain relatively large amounts of water.

B-11.2 H_2S Removal

Facilitated transport of H_2S through membranes may be feasible. Hydrogen sulfide is a weak acid (like CO_2) and appropriate agents for transporting H_2S may be found.

B-11.3 NH_3 Removal

In a similar manner, acid carrier may be found to permit the facilitated transport of NH_3 through the walls of hollow fiber membrane separators.

TABLE B-12
TRACE CONTAMINANT GENERATION RATES AND MAXIMUM
ALLOWABLE CONCENTRATIONS

	Est. Generation Rate (lb./hr. x 10^8)	Space Maximum Allowable Conc. (p.p.m.)
Ammonia	4150	25
Benzene	415	1
Carbon monoxide	115	25
Cyclohexane	85	30
Dioxane	42	5
Ethanol	415	50
Formaldehyde	42	0.1
Hydrogen	820	3,000
Hydrogen fluoride	125	0.1
Hydrogen sulfide	1.8	2
Methane	72,000	2,700
Methanol	415	40
Methylene chloride	42	10
Ozone	4.2	0.02
Sulfur dioxide	42	1
Toluene	415	20

B-12   INTRODUCTION

This section describes the analytical models used to describe those processes important to the HFM component sizing and system integration. Initial discussions treat the hydrostatic pressure loss in the process stream flowing through the tubular membranes and backpressuring effects of shell side geometry. Mass flow processes through microporous membrane walls are shown to be dominated by a wide range of physical phenomena with the final process model definition a strong function of permeant phase upstream, within and downstream from the membrane wall. Membrane geometry and wettability are considerations which influence the description of the mass transfer process. In this area we have considered "solid" vs. microporous membrane structures both of which may be homogenous or anisotropic. The facilitated transport obtained with coatings and fillers is also presented.

B-12.1   Tube Side Pressure Drop

For a steady flow of a Newtonian fluid in a tube of uniform diameter, the laminar pressure loss is described by the Hagen-Poiseuille relationship:

$$\Delta P = \frac{32\,\mu\,VL}{g_c D^2} \tag{1}$$

Although specifically applicable to incompressible fluid, the relationship applies to compressible fluids when the density is nearly constant or when:

$$\frac{\Delta P}{P} < 0.1$$

Equation 1 may also be expressed as the Fanning equation:

$$\Delta P = f\ \frac{L}{D}\ \frac{G^2}{2g_c\,\rho} \tag{2}$$

since for laminar flow:

$$f = \frac{64}{N_{Re}} = 64\,\frac{\mu}{DG} \tag{3}$$

In addition to the frictional loss within the tubes, entrance and exit losses must be considered. The assembly is best represented as an inward projecting pipe entrance and a projecting pipe exit producing a pressure loss as follows:

$$\Delta P = 1.78\ \frac{G^2}{2g_c\,\rho} \tag{4}$$

(Continued)

Total pressure loss for the tube side flow within the hollow fiber membrane can be
expressed as the sum of (2) and (4):

$$\Delta P = (1.78 + f\frac{L}{D})\ \frac{G^2}{2g_c\rho} \tag{5}$$

$$= (1.78 + 64\ \frac{\mu}{DG})\ \frac{G^2}{2g_c\rho} \tag{5a}$$

B-12.2 Shell Side Pressure Drop

Shell side pressure drop must be considered in HFM component design to provide an
operating knowledge of the local pressure on the discharge side of the membrane
material. Several factors must be included in this analysis to accurately model the
system.

1. Pressure difference across the membrane, and therefore mass flux,
decreases from tube inlet to outlet. Shell side tube bundle flow will
therefore have two components; flow normal to the axis and flow
parallel to the axis.

2. In either flow direction, there will be mass addition from the
downstream membranes. This mass addition is a variable
dependent on local membrane pressure differential.

3. Tube bundle geometry may vary significantly with position due to
the difficulty in maintaining precise dimensional control. Spacing
of the fine tubes and alignment, whether in-line or staggered, can
only be grossly defined for the actual hardware.

Initial analyses not considering multiple flow direction or wide variation in tube bundle
geometry have produced excessively conservative predictions and have not accurately
reflected the test data results.

As membrane technology increases and attempts are made to provide the ultimate
optimization in component weight and volume we may have to reevaluate the need for
an accurate math model in this area but further work is not warranted at this stage.
Minimal test data is sufficient to provide knowledge of geometry effects and will
suffice for the initial sizing and evaluation phase.

B-12.3 Microporous Membranes

In attempting to describe the analytical relationships governing the superficial
performance of microporous membranes we must first separate the potential

(Continued)

operating regimes of the system. Totally different processes and realtionships are involved when considering phase change across the membrane barrier as compared to those processes maintaining a constant phase across the system. As examples we will consider two concepts: one using the membrane as a microfilter with water present on both the tube and shell sides only in the liquid phases, and the second as a thermal sink using the heat of vaporization of a portion of the liquid water in the tube as it evaporates to a gas on the downstream or shell side.

Constant Phase Process

For the constant phase process, flow may be estimated using equation (1), assuming pore entrance and exit effects are negligible, as follows:

$$\Delta P = \frac{32 \mu \, VL}{g_c D^2} \tag{1}$$

$$= \frac{\mu \, GL}{D^2 \rho}$$

or,

$$G = \frac{\Delta P \, D^2 \rho}{\mu \, L} \,, \quad \frac{\text{lbs. of fluid}}{(\text{sec}) \, (\text{ft}^2)} \tag{6}$$

Assuming the following pore and system characteristics, we may proceed:

Membrane Wall Thickness, L = 25 microns
= 8.2×10^{-5} ft.
Membrane Open or Pore Area = .03 x Total Membrane Area
Nominal Protein Molecular
    Weight Cutoff = 5,000 to 30,000

or, Approximate Pore Diameter = 20 Angstrom Units
= 6.56×10^{-9} ft.

ΔP = 1 atm. = 2.12×10^3 psf

μ = 1.06×10^{-3} lb/sec-ft (H_2O @ 40°F)

ρ = 62.4 lbs H_2O/ft^3

$G = \dfrac{(2.12 \times 10^3) \, (6.56 \times 10^{-9})^2 \, (62.4)}{(1.06 \times 10^{-3})(8.2 \times 10^{-5})}$

$= 6.6 \times 10^{-5} \dfrac{\text{lbs } H_2O}{(\text{sec}) \, (\text{ft}^2 \text{ pore area})}$

$= 6.6 \times 10^{-5} \, (3600) \, (.03)$

$= .007 \dfrac{\text{lbs } H_2O}{(\text{hr}) \, (\text{ft}^2 \text{ membrane area})}$

(Continued)

This value is representative of flow through a homogenous membrane. The use of
anisotropic configurations in similar applications will result in flow increases
approximately two orders of magnitude higher due to the greatly reduced pore length.
It should be noted that the parameters governing the rate of transfer in this system are
primarily pore geometry and hydrostatic pressure differential.

During recent testing at Hamilton Standard, water transfer rates were found to exceed
these values by one to three orders of magnitude and to be independent of hydrostatic
pressure differential when used in a phase change mode - such as a water boiler. A
necessary conclusion can be made that the prior analysis does not represent the
system where the liquid and gaseous interface is in contact with the membrane surface.
The analysis does apply, however, when liquid is present on the membrane external
surfaces and the gas/liquid interface is separated from the membrane by a thickness
of liquid film. Under this condition, transmembrane flow will be correlated as a
function of hydrostatic pressure differential. This situation will be encountered when
vapor removal capacity is limited and water is allowed to condense and collect on the
tube external surfaces.

Phase Change Process

When the capacity for vapor removal is large, the external surfaces of the membrane
can be considered essentially dry and the liquid/gas interface now contacts some
portion of the membrane material. Surface tension characteristics become dominant
and must be considered in the analysis. Several factors will be presented for consi-
deration - they should not be construed as absolute contributors to the analysis but
only as potential contributors.

Critical Line Force

Critical Line Force, CLF, is the force necessary to overcome the resistance to
movement of a liquid-solid-vapor boundary line along a solid surface. In particular,
it is the force necessary to move liquid (such as water in the case we are considering)
through a hydrophobic capillary or the force necessary to push the liquid beyond the
confines of a hydrophilic capillary into an area where capillary forces are minimal
or nonexistent. For water, the CLF has been measured on Teflon and Polyethylene
to range between 9.72 and 14.0 Dynes/cm. The pressure necessary to cause move-
ment of the interface is calculated as follows:

$$\Delta P = \frac{CLF \text{ (Interface Length or Capillary Circumference)}}{\text{(Area Over Which Pressure is Exerted)}}$$

$$= \frac{CLF (2\pi r)}{(\pi r^2)} = \frac{2}{r} CLF \tag{7}$$

(Continued)

For pore diameters of 6.56×10^{-9} ft. as in the previous example,

$$\Delta P = \frac{(2)\ (10\ dynes/cm)}{\dfrac{(6.56 \times 10^{-9}\ ft)}{2}\ 30.48\ \dfrac{cm}{ft}}\ (1.45 \times 10^{-5}\ \dfrac{psi}{dyne/cm^2}) = 2900\ psi$$

Based on the magnitude of this value, we may conclude that hydrostatic pressure forces available in the system will not force liquid into a hydrophobic capillary or beyond a hydrophilic capillary.

Capillary Pressure Rise

The capillary pressure rise of water thru hydrophilic materials, such as cellulose or cellulose acetate, may be estimated as follows assuming a zero contact angle:

$$\Delta P = \frac{2\sigma}{r}$$

$$= \frac{2(72.3\ dyne/cm)}{(\dfrac{6.56 \times 10^{-9}}{2}\ ft)\ (30.48\ \dfrac{cm}{ft})}\ (1.45 \times 10^{-5}\ \dfrac{psi}{dyne/cm^2}) \qquad (8)$$

$$= 21,000\ psi$$

Referring to Equation 6 we can conclude that the capillary flow potential is approximately 10 lbs H_2O/(Hr) (Ft^2 membrane area) for the homogeneous membrane and some 100 times higher for the anisotropic configuration. It may now be concluded that capillary flow for wetted materials is not a limiting factor in the analysis.

Liquid Vapor Pressure

Due to the effects of surface tension, the vapor pressure of a liquid over a convex surface (such as a droplet) is greater than over a plain surface and conversely it is lower over a concave surface (the geometry which may be present in a wetted capillary) than over the plain surface. This phenomenon is described by the Kelvin equation:

$$\ln\ \frac{P_{high}}{P_{low}} = \frac{2\mu\sigma}{RT\rho\ r} \qquad (9)$$

For water at $40^{\circ}F$, $P = 6.3$ mmHg, the following values have been calculated:

Hamilton U
Standard DIVISION OF UNITED AIRCRAFT CORPORATION
A®

(Continued)

		$\dfrac{P_{high}}{P_{low}}$	Vapor Pressure, mmHg	
r (cm)	r (Angstroms)		Concave	Convex
10^{-7}	10	2.95	2.1	18.6
10^{-6}	100	1.114	5.7	7.0
10^{-5}	1,000	1.011	6.2	6.4
10^{-4}	10,000	1.001	6.3	6.3

Since we are working with micropore in the range of 10-30 Angstrom units the variation in vapor pressure can be significant and must be considered in the analysis. Data correlation, however, has not indicated any measurable reduction in vapor pressure, but has shown a potential increase in pressure. This could be explained (for the cases of the wetted materials) by capillary action or wicking beyond the end of what has previously been considered the "pore". Certainly, for the anisotropic materials this condition exists with the many fine fibers or ligaments of the matrix (substrate) providing both a wicking surface and a small convex diameter which could produce the increase in vapor pressure seemingly noted in test.

Differences in performance between the cellulose acetate and the cellulose may be explained in this manner since both units should not be limited by pore configuration - wicking capacity is orders of magnitude greater than transmembrane flows measured in test. The homogenous cellulose unit may simply have had limited evaporant surface area or, more likely, limited vapor pressure increase and exhibited lower performance. Further work, including microscopic examination, is warranted in this area to better define the pertinent parameters.

Hydrophobic Materials

When using Teflon, Silicone or Silicone/Polycarbonate microporous materials, the analysis must deal with a different situation than previously described. We have shown that the hydrostatic pressure is insufficient to force liquid in the capillaries in the size range of interest. Therefore, vaporization must originate at the inner diameter of the tube at the base of the pore. The strong convex shape of the partially penetrating liquid will produce an approximate three fold increase in the vapor pressure but gas flow thru the capillary is in the molecular or Knudson flow regime and subject to significantly increased resistance. The governing equation is as follows:

$$\omega = 16.5 \; \frac{r}{L} \; \Delta P \; \sqrt{\frac{M}{T}} \; A_T \qquad (10)$$

(Continued)

For a membrane bundle similar to that previously treated the flow rate is as follows:

Water at $60^{\circ}F$: P_{sat} = 13.2 mmHg

Rise Due to Bubble Geometry = 3 x 13.2 = 39.6 mmHg

Assume Shell Side Pressure = 9.6 mmHg

Pore ΔP = 30 mmHg = 83.4 psf

$$\dot{\omega} = (16.5) \frac{(6.56 \times 10^{-9})}{(8.2 \times 10^{-5})} (83.4) \sqrt{\frac{18}{520}} A_T$$

$$= .02 A_T \frac{\text{lbs } H_2O}{\text{Hr - Ft}^2} \text{ of Membrane Area}$$

This value may be raised by a factor as high as 100 when considering anisotropic geometrics but still falls short of the performance demonstrated by the cellulose acetate membranes.

Application of Data

From the previous analysis, it may be concluded that hydrophobic microporous membrane evaporator performance will be dominated by pore geometry (diameter and length) and differential vapor pressure across the membrane wall. Conversely, hydrophilic evaporator performance is dominated by conditions downstream from the pore structure. This includes not only the vapor pressure drop thru the tube bundle but the geometry of the membrane itself downstream of the capillaries (homogenous vs. anisotropic structure).

In both cases, the basic correlation can be based on constants evaluated from test data and representing the effects of membrane geometry. A major variable, however, will be the system driving force or differential partial pressure. Evaluation of data obtained to date has demonstrated this effect.

B-12.4 Activated Diffusion

Mass transport through "solid" polymeric materials, in contrast to mass transport through microporous structures (Knudsen flow or Poiseuille flow), occurs by activated diffusion. This takes place in three steps. First, the permeant "dissolves" in the permeable membrane on the side of its higher concentration. Then it diffuses through the membrane towards the side of the lower concentration, a process which depends on the formation of "holes" in the plastic network due to thermal agitation of the chain segments. Finally, the permeant becomes desorbed on the side of the lower concentration. In contrast to this, when permeating through porous materials, the permeating molecule does not change from undissolved to dissolved, and does not form transient "holes" in its passage.

(Continued)

The rules applying to permeability governed by activated diffusion are completely different from those of Knudsen flow. In activated diffusion, the rate of mass transport increases exponentially with temperature, is essentially independent of the hydrostatic pressure, and in many cases is independent of whether the penetrant is in the liquid form or in the form of saturated vapor. The chemical composition of the membrane and permeant is very important and the process is selective in the sense that a membrane will allow penetrants that are chemically similar to pass much faster than penetrants that are dissimilar.

In contrast to this, permeation through porous materials decreases with temperature (linearly in the case of Poiseuilles flow and with the square root in the case of Knudsen flow), is often highly dependent on the hydrostatic pressure and the state of aggregation of the permeant, and the permeability process is non-selective.

Definitions

To facilitate the ensuing discussion several terms will be defined. The rate of permeation, W, is the amount of material passing through a membrane per unit time. The permeability constant, P, a property of the barrier material, is defined as

$$P = \frac{W \text{ (Membrane Thickness)}}{\text{(Membrane Surface Area) (Partial Pressure Differential in Environments Separated by Membrane)}}$$

The diffusion constant, D, is:

$$D = \frac{\text{(Rate of Diffusion)}}{\text{(Membrane Surface Area) (Concentration Differential Within the Membrane)}}$$

This concentration is expressed as the quantity of permeant per unit volume of barrier material (usually standard cubic centimeter of gas per cubic centimeter of barrier material). The rate of diffusion equals the rate of permeation if the amount of permeant entering the membrane equals the amount that leaves it. The solubility coefficient, S, often called solubility, is:

$$S = \frac{\text{(Permeant Concentration within the Membrane)}}{\text{(Permeant Partial Pressure in Equilibrium with Membrane)}}$$

The permeability constant, P, of mass transfer occurring by activated diffusion is the product of the diffusion constant, D, and the solubility coefficient, S:

$$P = DS \tag{11}$$

(Continued)

From equation 11 it can be seen that if Fick's law, which requires that the diffusion constant be independent of the concentration of the permeant in the membrane, or if Henry's law, which requires that the solubility coefficient be independent of the pressure or activity of the permeant in the phase in equilibrium with the membrane, are not obeyed, then the permeability constant, P, will also be dependent on the vapor pressure or activity of the penetrant. This leads to complicated relationships, as will be discussed later, and detracts from the usefulness of the term P in calculating permeation rates.

The temperature dependence of P, D, and S can be expressed by Arrhenius type equations:

$$P = P_0 \exp(-E_p/RT) \tag{12}$$

$$D = D_0 \exp(-E_d/RT) \tag{13}$$

$$S = S_0 \exp(-\Delta H_s/RT) \tag{14}$$

where E_p is the activation energy for the overall permeation process and is equal to the sum of E_d, the activation energy for the diffusion process, and H_s the heat consumed on dissolving a mole of permeant in the membrane:

$$E_p = E_d + H_s \tag{15}$$

R and T are the gas constant and absolute temperature as usual. The heat of solution, H_s, can be further broken down into the heat of condensation and heat of mixing:

$$H_s = H_{cond} + H_m \tag{16}$$

Substituting the product of D_0 and S_0 for P_0 and the sum of E_d, H_{cond} and H_m for E_p in equation 12 results in equation 17:

$$P = D_0 S_0 \exp\left[-(E_d + H_{cond} + H_m)/RT\right] \tag{17}$$

Equation 17 will be referred to in explaining various types of dependence of the permeability constant on the experimental variables.

Factors Governing Rate of Permeation

The amount of material passing through a polymeric membrane depends on a number of parameters.

Nature of the Permeating Material - The simplest case is that of a permeant gas or a hard-to-condense vapor. Here the permeability increases with decreasing size of

(Continued)

the permeating molecule and is usually, but not always, independent of the chemical similarity of penetrant and membrane material. In contrast to permanent gases, liquids and easy-to-condense vapors show a high interaction between membrane and permeant.

Among the factors to consider when attempting to predict the permeability of an easily condensable vapor are the size of the penetrant molecule, the ease with which the penetrant can be condensed, and the similarity of the penetrant and membrane materials. The permeability increases with decreasing molecule size, with increasing ease of condensation. and with increasing similarity.

If the membrane has functional groups or chain segments chemically similar to the penetrant, such as cellophane and water, then the cohesive forces between the polymer and the vapor are large. This results in a large solubility of the permeant in the membrane, causing the permeability constant to increase for two reasons. First, since according to equation 11 the permeability is the product of the solubility and diffusion constants, this product increases. Second, the high concentration of the penetrant in the membrane causes it to swell, resulting in a less "tight" polymer network and this results in an increase of the diffusion constant which, in turn, results in a further increase of the product of equation 11.

If the permeant is dissimilar to the membrane material, such as is the case with polyethylene and water, then the cohesive forces of the vapor will be larger than the interaction forces between vapor and polymer and as a result the water molecules will tend to cluster together and not disrupt the polymer network. As a consequence, the permeability of water through polyethylene is much lower (70 to 400 times) than the permeability of water through cellophane. However, because of the ease with which water vapor is condensed, the permeability of water through PE is about 10 times larger than that of oxygen, a molecule of approximately equal size.

Nature of the Membrane Material – Various aspects of the membrane material influence the rate of permeation. These include its chemical composition, the similarity of the chemical composition to that of the permeant, the degree of cross-linking, the degree of crystallinity, the degree of plasticization and swelling by either a foreign plasticizer, a solvent, or by the permeant itself and sometimes the previous history of the material. In order to possess good transport properties, a polymeric material must fulfill two conditions: the structure must be such that it will not interfere with ease of the diffusion process and the polymer must possess chain structures or functional groups chemically similar to the penetrant molecule.

Two types of structures will interfere with the diffusion process. If the polymeric network is "tight" in the sense of resisting separation of the polymeric chains, then the energy needed to form a hole to accommodate a diffusing molecule will be large

(Continued)

thus the activation energy for the diffusion and permeation processes will be large
and the permeability constant will be small as it can be seen readily from equation
17. Such a "tightness" is encountered with materials possessing cross-links, a high
degree of symmetry, crystallinity, or strong cohesive forces brought about by
polarity. The polymer network will be "loose" if the material is plasticized or swollen
by either the permeant or another solvent or plasticizer.

A second type of structure interfering with the diffusion process is realized with
materials possessing regions inaccessible to the diffusing molecule. This forces
the molecule to diffuse around these regions and results in a longer diffusion path.
The net result is a decrease in the preexponential factors D_0 and P_0 of equations 12
and 13 and a consequent lower permeability. Such inaccessible regions are realized
by compounding elastomers with lamellar fillers or by having crystalline regions in
the polymer.

A membrane with a very high rate of transport can be obtained by filling the pores of
a microporous polymer with a material having a highly selective solubility or
reactivity with the permeant. Examples are the use of glycerine for facilitated water
transport and ammonium carbonate or sodium arsenate catalyzed cesium carbonate
for facilitated transport of both water and carbon dioxide. This separation of the
functions of structure and transport permits utilization of the most suitable polymers
to generate the membrane structure and the most suitable materials to facilitate
permeant transport.

Effect of Pressure Differential on the Permeability of Permanent Gases - The driving
force that causes permeation to take place, either by activated diffusion or by Knudsen
flow, is the presence of a pressure or partial pressure differential causing more
permeant to flow from the high concentration side of the membrane to its low con-
centration side than vice versa. This results in a net mass transport from the high
to the low concentration side.

The rate of permeation of a permanent gas or hard-to-condense vapor is usually
proportional to the pressure or partial pressure differential provided that 1) the
membrane had been exposed to the gas for a time sufficient to reach equilibrium,
2) the pressure is not so high that deviations from the gas law are appreciable, or
that the volume of the membrane, its crystallinity, or other structural features, such
as being above or below the glass temperature, are changed (these requirements are
usually fulfilled up to rather high pressures), and 3) the permeant does not degrade
the membrane chemically.

(Continued)

Effect of Vapor Pressure, Vapor Pressure Differential, and State of Aggregation
on the Permeability of Vapors and Liquids - In the case of vapors and liquids two
situations must be distinguished. The first includes systems in which the vapor does
not dissolve appreciably in the membrane. Under these conditions the rate of per-
meation is proportional to the vapor pressure differential between the ingoing and
outgoing surfaces of the membrane, as is the case for permanent gases. The rate of
permeation is also independent as to whether the ingoing side of the membrane is
exposed to the permeant in liquid state or to the saturated vapor.

The second group includes systems in which the permeant dissolves appreciably in
the membrane. In these systems, exemplified by a facilitated transport process,
Henry's law and Fick's law are not obeyed. The deviation is such that the solubility
increases with the concentration of the permeant in the membrane. As a consequence,
the rate of permeation increases faster than linearly with the vapor pressure differential
and is dependent not only on the pressure differential but also on the absolute vapor
pressure. As a further consequence, the permeability constant defined as the ratio of
the rate of permeation through a membrane of unit area and thickness to the pressure
differential, is not constant at all. Permeability "constants" for such systems are
valid only under the exact conditions of vapor pressure and vapor pressure differential
at which they were determined.

Attempts to predict behavior at one vapor pressure from data at a different vapor
pressure might lead to conclusions that are even qualitatively incorrect.

The rate of permeation for some systems, instead of varying linearly with the con-
centration or pressure differential varies exponentially with the concentration or
pressure at the ingoing surface and is essentially independent of the pressure
gradient or the pressure at the outgoing surface.

Effect of Hydrostatic Pressure on the Permeability of Liquids - The hydrostatic
pressure has only an insignificant effect on permeability processes occurring by
activated diffusion. A high hydrostatic pressure can affect permeability by changing
the membrane by altering its density, crystallinity, or glass temperature. Changes
of this nature result in a decreased rate of permeation.

Conversely, the high pressure will increase the diameter and thin the walls of the
hollow fibers - changes resulting in increased rate of permeation.

(Continued)

Effect of Area and Thickness - The rate of permeation is always proportional to the
area of the membrane and usually inversely proportional to its thickness if equilibrium
conditions have been established. If equilibrium has not been reached, then the time
needed to reach equilibrium is roughly proportional to the square of the thickness if
Fick's and Henry's laws are obeyed. Thus the thickness of the membrane improves
its contaminant removal properties much more for the preequilibrium period than it
does after reaching equilibirum.

Effect of Time - The simplest situation prevails when a membrane has been subjected
to a permeant for a long enough time to bring about equilibrium of the ingoing and
outgoing surfaces with the corresponding pressures. Under these conditions the rate
of permeation is constant. The most frequently met nonequilibrium situation exists
when a barrier free of permeant is initially subjected to zero pressures at the outgoing
side and to a finite constant pressure at the ingoing side. Here the rate of permeant
removal from the process stream starts at a maximum and decrease gradually until
equilibrium is reached.

Other nonlinear permeation rates are encountered if the membrane contains initially
more permeant that at the steady state conditions, in which case the permeant
removal rate increases with time until equilibrium is reached.

Effect of Temperature

1. Permeants That Do Not Swell the Membrane - The rate of permeation which
    occurs by activated diffusion usually increases exponentially with temperature
    if the permeant does not swell the membrane. The dependence is given by the
    Arrhenius type equation 12 and is exponential only if P_0 and E_p do not vary with
    temperature, a condition fulfilled if the temperature intervals are small and the
    membrane material has no second-order transition point in the temperature
    interval considered. The temperature dependence for a liquid that does not
    swell the membrane is steeper than the temperature dependence for a gas or a
    vapor. This is because the rate for a liquid is proportional to the permeability
    constant and to the vapor pressure, both of which increase exponentially with
    temperature, whereas for a gas or vapor kept at constant pressure the rate of
    permeation is temperature dependent only because of the temperature dependence
    of the permeability constant.

2. Permeants That Do Swell the Membrane - In the case of permeant-membrane
    systems in which the membrane swells, the situation is more complex.

(Continued)

In this case the rate of permeation of the vapor at constant pressure first decreases with decreasing temperatures as usual, then passes through a minimum and increases when the temperature is further decreased. The reason for this abnormal behavior is most readily explained by pointing out that lowering the temperature at constant vapor pressure causes an increase in the activity of the vapor (or the relative humidity) and thus favors condensation and solution of the vapor in the membrane. The resulting plasticization of the membrane increa the rate of diffusion.

Effect of Two Membranes in Series - The rate of permeation through a composite film is independent of the order in which the layers are assembled if the rate of permeation for each component is a linear function of the vapor pressure and if there are no barriers to diffusion due to interfacial phenomena between layers. The reciprocal of the rate, R, through the composite equals the sum of the reciprocals of what the rate would be if each component were used separately:

$$\frac{1}{W} = \frac{1}{W_1} + \frac{1}{W_2} \tag{18}$$

If the rate of permeation through one of the components is not a linear function of the pressure, then the rate through the composite will be dependent on the order. This rate will be larger if the film showing the larger pressure dependence is exposed to the higher pressure.

Application of Data

Before attempting to calculate the amount of penetrant passing through a membrane from basic permeability data, a number of factors must be considered or else an erroneous conclusion might be reached. The simplest situation arises if 1) the permeability constant for the temperature of application is known and has been determined by a reliable method, 2) the permeant does not swell or otherwise attack the membrane material, 3) the rate of permeation is proportional to the gas or vapor pressure differential, 4) the time of exposure is considerably longer than the time needed to reach equilibrium, and 5) the membrane is free of cracks and pinholes, and permeation occurs only by a process of activated diffusion.

Conditions 1 and 4 are usually fulfilled for the permeation of gases through all membranes and for the permeation of water through hydrophobic membranes.

If conditions 1 to 5 are fulfilled, then the rate of permeant entering or escaping through the membrane is calculated by multiplying the permeability constant by the area, and by the vapor or gas pressure differential, and dividing the product by the thickness of the membrane wall. The pressure to be used is the gas pressure in

Hamilton U
Standard A ®.
DIVISION OF UNITED AIRCRAFT CORPORATION

(Continued)

case of a gas, the partial pressure in the case of gaseous mixture, and the vapor
pressure at the temperature of application in the case of a liquid.

Situations Where the Permeability Constant is not Known at the Application
Temperature - If the permeability constant is known only at a temperature slightly
different than that of the application and the activation energy E_p is known, then the
permeability constant can be estimated from equation 19 provided that the membrane
material does not show a second order transition within the temperature interval
considered:

$$\log P_2 = \log P_1 + \frac{E_p}{0.0046} \left[\frac{1}{T_1} - \frac{1}{T_2} \right] \tag{19}$$

where P_1 and P_2 are the permeability constants at $T_1{}^\circ K$ and $T_2{}^\circ K$, and 0.0046 is the
product of the gas constant (expressed in kcal. per mole per degree) and the factor
2.3 converting natural logarithms to Briggsian logarithms. The activation energies
for most permeation processes vary within 5 to 16 kcal/mole. Equation 19 predicts
a doubling of the permeability constant every 25°C if the activation energy is 5 kcal/
mole, and every 8°C if the activation energy is 16 kcal/mole.

Situations Where the Rate of Permeation is not Proportional to the Pressure
Differential - The rate of permeation for gases usually varies linearly with the
pressure differential, but there are cases where an exponential dependence on
pressure at the ingoing surface is observed. In the case of liquids and vapors such
exponential dependencies are rather common and occur whenever the permeant swells
the membrane as discussed previously.

If the dependence of the rate of permeation on the vapor pressure differential is other
than linear, then the simple procedure given at the start of this section cannot be
followed. If permeability "constants" are reported in the literature, they can be used
only provided that the pressure and pressure differential as well as the temperature
of the service conditions are the same as those employed in determining the permeability
"constants". The temperature dependence of the rate is also more pronounced and
unpredictable for these systems than it is for systems with a linear variation of the
rate with pressure differential. The time needed to reach equilibrium is also usually
longer.

It follows that the prediction of performance from basic data is difficult for such
systems. The permeability constant can be used only if it applies to the particular
condition of concentration, pressure, or pressure differential of the application.
Such permeability constants are usually not available. They can often be estimated

(Continued)

by interpolation or extrapolations from permeability constants under other conditions if permeability constants are known under various conditions of concentration, pressure, and pressure differential.

B-13.1 Functions Summary

B-13.1.1 Gas Systems

A number of transport processes involving gases or vapors may be considered relative to hollow fiber membranes. In all cases the separation of a specific gas or vapor from other gases is desired. Examples are CO_2 removal from O_2, trace gas contaminants removal from O, H_2O vapor removal from O_2.

From discussions and data presented earlier, recommendations of membrane types and membrane materials can be made as follows:

CO_2 Removal from O_2

1. Separation through microporous membrane would probably be ineffective.

2. Diffusive transport of CO_2 is more effective than that of O_2, but the relative partial pressures of the gases in the mixtures of interest make the entire process ineffective.

3. Facilitated transport of CO_2 using a microporous membrane in which all the pores or the pores in a thin surface skin are filled with a liquid containing a carrier for CO_2 appears effective. Here the O_2 is held back by the liquid diffusion barrier and the CO_2 is carried chemically through the barrier.

Trace Gas Removal From O_2

The problem is similar to but more difficult than CO_2 removal because of very low contaminant partial pressures. For this reason sieve type membranes and diffusive membranes are unattractive.

Facilitated transport of CO, H_2S, NH_3 trace contaminants is possible but has not been demonstrated.

Catalytic oxidation of CO at the surface of hollow fiber membranes and facilitated transport of the product CO_2 is an attractive possibility. Incorporation of catalysts in hollow fiber membranes has been demonstrated.

Water Vapor Removal

The flux of water vapor through microporous cellophane has been demonstrated to be rapid. Permeability of cellophane by O_2 is reported to be very low. Hollow fiber membranes of this material are prime candidates for separation of water vapor from oxygen.

(Continued)

A potential problem may be an increased permeation of O_2 through cellophane swollen with water. This would decrease the efficiency of the separation.

B-13.1.2 Liquid Systems

The principal processes of concern which involve liquid components are heat rejection and water purification. The heat rejection involves the evaporation of liquid water or ice; the water purification involves removal of water from nonvolatile contaminants by reverse osmosis or vapor diffusion.

Heat Rejection

The process can be accomplished using porous hollow fibers which are either hydrophilic or hydropholic.

With hydrophilic (wetting) membranes liquid water fills the membrane pores and evaporation occures on the gas side of the membrane. Leaking of water with loss of cooling efficiency is possible with this system. Regenerated microporous cellulose is an example of a candidate material.

With hydrophoblic (non-wetting) membranes water is excluded from the membrane pores and evaporation occurs on the liquid side of the membrane. Plugging of membrane pores by particulates in the water is minimized and liquid water loss is prevented. Hydrophobic microporous polypulfone hollow fibers is a candidate material for this application. A second acceptable material is Kynar – a fluorocarbon polymer.

Water Recovery:

Water Recovery by reverse osmosis would make use of hollow fiber membranes of cellulose acetate made using some modification of the method of Loeb and Sourirajan. Systems using this material are under extensive development.

Water recovery by vapor diffusion (pervaporation) can be carried out with either wetting or nonwetting microporous membranes.

Nonwetting membranes are the materials of choice since contaminants in the water cannot enter and accumulate in the membrane pores and since the possibility of liquid water formation on the gas side of the membrane is prevented. The material selected should be from the group-polysulfone, kynar and teflon.

B-13.1.3 Gas-Liquid Systems

Water deaeration is the only process presently within this category. The require-
ment of the process is that noncondensable gases be removed from water, therefore
the gases should permeate the membrane and liquid water be excluded (water vapor
loss should also be minimized unless the two processes of deaeration and heat
rejection are combined). The hollow fiber membranes most suitable are believed
to be those made from Kynar, teflon or polysulfone.

B-13.1.4 Gas-Solid Systems

A filter for the removal of particulates from gas should have as the hollow fiber a
material which can be produced with a thin, macroporous skin and a coarse micro-
porous skin and a coarse macroporous spongy support structure. The filter should
be operated in a mode such that the gas to be filtered first contacts the macroporous
side of the fiber and then permeates through the microporous layer.

Polysulfone fibers produced by Amicon, teflon, Kynar and tedlar are candidate
materials for this application.

B-13.1.5 Liquid-Solid Systems

Hollow fiber membranes which are wettable and microporous appear to be optimal
for this process. As in the gas-solid filter, maximum filter life would be attained
by using an asymmetric fiber with the spongy support side in contact with the
contaminated liquid. The material of choice is the cellulose acetate asymmetric
membrane developed for reverse osmosis use.

BIBLIOGRAPHY

(a)   H. H. Hoehn and D. G. Pye – U.S. Patent 3,497,451 (1970)

(b)   M. I. Mahon, Proceedings-Desalination Research Conference
National Academy of Science – National Research Council
Publication 942, 345-354 (1963)

(c)   R. F. Mattson and V. J. Tomsic, Chem. Eng. Progr. 65 (1), 62-68
(1969)

(d)   E. A. McLain and H. I. Mahon, U.S. Patent 3,423,491 (1969)

(e)   W. E. Skiens, U.S. Patent 3,532,527 (1970)

(f)   M. E. Cohen and B. Riggleman, Office of Saline Water Research and
Development Progress Report No. 400, U.S. Department of the Interior,
1969

(g)   T. A. Orofino, Office of Saline Water Research and Development Progress
Report No. 549, U.S. Department of the Interior, 1970

(h)   L. W. Henderson, C. Ford, C. K. Colton, L. W. Bluemle, and H. J.
Bixler, Trans. Am. Soc. Artificial Internal Organs 16, 107-114 (1970)

(i)   Oil Gas J. 68 (12), (March 23, 1970)

(j)   Oil Gas J. 68 (24), 124 (June 15, 1970)

(k)   R. P. deFilippi, F. C. Tompkins, J. E. Porter, and G. W. Harris,
Artificial Heart Program Conference Proceedings, U.S. Government
Printing Office, 1969, pp. 347-355

(l)   B. J. Lipps, W. E. Skiens, E. A. McLain, and P. D. Oja. Artificial
Heart Program Conference Proceedings, U.S. Government Printing O
Office, 1969, pp. 357-364

(m)   T. L. Williams, L. H. Bosher, T. Nakamura, Artificial Heart Program
Conference Proceedings, U.S. Government Printing Office, 1969, pp.
365-371

(o)   S. Loeb and S. Sourirajan, UCLA Engr. Report 60-60 (1960);
Advan. Chem. 38, 117 (1963)

BIBLIOGRAPHY (CONTINUED)

(p)   R. Block, O. Kedem, and D. Vofsi, Polymer Letters $\underline{3}$, 965 (1965)

(q)   R. M. Barrer, Diffusion in and Through Solids, Cambridge University Press, London, (1951)

(r)   P. C. Carmen, Flow of Gases Through Porous Media, Academic Press, London, (1956)

(s)   S. Loeb and S. Sourirajan, UCLA Department Engr. Report No. 60-$\underline{60}$ (1960)

(t)   P. Meares, J. Am. Chem. Soc. $\underline{76}$, 3415 (1954);
Trans. Faraday Soc. $\underline{53}$, 101 (1957)

(u)   A. S. Michaels, W. R. Vieth, and J. A. Barrie, J. Appl. Phys. $\underline{34}$, 1, 13 (1963)

(v)   V. Stannett and M. Szuarc, J. Polymer Science $\underline{16}$, 89 (1955)

(w)   F. A. Long and L. J. Thompson, J. Polymer Science $\underline{14}$, 321 (1954)

(x)   V. Stannett and M. Szuarc, Tappi Report 1954-1955

(y)   H. J. Bixler, A. S. Michaels, and M. Salame, J. Polymer Science (A) $\underline{1}$, 895 (1963)

(z)   I. Sobolev, J. A. Meyer, V. Stannett, and M. Szuarc J. Polymer Science $\underline{17}$, 417 (1955)

(aa) W. J. Ward III, and W. L. Robb, Science $\underline{156}$, 1481 (1967)

(bb) W. J. Ward III, AICH J$\underline{16}$, No. 3, 405 (1970)

(cc) J. G. Tajar, and I. F. Miller, AIChE J. $\underline{18}$, 78 (1972)

Hamilton Standard
DIVISION OF UNITED AIRCRAFT CORPORATION
U
A®

TABLE OF SYMBOLS

P = Pressure, lb_f/ft^2

μ = Absolute Viscosity, lb/sec-ft

L = Length, ft.

D = Diameter, ft.

ρ = Density, lbs/ft^3

g_c = Constant, 32.2 ft-lbs/lb_f - sec^2

f = Friction Factor, Dimensionless

G = Mass Velocity, lb/sec-ft^2

N_{Re} = Reynolds Number, Dimensionless

V = Velocity, ft/sec.

r = Radius, ft.

σ = Surface Tension, dyne/cm

CLF = Critical Line Force, dyne/cm

R = Universal Gas Constant

M = Molecular Weight

T = Absolute Temperature, $^\circ R$

$\dot{\omega}$ = Weight Flow, lbs/hr

A_T = Total Membrane Area, ft^2

W = Rate of Permeation

P = Permeability Constant

D = Diffusion Constant

S = Solubility Coefficient

E = Process Activation Energy

H = Enthalpy

APPENDIX B

HOLLOW FIBER MEMBRANE SYSTEMS

BREADBOARD SYSTEMS TEST PLAN

HAMILTON STANDARD Division of UNITED TECHNOLOGIES™

HOLLOW FIBER MEMBRANE SYSTEMS

BREADBOARD SYSTEMS TEST PLAN

PREPARED UNDER CONTRACT NAS 9-14682

BY

HAMILTON STANDARD
DIVISION OF UNITED TECHNOLOGIES CORPORATION
WINDSOR LOCKS, CONNECTICUT   06096

FOR

NATIONAL AERONAUTICS AND SPACE ADMINISTRATION
LYNDON B. JOHNSON SPACE CENTER
CREW SYSTEMS DIVISION
HOUSTON, TEXAS   77058

JUNE 1976

PREPARED BY: _____
R. PETILLO
SENIOR TEST ENGINEER

APPROVED BY: _____
G. ROEBELEN
PROGRAM ENGINEER

APPROVED BY: _____
F. GOODWIN
PROGRAM MANAGER

1.0   SCOPE

This plan of test defines the Breadboard System test program to
be performed by Hamilton Standard and Amicon Corporation on the
Hollow Fiber Membrane breadboard units. The test program is in-
tended as a means for varying performance and control modes,
for evaluating off-design conditions, and for establishing feasi-
bility of the selected applications.

TEST SEQUENCE

The Performance Test Program consists of tests performed as
follows:

   1.   Bacteria Filtration Unit

         Proof pressure test

         Leakage/permeation test

         Bacterial filtration test

   2.   Deaeration Unit

         Proof pressure test

         Leakage/permeation test

         Deaeration test of dissolved oxygen in water at mission
         design temperature, flow, and pressure conditions.

   3.   Heat Rejection Unit

         Proof pressure test

         Leakage/permeation test

         Heat rejection at mission design conditions of tempera-
         ture, flow, and environmental pressure.

         Off-design conditions of heat loads, flow versus pres-
         sure drop characteristics determination, and variations
         of vacuum environment to determine design margin.

Deviation from the test procedure requires approval of the cog-
nizant Program Engineer.

TEST ENVIRONMENT

The test environment for the heat rejection and deaeration tests
will be vacuum. The bacteria test will be at ambient conditions.

4.0   TEST EQUIPMENT

The heat rejection and deaeration testing will be performed in the Rig 8 vacuum facility of the Hamilton Standard Space Systems Department Space Laboratory. The bacterial filtration testing will be performed at Amicon Corporation.

5.0   DEFINITION OF TESTS

5.1   Bacterial Filtration Unit Testing

5.1.1   Instrumentation and Equipment

Quantity	Items
1	Reservoir with Injection Port Capacity
1	Valve, Shutoff
1	Module Holder
1	Pressure Gauge, 0-25 psig ± 0.02 psi

5.1.2   Test Setup

This entire test sequence is performed in the Amicon Corporation Laboratory. Figure 1 schematically illustrates the leakage/permeation and proof pressure test setup, and Figure 2 schematically illustrates the bacterial filtration test setup.

5.1.3   Test Procedure

a.   A bacteria filtration breadboard module P/N 70087G1 shall be placed into the holding fixture and all lines plumbed as shown in Figure 1.

b.   Proof pressure test the unit by slowly increasing the nitrogen pressure to 18 ± 0.1 psig and hold for 10 minutes minimum. Visual observation of the fibers shall be made and recorded with special attention to rupture or any other physical change in the fibers and module. Damaged fibers shall be cause for rejection of the module.

c.   Leak check the unit by nitrogen retention on the inside of the hollow fibers. Apply nitrogen at 10 ± 0.1 psig to the fibers and hold for 20 minutes minimum. Leakage in excess of 2 cc/min shall be cause for rejection of the module.

d.   Replumb the holding fixture per Figure 2. The bacterial filtration test shall be performed by injecting the bacteria agents shown below into the distilled water reservoir, shown in Figure 2, to create a challenge solution.

HAMILTON STANDARD Division of UNITED TECHNOLOGIES
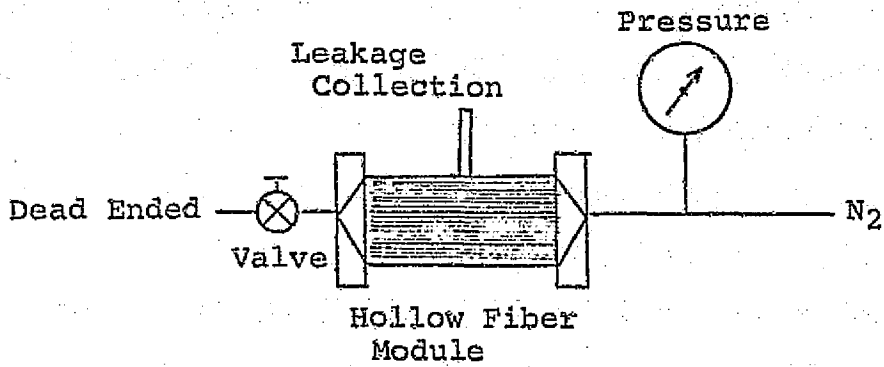
FIGURE 1 PROOF PRESSURE AND LEAKAGE/PERMEATION TEST SETUP
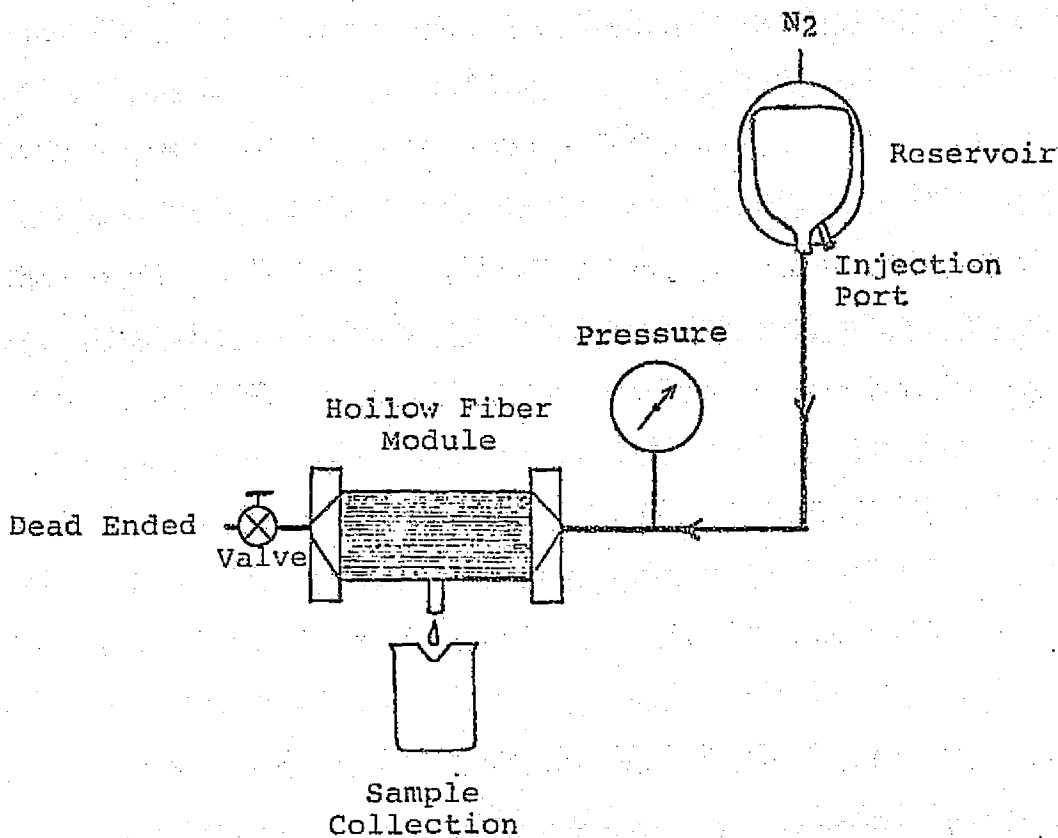
FIGURE 2 BACTERIAL FILTRATION SETUP

5.1.3   (Continued)

Agents	Concentration
Pseudomonas Aeruginosa	10^6 colony counts/cc
Escherichia Coli	10^6 colony counts/cc
Staphylococcus Aureus	10^6 colony counts/cc
Streptoccoccus Pyrogens	10^6 colony counts/cc
Klebsiella	10^6 colony counts/cc
Proteus Vulgaris	10^6 colony counts/cc
Salmonella Typhosa	10^6 colony counts/cc

e.   Pressurize the challenge solution to 10 ± 0.1 psig.

f.   The collected throughput solution shall be analyzed for bacteria presence and the quantity recorded. Presence of any listed bacteria shall be cause for rejection.

g.   At the completion of the test, the HFM module shall be sterilized and sealed in an airtight container.

5.1.4   Test Requirements

The following data shall be recorded for the above tests:

a.   Proof Pressure Test

1. Module serial number
2. Pressure level, psig
3. Duration at pressure level
4. Visible effects

b.   Leakage/Permeation Test

1. Module serial number
2. Pressure level, psig
3. Duration at pressure level
4. Leakage rate, cc/min.

c.   Bacteria Filtration Test

1. Module serial number
2. ATCC numbers
3. Challenge fluid, colony counts/cc
4. Ultrafiltration, colony counts/cc

5.2   Deaeration Unit Testing

5.2.1   Instrumentation and Equipment

Qty	Item	Range/Cap.	Accuracy
1	Flowmeter	0-42 ml./min	+2% F.S.
1	Supply Tank	100 cc minimum	
1	Supply Tank	9 Gallons	
1	Pressure Gage	0-15 psia	+0.02 psi
1	Hatch Oxygen Analysis Kit	OX-2P	
	Distilled Water	9 Gallons	
	Regulated Gaseous Oxygen		
	Regulated Gaseous Nitrogen		
2	Sample Collection Bottles	20 cc	
3	Valve, Shutoff		
2	Module Holders		
1	Pressure Gage	0-25 psig	+0.02 psi

5.2.2   Test Setup

The leakage/permeation and proof pressure tests are performed in the Amicon Corporation Laboratory per Figure 3.

The dissolved oxygen tests are performed on Rig 8 of the Hamilton Standard Space Systems Department Space Laboratory. Figure 4 schematically illustrates this test setup.

5.2.3   Test Procedure

a. A hollow fiber membrane module P/N70087G3 shall be placed into the holding fixture and all lines plumbed as shown in Figure 3.

b. Proof pressure test the unit by slowly increasing the H_2O pressure to 18 + 0.1 psig and hold for ten minutes minimum. Visual observation of the fibers shall be made and recorded with special attention to rupture or any other physical change in the fibers and module. Damaged fibers shall be cause for rejection of the module.

c. Leak check the unit by H_2O retention on the inside of the hollow fibers. Apply H_2O at 10 + 0.1 psig to the fibers and hold for 20 minutes minimum. Leakage in in excess of 0.8 cc/min shall be cause for rejection of the module.

d. Remove the breadboard HFM module from the pressure test holding fixture and install in the holding fixture located in the bell jar of Rig 8 and plumb the hardware per Figure 4.
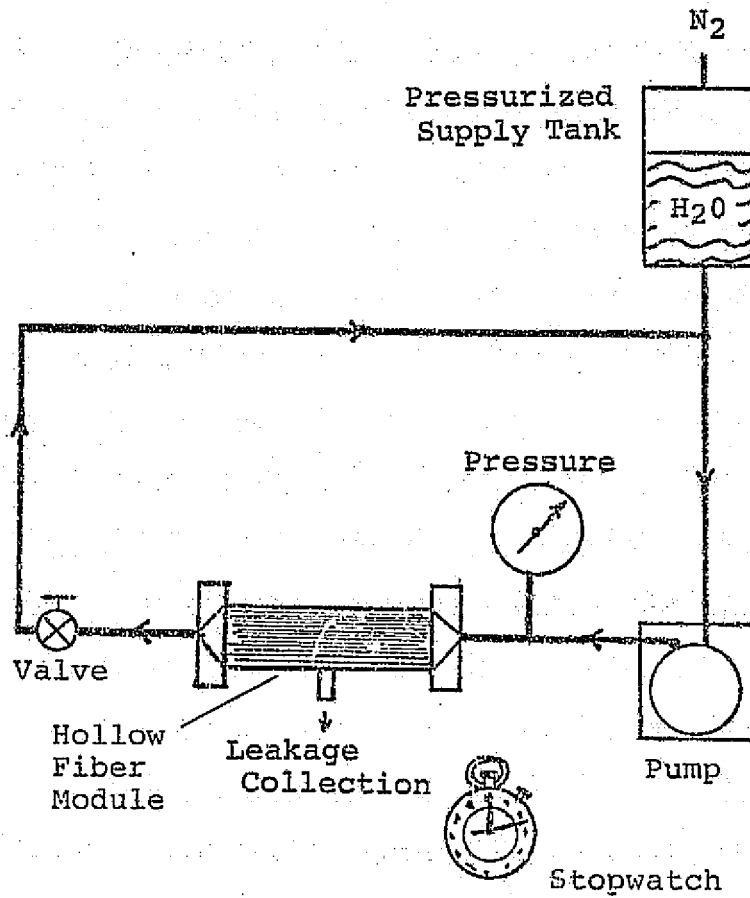
FIGURE 3 PROOF PRESSURE AND LEAKAGE/PERMEATION TEST SETUP
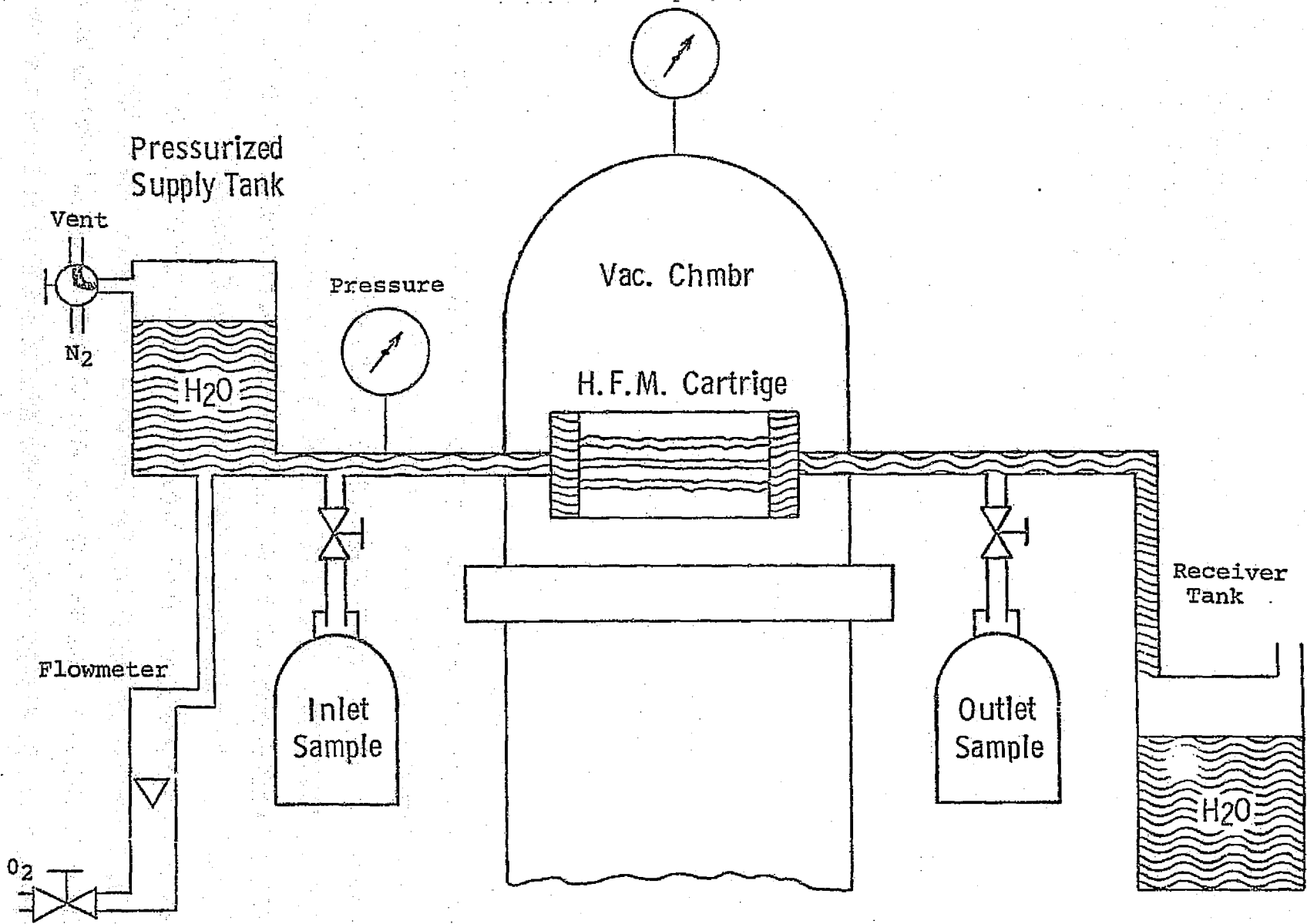
FIGURE 4 DISSOLVED OXYGEN TEST

5.2.3   (Continued)

e.   Fill the supply tank to capacity with distilled water at room temperature and connect a regulated gaseous nitrogen source.

f.   Bubble gaseous oxygen into the supply water at 24 $\pm$ 0.5 psia and at 42 $\pm$ 2 cc/min until desired level of dissolved oxygen is achieved. Shut off O_2 supply.

g.   Reduce chamber pressure to 0.5 $\pm$ 0.02 psia.

h.   Apply 10 $\pm$ 0.1 psig of nitrogen to the supply tank and remove a sample of inlet water by filling to capacity a 20 cc sample bottle. Secure the cap immediately and identify the sample.

i.   Allow water to flow through the HFM cartridge at the rate of 100 $\pm$ 2 lb/hr.

j.   Remove a sample of water on the outlet side of the HFM cartridge by filling to capacity a 20 cc sample bottle, capping tightly and identify.

k.   Repeat step (i) for 50 $\pm$ 2 lb/hr and 25 $\pm$ 2 lb/hr and perform step (j) at each condition.

l.   Reduce chamber pressure to 0.3 $\pm$ 0.02 psia and repeat steps (i) and (j).

m.   Shut down flow and raise chamber pressure to atmospheric pressure.

n.   Analyze dissolved oxygen in the five samples collected using a Hatch Analysis Kit OX-2P and record results.

5.2.4   Test Requirements

The following data shall be required for the above tests:

a.   Proof Pressure Test

1.   Module serial number
2.   Pressure level, psig
3.   Duration at pressure level
4.   Visible effects

5.2.4   (Continued)

       b. Leakage/Permeation Test

          1. Module serial number
          2. Pressure level, psig
          3. Duration at pressure level
          4. Leakage rate, cc/min.

       c. Deareation Test (Dissolved Oxygen)

          1. Chamber pressure, psia
          2. Water flow, lbs/hr
          3. Temperature in and out, °F
          4. Pressure in and out, psia
          5. Duration of gas flow in supply water

5.3   Heat Rejection Unit Testing

5.3.1   Instrumentation and Equipment

Qty	Item	Range/Cap	Accuracy
2	Thermocouples, Type K	40-120°F	+2°F
2	Pressure Gages	0-30 psia	+0.1 psi
1	Differential Pressure Gauge	0-300 in. H_2O	+ in. H_2O
1	Vacuum Gauge, Hastings	0-1000 mmHg Abs.	+2% Angul. Defl.
1	Flowmeter	0-400 lb/hr	+2% F.S.
1	Water Supply Tank with Heater		
	Distilled Water		
	Regulated Gaseous Nitrogen		
2	Valve, Shutoff		
2	Module Holders		
1	Pressure Gage	0-25 psig	+0.02 psi

5.3.2   Test Setup

The leakage/permeation and proof pressure tests are performed
in the Amicon Corporation Laboratory per Figure 3.

The heat rejection test is performed on Rig 8 in the Hamilton
Standard Space Systems Department Space Laboratory. Figure 5
schematically illustrates this test setup.

5.3.3   Test Procedure

       a. A hollow fiber membrane module P/N70087G2 shall be
          placed into the holding fixture and all lines plumbed
          as shown in Figure 3.

5.3.3   (Continued)

b. Proof pressure test the unit by slowly increasing the H2O pressure to 18 + 0.1 psig and hold for ten minutes minimum. Visual observation of the fibers shall be made and recorded with special attention to rupture or any other physical change in the fibers and module. Damaged fibers shall be cause for rejection of the module.

c. Leak check the unit by H2O retention on the inside of the hollow fibers. Apply H2O at 10 ± 0.1 psig to the fibers and hold for 20 minutes minimum. Leakage in excess of 5.5 cc/min shall be cause for rejection of the module.

d. Remove the module from the pressure test holding fixture and install in the holding fixture located in the bell jar of Rig 8, and plumb the hardware and wiring per Figure 5.

e. Fill supply tank with five gallons minimum of distilled water and actuate pump with the pump bypass valve open.

f. Heat water in supply tank to 65°F ± 2°F.

g. Open valve to HFM unit and reduce bypass to allow 300 ± 8 lb/hr to flow through the cartridge.

h. Reduce bell jar pressure to 9.8 ±0.2 mmHg absolute.

i. Maintain 300   8 lb/hr flow through cartridge for at least 10 minutes.

j. Record inlet and outlet temperatures, differential pressure, and flow.

k. Repeat (i) and (j) for 240 ± 8 lb/hr, 180 ± 8 lb/hr, 90 ± 8 lb/hr, and 50 ± 8 lb/hr successively.

l. Reduce chamber pressure to 8.6 + 0.2 mmHg absolute and repeat steps (f), (i), (j), and (k).

m. Reduce supply tank temperature to 55°F ± 2°F and repeat steps (i), (j), and (k).

n. Increase supply tank temperature to 90°F ± 2°F and repeat steps (h), (i), (j), and (k).
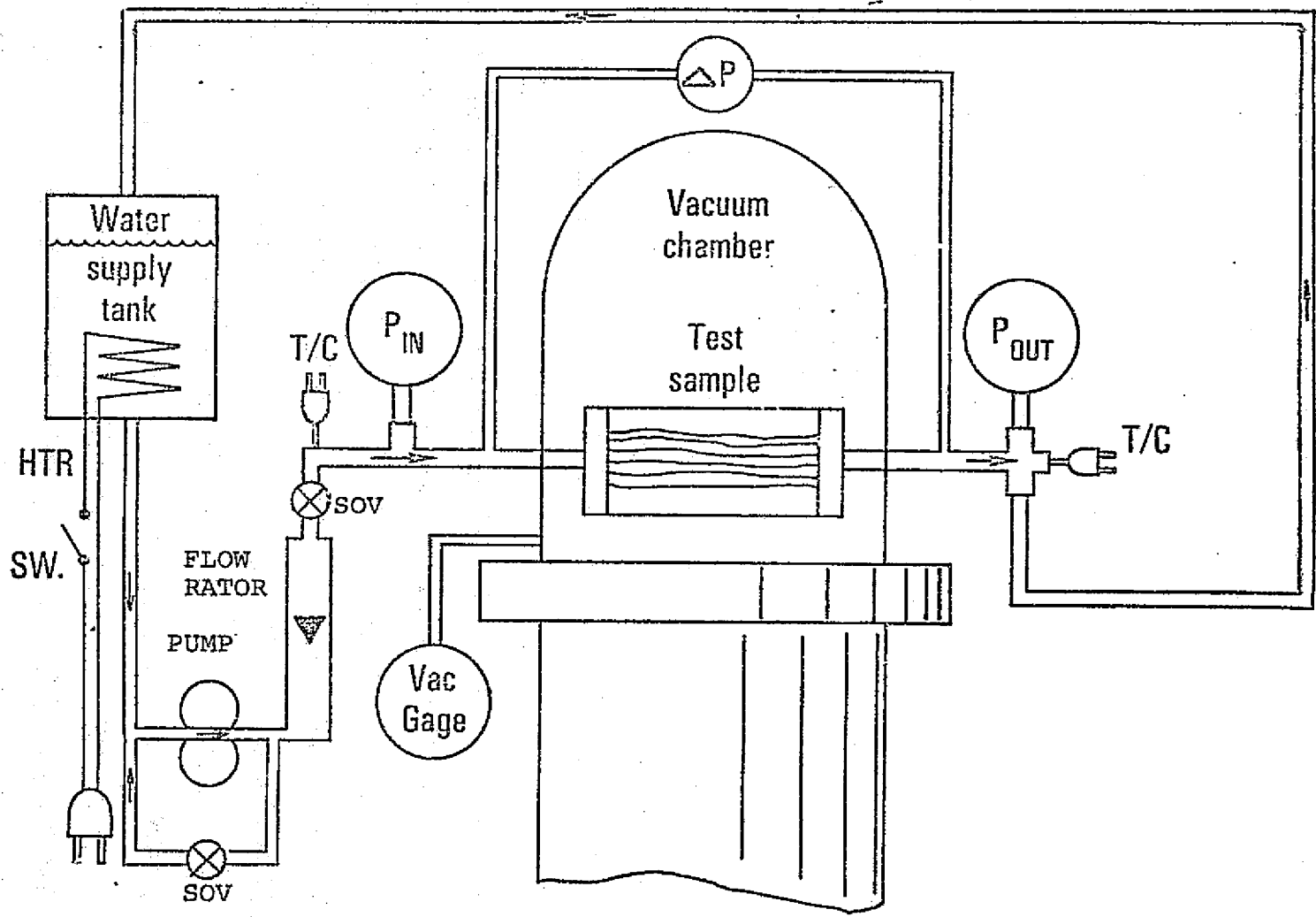
FIGURE 5   HEAT REJECTION TEST

5.3.4   Test Requirements

The following data shall be required for each of the above tests:

a. Proof Pressure Test

1. Module serial number
2. Pressure level, psig
3. Duration at pressure level
4. Visible effects

b. Leakage/Permeation Test

1. Module serial number
2. Pressure level, psig
3. Duration at pressure level
4. Leakage rate, cc/min.

c. Heat Rejection

1. Pressure, module, in and out, psia
2. Differential pressure, module, in. H_2O.
3. Water temperature, in and out, °F
4. Water flow, lbs/hr
5. Chamber pressure, mmHg abs.

From the above data, delta temperature, heat load (Q), and the conductance (UA) shall be calculated. From the water vapor partial pressure at inlet, and outlet water temperatures the log mean partial pressure of the water vapor in the HFM tubes shall be calculated.

SAMPLE LOG SHEETS

Hamilton Standard DIVISION OF UNITED AIRCRAFT CORPORATION

U A

WINDSOR LOCKS, CONNECTICUT 06096

SPACE & LIFE SYSTEMS LABORATORY

LOG OF TEST

TYPE OF TEST
H.F.M PERMEATION/BACTERIAL
TEST ENGINEER
NAME OF CO. **AMICON**
PROJECT & ENG. ORDER NO.

SHEET	OF	DATE	
TEST PLAN NO.			
MODEL NO.			
PART NO.			
SERIAL NO.			
OPERATORS			

LEAKAGE RATE AT ___ PSIG - AFTER ___ MIN. : ___ CC/MIN

PROOF PRESSURE AT 18 PSIG - OBSERVATIONS AFTER 10 MINUTES :

COLONY COUNTS /CC

AGENT	ATCC. NO	CHALLENGE FLUID	ULTRA FILTRATE
PSEUDOMONAS AERUGINOSA			
ESCHERICHIA COLI			
STAPHYLOCOCCUS AUREUS			
STREPTOCOCCUS PYROGENS			
KLEBSIELLA			
PROTEUS VULGARIS			
SALMONELLA TYPHOSA			

B-16

REMARKS:

18045

HSF-175.1A 1/66

Hamilton Standard DIVISION OF UNITED AIRCRAFT CORPORATION
WINDSOR LOCKS, CONNECTICUT 06096

U A

SPACE & LIFE SYSTEMS LABORATORY
LOG OF TEST

TYPE OF TEST	
H.F.M. HEAT REJECTION	
TEST ENGINEER	
NAME OF RIG #8	
PROJECT & ENG. ORDER NO.	

SHEET OF	
TEST PLAN NO.	
MODEL NO.	
PART NO.	
SERIAL NO.	
OPERATORS	

P_{IN}	P_{OUT}	ΔP	ΔP		TEMP IN	TEMP OUT	ΔT		FLOW			P_{CH}		TEMP SINK	Q		UA	P_{H_2O} IN	P_{H_2O} OUT	$\ln P_{H_2O}$
Psia.	Psia.	Psi	IN.H2O		°F	°F	°F		%	LBS/HR		MM Hg		°F	BTU/HR		BTU/HR/°F	mm Hg	NM Hg	mm Hg

B-17/B-18

PROOF PRESSURE AT ____ PSIG - OBSERVATIONS AFTER ____ MINUTES:

SVHSER 7100
C46-01

HAMILTON STANDARD Division of UNITED TECHNOLOGIES™

APPENDIX C

BACTERIA FILTRATION TECHNICAL REPORT

GRACE D. BROWN, PH.D.

24 PARKSIDE DRIVE

JAMAICA PLAIN, MASS. 02130

(617) 522-4838

MICROBIOLOGIST
AND
INDUSTRIAL
CONSULTANT

September 20, 1976

Mr. Micheal Lysat
Amicon Corporation
25 Hartwell Avenue
Lexington, Ma. 02173

TECHNICAL REPORT

DATE - August 18, 1976

SPECIMEN - Amicon Filter

SERIAL NUMBER - GM 80 (CB 21) 2

TEST PERFORMED - challange of filter with known amounts of bacteria

and viruses suspended in sterile distilled water. The bacteria and

viruses used were of the same ATCC strains as those used in the previous

testing of the Amicon Ultrafilter # GM-80.

BACTERIAL SPECIES USED:	ATCC#
1. Pseudomonas aeruginosa	9721
2. Escherichia coli	25922
3. Klebsiella species	23557
4. Salmonella typhosa	6380
5. Proteus vulgaris	13311
6. Staphylococcus aureus	12600
7. Streptococcus pyrogens	10389

The bacterial suspensions were fed through the filter in 10,000
organisms doses until a total of 1 million organisms were achieved.
At each progressive step, samples were taken in duplicate and plate counts
preformed.

RESULT: In each case the plate counts were negative after 72 hours.

VIRUSES USED: ATCC#

1. Coxsackie virus   A4 -27 millimicrons   VR 27
2. Echo Virus # 2   19   "   VR 32
3. Adenovirus- Human   1-85   "   VR 1
4. Herpes simplex   120-180 "   VR 539
5. Vacinnia   150-300 "

RESULT OF CHALLANGE:

The viral challanges were performed in the same manner as the preceeding

Adenovirus, Herpes simplex and Vacinnia virus withheld the challange
to 150,000 organisms per cc. at which time there was growth.

The Coxsackie and Echo viruses would only withhold the challange
to 45,000 organisms per cc.

The results indicate that the filter will withstand bacterial
contamination in large numbers. Viruses are filtered according to
the number present and the size of the virus.

It is extremely unlikely that viral contamination would reach the
extent to that of the experminental challange.

Submitted September 20, 1976

Grace D. Brown

APPENDIX D

HOLLOW FIBER MEMBRANE SYSTEMS

BREADBOARD SYSTEMS TEST LOG SHEETS

Hamilton Standard DIVISION OF UNITED AIRCRAFT CORPORATION
WINDSOR LOCKS, CONNECTICUT 06096

SPACE & LIFE SYSTEMS LABORATORY
LOG OF TEST

TYPE OF TEST MODULE
BACTERIAL RETENTION
TEST ENGINEER -
NAME OF THE CO.
AMICON
PROJECT & ENG. ORDER NO.

SHEET 1 OF 1   DATE 8/11/76
TEST PLAN NO. 5.1.3
MODEL NO.
PART NO. P/N 7008761
SERIAL NO. (B-21-1) 001
OPERATORS F. MUOLO

PROOF PRESSURE AT 18 PSI OBSERVATIONS AFTER 10 MIN:
NO VISIBLE DEFECTS IN FIBERS OR MODULE. POLYETHYLENE SLEEVE TAPED TO MODULE

GAS FLUX AT 10 PSI TRANSMEMBRANE PRESSURE:

TIME (MIN)	GAUGE READING	FLUX IN CC/MIN
1	10 PSI	0
2	10 PSI	0
5	10 PSI	0
10	10 PSI	0
15	10 PSI	0
20	10 PSI	0

D-1

SVHSER 7100

REMARKS:

13451

TYPE OF ~~TEST~~ MODULE	SHEET 1 OF 1	DATE 8/10/76
BACTERIA RETENTION	TEST PLAN NO. 5.1.3.	
TEST ENGINEER	MODEL NO.	
	PART NO. P/N 7008761	
NAME OF ~~RIG~~ CO.	SERIAL NO. (B-21-2) 002	
AMICON	OPERATORS F. MUOLO	
PROJECT & ENG. ORDER NO.		

PROOF PRESSURE AT 18 PSI OBSERVATIONS AFTER 10 MIN.
NO VISIBLE DEFECTS IN FIBERS OR MODULE.
POLYETHYLENE SLEEVE TAPED TO UNIT.

GAS FLUX AT 10 PSI TRANS MEMBRANE PRESSURE:

TIME (MIN)	GAUGE READING	FLUX IN CC/MIN
1	10 PSI	O
2	10 PSI	O
5	10 PSI	O
10	10 PSI	O
15	10 PSI	O
20	10 PSI	O

WATER FLUX AT 3 PSI:
PRESSURE IN = 4 PSI
PRESSURE OUT = 2 PSI
FLUX = 170 CC/MIN

UNIT BLUE DEXTRAN TESTED, PACKAGED IN FORMALIN, SENT
FOR BACTERIA RETENTION.

D-2

SVHSER 7100

REMARKS:

13454

Hamilton Standard DIVISION OF UNITED AIRCRAFT CORPORATION
WINDSOR LOCKS, CONNECTICUT 06096

SPACE & LIFE SYSTEMS LABORATORY

LOG OF TEST

TYPE OF TEST MODULE

DEAERATION

TEST ENGINEER

NAME OF RIG CO.

AMICON

PROJECT & ENG. ORDER NO.

SHEET 1 OF 1 . DATE 8/27/76

TEST PLAN NO. 5.2.3.

MODEL NO.

PART NO. P/N 70087G3

SERIAL NO. (C-16-2) 001

OPERATORS F. MUOLO

PROOF PRESSURE AT 18 PSI: OBSERVATIONS AFTER 20 MINUTES.
NO VISIBLE DEFECTS IN FIBERS OR MODULE.

PERMEATE RATE AT 10 PSI:
29 CC COLLECTED STEADILY FOR 20 MIN.
PERMEATE RATE 1.45 CC/MIN.

UNIT RECHECKED FOR LEAKS BY THE BLUE DEXTRAN
PROCEDURE. PERMEATE CLEAR NO LEAKS.

D-3

SVHSER 7100

REMARKS:

13456

U
A

TYPE OF ~~TEST~~ MODULE	SHEET 1 OF 1	DATE 8/27/76
DEAERATION	TEST PLAN NO. 5.2.3	
TEST ENGINEER	MODEL NO.	
	PART NO. P/N 7008763	
NAME OF ~~BIG~~ CO.	SERIAL NO. (C-16-4) 002	
AMICON	OPERATORS F MIVOLO	
PROJECT & ENG. ORDER NO.		

PROOF PRESSURE AT 18 PSI : OBSERVATIONS AFTER 20 MINUTES:
NO VISIBLE DEFECTS IN FIBERS OR MODULE

PERMEATE RATE AT 10 PSI :
20 CC COLLECTED STEADILY FOR 20 MIN.
PERMEATION RATE 1.0 CC/MIN.

UNIT RECHECKED FOR LEAKS BY THE BLUE DEXTRAN
PROCEDURE . PERMEATE CLEAR NO LEAKS.

D-4

SVHSER 7100

REMARKS:

13455

TYPE OF TEST		SHEET	OF	DATE
H.F.M DEAERATION		1	1	9-2-76

TEST ENGINEER: R. PETILLO
NAME OF RIG: #8
PROJECT & ENG. ORDER NO.

TEST PLAN NO. 9-14682
MODEL NO. (C16-4)
PART NO. 70087G3
SERIAL NO. 002
OPERATORS V. Sandberg

P_{IN}	P_{OUT}	ΔP	∠	T_{IN}	T_{OUT}	ΔT	FLOW			P_{ch}	WATER SUPPLY	WATER SAMPLE	$mg\,O_2$ per Hr				
Psia	Psia	Psi		°F	°F	°F	%	LBS/HR		Psia	GAL	#					
19.5	14.8	4.7		71.7	71.2	0.5	24	100		0.5	8.5	1	5		BUBBLED O_2 @		
17.1	14.4	2.7		73.2	72.9	0.3	13	50		0.5	—	2	5		ATMOSPHERIC PRESS		
15.2	14.3	0.9		73.1	71.6	1.5	6	25		0.5	—	3	4				
19.8	14.7	5.1		73.2	66.6	6.6	24	100		0.3	—	4	4				
							WATER	SATURATION				0	7				
19.4	13.7	5.7		74.1	73.1	1.0	24	100		0.5		1	9		BUBBLED O_2 to		
20.8	18.3	2.5		75.6	74.9	0.7	13	50		0.5		2	8		24.1 PSIA		
17.9	16.8	1.1		75.2	74.2	1.0	6	25		0.5		3	6				
21.0	15.5	5.5		75.7	65.3	10.4	24	100		0.3		4	9				
—							WATER	SATURATION				0	13				

D-5

SVHSER 7100

REMARKS:

13716

Hamilton Standard
DIVISION OF UNITED AIRCRAFT CORPORATION
WINDSOR LOCKS, CONNECTICUT 06096

UA

SPACE & LIFE SYSTEMS LABORATORY
LOG OF TEST

TYPE OF TEST	Hollow Fiber Membrane Deaeration
TEST ENGINEER	Petillo
NAME OF RIG	8
PROJECT & ENG. ORDER NO.	C46-000-001A

SHEET 1 OF 1	DATE 9-20-76
TEST PLAN NO.	
MODEL NO.	
PART NO.	70087G3
SERIAL NO.	002 (C-16-4)
OPERATORS	Laszczyk

D-6

9-20-76

SVHSER 7100

TIME		Pin PSIA	Pout PSIA		Tin °F	Tout °F		Pcham. PSIA		F/R %	Flow PPH		Saturation Press PSIA	F/R %		Sample	Dissolved O2 mg/L	
11:25	START	FLOW	THRU	HFM										ⓐ				
1130		19.2	15.65		89.7	72.8		.40		17	20.							
1140		19.2	15.6		90.0	71.6		.38		17	20.							
1200		19.15	15.5		90.0	72.3		.40		17.5	72.							
12:15		19.05	15.4		89.7	72.3		.40		17.5	72.							
12:20	STOP		WATER	SAMPLE	TAKEN	FROM	PIG										5	
																	5	
12:45	START	O2	SATURATION										22.	8+				
1330													22.8	7.5				
1415													22.8	7.5				
1515													22.9	7.5				
						ⓒ											30	BASELINE
1519		20.5	15.2		72.3	71.1		.49		25	110					1	30	
1523		21.7	19.2		72.6	70.8		.49		12.5	50					2	26	
1527		22.2	21.3		72.6	69.1		.49		6	25					3	16	
1532		20.4	13.9		72.6	64.0		.34		25	110					4	27	
0900																	32	BASELINE
0925		20.1	13.9		70.6	69.6		.50		25	110					1	21	
0930		21.3	18.4		70.8	69.3		.50		12.5	50					2	18	
0935		22.0	20.9		70.8	67.9		.50		6	25					3	13	
0942		20.	13.85		70.9	65.1		.30		25	110					4	21	

REMARKS: ① SiSi BALL.

13509

Hamilton Standard DIVISION OF UNITED AIRCRAFT CORPORATION

WINDSOR LOCKS, CONNECTICUT 06096

SPACE & LIFE SYSTEMS LABORATORY

LOG OF TEST

TYPE OF TEST	SHEET 1 OF 1 DATE 9-21-76
Hollow Fiber Membrane Deaeration	TEST PLAN NO.
TEST ENGINEER PETILLO	MODEL NO.
NAME OF RIG 8	PART NO. 7008763
	SERIAL NO. 002 (C-16-4)
PROJECT & ENG. ORDER NO. C46-000-001A	OPERATORS LASZCZYK

TIME	P_{IN} PSIA	P_{OUT} PSIA	T_{IN} °F	T_{OUT} °F	P_{CHAM} PSIA	AIR %	Flow PPH	SATURATION PRESS PSIA	F/R %	SAMPLE	DISSOLVED O_2 Mg/L			
										BASELINE	21			
1235	19.9	13.7	70.7	69.8	.50	25	110			1	17			
1240	20.9	19.9	70.8	69.5	.50	12.5	50			2	16			
1245	21.7	20.5	70.7	68.1	.50	6.	25			3	11			
1250	19.9	13.7	70.8	65.6	.30	25	110			4	18			

REMARKS

SVHSER 7100

13510

Hamilton Standard
DIVISION OF UNITED AIRCRAFT CORPORATION
WINDSOR LOCKS, CONNECTICUT 06096

HSF-175 IA 1/06

SPACE & LIFE SYSTEMS LABORATORY
LOG OF TEST

TYPE OF TEST	
H.F.M. HEAT REJECTION	
TEST ENGINEER	R. PETILLO
NAME OF RIG	#8
PROJECT & ENG. ORDER NO.	

SHEET 1 OF	DATE 8-30-76
TEST PLAN NO.	9-14682
MODEL NO.	2400-3A-1
PART NO.	7008762
SERIAL NO.	001
OPERATORS	G. HOWE

P_{IN}	P_{OUT}	ΔP	ΔP		TEMP IN	TEMP OUT	ΔT	LN T	FLOW		$P_{Ch.}$	TEMP SINK	Q		UA	P_{H_2O} IN	P_{H_2O} OUT	LN P_{H_2O}
Psia	Psia	Psi	IN H2O		°F	°F	°F	°F	%	LBS/HR	mmHg	°F	BTU/HR		BTU/HR/°F	mmHg	mmHg	mmHg
21.3	18.0	3.3	89		88.7	78.0	10.7	31.35	62	260	9.8	51.7	2882		88.74	34.7	24.6	19.41
20.4	17.5	2.9	83		89.8	78.9	10.9	32.34	58	240	9.8	51.7	2616		90.89	36.0	25.4	
19.1	17.1	2.0	57		90.0	76.1	13.9	30.63	44	180	9.85	57.9	2502		81.68	36.1	23.1	
17.6	16.8	0.8	24		89.3	68.8	20.5	25.70	22	90	9.9	52.0	1845		71.79	35.4	18.0	
17.1	16.7	0.6	18		89.0	62.6	26.4	21.46	13	50	9.3	51.7	1320		61.51	35.0	14.6	
27.4	21.8	5.6	157		54.7	53.0	1.7	5.81	72	300	8.6	48.0	510		87.78	10.9	10.3	
25.1	20.9	4.2	119		54.4	52.5	1.9	5.39	58	240	8.6	48.0	456		84.60	10.8	10.1	
23.5	20.5	2.0	86		54.6	52.2	2.4	5.31	44	180	8.6	48.0	432		81.36	10.9	10.0	
22.0	20.0	2.0	39		55.9	51.9	4.0	5.04	22	90	8.7	48.6	360		71.43	11.4	9.9	
20.5	19.7	0.8	21		56.9	50.5	6.4	5.04	13	50	8.6	48.0	320		63.49	11.8	9.4	
23.7	17.7	5.0	165		53.1	52.2	0.9	4.64	72	300	8.6	48.0	270		58.19	10.3	10.0	
21.4	16.8	4.6	127		53.3	53.2	1.1	4.73	58	240	8.6	48.0	264		55.81	10.4	10.0	
19.4	16.1	3.3	93		53.0	51.2	1.8	4.03	44	180	8.6	48.0	324		80.39	10.35	9.6	
16.9	15.3	1.7	43		55.0	51.2	3.8	4.85	22	90	8.6	48.0	342		70.58	11.1	9.6	
16.1	15.1	1.0	27		56.9	50.7	6.2	5.20	13	50	8.6	48.0	310		59.62	11.8	9.4	

REMARKS: PROOF PRESS AT 18 PSIG FOR 14 MIN. OBSERV.: NO VISIBLE DAMAGE TO FIBER & HOLDER. LEAKAGE/PERM. AT 10 PSIG FOR 20 MIN. LEAKAGE: 4.8 CC. LEAK RATE 0.24 CC/MIN.

D-8

13904

Hamilton Standard DIVISION OF UNITED AIRCRAFT CORPORATION
WINDSOR LOCKS, CONNECTICUT 06096

U A

SPACE & LIFE SYSTEMS LABORATORY
LOG OF TEST

TYPE OF TEST: H.F.M. HEAT REJECTION

TEST ENGINEER: R. PETILLO

NAME OF RIG: #8

PROJECT & ENG. ORDER NO.

TEST PLAN NO. 9-14682
MODEL NO. 2400-3A-2
PART NO. 70087G2
SERIAL NO. 002
OPERATORS: V. SANDBERG

P_IN	P_OUT	ΔP	ΔP		TEMP IN	TEMP OUT	ΔT	L/ΔT	FLOW			P_ch	↙	TEMP SINK	Q		UA	P_H2O IN	P_H2O OUT	LN P_H2O
Psia	Psia	Psi	in H₂O		°F	°F	°F	°F	%	LBS/HR		mmHg	↙	°F	BTU/HR		BTU/HR/°F	mmHg	mmHg	mmHg
23.4	17.1	6.3	174		56.2	54.4	1.8	7.26	72	300		8.6	48.0	48.0	540		74.38	11.6	10.8	2.58
21.3	16.4	4.9	136		55.1	52.9	2.2	5.99	38	240		8.6	48.0	48.0	528		89.03	11.1	10.2	2.02
19.2	15.7	3.8	98		55.1	53.1	2.0	6.04	44	180		8.6	48.0	48.0	360		59.60	11.1	10.3	2.07
16.3	15.0	1.3	36		56.3	52.2	4.1	6.01	22	90		8.6	48.0	48.0	369		61.80	11.6	10.0	2.10
15.5	14.8	0.7	18		55.9	50.7	5.2	4.84	13	50		8.6	48.0	48.0	260		53.72	11.4	9.4	1.60
23.0	17.0	6.0	166		64.1	61.4	2.7	10.99	72	300		9.8	51.7	51.7	810		73.70	15.3	13.9	4.77
20.7	16.2	4.5	126		64.0	60.7	3.3	10.96	58	240		9.65	51.3	51.3	792		72.26	15.2	13.6	4.70
18.9	15.7	3.2	89		64.1	60.0	4.1	10.21	44	180		9.8	51.7	51.7	728		72.28	15.3	13.2	4.37
16.4	15.05	1.3	38		64.7	57.8	6.9	9.33	22	90		9.7	51.5	51.5	621		66.56	15.6	12.2	3.96
15.6	14.75	0.8	21		56.3	55.9	10.4	8.35	13	50		9.8	51.7	51.7	520		62.28	16.5	11.4	3.56
23.0	17.2	5.8	163		64.7	61.3	3.4	14.94	72	300		8.6	48.0	48.0	1020		68.27	15.6	13.8	6.06
20.7	16.4	4.3	119		64.8	60.8	4.0	14.71	58	240		8.6	48.0	48.0	960		65.26	15.7	13.6	5.99
18.9	15.7	3.2	88		64.8	59.8	5.0	14.15	44	180		8.6	48.0	48.0	900		63.60	15.7	13.2	5.76
16.4	14.9	1.5	38		65.9	57.4	8.5	13.20	22	90		8.6	48.0	48.0	765		57.95	16.2	12.1	5.39
15.6	14.8	0.8	21		65.9	54.5	11.4	11.25	13	50		8.6	48.0	48.0	570		50.67	16.2	10.8	4.36

REMARKS: PROOF PRESS AT 18 PSIG FOR 14 MIN. OBSERV: NO VISIBLE DAMAGE TO FIBER & HOLDER
LEAKAGE/PERM AT 10 PSIG FOR 20 MIN LEAKAGE: 10.1 CC, LEAK. RATE 0.505 CC/MIN

D-9

SVHSER 7100

3727

HSF-175.1A 1/66

Hamilton Standard DIVISION OF UNITED AIRCRAFT CORPORATION
WINDSOR LOCKS, CONNECTICUT 06096

UA

SPACE & LIFE SYSTEMS LABORATORY
LOG OF TEST

TYPE OF TEST
H.F.M. HEAT REJECTION
TEST ENGINEER
R. PETILLO
NAME OF RIG
± 8
PROJECT & ENG. ORDER NO.

SHEET 2 OF 2 DATE 9-1-76
TEST PLAN NO. 9-14682
MODEL NO. 2400-3A-2
PART NO. 7008762
SERIAL NO. 001
OPERATORS V. SANDBERG

P_{IN}	P_{OUT}	ΔP	ΔP		TEMP IN	TEMP OUT	ΔT	$LN\Delta T$	FLOW		P_{ch}		TEMP SINK	Q		UA	P_{H_2O} IN	P_{H_2O} OUT	$LN P_{H_2O}$	
P_{sia}	P_{sia}	P_{si}	$IN H_2O$		°F	°F	°F	°F	%	LBS/HR	mmHg		°F	BTU/HR		BTU/HR°F	mmHg	mmHg	mmHg	
21.8	16.8	5.0	138		88.1	79.4	8.7	31.85	72	300		9.8		51.7	2610		81.95	34.1	25.8	19.86	
19.8	16.2	3.6	100		88.0	78.0	10.0	31.03	58	240		9.8		51.7	2400		77.34	34.0	24.6	19.12	
18.1	15.6	2.5	69		88.2	75.9	12.3	29.93	44	180		9.8		51.7	2214		73.97	34.2	22.9	18.17	
16.2	14.9	1.3	31		89.0	69.7	19.3	26.49	22	90		9.8		51.7	1737		65.57	35.1	18.6	15.64	
15.3	14.7	0.6	17		89.4	63.6	25.8	23.37	13	50		9.8		51.7	1290		57.67	35.5	15.0	12.83	

REMARKS:

Hamilton Standard — Division of United Aircraft Corporation
WINDSOR LOCKS, CONNECTICUT 06096

UA

SPACE & LIFE SYSTEMS LABORATORY
LOG OF TEST

TYPE OF TEST
H.F.M HEAT REJECTION

TEST ENGINEER
R. PETILLO

NAME OF RIG
8

PROJECT & ENG. ORDER NO.

P_{IN}	P_{OUT}	ΔP	ΔP		TEMP IN	TEMP OUT	ΔT	LN ΔT		FLOW			P_{ch}		TEMP SINK	Q		UA	P_{H_2O} IN	P_{H_2O} OUT	LN P_{H_2O}	TIME @ CONDIT
Psia	Psia	Psi	inH2O		°F	°F	°F	°F		%	LBS/HR		mmHg		°F	BTU/HR		BTU/HR/°F	mmHg	mmHg	mmHg	MIN
22.8	17.6	5.2	140		54.6	52.1	2.5	5.25		72	300		8.6		48.0	750		142.9	10.9	9.9	1.75	5
20.8	16.8	4.0	110		54.0	51.8	2.2	5.99		58	240		8.5		47.6	528		101.1	10.7	9.8	1.71	5
19.1	16.0	3.1	81		53.8	50.6	3.2	3.99		44	180		8.6		48.0	576		144.4	10.6	9.4	1.24	5
16.8	15.3	1.5	40		55.1	49.9	5.2	3.94		22	90		8.6		48.0	468		118.8	11.1	9.2	1.33	5
16.0	14.9	1.1	26		57.0	49.5	7.5	4.19		13	50		8.6		48.0	375		89.5	11.9	9.1	1.48	5
22.6	17.6	5.0	133		63.1	57.0	6.1	11.78		72	300		8.6		48.0	1830		155.3	14.8	11.9	4.60	5
20.5	16.8	3.7	100		63.6	56.4	7.2	11.22		58	240		8.65		48.4	1728		154.0	15.0	11.6	4.43	5
18.8	16.1	2.7	71		63.9	55.3	8.6	11.05		44	180		8.6		48.0	1548		140.1	15.2	11.2	4.29	5
16.7	15.4	1.3	32		64.4	52.0	12.4	8.79		22	90		8.6		48.0	1116		127.0	15.4	9.9	3.32	5
15.9	15.2	0.7	18		66.0	49.9	16.1	7.16		13	50		8.6		48.0	805		112.4	16.3	9.2	2.78	5
22.3	17.5	4.8	131		63.1	58.1	5.0	8.66		72	300		9.8		51.7	1500		173.2	14.8	12.4	3.67	5
20.3	16.8	3.5	96		63.8	57.8	6.0	8.97		58	240		9.75		51.5	1440		160.5	15.2	12.2	3.75	5
18.7	16.1	2.6	70		64.4	57.2	7.2	8.60		44	180		9.8		51.7	1296		150.7	15.4	12.0	3.64	5
16.7	15.4	1.3	32		65.5	54.5	11.0	6.90		22	90		9.8		51.7	990		143.5	16.0	10.9	2.95	4
15.9	15.2	0.7	19		67.0	53.0	14.0	5.68		13	50		9.8		51.7	700		123.2	16.8	10.3	2.46	4

REMARKS: PROOF PRESS AT 18 PSIG FOR 10 MIN — NO VISIBLE DAMAGE OR LEAK AROUND
HOLDER & FITTINGS
LEAKAGE/PERM AT 10 PSIG FOR 20 MIN. 11.8 CC (.59 CC/MIN.)
" " " " " " AFTER SURFACTANT COATING 17.5 CC (.875 CC/MIN)

13.

Hamilton Standard
DIVISION OF UNITED AIRCRAFT CORPORATION
WINDSOR LOCKS, CONNECTICUT 06096

U A

SPACE & LIFE SYSTEMS LABORATORY
LOG OF TEST

TYPE OF TEST	H.F.M. HEAT REJECTION
TEST ENGINEER	R. PETILLO
NAME OF RIG	#8
PROJECT & ENG. ORDER NO.	

SHEET 2 OF 7 DATE 9/8/76	
TEST PLAN NO. 9-14682	
MODEL NO. 2400-3A-3	
PART NO. 700876-2	
SERIAL NO. 004	
OPERATORS V. Sandberg	

HSF-175 1A 1/66

P_{IN} PSIG	P_{OUT} PSIA	ΔP PSI	ΔP inH2O	TEMP IN °F	TEMP OUT °F	ΔT °F	LN ΔT °F	FLOW %	FLOW LBS/HR	Pch mmHg	TEMP SINK °F	Q BTU/HR	UA BTU/HR°F	P_{H2O} IN mmHg	P_{H2O} OUT mmHg	LN P_{H2O} mmHg	TIME @ ... MIN
21.2	17.3	3.9	106	91.1	74.1	17.0	30.62	72	300	9.6	51.2	5100	166.56	37.5	21.6	18.35	
19.6	16.6	3.0	81	89.7	71.6	18.1	27.57	58	240	9.9	52.1	4344	151.56	35.9	19.8	16.67	
19.2	16.0	2.2	58	89.3	68.5	20.8	25.82	44	180	9.8	51.7	3744	145.00	35.2	17.8	15.06	
16.4	15.3	1.1	28	89.6	60.6	29.0	20.02	22	90	9.8	51.7	2610	130.37	35.8	13.5	11.44	
15.8	15.0	0.3	17	90.1	55.5	34.6	14.96	13	50	9.8	51.7	1730	115.64	36.1	11.3	8.66	
21.4	17.4	4.0	103	87.3	72.4	14.9	27.28	72	300	9.85	51.9	4470	163.36	33.2	20.4	16.11	

D-12

SVHSER 7100

REMARKS:

14156

Hamilton Standard DIVISION OF UNITED AIRCRAFT CORPORATION
WINDSOR LOCKS, CONNECTICUT 06096

UA

SPACE & LIFE SYSTEMS LABORATORY
LOG OF TEST

TYPE OF TEST	
TEST ENGINEER	
NAME OF RIG	
PROJECT & ENG. ORDER NO.	

SHEET _1_ OF _1_ DATE 9/29/76	
TEST PLAN NO.	9/30/76
	10/1/76
MODEL NO.	
PART NO. 70087-G2	
SERIAL NO. 002 (2400-3R-2)	
OPERATORS	

① PRE-VIBRATION LEAK TEST: 9/29/76
@ 10 PSIG LEAK 2.8 CC IN 20 MIN ✓ RATE 0.14 CC/MIN

② VIBRATION TESTING PERFORMED TO SPACE LAB QUAL & DURATION LEVELS: 9/30/76
NO VISIBLE DAMAGE NOTED

③ POST-VIBRATION LEAK TEST: 10/1/76
@ 10 PSIG LEAK 3.0 CC IN 20 MIN ✓ RATE 0.15 CC/MIN

D-13/D-14

SVHSER 7100

REMARKS:

14168